Preface

Special Issue on Up-to-Date Problems in Modern Railways

The topic is significant and researched in detail worldwide in engineering. Guest Editors, some of the best and well-known researchers in Middle and East Europe in this field, are the warrant for the quality of the collected papers.

This Special Issue aimed to provide a premier international platform for a wide range of professions to discuss and present the most recent challenges and developments in *Up-to-date problems in modern railways*. The special issue was open to submitting novel and high-quality research contributions (research and review papers). The topics are from the railway vehicle across the track, even until the subsoil, but they connect the engineering (civil, mechanical, vehicle, electrical engineering, mechatronics, etc.) area.

The collected papers contain new laboratory tests, field/in-situ tests, numerical modeling, railway diagnostics, etc., with up-to-date methods.

We are very grateful to all the authors for their enthusiasm during the preparation of contributions for this special issue and for sharing their research with us, especially for this occasion.

Last but not least, we are honestly thankful to the editorial board of journal Acta Polytechnica Hungarica for making this issue possible, as well as Prof. Dr. Péter Baranyi, Rector of Széchenyi István University, Győr, the organizer of this Special Issue.

It is planned to continue the first part of the Special Issue in the future, i.e., further number is under preparation in Acta Polytechnica Hungarica journal.

Dragan Marinkovic, Dmytro Kurhan, Mykola Sysyn and Szabolcs Fischer

Guest Editors

Laboratory Tests and FE Modeling of the Concrete Canvas, for Infrastructure Applications

Balázs Eller, Movahedi Rad Majid, Szabolcs Fischer

Széchenyi István University
Egyetem tér 1, H-9026 Győr, Hungary
{eller.balazs,majidmr,fischersz}@sze.hu

Abstract: The Concrete Canvas (CC) material, is a promising material for application in many civil engineering fields, such as, water construction, pipelining, slope protection, military applications, etc. The authors believe that this material has more potential and could be helpful in infrastructure applications. The infrastructure design requirements are known; the CC has to be fit into the track structure. Several relevant investigations were performed to show the materials adequacy, and using collected data, FE (Finite Element) models were built to determine more of the physical parameters. From the results and the hardening experiences, it can be stated, that after the laying of CC and the spraying of water, the material has to be loaded to reach the best shape and push the material down to the supporting protection layer. In FE modeling, it was shown that the material is a composite structure, i.e. one material's physical properties is not enough for modeling (it has to be improved). Moreover, it means that dynamic examinations can be initiated.

Keywords: GCCM; ConcreteCanvas; railway; substructure; FE modeling

1 Introduction

The development of infrastructural technologies are continuous [1-4]. The new methods always solve exisiting problems, give more opportunities or cost-effective solutions [5-8]. In this study, the authors also try to find solutions for drainage, adequate separation and strengthening. These problems can be a problem in road operation, too, but most problems occur in railways. Therefore, cost-effective technologies are needed, and it is especially true at the renewing of the local substructure problems. The local substructure problems mean a problem in a short section, for example, from 2 meters to 50-100 meters. The renewing of these cannot be done locally. Usually, it needs earthwork technology to renew the protection layer and the whole superstructure. If the drainage can't be handled, the problem will come back in a short time. The problems and the possible solutions were summarized in [9] [10].

The material which can allow us to improve these segments is the application of geosynthetic cementitious composite mats (GCCMs). The authors mainly investigate the most promising type of the GCCMs, the Concrete Canvas (CC). It was developed by Berwin and Crawford, in 2005. [11]. This technology until this time is mainly used in water construction, while it is an alternative solution for shotcrete. It is presented in several case studies, such as slope protection [12], a trackway for vehicles, pedestrians or a protection layer for pipe and lining [11]. Even so, the CC is barely investigated in the professional literature yet. The CC is available in 5, 8 and 13 mm thicknesses (CC5, CC8 and CC13, respectively). The mat is a cement-impregnated fabric. It contains a 3D fiber matrix with a special cement mixture, while the upper plane is a non-woven geotextile, and the lower plane is a PVC waterproofing layer [9]. The structure of the material can be seen in Fig. 1 (left). After it is hydrated by water, the material reaches high rigidity and strength according to the date scripts; it reaches 80% of the final physical properties. [13] [14].

The technology has drawbacks. For example, water access can be a problem, especially at railways, where access to the problematic section is nearly impossible on the road. In this case, an additional railway vehicle is required. In road construction, it is a much easier task.

The density of the CC at non-bound form is 1300-1500 kg/m^3 thanks to the dry cement powder in the structure. After the hydration, the final density increased by 25-30%, to 1700-2000 kg/m^3. The density of the regular concrete is 2200-2400 kg/m^3 [11] [15].
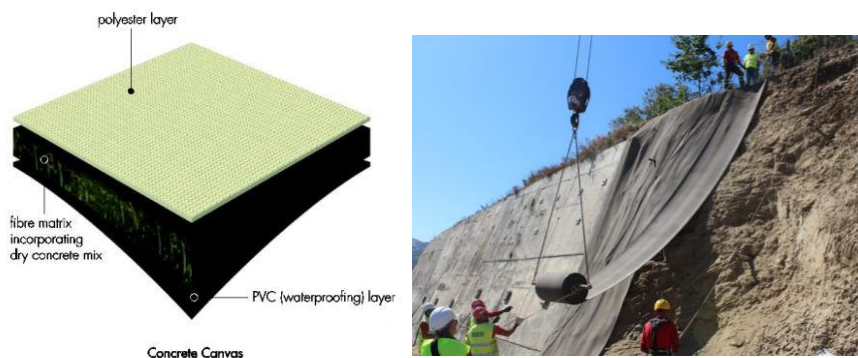

Figure 1
The structure and the application of CC [11]

In [16-18], the mechanical strength and the volume stability were described. The upper polyester layer has been woven in two directions. The longitudinal direction is more robust. The other variables are the type of the 3D fiber and the type/composition of cement.

The material is a perfect solution for slope protection (Fig. 1, right), and several examinations were made, which gave good results. [19] [20] In place of the shotcrete layer, the CC hardens faster, and the properties are better or the same. The manufacturer shows several case studies on these topics [11]. Furthermore, thanks to its nearly waterproof property, the soil does not absorb water from the rain, so the moisture content does not generate problems.

This article aims to introduce the our laboratory investigations and, based on the results, draw any conclusions concerning the applications in infrastructure construction, mainly from railway aspects.

2   Laboratory Examinations

To examine the material's behavior at railway or road circumstances, we have to think about how much force (load) can occur on the material. First, the material has to deal with static loads. In the aspect of roads, the max. axle load is approx. 100 kN, while the max. axle loads at the railways are 225 kN (in Hungary). Other countries use larger axle loads (250 kN or more), but the authors investigate the Hungarian conditions primarily. On the other hand, the axle load is not the only load on the structure; the superstructure of the railway has its own dead load, too. But this dead load is appropriate to create the ideal plane of the CC layer on the protection layer. Among the types of material, the authors decided to investigate the 13 mm thick material because in this kind and amount of loading, the thicker is the better choice.

Suppose the static loads cannot occur problems in the material, and the physical properties give a continuously appropriate layer. The second step is to investigate the material for dynamic loads. The load distribution at the railways is particular; it spreads by a nominal degree of 45° (see Fig. 2).
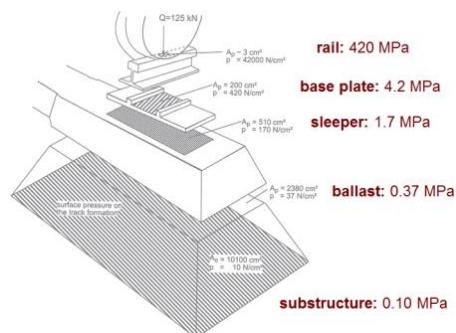

Figure 2
Load distribution at railways [21]

In the professional literature, several tests were shown in [12-15, 18, 22, 23], like puncture test, 3-point bending test, tensile test, etc. We studied and tried the different tests, and finally, the authors selected the following relevant static laboratory tests:

- Four-point bending test (in place of three-point bending test)
- Compressive strength test
- Puncture test

2.1. Four-Point Bending Test

According to previous experiences, the 4-point bending test was chosen in place of the three-point test because shear loads were occurring at the latter test. It could be complicated at the finite element modeling (FEM). 350×200 mm samples were cut from CC13, and these were divided into three 100 mm sections. The illustration of this test can be seen in Fig. 3 (left and right). The movement (displacement) of the edges was measured in the middle; blue arrows signed it.
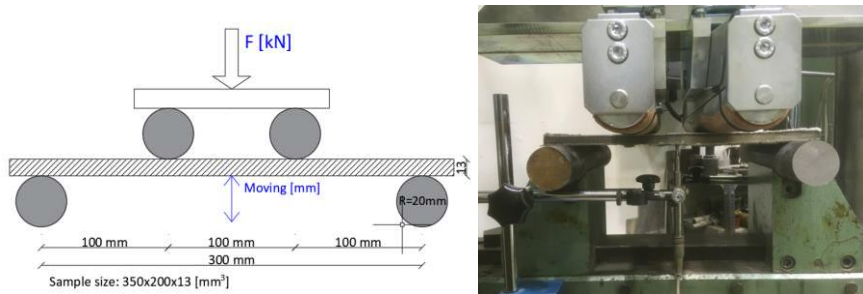

Figure 3
Four-point bending test

2.2. Compressive Strength Test

Compressive strength tests were not found in the authors' research, so this test was planned based on our ideas. The unique cement powder mixture was not available for the authors, so they had to think of another way to measure the compressive strength and calculate the material's Young's modulus. Finally, it was decided to cut 300×300 mm size tables from CC13. The material was loaded slowly until 200 kN. The movement was measured in every corner, and then the average movement (displacement) was calculated from the four values. The illustration of this test can be seen in Fig. 4 (left and right). Another essential part is the making of the samples. The CC has to be covered with weight after hydration. If not, the material can be 'wavy', which can be a problem at the test.

If the surface is not flat and one or two corner bends up, the result of the average movement can be larger than the real value, so false values can be received. If these columns of data are deleted, the average would not be so accurate.
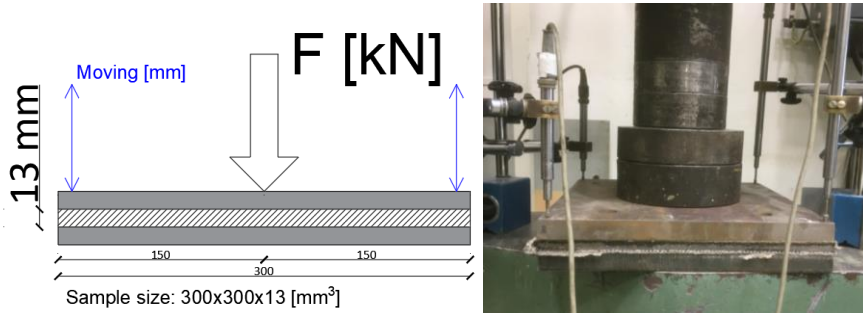

Figure 4
Compression strength stress

2.3. Puncture Test

This test was performed according to the concerning ISO standard [24] (see Figs. 5 and 6). In [13], puncture tests were executed on GCCM materials. This test is usable at modeling real circumstances when there is no support under the CC layer (especially at railways, at local failures). At this test $250{\times}250$ mm^2 samples were cut, and these were fixed to two circle profiles, with a minimum diameter of 150 mm. The material got no lower support, while a 50 mm diameter plunger loaded it. The material was loaded until the first crack, and then it was loaded continuously until the textile and the PVC layer were also torn.
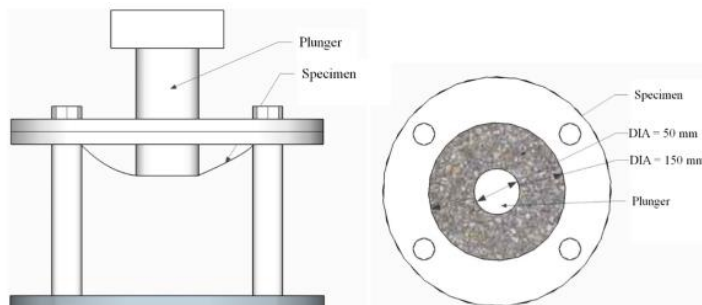

Figure 5
Puncture test [5]

Figure 6
The deformation after the puncture test

3   Results

3.1.   Four-Point Bending Test

According to the manufacturer's data script (datasheet), the initial break occurs at>4 MPa, while the final break occurs at >6 MPa [25]. Compared to the measured data, the authors determined lower stress until the initial break. The measured results can be seen in Table 1. It can be observed that the direction of the woven makes a difference in the stress of the initial break. On the other hand, the bending stress does not reach 80% after 24 hours, while the deflection is larger than the hardened types. It is because the material is plastic at this time. Because of this plastic behavior, the CC takes the shape of the lower plane of the ballast bed [25].

It can be seen in Table 1 that there is constant stress increasing at the longitudinal direction, while at the transversal direction, the 7-day samples were more rigid and robust than the 28-day samples. It is probably the problem of hydration; if the water spraying is not even, the rigidity of the CC layer will not be the same at every point. Thanks to this, the standard deviation is quite significant. The table also shows that the bending was between 0.51-1.10 mm in every case, which is a tiny difference.

The calculated data are low values. If Fig. 2 is rechecked, it can be noticed that the nominal/assumed load on the plane of the protection layer is only 0.1 MPa (with 250 kN axle load and without deadweight, which is negligible compared to the axle load). Of course, it is not accurate and different in real, because the distribution of the loads is going through ballast particles, but it is suitable for

illustration. One day after the hydration, the lowest bending stress is much larger than the loading on the plane of the protection layer. The support under the CC layer is assumed to be continuous and adequate, so the breakage will not happen predictably.

Table 1

Results of the four-point bending test

	Stress [Mpa]	Woven		Stress [MPa]	Woven	Diff.
Results after 1 day						
Average:	**3.01**	longitudinal	Average:	**2.15**	transversal	37.2%
Standard dev.:	0.05		Standard dev.:	0.02		
Difference [%]:	17.75		Difference [%]:	7.20		
average deflection until the first crack: 0.73 and 0.51						
Results after 7 day						
Average:	**5.60**	longitudinal	Average:	**3.87**	transversal	38.3%
Standard dev.:	0.13		Standard dev.:	0.07		
Difference [%]:	27.07		Difference [%]:	16.70		
average deflection until the first crack: 0.63 and 0.63						
Results after 28 day						
Average:	**7.83**	longitudinal	Average:	**2.38**	transversal	229.5%
Standard dev.:	0.15		Standard dev.:	0.08		
Difference [%]:	19.48		Difference [%]:	32.14		
average deflection until the first crack: 1.1 and 0.95						

Using the received and the given data, the examination model was built (Fig. 7). Without knowing the correct material parameters, the authors used the calculated Young's modulus from the compression test. The results were not the same on the model and from the laboratory measurements. The experience is that only Young's modulus is not enough to build the material model because unreal ending values were obtained. On the other hand, the bending results were not the same at the different woven directions, which also occurs some problem at the illustration of the correct movement. In Fig. 7, it can be seen a sample with a weaving of the longitudinal direction. The average load was given, while the Young's modulus was from the compression test. The deflection is nearly 8 mm, while the average movement (displacement) until the first break was 1.1 mm.
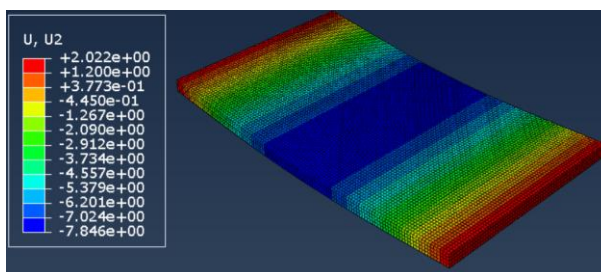

Figure 7

The model of the four-point bending test

It can be stated that the model needs more parameters; on the other hand, a new composite structure with different parameters had to be built. The concrete layer is only 11 mm of the 13 mm total thickness, so only the concrete parameters will show false results.

3.2.   Compressive Strength Test

The measuring of the compressive strength is important because it was needed to determine the material's Young's modulus. The data obtained are plotted on a graph, and then the load section where the chart has the most significant slope is selected. After that, using the "least squares" method, a straight line was calculated that best fits the data, and then returned an array that described the line was returned. From that, the Young's modulus was able to be received, which can be seen in Table 2. The first problem is the high standard deviation. As it was mentioned earlier in Chapter 3.1, the problem can be unequal hydration.

Table 2
Results of the compression test

1 days	150 kN - end [Mpa]	28 days	150 kN - end [Mpa]
1120/1	346.054	1218/1	515.301
1120/2	736.230	1218/2	495.089
1120/3	592.656	1218/3	480.585
1120/4	303.246	1218/4	507.845
1120/5	328.415	1218/5	645.734
1120/6	422.053	1218/6	733.183
0520/1	444.889	0615/1	419.886
0520/2	broken	0615/2	424.524
0520/3	367.083	0615/3	489.860
0520/4	785.690		
Average	480.702	Average	523.556
E=480.7 Mpa		E=523.6 Mpa	
Stand. Dev.	180.724	Stand. Dev.	102.184
Diff. [%]	38.092	Diff. [%]	18.207
Calculation with full thickness			

The results were used at modeling (see Fig. 8) to check the correlation between the calculated data and the measured compression. The average compression at the measurements was 1 mm. Using the calculated Young's modulus at the modeling, the received compression was not the same as the laboratory measurements. The result of the modeling was 0.028 mm as opposed to the 1 mm average compression. The problem can be found at the layer structure, again. The upper ~1 mm woven textile and the lower ~1 mm PVC layer can be compressed easier, but on the other hand, this 2 mm means 15.4% of the

structure's thickness. These thin layers cannot be removed. One solution is to build the composite model structure from the three materials, but the validation can again be a problem at the two thin layers. The second solution is checking the shorter range in the elongation and loading graph, which could improve the received 'E'. But in this case, while the material could be more robust, the compression will be lower. In our opinion, both solutions need to be used to make this test result more correct.
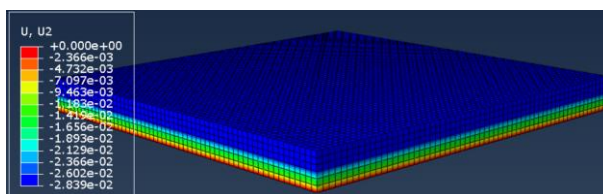

Figure 8
Modeling of the compression test

However, these tests were not successful from modeling; it was helpful to see that the CC layer is not being broken under the high load. It means that it can handle the static loads which are being occurred under the railway structure.

3.3. Puncture Test

According to the loadings of Fig. 1 and the test results, the puncture at operation circumstances can only happen in special cases; usually, the material is strong enough to support the railway superstructure and the static loads.

Table 3
Results of the puncture test

Puncture test											
1 day after hydration				7 days after hydration				28 days after hydration			
#	Stress [Mpa]	Average	Stand.dev.	#	Stress [Mpa]	Average	Stand.dev.	#	Stress [Mpa]	Average	Stand.dev.
1.	0.976	**0.927**	**0.043**	1.	1.388	**1.135**	**0.227**	1.	0.916	**1.170**	**0.230**
2.	0.904			2.	1.349			2.	1.392		
3.	0.896			3.	1.081			3.	1.547		
4.	0.886			4.	1.211			4.	1.043		
5.	0.986			5.	1.239			5.	1.116		
6.	0.916			6.	0.799			6.	1.212		
				7.	0.877			7.	0.965		
		Standard dev. [%]	**4.619**			Standard dev. [%]	**19.990**			Standard dev. [%]	**19.698**
Hardened: 79.23%				**Hardened: 97.01%**				**Hardened: 100%**			

In Table 3, the results are shown. The values marked in grey are the stresses at which the first crack occurred. The marked values typically happen at a deflection of 9-11 mm; at this point, the concrete layer breaks. Regardless of the hardening,

only the non-woven textile and the PVC layer holds the structure together, after the first crack. Up to an average value of 1.59 MPa, the PVC layer does not rupture, which typically means an elongation of 45-50 mm. Until this point, the CC layer is still watertight.
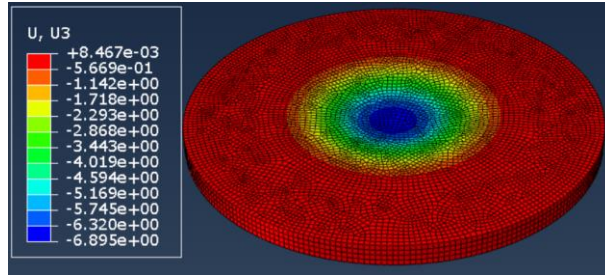

Figure 9
Modeling of the puncture test

The modeling showed a deflection of ~6.9 mm. At the measurement, the authors received the max. stress which eliminates the resistance of the concrete in the structure. This value is an appropriate average value because the mentioned 9-11 mm deflection does not mean the first break in the sample. It was mentioned at the compression test that more correct properties have to be determined. After that, the appropriateness of the just received value can be checked.

In the future (similar during dynamic and field tests, and FE modeling) the effect of sharp stones onto the CC material has to be considered and modeled.

Conclusions

The CC is easy to handle, conversly, water access, at the railways can cause problems. Therefore, the hydration of the material is very variable, which statement is determined by the standard deviation of the test results. According to the results, the 20% standard deviation is nearly normal for this type of material.

From the results and the hardening experiences mentioned in Chapter 2.2, it can be stated that after the application of CC and the spraying of water, the material has to be loaded to reach the best shape and push the material down to the supporting protection layer.

In the FE modeling, it could be seen that this type of material is a composite structure, so using only one material's physical properties is not enough. Therefore, for accurate and useful modeling, the structure materials have to be investigated separately.

According to the results of our examinations, the CC material is appropriate to give support during the static loads in railway infrastructure applications. Moreover, it means that the prepared dynamic examinations can be started.

References

[1]   M. Kurhan, D. Kurhan, R. Novik, S. Baydak, N. Hmelevska, Improvement of the railway track efficiency by minimizing the rail wear in curves. IOP Conference Series: Materials Science and Engineering, Vol. 985, No. 1, 2020, 012001

[2]   M. Sysyn, U. Gerber, O. Nabochenko, V. Kovalchuk, Common crossing fault prediction with track based inertial measurements: Statistical vs. Mechanical approach, Pollack Periodica, Vol. 14, No. 2, 2019, pp. 15-26

[3]   A. J. Tigh Kuchak, D. Marinkovic, M. Zehn,, Finite element model updating - Case study of a rail damper. Structural Engineering and Mechanics, Vol. 73, No. 1, 2020, pp. 27-35

[4]   U. Gerber, M. Sysyn, J. Zarour, O. Nabochenko, Stiffness and strength of structural layers from cohesionless material. Archives of Transport, Vol. 49, No. 1, 2019, pp. 59-68

[5]   A. Kampczyk, K. Dybeł, The fundamental approach of the digital twin application in railway turnouts with innovative monitoring of weather conditions. Sensors, Vol. 21, No. 17, 2021, 5757

[6]   A. Matejov, J. Šestáková, The Experiences with utilization of BIM in railway infrastructure in Slovak Republic and Czech Republic. Transportation Research Procedia, Vol. 55, 2021, pp. 1139-1146

[7]   A. Németh, S. Fischer, Investigation of glued insulated rail joints applied to CWR tracks. Facta Universitatis-Series Mechanical Engineering, 2021, 7642

[8]   S. Fischer, Investigation of effect of water content on railway granular supplementary layers. Naukovyi Visnyk Natsionalnoho Hirnychoho Universytetu, No. 3, 2021, pp. 64-68

[9]   B. Eller, S. Fischer, Review of the modern ballasted railway tracks' substructure and further investigations. Nauka ta Progres Transportu, Vol. 84, No. 6, 2019, pp.72-85

[10]   B. Eller, S. Fischer, Tutorial on the emergence of local substructure failures in the railway track structure and their renewal with existing and new methodologies. Acta Technica Jaurinensis, Vol. 14, No. 1, 2021, pp. 80-103

[11]   Concrete Canvas Ltd. https://www.concretecanvas.com [online, last visited on: 2021.10.15]

[12]   H. Li, H. Chen, X. Li, F. Zhang, Design and construction application of concrete canvas for slope protection. Powder Technology, Vol. 344, 2018, pp. 937-946

[13] T. Jirawattanasomkul, N. Kongwang, P. Jongvivatsakul, S. Likitlersuang, Finite element analysis of tensile and puncture behaviours of geosynthetic cementitious composite mat (GCCM) Composites Part B, Vol. 154, 2018, pp. 33-42

[14] P. Jongvivatsakul, T. Ramdit, P. T. Ngo, S. Likitlersuang, Experimental investigation on mechanical properties of geosynthetic cementitious composite mat (GCCM) Construction and Building Materials, Vol. 166, 2019, pp. 956-965

[15] F. Zhang, H. Chen, X. Li, H. Li, T. Lv, W. Zhang, Y. Yang, Experimental study of the mechanical behavior of FRP-reinforced concrete canvas panels. Composite Structures, Vol. 176, 2017, pp. 608-616

[16] F. Han, H. Chen, X. Li, B. Bao, T. Lv, W. Zhang, W. Hui Duan, Improvement of mechanical properties of concrete canvas by anhydrite-modified calcium sulfoaluminate cement. Journal of Composite Materials, Vol. 50, No. 14, 2015, pp. 1937-1950

[17] F. Han, H. Chen, W. Zhang, T. Lv, Y. Yang, Influence of 3D spacer fabric on drying shrinkage of concrete canvas. Journal of Industrial Textiles, Vol. 45, No. 6, 2016, pp. 1457-1476

[18] Han, F., Chen, H., Jiang, K., Zhang, W., Lv, T., & Yang, Y. (2014) Influences of geometric patterns of 3D spacer fabric on tensile behavior of concrete canvas. Construction and Building Materials, 65, 620-629

[19] H. Li, H. Chen, L. Liu, F. Zhang, F. Han, T. Lv, W., Zhang, Y. Yang, Application design of concrete canvas (CC) in soil reinforced structure. Geotextiles and Geomembranes, Vol. 44, No. 4, 2016, pp. 557-567

[20] H. Li, H. Chen, X. Li, F. Zhang, Design and construction application of concrete canvas for slope protection. Powder Technology, Vol. 344, 2019, pp. 937-946

[21] S. Fischer, B. Eller, Z. Kada, A. Németh, Railway Construction (lecture note). Széchenyi István University, Faculty of Architecture, Civil- and Transport Engineering, Department of Transport Infrastructure, 2015

[22] T. Jirawattanasomkul, N. Kongwang, P. Jongvivatsakul, S. Likitlersuang, Finite element analysis of tensile and puncture behaviours of geosynthetic cementitious composite mat (GCCM) Composites Part B: Engineering, Vol. 165, 2019, pp. 702-711

[23] F. Han, H. Chen, W. Zhang, T. Lv, Y. Yang, Influence of 3D spacer fabric on drying shrinkage of concrete canvas. Journal of Industrial Textiles, Vol. 45, No. 6, 2016, pp. 1457-1476

[24] ISO 12236:2006 Geosynthetics – Static puncture test (CBR test)

[25] European Technical Assessment (2019) ETA-19/0086 of 22/03/2019

Optimization of Lubricant Consumption in the Wheel/Rail Friction System

Vyacheslav T. Volov[1], Aleksey A. Bondarenko[1], Dmitriy V. Ovchinnikov[1], Vitaliy V. Atapin[1], Lei Kou[2]

[1]Samara State Transport University
First Bezimyannii per.18, 443066 Samara, Russia
volovvt@samgups.ru, bondarenko@infotrans-logistic.ru,
ovchinnikov@samgups.ru, atapin@infotrans-logistic.ru

[2]Institute of Railway Systems and Public Transport, TU-Dresden
Hettnerstr. 1, 01069 Dresden, Germany
lei.kou@tu-dresden.de

Abstract: The work examines the results of the study aimed at minimizing the consumption of lubricants in the wheel/rail interface. A numerical simulation of a circular slip path was carried out based on the theory of experiment planning. The simulation was performed depending on the wheel radius, the difference between the radii of the wheels contacting the flange and rim with the railhead, the taper angle of the flange and the angle of attack. According to Box-Wilkson steepest ascent method, geometrical parameters of the wheel/rail interface were obtained, making it possible to reduce the circular slip path by 30%. These results can significantly decrease the number of relevant field studies and lubricant consumption in the wheel-rail system. Mathematical modeling enabled the analysis of the stress-strain state of the "wheel-rail" system, at lateral contact, with the addition of friction forces to the contact zone. The simulation results show the importance of using rail lateral lubrication as one of the means to extend the service life of this expensive track structure, in small radius curves.

Keywords: slip path; angle of attack; flange angle; regression equation; Box-Wilkson method; track infrastructure; rail lubrication; stationary rail lubricators; mobile rail lubricators; stress calculation; lateral contact; moment of forces

1   Introduction

A rail lubrication is an important maintenance technique that decreases rail-wheel friction and therefore can cause the significant reduction of rail wear and rail contact (RCF) defects in railway curves. This results in extending the life cycle of rails, improvement the wheel-rail contact and decreasing the overall life cycle costs. The research of rail lubrication is presented by many studies of the last years. The experimental investigation [1] was carried out to study and compare the response to cyclic loading of the high-performance railway wheel steels ER8 EN13262. Rolling contact tests were performed with the same contact pressure, rolling speed and sliding ratio, varying the lubrication regime to simulate different climate. The distribution of crack length and depth at the end of the dry tests was analyzed to quantify the damage. A comprehensive review of recent research in wheel-rail contact tribology and lubrication is presented in [2]. An experimental investigation of the lubricant Optimization is presented in [3] using a test rig from a scaled wheel and a short section of rail, and a modern trackside lubricator set-up. The results showed that increasing pickup of grease can be expected when an additional component was fitted to a regular grease delivery unit on the rail. The effect of temperature on bulb size of grease was also investigated. The paper [4] provides a study of the effectiveness of the technology of lubrication of the rail roll surface in the curve by the locomotive in the train. The reduction of the lateral impact on the track by reducing the constant of friction on the roll surface of the internal rail and the side surface of the outer railhead is indicated. The research [5] presents designing of disc-on-disc wear testing instrument with wheel material and rail one specimen. Dry lubricant used was graphite bar polished onto wheel specimen surface. The result of research showed that graphite could adhere to wheel surface and penetrate into the cracks of contact between wheel and railway. In the study [6], the influence of three commercially applied railway greases on the wear and friction behavior, as well as, the load-carrying ability, were investigated. The test results explained that the rail curve greases are very soft in texture yet have the stable structure over a high-temperature range. The pin-on-disc test model system was used in [7] to simulate contact-wear between wheel flange and rail gauge corner in dry and lubricated tests. The results show that for the lubricated tests, mass loss was significantly lower and regardless of both, hardness ratio and normal load, than in the other tests. The study [8] evaluates the effect of roughness and temperature on the friction coefficient of wheel and rail materials by applying different amounts of railway lubricant grease using a pin-on-disc tribometer and simulating a wheel-flange and rail-gauge contact pressure. The results show that for a well-lubricated contact, the rougher surfaces yield a lower friction coefficient for the same contact pressure and sliding velocity.

The wheel-rail interaction is a key issue of railway vehicle dynamics that influence rail wear and RCF defects. Many scholars have done in-depth research on this issue [9-17]. Especially when the train passes through the high-speed

curve, the influence of the line change on the interaction on the wheel-rail is more severe, the impact force of the wheel-rail is greater, and the damage to the wheel-rail system structure will be further aggravated, which will affect the safety, stability and stability of the train operation. The modeling, analysis and evaluation methods of vehicle curve passing performance are the key points of wheel-rail relationship research [18-21]. Rapid wear and tear not only consumes a lot of maintenance labor force, but also requires frequent damage detection [22], which will make a lot of investment. There are some outstanding research results. Yang G. et al used the modified Elkins wear index method and the ANSYS and SIMPACK co-simulation method to study the influence of the wheel-rail contact geometric parameters under a high-speed train on wheel-rail wear [23]. The Lagrangian Euler finite element wheel-rail rolling contact model was established by Chang C. and Wang C. to study the various aspects of the wheel-rail contact system. It provides a stable and predictable rolling contact model for different materials and geometric configurations. At the same time, it analyzes the distribution of contact stress, contact mode and relative sliding velocity. The rotation and distribution of friction in the contact mode have a huge impact on the wheel-rail system in terms of vibration, adhesion and wear [24]. The paper [25] presents an innovative solution for monitoring the status of temperature and other atmospheric conditions. The solution is an effective support for the application of digital twins to railway turnouts and ongoing surveying and diagnostic work of other elements of rail transport infrastructure. N. Costa J. et al. proposed a new method was proposed to model the track so that it can be properly aligned with the body [26]. Milošević M et al use the finite element model to calculate the residual stress inside the track in the wheel-rail contact [27].

At present, there are few related results to study the curve passing performance through the establishment of dynamic models. Numerous studies have shown that the wheel-rail creep rate has an important impact on wheel-rail wear. The sharp change in stress state from tension to compression is the most unfavorable condition for wheel-rail operation and lubricants can improve this unfavorable condition. Taking into account the current share of railway curves in Russia, this paper uses experimental planning theory tools to numerically optimize the geometric parameters of the circular slip path. Using the Box-Wilkson steepest ascent method, the parameters of the wheel-rail geometric interface and the 3D finite element model are obtained. The use of lubricants is quantitatively evaluated. This verifies the possibility of track lateral lubrication as a means to extend the service life of this expensive track structure on a small radius curve.

2   The Wear of Rails and Wheelsets in Curves

Changes in the traffic mode, the state of the rolling stock and rail track have a significant impact on the nature of their interaction. They form one of the main factors that cause rail track irregularities in curves, wheelsets and rail wear. Over 80% of rail damage leading to their failure proved [28-30] to be on curves. This is primarily rail wear out caused by the impact of rolling stock wheels. New rolling stock wheels have the tread conicity of 1/20, which enables to pass curves with a radius of 1100 m and over, eliminating slip rolling. Such a slip is inevitable if the curve radius is less than 1100 m, wheels have other values of conicity, or design features of the wheelsets in a car bogie. There is a longitudinal slip of the inner wheels (blocking) or sliding of the outer wheels on the rails, thus resulting in intense wear of the rails. Large-scale inspection of wheelsets revealed only up to 10% have a conicity of 1/20, others have a higher conicity (or even have negative values). The share of track curves with an average radius of 350-1100 m on the network of the Russian Federation amounts to about 40%. For example, the length of such sections is about 56% at one of the enterprises of the track facilities of the Kuibyshev railway. (Fig. 1)
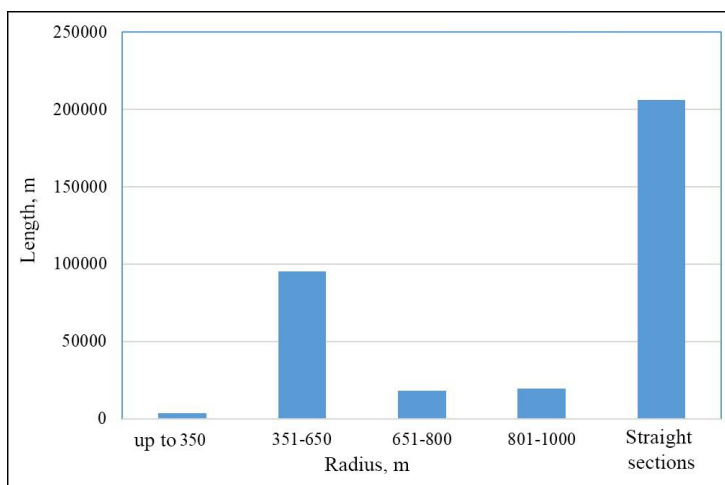

Figure 1
The share of curves at one of the enterprises of railway track facilities

The main measures to reduce the wear of rails and wheelsets in curves include the use of various lubricants, which are applied to the working surface of the railhead by different facilities and in different ways [31] [32]. In Russia at present, the number of modern rail lubricating cars is about 95 units. In addition, there are 89 mobile rail lubricators built based on reequipped locomotives.

The network operates 8.893 stationary rail lubricators (SRL), of which 8.514 (95.7%) are of modern type SRL. Stationary lubricators with one (SRL-02, Fig. 2) and two (SRL-02-04) nozzles and lubricators with feeder plates (SRL-02-06) are used. The lubricant is supplied with compressed nitrogen or air.

These modifications (with two nozzles) can be used both in curves exceeding 300 m in length and at turnouts. Single-nozzle modification is used on conventional turnouts, whereas double nozzle one is applied to symmetrical switches. Lubricators SRL02 and SRL-02-04 provide lubricant supply to the working surface of the rail through nozzles that are installed inside the track. They do not have direct contact with the rail and wheel.

Figure 2
Stationary rail lubricator (SRL-02)

In this regard, one of the major objectives in the wheel/rail interface operation is to conclude the optimal values of lubricant consumption parameters. These parameters ensure reduced dynamic forces impact, thus achieving a decrease in the wear of the rails and bogies of the railway vehicle. At the same time, the following problems are not fully solved: optimizing lubricant consumption and the effect of lubricant on the malfunctioning in the wheel/rail interface. It is especially important for ensuring safe movement of trains on sections of high-speed and heavy-weight traffic due to increased axial loads. The primary aim of this study is to determine the optimal values of lubricant consumption parameters.

3   Lubricant Consumption Parameters

According to the classical ideas of the modern theory of friction and wear, an equilibrium roughness of the contacting surfaces are formed in the process of wheel flanges slipping along the side of the railhead [33-35]. If there are not any micro irregularities, they are formed and gradually expand to the size of the equilibrium roughness. If there are initial micro-irregularities, they are smoothed by the micro-cutting of the metal (the tops of the protrusions) and it develops an equilibrium roughness.

The size of the micro-irregularities corresponding to the equilibrium roughness depends on many factors: specific pressure in the contact patch, metal hardness, lubrication, low temperature effect, slipping speed, etc. However, the most important of them is the slip. The studies [28-30] [33-35] showed that such types of slip as pseudo-slip, called "creep", slip caused by the common spinning of contacting surfaces, called "spin", and cross-slip have little impact on the lateral wear of rails and wheel flanges. This process is mainly caused by the inevitable circular slip of the pressed wheel flange along the side of the railhead during their two-point contacting, as well as the longitudinal slip of the wheel along the rail due to different lengths of the outer and inner rails in a curve and different lengths of wheel circles on these rails. Longitudinal slip along the outer rail occurs only in case of an excessive height of the outer rail.

This study proposes a solution to the problem of defining optimal values of the parameters of the wheel/rail interface corresponding to the minimum circular slip distance, which in turn leads to a lower consumption of expensive lubricants. The instruments of the experiment planning theory were used for determining the optimal geometric parameters of the wheel/rail interface [36].

Numerical optimization of the geometric parameters of the "wheel-rail" system according to the formula (1) using experiment planning and the Box-Wilkson gradient method allows to significantly narrow the search area for optimal geometric parameters in real conditions of a field experiment.

The final formula for determining the circular slip path along the length L, depending on the angle of attack α and the taper angle of flange φ for new rails, has the following form (the design scheme is shown in Figure 3):

$$\Delta l_{\rho} = \frac{L(r + \Delta r)\sqrt{1 + \dfrac{\tan^2 \phi \tan^2 \alpha}{1 - \tan^2 \phi \tan^2 \alpha}}}{r} - L \tag{1}$$

Where:

L -   The distance at which the wheel makes n revolutions

Δr -   The difference between the radii of the circles of contact with the flange
            and rim of the wheel with the rail head and the radius of the wheel in the
            section of the rolling circle

r -   Wheel radius

α -   Angle of attack
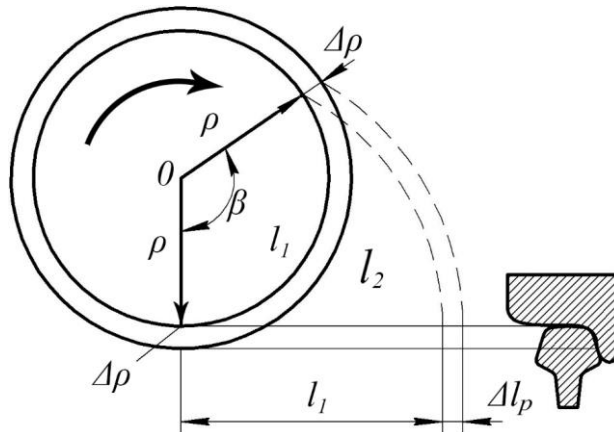
φ -   Taper angle of the flange

Figure 3
Diagram of the formation of a circular slip of the flange along the side of the railhead

The following factors were selected as the main ones: wheel radius (x_1), the
difference between the flange tangent radius and side of the rim with the top of the
railhead (x_2), flange angle (x_3), angle of attack (x_4). For the experiment, the
following levels of factors were chosen:

1) For factor (ρ): 0.9 m is the lower level; 0.95 m is the main level; 1.0 m is
   the top level of the factor

2) For factor ($\Delta \rho$): 0.01 m is the lower level; 0.015 m is the main level; 0.02
   m is the top level of the factor

3) For factor (φ): 60 deg is the lower level; 70 deg is the main level; 80 deg is
   the top level of the factor

4) For factor (α): 30 min is the lower leve; 40 min is the main level of the
   factor; 50 min is the top level of the factor

The encoding of the natural values of the factors will be performed according to
the following formula:

$$x_i = \frac{\tilde{x}_i - x_{i0}}{J_i} \tag{2}$$

where

x_i is the natural value of the factor,

$\widetilde{x}_{i0}$ is the main level of the factor,

J_i is the interval of variation of the factor.

As a result of coding, all the top levels of the selected factors will take the value +1, the lower levels -1, and the main level of the factors will be zero.

In the numerical experiment, a two-level orthogonal plan 2^4 was used, i.e., a full factorial experiment was conducted. The coefficients of the regression equation were determined from the range of application of the factors of the experiment [27]:

$$B = \left(A^T \cdot A\right)^{-1} A^T \cdot Y \tag{3}$$

A is shown in equation (5); B is shown in equation (6); Y is shown in equation (7).

Regression equation has the following form:

$$\begin{aligned}
Y = {}& b_0 + b_1 X_1 + b_2 X_2 + b_3 X_3 + b_5 X_1 X_2 + b_6 X_1 X_3 + b_7 X_1 X_4 + \\
& b_8 X_2 X_3 + b_9 X_2 X_4 + b_{10} X_3 X_4 + b_{11} X_1 X_2 X_3 + b_{12} X_1 X_2 X_4 + \\
& b_{13} X_1 X_3 X_4 + b_{14} X_2 X_3 X_4 + b_{15} X_1 X_2 X_3 X_4
\end{aligned} \tag{4}$$

In equation (4):
$$X_1^{max} = 1\,m;\ X_1^{min} = 0.9\,m;\ X_2^{max} = 0.025\,m;\ X_2^{min} = 0.015\,m;$$
$$X_3^{max} = 80\,\mathrm{deg};\ X_3^{min} = 70\,\mathrm{deg};\ X_4^{max} = \frac{5}{6}\,\mathrm{deg};\ X_4^{min} = \frac{1}{2}\,\mathrm{deg}$$

where the values of bi are determined by the vector column B of the equation (8). In the equation (9), Y is the function of the circular slip path $\Delta l\rho$.

The matrix of the numerical experiment was determined by encoding the main factors (2) and their interactions of the second, third, and fourth order (equation (4)) and has the following form:

$$
A = \begin{pmatrix}
1 & 1 & 1 & 1 & 1 & 1 & 1 & 1 & 1 & 1 & 1 & 1 & 1 & 1 & 1 & 1 \\
-1 & 1 & -1 & 1 & -1 & 1 & -1 & 1 & -1 & -1 & 1 & -1 & 1 & -1 & 1 & 1 \\
-1 & -1 & 1 & 1 & -1 & -1 & 1 & 1 & -1 & 1 & 1 & -1 & -1 & 1 & 1 & -1 \\
-1 & -1 & -1 & -1 & 1 & 1 & 1 & 1 & -1 & -1 & -1 & 1 & 1 & 1 & 1 & -1 \\
-1 & -1 & -1 & -1 & -1 & -1 & -1 & -1 & 1 & 1 & 1 & 1 & 1 & 1 & 1 & 1 \\
1 & -1 & -1 & 1 & 1 & -1 & -1 & 1 & 1 & -1 & 1 & 1 & -1 & -1 & 1 & -1 \\
1 & -1 & 1 & -1 & -1 & 1 & -1 & 1 & 1 & 1 & -1 & -1 & 1 & -1 & 1 & -1 \\
1 & -1 & 1 & -1 & 1 & -1 & 1 & -1 & -1 & -1 & 1 & -1 & 1 & -1 & 1 & 1 \\
1 & 1 & -1 & -1 & -1 & -1 & 1 & 1 & 1 & -1 & -1 & -1 & -1 & 1 & 1 & 1 \\
1 & 1 & -1 & -1 & 1 & 1 & -1 & -1 & -1 & 1 & 1 & -1 & -1 & 1 & 1 & -1 \\
1 & 1 & 1 & 1 & -1 & -1 & -1 & -1 & -1 & -1 & -1 & 1 & 1 & 1 & 1 & -1 \\
-1 & 1 & 1 & -1 & 1 & -1 & -1 & 1 & -1 & 1 & -1 & 1 & -1 & -1 & 1 & 1 \\
-1 & 1 & 1 & -1 & -1 & 1 & 1 & -1 & 1 & -1 & -1 & 1 & -1 & -1 & 1 & -1 \\
-1 & 1 & -1 & 1 & 1 & -1 & 1 & -1 & 1 & 1 & -1 & -1 & 1 & -1 & 1 & -1 \\
-1 & -1 & 1 & 1 & 1 & 1 & -1 & -1 & 1 & -1 & -1 & -1 & -1 & 1 & 1 & 1 \\
1 & -1 & -1 & 1 & -1 & 1 & 1 & -1 & -1 & 1 & -1 & 1 & -1 & -1 & 1 & 1
\end{pmatrix}
\tag{5}
$$

$$
B = \begin{pmatrix}
13.5 \\
-0.668 \\
3.171 \\
0.545 \\
0.414 \\
-0.167 \\
-5.77 \times 10^{-4} \\
-4.67 \times 10^{-4} \\
2.83 \times 10^{-3} \\
2.13 \times 10^{-3} \\
0.257 \\
-1.32 \times 10^{-4} \\
-1.29 \times 10^{-4} \\
-2.64 \times 10^{-4} \\
1.35 \times 10^{-3} \\
-5.39 \times 10^{-5}
\end{pmatrix}
\tag{6}
$$

$$
Y = \begin{pmatrix}
10.2 \\
9.18 \\
16.8 \\
15.2 \\
10.7 \\
9.75 \\
17.4 \\
15.8 \\
10.5 \\
17.2 \\
15.5 \\
12.1 \\
11.1 \\
18.8 \\
17.1 \\
9.49
\end{pmatrix}
\tag{7}
$$

And searching for the minimum slip path, the Box-Wilson method or the steep ascent method was applied. Moving along the gradient from the center of the experiment, the minimum value of the slip path was obtained, equal to $\Delta l\rho$, = 6.07 m, which is 30% less than the previously obtained values when moving from other centers of the numerical experiment. This determines the completion of the numerical optimization of the circular slip path.

Numerical optimization of the geometrical parameters of the circular slip path (1) when using the tools of the theory of experiment planning is a preliminary stage, which makes it possible to reduce the subsequent costly field experiment significantly. The choice of the theory of experiment planning as an optimization tool [36] is explained by the fact that it is widely used by scientists and production workers in the study of various processes and devices. The change in the optimization tools in the numerical simulation and the subsequent field experiment is, in the authors' opinion, inexpedient. The resulting reduction in the circular slip path by optimizing the geometric parameters of the wheel/rail interface leads to lower consumption of lubricants.

4   Finite Element Models

The use of lubrication in curves also affects the stress-strain state of the "wheel-rail" system. Friction forces in the lateral contact zone of the wheel flange and the railhead change the configuration of interaction, adding significant longitudinal forces to the contact zone, the maximum value of which is limited by the friction force in the contact zone until the moment of slipping. A quantitative assessment of the above phenomenon was carried out in the environment of finite element modeling - a modern method that is widely used to solve a wide range of problems, including problems of mechanics of deformable solids and others [37, 38]. For this, three-dimensional model of the interaction of a new wheel and a new rail with full geometric similarity to full-scale structures has been developed - GOST 10791-2011 and GOST R 51685-2013.
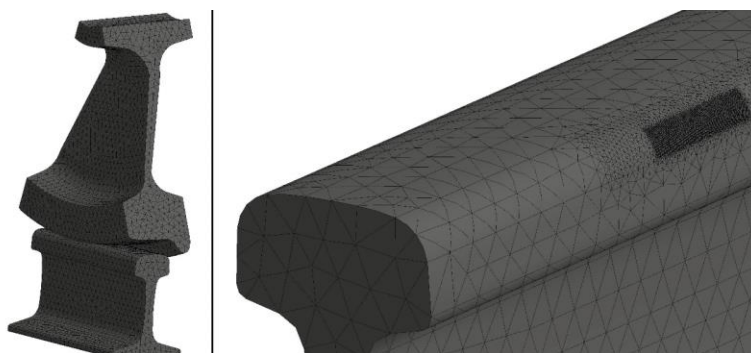

Figure 4
Finite element model of the "wheel-rail" system

The capacity of finite element models is about 850 thousand knots. In the contact area, the element size is significantly reduced (0.3-0.4 mm) for the most accurate display of the calculation results.

The wheel acts on the rail with a lateral force of 10 tons - these are the values of lateral forces that have been experimentally recorded in small-radius curves and are confirmed by the results of modeling the dynamics of the interaction between the track and rolling stock. Thus, the maximum torque before the start of the slip process will be:

$$M_{max} = F_{fr} \cdot l \tag{8}$$

where l – the shoulder of the moment of forces and the distance from the axis of rotation of the wheel to the point of the flange contact.

The maximum value of the frictional forces depends on the side load and the coefficient of friction (adhesion) μ:

$$F_{fr} = F_{ax} \cdot \mu \quad F_{fr} = F_{ax} \cdot \mu \tag{9}$$

When assessing the stress-strain state of the lateral contact, the value of l is determined as the distance from the axis of rotation of the wheel to the point of the flange contact.

When solving, the following boundary conditions and loads were used:

- Anchoring is modeled along the rail foot area,

- The contact surface of the wheel and axle moves with two-point contact in the vertical and horizontal direction,

- Other elements are not fixed,

- The force is applied using a "distance point", which makes it possible to simulate the effect of axial load as close as possible to the real physical process that occurs during contact.

Initial data parameters:

- Wagon wheel with a diameter of 950 mm,

- Lateral force 10 tons,

- Values of torques (justify where and under what conditions slip lengths):

  2.91 kN m   5.82 kN m   8.73 kN m   11.64 kNm,

- The axle of the wheel is in a vertical position,

- Rail axis with an inclination of 1/20,

- Contact surfaces in accordance with the specified profile.

The contours of equivalent stresses, as well as normal stresses on the side surface of the rail, including when adding torque, are shown in Figures 5 and 6.
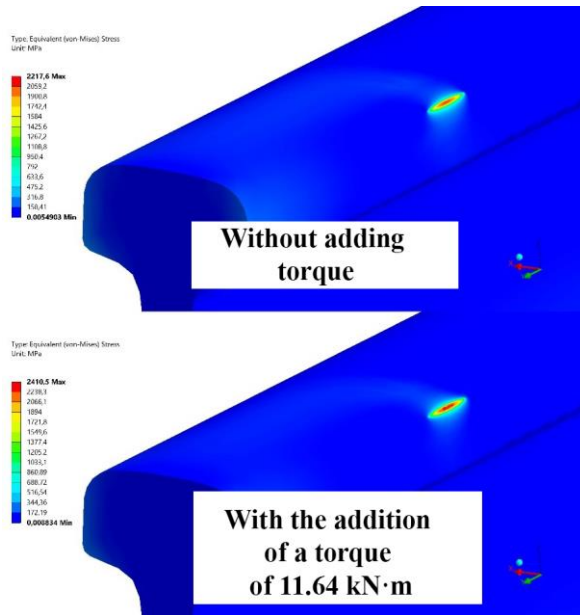
Figure 5
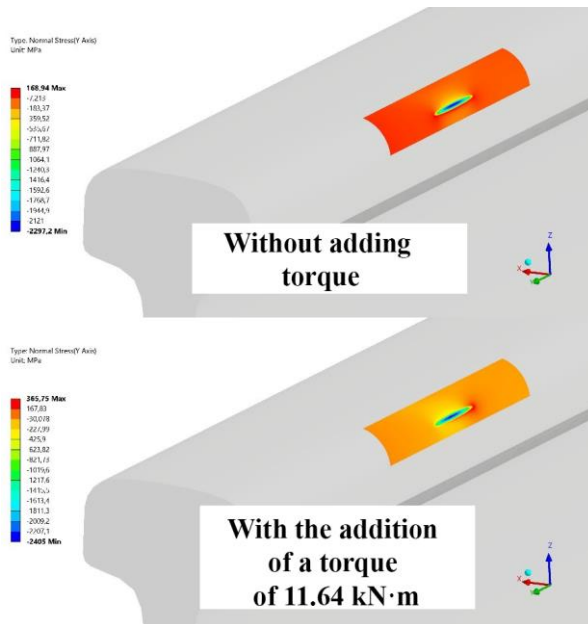Equivalent stresses on the rail surface

Figure 6
Normal stresses on the rail surface

The results are summarized in Table 1.

Table 1

Stress-strain state of the "wheel-rail" system in the study of the influence of the friction force in the contact zone

Torque value, Nm	Equivalent stresses, MPa	Normal stresses, MPa	
		Minimum value	Maximum value
0	2217.6	-2297.2	168.94
2910	2225.7	-2307	187.3
5820	2247.1	-2328.7	253.79
8730	2311.1	-2339.5	312.18
11640	2410.5	-2405	365.75

The increase in the equivalent stresses is about 9%, while the increase in the maximum normal stresses on the surface is more than 116%, i.e., more than 2 times. From the point of view of the durability of rail steel, the most unfavorable operating conditions are sharp changes in the stress state from tension to compression and vice versa. When the torque is added, which can be characterized as the addition of the friction coefficient to the contact zone, a sharp increase in compressive stresses on the side surface of the rail is observed together with the same lateral force. Thus, the reduction of the friction coefficient with the help of lubrication is currently an urgent task from the standpoint of increasing the durability of rail steel in small-radius curves.

Conclusions

As a result of the analysis and planning of the numerical experiment, the optimal geometric parameters of the wheel/rail interface were found, allowing to reduce the circular slip path by 30%. However, the obtained theoretical result can only be the basis for real field planning of an experiment, which makes it possible to significantly narrow the area of the most important geometric parameters for optimizing the wheel/rail interface. Reducing the circular slip path will lower the consumption of expensive lubricants.

Mathematical modeling confirmed the relevance and importance of the use of lubricants, in the lateral contact zone of the "wheel-rail" system, as one of the means of extending the rail service life, in small radius curves.

References

[1]   Faccoli, M., Petrogalli, C., Lancini, M., Ghidini, A., Mazzù, A. Rolling. Contact Fatigue and Wear Behavior of High-Performance Railway Wheel Steels Under Various Rolling-Sliding Contact Conditions. Journal of Materials Engineering and Performance. 2017, 26(7), pp. 3271-3284

[2]   Olofsson, U., Lyu, Y. Open System Tribology in the Wheel-Rail Contact-A Literature Review. Applied Mechanics Reviews. 2017, 69(6), p. 060802

[3] Temple, P. D., Harmon, M., Lewis, R., Temple, B., Jones, D. Optimisation of grease application to railway tracks. Proceedings of the Institution of Mechanical Engineers, Part F: Journal of Rail and Rapid Transit. 2018, 232(5), pp. 1514-1527

[4] Kossov, V., Lunin, A., Spirov, A., Ivaškovska, N., Nikolajevs, A. The technology of rail lubrication by the hauling locomotive in train formation. Procedia Computer Science. 2019, 149, pp. 331-335

[5] Suparno, J., Halim, D. A., Junaidi, Effendy, M., Jamari, J. Materials Science. 2019, 961, pp. 126-133

[6] Razak, I. H. A., Ahmad, M. A., Puasa, S. W. Tribological and physiochemical properties of greases for rail lubrication. Tribology Online. 2019, 14(5), pp. 293-300

[7] Viana, T. G., Tressia, G., Sinatora, A. Sliding wear of rail and wheel steels: Effect of hardness ratio, normal load and lubrication. Tribology in Industry 2020, 42(3), pp. 428-442

[8] Vásquez-Chacón, I. A., Gallardo-Hernández, E. A., Moreno-Ríos, M., Vite-Torres, M. Influence of surface roughness and contact temperature on the performance of a railway lubricant grease. Materials Letters. 2020, 285, p. 129040

[9] Jover, V., Gaspar, L., Fischer, S. Investigation Of Geometrical Deterioration of Tramway Tracks. Science and Transport Progress. Bulletin of Dnipropetrovsk National University of Railway Transport: 2020, 2(86), pp. 46-59

[10] A. Nemeth, S. Fischer, Investigation of glued insulated rail joints with special fiber-glass reinforced synthetic fishplates using in continuously welded tracks. Pollack Periodica. 2018, 13(2), pp. 77-86

[11] Shvets, A. O. Dynamic interaction of a freight car body and a three-piece bogie during axle load increase. Vehicle System Dynamics, AHEAD-OF-PRINT, 2021, pp. 1-23

[12] He, C., Zhou, S., Di, H., Zhang, X. Effect of longitudinal joint on train-induced vibrations from subway shield-driven tunnels in a homogeneous half-space, International Journal of Transportation Science and Technology, 2021

[13] Shvets, A. O. Analysis of the dynamics of freight cars with lateral displacement of the front bogie. Advanced Mathematical Models and Applications, 2021, 6(1), pp. 45-58

[14] Xu, J., Ma, Q., Wang, X., Wang, P., Wei, X., M. Ahmadian. Investigation on the motion conditions and dynamic interaction of vehicle and turnout due to differential wheelset misalignment, Vehicle System Dynamics, 2021, pp. 1-21

[15]   Dmitry Ovchinnikov, Alexey Bondarenko, Lei Kou, Mykola Sysyn. Extending service life of rails in the case of a rail head defect. Građevinar. 2021, pp. 177-183

[16]   Mykola Sysyn, Ulf Gerber, Franziska Kluge, Olga Nabochenko, Vitalii Kovalchuk. Turnout remaining useful life prognosis by meansof on-board inertial measurements on operationaltrains. International Journal of Rail Transportation. 2019, 8(1), pp. 1-23, DOI: 10.1080/23248378.2019.1685918

[17]   Dmytro Kurhan. Determination of Dynamic Loads From the Wheel on the Rail For High-Speed Trains. Science and Transport Progress Bulletin of Dnipropetrovsk National University of Railway Transport. 2015, 3(57)

[18]   Kurhan, D., Kurhan, M., Husak, M. Impact of the variable stiffness section on the conditions of track and rolling stock interaction IOP Conference Series: Materials Science and Engineering. 2014, 985(1), p. 012005

[19]   Yuan Gao , Jingmang Xu , Yibin Liu , Zhiguo Dong , Ping Wang, Ziqing Jiang. An investigation into transient frictional rolling contact behaviour in a switch panel: validation and numerical simulation. Vehicle System Dynamics, 2014, DOI: 10.1080/00423114.2020.1802492

[20]   Mykola Sysyn, Franziska Kluge, Dmitri Gruen, Vitalii Kovalchuk, Olga Nabochenko. Experimental Analysis of Rail Contact Fatigue Damage on FrogRail of Fixed Common Crossing 1:12. Journal of Failure Analysis and Prevention. 2019, 19(21)

[21]   Vitalii Kovalchuk, Mykola Sysyn, Ulf Gerber, Olga Nabochenko, Jandab Zarour, Dehne Stefan. Experimental investigation of the influence of train velocity and travel direction on the dynamic behavior of stiff common crossings. Facta University, Series: Mechanical Engineering. 2019, 17(3), pp. 345-356

[22]   Banić M., Miltenović A., Pavlović M., Ćirić I. Intelligent machine vision based railway infrastructure inspection and monitoring using UAV. Facta University, Series: Mechanical Engineering. 2019, 17(3), pp. 357-364

[23]   Yang G., Zhao F., Li Q., Liang Y., Lin G. Study of Influences of High-speed Train Wheel-rail Contact Geometric Parameters on Wheel-rail Wear. Journal of the China Railway Society, 2019, 41(2), pp. 50-56

[24]   Chang C., Wang C. Wheel-rail steady state rolling contact analysis based on ale finite element method. China Railway Science. 2009, 30(2), pp. 87-93

[25]   Kampczyk, A., Dybeł, K. The fundamental approach of the digital twin application in railway turnouts with innovative monitoring of weather conditions. Sensors. 2021, 21(17), p. 5757

[26]   J. N. Costa, P. Antunes, H. Magalhães, J. Pombo, J. Ambrósio. A finite element methodology to model flexible tracks with arbitrary geometry for railway dynamics applications. Computers and Structures. 2021, 254(1)

[27]   Milošević M., Miltenović A., Banić M., Tomić M. Determination of residual stress in the rail wheel during quenching process by FEM simulation. Facta University, Series: Mechanical Engineering. 2017, 15(3), pp. 413-425

[28]   Verigo M. F. Vzaimodeystvie puti i podvizhnogo sostava v krivykh malogo radiusa i borba s bokovym iznosom relsov i grebney koles [Interaction of the track and rolling stock on the curves of small radius and the fight against lateral wear of rails and wheel flanges] Moscow, PTKB TSP MPS, 1997

[29]   Lysiuk V. S., Bugaenko V. M. Povrezhdeniya relsov i ikh diagnostika [Rail damage and diagnostics] Moscow, IKTS Akademkniga, 2006, p. 638

[30]   Lysiuk V. S. Prichiny i mekhanizm bokovogo iznosa relsov i grebny koles [Causes and mechanism of lateral wear of rails and wheel flanges] Put i putevoe khozyaystvo, 1997, pp. 13-19

[31]   The concept of development of the technology of lubrication of the contact zone "wheel-rail" in JSC "Russian Railways": approved by order of JSC RZD dated January 16, 2015, 60(5)

[32]   E. V. Eliseev, O. A. Pashenceva, A. I. Gosman, D. B. Konovalov. Sistemy smazki: effektivnoe umen'shenie iznosa [Lubrication systems: effective reduction of wear] Put' i putevoe hozyajstvo, 2012, 1, pp. 5-9

[33]   Harris U. J., Zakharov S. M., Landgren J., Turne Kh., Eberson V. Obobshchenie peredovogo opyta tyazhelovesnogo dvizheniya: voprosy vzaimodeystviya kolesa i rel'sa [Generalization of advanced experience on heavy-weight movement: issues of wheel and rail interaction, English-Russian translation] Moscow, Intext, 2002, p. 408

[34]   Broek D. M. Osnovy mekhaniki razrusheniya [Elementary engineering fracture mechanics, English-Russian translation] Moscow, Vysshaya shkola, 1980, p. 368

[35]   Krachsavskiy I. B., Dobychin N. M., Kombalov V. S. Osnovy raschetov na trenie i iznos [Basics of calculations for friction and wear] Moscow, Mashinostroenie, 1997, p. 526

[36]   Adler A. S., Markova R. N., Granovskiy V. N. Planirovanie optimalnogo eksperimenta [Planning an optimal experiment] Moscow, Nauka, 1976

[37]   D. V. Ovchinnikov, V. A. Pokatskiy. Assessment of the stability of a continuous welded track using the finite element method. Modern issues in railway track design, construction and operation, 2012, pp. 206-210

[38]   Dmitry Ovchinnikov, Vladimir Pokatsky, Damir Gallyamov. Factors Affecting the Dynamic Rail Canting of the Railway Track Transportation Research Procedia, 2021, 54, pp. 544-551

Investigation of the Effects of Thermit Welding on the Mechanical Properties of the Rails

Vivien Barna[1], András Brautigam[1], Bence Kocsis[2], Dóra Harangozó[2], Szabolcs Fischer[2]

[1]Budapest Transport Privately Held Corporation (BKV)
Akácfa u. 15, H-1072 Budapest, Hungary
{barnav,brautigama}@bkv.hu

[2]Széchenyi István University
Egyetem tér 1, H-9026 Győr, Hungary
{kocsis.bence,harangozo.dora,fischersz}@sze.hu

Abstract: This current paper deals with the investigation of the variation of the hardness of the rail steel material in the heat-affected zone (HAZ) of a rail joint made by thermit welding (TW). The tested rail is a normal R260 type rail steel category; its production date is 1977, the rolling mill was Diosgyor (Hungary), rail profile is MÁV 48.5. This rail has not been in railway track before the test. The authors performed hardness tests on the rail head's surface even after the rail welding, as well. After the welding and hardness tests, the rail joint was cut with +/–200 mm by a rail cutter and transported to the laboratory. Water jet cutting was applied to shape six longitudinal direction slices with five vertical cutting lines from the rail piece's head. The slices' length was 400 mm, the width of these slices was approx. 10 mm; the TW rail joint was in the mid-point of the slices. Micro-Vickers (HV10) hardness tests were executed on these slices, in the –150...+150 mm interval lengthwise and in the 3, 6, and 10 mm depth points below the rail head's top surface. As a result, the authors received a very detailed hardness functions of the HAZ of rail joint made by TW. These variation functions were compared to the official Elektrothermit's SoW-5 hardness tests' results. It can be concluded that the variation of the hardness of rail steel in the area of the HAZ correlated with the Elektrothermit's results; however, there were some critical points where significant differences were able to be found. The highest deviation was concluded in 50 mm distance measured from the axis of welded rail joint. The authors gave possible valuable explanations for these phenomena.

Keywords: thermit rail welding; HAZ; heat-affected zone; welded rail joint; Brinell Hardness

1   Introduction

Transportation via railway is an especially highlighted logistical process that highly affects the railway rail itself (in the following, the authors use the single word: rail, instead of railway rail). Many researchers dealt with the rail itself in their research [1-4]. It is worth mentioning the rail wear process and its minimizing in curves [1]; the rail's and wheel's corrugations, and the related modified bearing capacity [2]; hence Kuchak et al. [3] published the finite element modeling of rail dampers that is important regarding the environmental aspects. Kazemian et al. [4] dealt with the condition monitoring of vibration of ballasted tracks in Iran where rail problems were detected. The ballast breakage effect is also an essential phenomenon connecting the environment protection due to the increased demand for ballast screening and dust pollution. Benmebarek and Movahedi [5] investigated the DEM modeling of crushable granular materials, while Sysyn et al. [6] executed laboratory tests with the ballast interlocking. Ballast interlocking is a significant area that is related to the geometrical deterioration of the railway tracks, which can be increased by geosynthetic inclusions.

In the case, precise geodetical measurements and complex integrated infrastructural are discussed regarding railways, the publications of Kampczyk and Dybel [7], as well as Matejov and Sestakova [8] can be instanced. The BIM in railway [8] became an up-to-date solution for design, planning, and of course, construction, maintenance, and diagnostics. The laser scanner technology [7] is adequate for receiving huge and helpful 3D point cloud and surfaces in them planning procedure is able to be eased.

This current paper aims to investigate the welded rail joints from the aspect of the hardness variation, mainly in the heat-affected zone (HAZ). For the understanding of rail joints and welding, the authors introduce the relevant knowledge, bases related to them.

The particular cross-section of the rail is manufactured by rolling, which borders the length of the rods/blocks. It stimulated the development of different rail connection technologies. Permanent and non-permanent rail joints also exist which have to meet the following requirements [9]:

- be able to bear with dynamic vertical and lateral loads in the absence of continuity;
- the formation or limit the size of altitude and horizontal steps between the rail ends;
- secure the movements of the rail ends caused by longitudinal loads (dilatation) without damaging the structure beside appropriate fishplate resistance;
- contain as few parts as possible;

- be easy and fast to construct and to change parts;

- meet the requirements of the interlocking and signaling system and general railway safety.

Rail joints can be permanent and non-permanent types [10]. The most common permanent type rail joint is the rail welding. The authors only deal with the welded rail joints in this article.
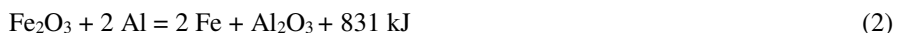
Welding technologies provide a possibility for permanent rail joints. These can be divided into two groups: fusion and pressure welding techniques (however, some railway companies apply arc welding). The most commonly used pressure technology is the flash-butt welding. In contrast, arc and thermite welding (Fig. 1) are the most frequent fusion techniques (identifications detailed in MSZ EN ISO 4063:2016 [11]).

Figure 1
Thermite welding (own made photo of S. Fischer)

Thermite welding was patented in 1895 in the German Empire and is still considered significant in the present. Although however, in constructing new rails, flash-butt welding took the lead, respecting the quantity. Still, in the case of maintenance and closing welds of standard gauge railways and subways, thermite welding became the most widespread technology. A chemical reaction takes place during the process; iron-oxide is reduced to pure iron by aluminum accompanied by heat generation while aluminum-oxide forms (Eqs. 1-3).

$$3\ FeO + 2\ Al = 3\ Fe + Al_2O_3 + 679\ kJ \tag{1}$$

$$Fe_2O_3 + 2\ Al = 2\ Fe + Al_2O_3 + 831\ kJ \tag{2}$$

$$3\ Fe_3O_4 + 2\ Al = 9\ Fe + 4\ Al_2O_3 + 782\ kJ \tag{3}$$

The welding process consists of the following steps:

- a fireproof mold is applied to the rail, fixed by a clamping device to the rail ends;

- the material of the rail is medium or high carbon steel (0.38…1.07%) [12], which needs proper preparation before welding. The large cross-section also requires a preheating;

- the mixture of aluminum powder and iron oxide is poured into an adequate crucible and ignited with the help of barium peroxide (1300 °C), then loaded into the prepared mold. Nowadays, durable molds are replaced by prepared disposable crucibles; the loading into the mold is an automatic process through a tap at the bottom of the crucible. The thermite steel is followed by the slag to the mold and also to the slag bowls outside the mold. The overheated thermite steel (might be 2400 °C hot) melts the rail ends, forming a continuous joint.

The high temperature of the welding process changes the pearlitic microstructure and the mechanical properties of the rail steels inevitably [13-15]. An especially hard cross-section can be found in the heat-affected zone (HAZ), leading to fatigue fracture. A softer 'zone' created by partial cementite 'spheroidization' with reduced hardness and strength can be the spot of plastic deformation, which is a significant problem for maintenance. Most of the literature only deals with one or the other phenomena, but they should be handled together. The division of the heat-affected zone into three parts is presented in Fig. 2.
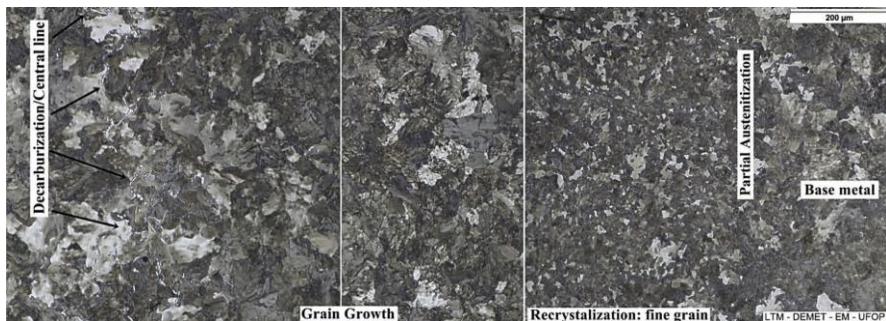

Figure 2
Changes of microstructure in the cross-section of the rail head, near the welded joint [13]

However, another study [16] confutes the significant effect of the retardation of cooling, except to reduce the maximum hardness in the HAZs of alloy rails by about 1-3 HRC.

Figure 3 presents a detailed hardness test. The centerline of the weld under the contacting surface shows a hardness of approximately 300 HV. This value is reduced by 50 HV at a distance of 20 mm from the centerline [14]. Thus, the hardness of the web of the rail is higher than in the case of rail head and foot.

In the case of aluminothermic weldings, the lower hardness of the weld can be caused by the changed chemical composition according to the applied welding material. Still, the hardness of the weld connot be less than the hardness of the base steel, which can be eliminated by proper material choice [17]. More studies demonstrate the applicability of the higher hardness limit of 350 HV [18-19].
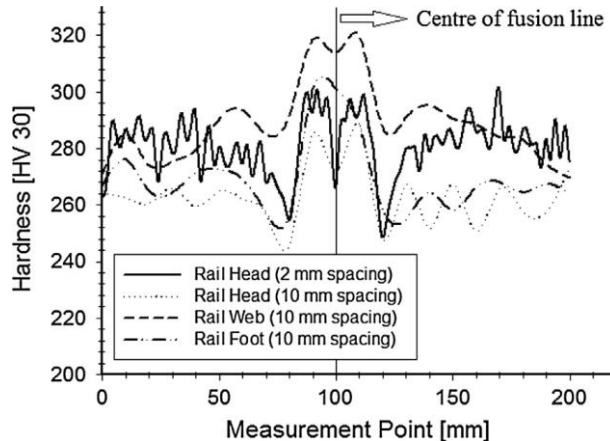

Figure 3

Hardness values in different cross-sections across the weld collar [14]

2   Methods and Applied Materials

In this paper the authors examined a TW rail joint based on the variation of hardness of the rail head in the HAZ. The current rail has not been built into the track, it has not been 'suffered' from traffic load anytime. The rail profile was MÁV 48.5 (see Fig. 4), the rail steel category was R260 according to the EN 13674-1 standard, the production year was 1977. The applied TW technology was SoW-5. The welding was made by the Budapest Transport Privately Held Corporation (BKV).

After the welding process, the rail piece was cut to 60 centimeters length from the rail, using a 'quick disc cutter' (i.e. rail cutter). The TW rail joint was in the middle of this rail lengthwise. In this manner, the measured hardness values of the rail joint and the HAZ were not affected by the heat input during cutting. In the laboratory the +/–150 mm long section was considered. Hardness tests were executed on the rail head's surface using a a Sauter HMO-3 type instrument, which measures in Leeb scale that is transformed into HB unit.

This above-mentioned TW rail joint was then examined in the laboratory of Audi Hungaria Faculty of Automotive Engineering at Széchenyi István University,

whose rail head was cut into six slices with a high-pressure water jet cutter (see Fig. 4). The slices had equal width; the cutting planes were vertical and parallel to the longitudinal axis. The advantage of this cutting technology is that the material to be tested is not exposed to heat. Furthermore, the separation is done mechanically, so the cut surface is smooth, free of burrs, and no hardening occurs, so the hardness values of the welding environment are not affected by the cut. Only one side of the cut rail slices was ground flat (i.e., only one side of the originally connecting surfaces was tested), then hardness tests were executed in the 3, 6, and 10 mm depth measured from the rail's top surface. The measurements were performed at every 5 millimeters in the whole +/–150 mm length.
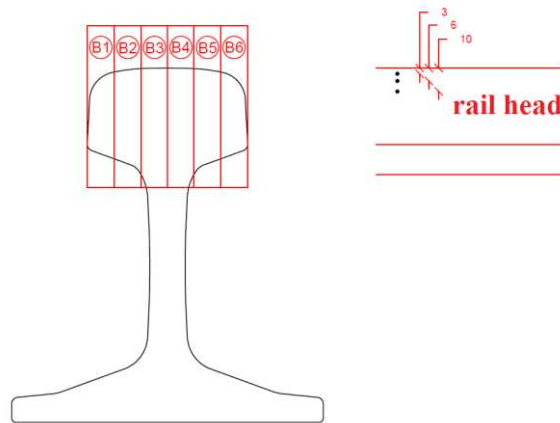

Figure 4

Scheme of the cutting of the rail head for further hardness test (slice 'B6' is at the inner gauge corner)

In the laboratory, the measured hardness values were reported in Vickers hardness (HV10), so for the sake of clarity, the authors converted the results to Brinell Hardness (HB) and displayed them in the tables. The instrument was a KB 30/KB Prüftechnik automatic micro-hardness tester machine. The measured values can be assumed as symmetric schemes related to the welded rail joint mid-axis. Due to the supposed same properties of the welded rail and the TW rail joint in both directions, the water jet cutting was performed only on the rail piece to the right of the TW rail joint's center (i.e., the right-hand side is seen from the track axis).

As a result, the authors prepared a very detailed hardness 'map' of the hardness variation of HAZ of TW rail joint. Furthermore, these variation functions were compared to the official SoW-5 functions, and the own measurements on the rail head's surface. The connecting results are detailed in Chapter 3.

3   Results and Discussion

The measured Brinell Hardness values of the tested TW rail joint are published in Figs. 5-7. The values (series B1…B6) are related to 3, 6, and 10 mm below the surface. These figures also contain the results of the own hardness tests related to the rail head's surface (i.e., these values are average values considering more measurements at these lines). In Figs. 5-7 there is an additional line: it is the official SoW-5 hardness series [20] measured by Elektro-Thermit.

It can be concluded that the approximate shape of the functions are quite similar, and they have steps/jumps in the 40…50 mm interval from the TW rail joint's axis, which is the outer borderline of the HAZ.
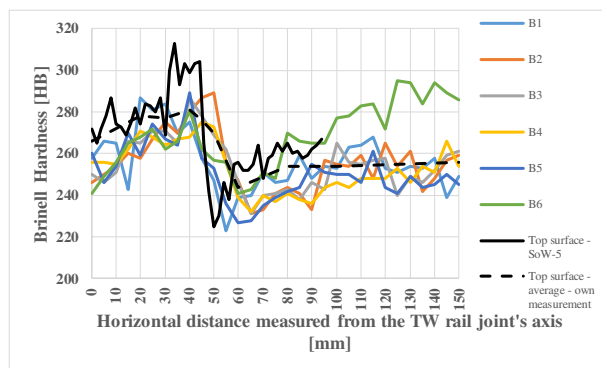

Figure 5

Results of hardness test in the 3 mm depth measured from the rail head's top surface
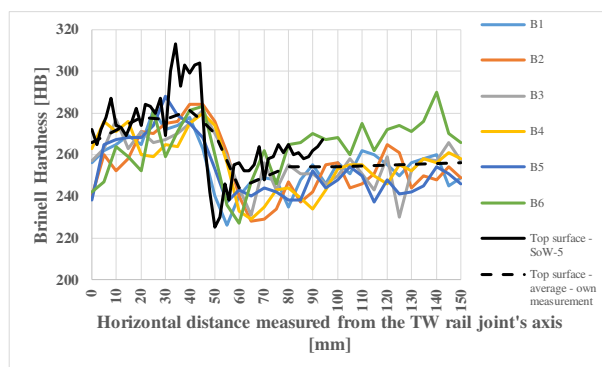

Figure 6

Results of hardness test in the 6 mm depth measured from the rail head's top surface
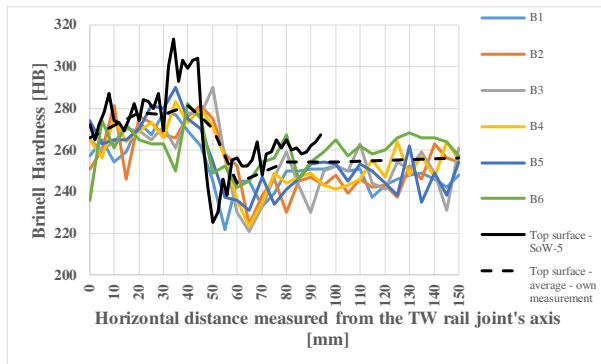
Figure 7

Results of hardness test in the 10 mm depth measured from the rail head's top surface

The ratios (rates) are given in Figs. 8-10, considering and comparing with SoW-5 technology's official hardness diagram's values [20], they are calculated in percentages. If the received rate (percentage) is higher than 100%, the authors' measured results are higher than the official values from the SoW-5 diagram. In the SoW-5 diagram the values are presented in each 2 mm values lengthwise; the authors' measurements were executed in every 5 mm point. It is resulted that the rates are calculated only in every 10 mm point because the authors didn't want to interpolate the hardness values that can cause inadequate approximation.
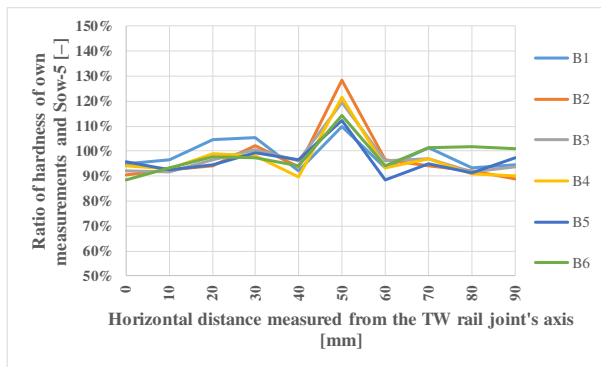

Figure 8

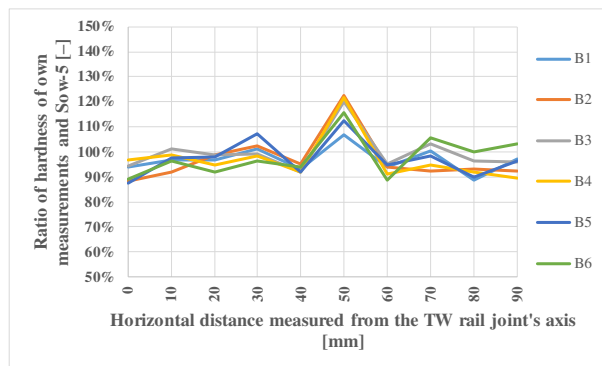Hardness ratio in the 3 mm depth measured from the rail head's top surface

Figure 9

Hardness ratio in the 6 mm depth measured from the rail head's top surface
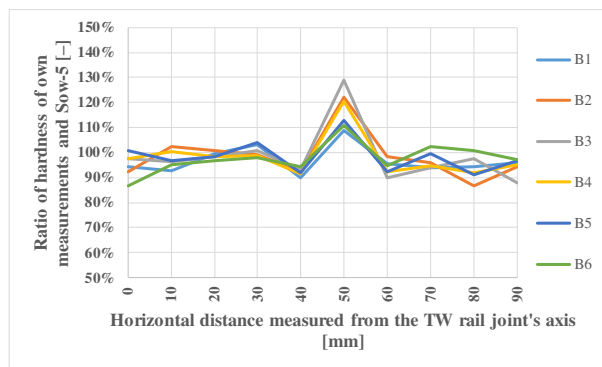
Figure 10

Hardness ratio in the 10 mm depth measured from the rail head's top surface

There are significant peak values (approx. 110-130%) in the 50 mm zone from the axis of the welded rail joint in every depth value (i.e., 3, 6, and 10 mm, respectively). Next to them, the average values seem to be in the 90-100% range.

Additionally, the authors introduce a figure about the surface measurements in Fig. 11. The base calculation procedure is the same as in Figs. 8-10, but it has to be mentioned that own made hardness measurements on rail's surface were performed at the field, even after the rail welding. It means that the signed distances are not as accurate as in the laboratory. The field hardness tests were executed by a Sauter HMO-3 type instrument.

Figure 11
Hardness ratio on the rail head's top surface

The differences can be explained with the following statements:

- the rail and air temperature values might not have been the same in the two compared procedures, i.e., during the thermit welding.
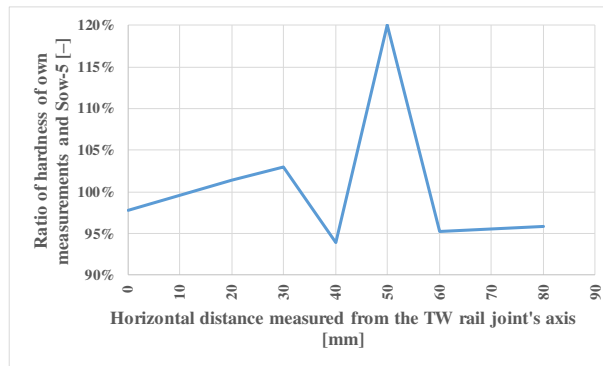
- The different cooling speed values of the welded joints and the connecting rails can cause significant differences also in hardness values.

- Considering the B1 and B6 slices (due to symmetry), mainly in the +70…+150 mm zone, the differences in the measured hardness values can be explained by the base material's not exact purity and homogenity. This variation cannot be found neither in the pairs B2-B5, nor B3-B4.

- Unfortunately, it is not evident and precisely known whether which rail rolling mill produced the rail sample that the Elektro-Thermit considered. The quality of the rail steel material exceptionally influences the hardness values of the rail, mainly the hardness of the material far from the surface. The quality of the rails, which were rolled in Diósgyőr in the past, is not sufficient. The measurable hardness values of this kind of rail sometimes cannot reach the qualification Brinell Hardness values, not only on the rail head's surface even in higher depths; it is a property of this rail steel materials).

- Differences in welding practice and technology: width of the set welding gap, thickness of the sealing, width of the casting moulds, effect of the surface quality during hardness test, fineness of the grinding after welding. The time difference in pre-heating, application of crucible and ignition, time parameters in technology, and their increasing in given cases are factors in which you shouldconsider the welding practice (human factor).

The relatively high values (110-120%) in Figs. 8-11 can be resulted by the significantly quick cooling procedure at the borders of the ceramic casting moulds (see Figs. 2 and 3). Below the casting moulds, the steel temperature can remain 700-750 °C, or higher. It causes that the rail steel can be quenched. The rail parts/sections where there is no covering by casting moulds, the rail temperature remains below 650 °C. In these zones, the steel can't be quenched, and they are the so-called softening zones. However, in the zones where the rail temperature is below 650 °C, the softening effect can't be seen.

Conclusions

The authors presented the results of laboratory and field tests of a welded rail joint. The welding technology was SoW-5 type thermit welding (TW), while the rail profile was MÁV 48.5. This rail has not been in railway track before the test. The investigation focused on the variation of the hardness of rail steel in the HAZ of the welded rail joint. The authors carried out hardness tests on the rail head's surface even after the rail welding, as well. After the field hardness tests and welding, the rail joint was cut with +/–200 mm by a rail cutter and transported to the laboratory. Water jet cutting was applied to shape six longitudinal slices from the rail piece's head. Micro-Vickers (HV10) hardness tests were made on these slices, in the –150…+150 mm interval lengthwise and in the 3, 6, and 10 mm depths. The HV10 hardness values were transformed to Brinell Hardness, and the field measurements' Leeb scale was also exchanged to Brinell Hardness.

The results were drawn in charts, figures, in which the Elektro-Thermit's official hardness function was taken into consideration related to HAZ of welded rail joint made by SoW-5 TW technology.

The authors received significantly detailed results because these measurements have not been published earlier in other research papers in different depths and in different horizontal positions in the rail head. The hardness measurement series was compared the SoW-5 technology's hardness test's results.

Based on the comparisons, the authors were able to draw conclusions. They stated that the received hardness tests functions are quite similar to the SoW-5's diagram (shape and scheme). It can be seen a significant peak at the position of 50 mm, measured from the axis of the welded rail joint (see Figs. 8-11, the mentioned value is approx. 120-130%). In the most cross-sections, the authors' results are in accordance with the SoW-5 function; they are in the 90-100% range (see Figs. 8-11). There are not too high differences in hardness values considering different depths and positions in the rail head. There is an outlier, e.g. B6 slice.

The authors gave all the possibilities that can be the reasons for the differences in measured hardness values. The tested rolled rail from the rolling mill Diósgyőr (Hungary) and the applied technology, as well as its details, properties significantly influence the results.

The authors conceive the possible further investigation as below:

- more types of welding technologies can be considered, e.g., flash butt welding, electric arc welding; and the main differences can be concluded with detailed comparison,

- heat treated and/or quenched base steel materials can be taken into consideration, etc.

Acknowledgement

References

[1]   M. Kurhan, D. Kurhan, R. Novik, S. Baydak, N. Hmelevska, Improvement of the railway track efficiency by minimizing the rail wear in curves. IOP Conference Series: Materials Science and Engineering, Vol. 985, No. 1, 2020, 012001

[2]   V. Kovalchuk, M. Sysyn, Y. Hnativ, A. Onyshchenko, M. Koval, O. Tiutkin, M. Parneta, Restoration of the Bearing Capacity of Damaged Transport Constructions Made of Corrugated Metal Structures. Baltic Journal of Road and Bridge Engineering, Vol. 16, No. 2, 2021, pp. 90-109

[3]   A. J. Tigh Kuchak, D. Marinkovic, M. Zehn, Finite element model updating - Case study of a rail damper. Structural Engineering and Mechanics, Vol. 73, No. 1, 2020, pp. 27-35

[4]   M. Kazemian, F. Astaraki, M. R. Movahedi, A. Taheri, Condition monitoring of vibration at weak parts of rail for ballasted railway tracks in Iran. Journal of the Korean Society for Railway, Vol. 24, No. 6, 2021, pp. 544-551

[5]   A. Benmebarek, M. R. Movahedi, DEM modeling of crushable grain material under different loading conditions. Periodica Polytechnica Civil Engineering, Vol. 65, No. 3, 2021, pp. 935-945

[6]   M. Sysyn, O. Nabochenko, V. Kovalchuk, M. Przybyłowicz, S. Fischer, Investigation of interlocking effect of crushed stone ballast during dynamic loading. Reports in Mechanical Engineering, Vol. 2, No. 1, 2021, pp. 65-76

[7]   A. Kampczyk, K. Dybeł, Integrating surveying railway special grid pins with terrestrial laser scanning targets for monitoring rail transport infrastructure. Measurement: Journal of the International Measurement Confederation, Vol. 170, 2021, 108729

[8]   A. Matejov, J. Šestáková, The Experiences with utilization of BIM in railway infrastructure in Slovak Republic and Czech Republic. Transportation Research Procedia, Vol. 55, 2021, pp. 1139-1146

[9]   J. Gajári, Railways I., 1983, Tankönyvkiadó, Budapest, in Hungarian

[10]   A. Németh, S. Fischer, Investigation of glued insulated rail joints applied to CWR tracks. Facta Universitatis-Series Mechanical Engineering, 2021, 7642

[11]   MSZ EN ISO 4063:2016: Welding and allied processes. Nomenclature of processes and reference numbers, 28 p.

[12]   MSZ EN 13674-2:2020: Railway applications. Track. Rail. Part 2: Switch and crossing rails used in conjunction with Vignole railway rails 46 kg/m and above, 112 p.

[13]   R. R. Porcaroa, G. L. Fariaa, L. B. Godefroida, G. R. Apolonioa, L. C. Cândidoa, E. S. Pinto: Microstructure and mechanical properties of a flash butt welded pearlitic rail. Journal of Materials Processing Tech., Vol. 270, 2019, pp. 20-27

[14]   Y. Sarikavak, O. S. Turkbas, C.Cogun: Influence of welding on microstructure and strength of rail steel. Construction and Building Materials, Vol. 243, 2020, 118220

[15]   C. Meric, E. Atik, S. Sahin: Mechanical and metallurgical properties of welding zone in rail welded via thermite process. Science and Technology of Welding and Joining, Vol. 7, No. 3, 2002, pp. 172-176

[16]   L. C. Schroeder, D. R. Poirier The Mechanical Properties of Thermite Welds in Premium Alloy Rails. Materials Science and Engineering, Vol. 63, 1984, pp. 1-21

[17]   BSI Standards Limited, Railway applications. Track. Aluminothermic welding of rails. Qualifications of aluminothermic welders, approval of contractors and acceptance of welds. 2017

[18]   W. A. Bruce, B. C. Etheridge, V. R. Arnett, Development of Heat-Affected Zone Hardness Limits for In-Service Welding. Tech Report, DOT Project No. 216, ENAUS826BBRUCE, Project No. 82673428, 2009, https://trid.trb.org/view/1475729/ [online, last visited on: 2021.09.28]

[19]   Further Development of Heat-Affected Zone Hardness Limits for In-Service Welding, Proceedings of the 2012 9th International Pipeline Conference, Canada, IPC2012-90095, pp. 71-81

[20]   Elektrothermit, Thermit SoW-5, https://www.elektro-thermit.de/fileadmin/ et/user_upload/PDF/Produktbrosch%C3%BCren/SOW5_DEF.pdf   [online, last visited on: 2021.09.28]

Prediction of Dynamic Response of Vibration Isolated Railway Obstacle Detection System

Milan Banić[1], Ivan R. Pavlović[1], Aleksandar Miltenović[1], Miloš Simonović[1], Marko Mladenović[2], Dragan Jovanović[1], Milan Rackov[3]

[1] University of Niš, Faculty of Mechanical Engineering
Aleksandra Medvedeva 14, 18000 Niš, Serbia; milan.banic@masfak.ni.ac.rs,
pivan@masfak.ni.ac.rs, aleksandar.miltenovic@masfak.ni.ac.rs,
milos.simonovic@masfak.ni.ac.rs, dragan.jovanovic@masfak.ni.ac.rs

[2] Harder Digital SOVA, Bulevar Cara Konstantina 80, 18000 Niš, Serbia;
marko.mladenovic@hdsova.rs

[3] University of Novi Sad, Faculty of Technical Science
Trg Dositeja Obradovića 6, 21000 Novi Sad, Serbia; racmil@uns.ac.rs

Abstract: The prototype of the on-board Obstacle Detection System (ODS), for GoA2 freight trains, was developed in the frame of H2020 project SMART. The developed prototype uses vision-based sensors, for environmental perception and obstacle detection. As severe image distortions while capturing imaging data can occur due to vibrations of the moving vehicle, the ODS of autonomous rail vehicles must be isolated from vibrations transmitting from the vehicle to have reliable image acquisition and post process analysis. The passive vibration isolation system was specially designed for suppression of moving rail vehicle vibrations during development of the ODS prototype. The paper presents the designed passive vibration system, as well as, experimental verification of its performance in operational conditions. Furthermore, two viscoelastic constitutive models, Voigt-Kelvin and Voigt-Maxwell, were applied to predict the dynamic response of vibration isolated ODS by using the real experimental data as system excitation.

Keywords: dynamic response; railway obstacle detection; vibration isolation; transmissibility of vibrations

1   Introduction

In many applications, the presence of harmful vibrations is unavoidable which is reducing the designed performance of machines and systems while emitting noise to environment [1]. The harmful vibrations in engineering, not only affect the use and working efficiency of precision instruments, but they may also trigger damage

and accordingly, compromise structural integrity [2] [3]. Cameras and other vision sensors, as precision instruments mounted on vehicles, are especially sensitive to vibrations [4].

Autonomous rail vehicles for environment perception and obstacle detection by vision-based sensors must have image stabilization to have reliable image acquisition and post process analysis [5]. It can be found in many sources that, at frequencies greater than 5 Hz, severe image distortions can occur [6]. With high image resolution, large optical zooming of the image and at low lighting conditions, the image distortion problem, due to vibrations, becomes more notable [6]. Many different image stabilization techniques have been developed to prevent distortion of image quality due to vibrations. Image stabilization techniques can be classified into four major categories: optical stabilization, digital stabilization, electro-mechanical and mechanical stabilization [7].

Mechanical stabilization operation principle is the isolation of the vision-based sensors from the vibration source. This way, vibrations cannot be suppressed completely, but amplitude of vibrations are significantly reduced, enabling further optical or digital stabilization [8]. Mechanical stabilization is done by implementing isolation devices made from materials possessing properties of elasticity and damping [9]. The mechanical isolators for imaging applications can be categorized in three major groups: solid viscoelastic dampers (rubber or rubber – metal springs); hysteretic isolators (metal springs, wire rope isolators); hysteretic-viscoelastic fluid isolators (combination of metal springs with fluid dampers). Isolation devices can realize vibration isolation in a wide range of frequencies, but only when the excitation frequency is $\sqrt{2}$ times higher than the natural frequency of vibrating system [10]. The rubber or rubber-metal springs are most often used as mechanical stabilization vibration isolators. Special types of rubber-metal springs were developed for isolation of sensitive instrumentation, measuring equipment and vision-based sensors. Noted springs for sensitive equipment have low natural frequency and ability to isolate vibrations in all three directions - vertical, lateral, and longitudinal.

Prediction of dynamic response, transmissibility and stability are major concern during the design of rubber-metal vibration isolators; thus a large number of authors deals with noted topics. The authors use analytical models solved directly or numerically [11-14] and finite element simulations with rubber constitutive models [15-17] to predict dynamic response and the transmissibility of vibration isolators. In most of the studies by other authors, the disturbing force is modelled as a sinusoidal input or as a white noise [18] to predict the dynamic response, transmissibility, and stability.

The development of railway transportation will be an increasingly important task for further developing of society in the 21st Century [19]. To contribute to railway transport increase of quality, effectiveness, and capacity while opposing the strong competence of other transport means [20], the prototype of the on-board Obstacle

Detection System (ODS) for GoA2 freight trains was developed in the frame of H2020 project SMART [21]. As the ODS uses vision-based sensors for environment perception, the passive vibration isolation system was specially designed for suppression of vibrations transmitting from the moving vehicle to the ODS. The paper presents the designed passive vibration system, as well as experimental verification of its performance in operational conditions for a cargo train in service. Furthermore, the viscoelastic Voigt-Kelvin and Voigt-Maxwell constitutive models were applied to predict the dynamic response by using the real experimental data for excitation of the system. The parameters of Voigt-Kelvin and Voigt-Maxwell models were determined by Monte Carlo simulation.

2   Vibration Isolation of the Railway ODS

The on-board freight train ODS prototype integrates three RGB cameras, thermal, night vision camera, and a 3D laser scanner (LiDAR) integrated into custom developed housing [8] as shown in Figure 1. The ODS housing is supported by the mounting plate rigidly connected to locomotive car body below the locomotive headlights. To prevent transmission of vibrations from the moving vehicle, via the mounting plate, to the ODS housing and thus, vision-based sensors, a passive vibration isolation system was designed.

Figure 1
The SMART ODS prototype mounted onto the Serbia KARGO 444-018 locomotive [22]

As previously stated, for vibration isolation it is necessary that excitation frequency is $\sqrt{2}$ times higher than the natural frequency of vibrating system - ODS housing and isolator assembly. The problem with vibrations transmitting from the rail vehicle to the ODS lies in the fact that there are multiple excitation frequencies which are not known. If one observes the diagram from Figure 2 it is

evident that series 444 locomotive (SMART ODS evaluation vehicle) traveling at 75 km/h at straight line has multiple resonant frequencies. In such case, widely adopted approach is to lower the vibrating system natural frequency, as much as possible, to achieve higher ratio between the excitation and vibrating system frequency. This is achieved by lowering the isolator stiffness which leads to larger displacement, thus lower vibrating system natural frequency, but the expense of static bearing capacity as it can become insufficient.
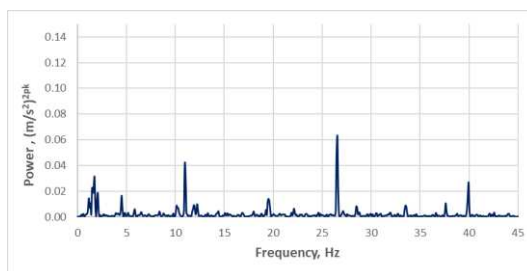

Figure 2

Vibration spectre of Serbia KARGO series 444 locomotive car body at 75 km/h on straight line [7]

Furthermore, the damping ratio should be as large as possible as high damping will reduce the maximum possible transmissibility when the excitation frequency value is around natural frequency of the vibrating system. By analysis of vibration spectre given in Figure 2, it is evident that the natural frequency of the vibrating system must be below 8 Hz to isolate vibrations for a vehicle resonant frequency of around 11.5 Hz. The first 2 resonant frequencies (at ≈2 and ≈4 Hz) can be neglected due to lower amplitude and the already stated fact that vibrations bellow 5 Hz will not downgrade quality of acquired images or can be easily mitigated with digital and optical stabilization. Based on requirements discussed above and due to good damping characteristics, and good static bearing capacity it was decided to design the vibration isolation system with rubber - metal springs. In principle, mechanical suppression of low frequency vibrations is possible only with a negative damping system which is not feasible for usage on the vehicle. The goal of adopted approach is to have a simple and low-cost vibration suppression system with proven service reliability. Furthermore, it was envisioned to use rubber-metal mounts already available on the market to decrease the system costs [23].
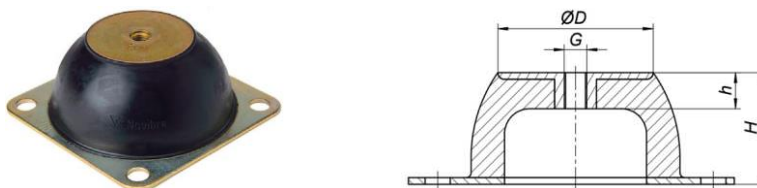

Figure 3

Bell-shaped rubber metal spring [24]

As desired vibration system natural frequency must be below 8 Hz, the selection was made to use the bell-shaped mount (Figure 3) which has a large deflection, as it is considered as most suitable rubber-metal mount for isolating the low frequency vibrations. Furthermore, it isolates vibration in all three directions, and it is suitable for shock suppression due to large deflection capacity.

The mass of the integrated ODS housing was intentionally increased to 160 kg by adding of ballast to increase the spring deflection and system inertia [25]. The number of mounts was selected as 4 to keep the uniform distribution of load across mounts and increase system stability. By usage of Trelleborg selection diagrams [24], the mount M50-40 was selected according to load per mount of 40 kg. The selected mount provides vibrating system natural frequency of 7.5 Hz, which is agreement with the requested value < 8 Hz. The resonance region for selected mount is between 5.5 and 10.5 Hz which ensures that all the vehicles resonant frequencies are outside the vibrating system resonance region. For largest vehicle resonant frequency of 27 Hz (Figure 2), the isolation efficiency is 72%.
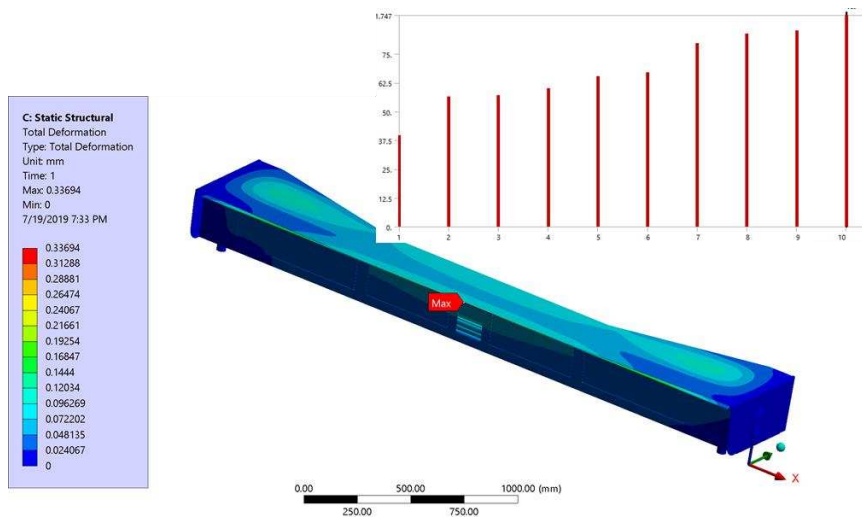
Figure 4

Deformed shape of integrated ODS housing for a static structural analysis and its natural frequencies in the range 0-100 Hz

Finally, it is necessary to determine integrated ODS housing natural frequencies to ensure that they are not the resonance region, as the ODS housing would be exited form moving vehicle vibrations in noted frequency region and resonance would occur. The natural frequencies of integrated ODS housing with of all the internal components and added ballast were determined by modal analysis (with static structural pre-stress analysis) in ANSYS Workbench software. The modal analysis was performed for a range between 0 and 100 Hz. The results of the modal analysis of a deformed ODS housing are shown in Figure 4. The primary natural

frequency is close to 38 Hz which is well within the isolation range (>10.5 Hz) For the integrated ODS housing primary natural frequency the isolation efficiency of the designed vibration suppression system is 87.5%.

3   Experimental Determination of ODS Dynamic Response

The evaluation of prototype of the freight onboard ODS, as well as the designed passive vibration isolation, was performed during the tests in operational traffic. The tests were performed on the railway line between Niš Marshaling Yard and station Ristovac, on the pan European 'corridor X'. A prototype of ODS was mounted on Locomotive 444-018, that pulled 21 wagons, with total mass of 1194 t and a total train length of 458 m, as shown on Figure 5. The test track length was 120 km, the average speed was 34 km/h and the test run lasted 3.5 h [22]. On the straight rail-tracks sections, between Niš Marshalling Yard and station Grdelica, the maximal train speed was 80 km/h.

Figure 5
Locomotive 444-018 with mounted prototype ODS pulling a train during evaluation tests before leaving the Niš Marshalling Yard [22]
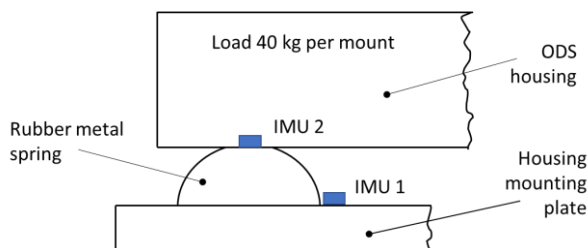

Figure 6
Positioning of IMU's on the housing mounting plate and inside the ODS housing

The vibration of the mounting plate and the ODS housing were recorded during the evaluation run by two triaxial Inertial Measurement Units (IMU's) positioned on the mounting plate and in the ODS housing as shown in Figure 6.

The acquisition device captured data from the IMU's at 75 Hz. The vibrations were recorded on a straight line, in curves, during the crossing of the bridges and passing over the switches. As the train was following the operational speed profile, the vibrations were recorded at multiple train speeds.
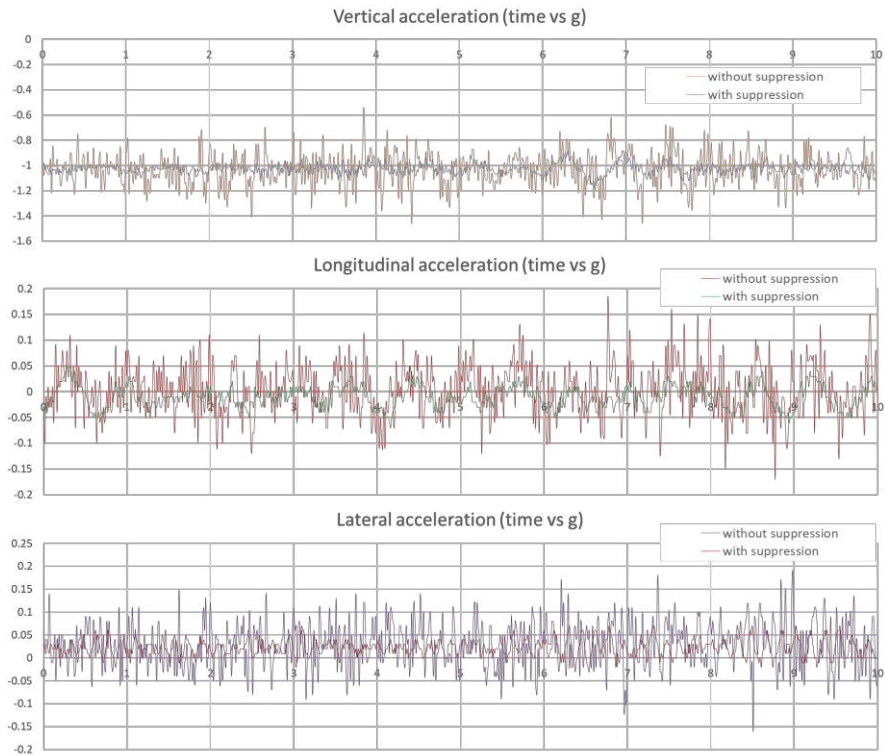
Figure 7

Vibrations of mounting plate (without suppression) and ODS housing (with suppression) on a straight part of the track at 80 km/h in vertical, longitudinal and lateral direction

Figure 7 shows the 10 second interval of measured vibrations on a straight track at train speed of 80 km/h. It is evident from the diagrams shown on Figure 7 that the designed vibration isolation system significantly reduces the amplitude of vibrations in all three directions. As expected, due to largest deflection of the rubber - metal spring in the vertical direction, the degree of isolation is largest in the vertical direction. The vibration isolation performance in lateral direction is somewhat better than in longitudinal direction. This can be explained by lower excitation signal frequency in the longitudinal direction, which leads to higher transmissibility due to smaller value of ratio of excitation frequency and natural frequency of the vibrating system.

4   Prediction of Dynamic Response

Following the experimental acceleration measurements in vertical direction from Figure 6 and mass per one mount of 40 kg, the stochastic acting force in vertical direction without and with vibration suppression is calculated and presented in Figure 8.
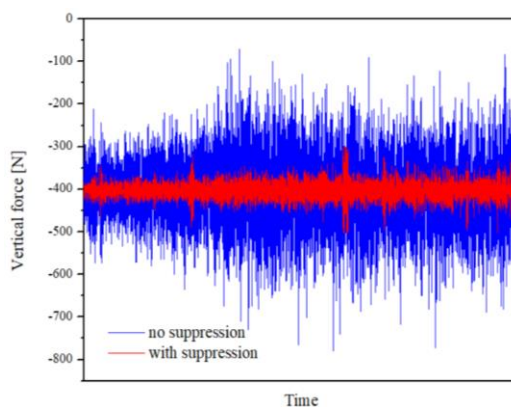
Figure 8
Calculated acting force in vertical direction

According to the designed vibration suppression used to isolate ODS housing from vibrations, the viscoelastic Voigt-Kelvin and Voigt-Maxwell models were applied for ODS housing stochastic vibrations analysis.

First, because of its simplicity, the Voigt-Kelvin model, was employed. This model consists of parallel connected spring and dashtop as shown in Figure 9.
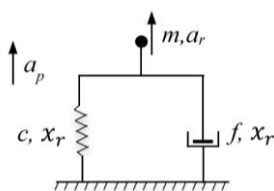
Figure 9
Voigt-Kelvin constitutive model

In applied Voigt-Kelvin constitutive model, c is spring stiffness, f is damping coefficient, m presents the mass of analyzed system (load per ODS housing mount of 40 kg) where a_r ($\ddot{x}_r$) presents relative system acceleration which corresponds to measured acceleration data of ODS housing. On the other hand, a_p is measured acceleration of the ODS housing mounting plate. According to dynamics of

relative movement, the model from Figure 8 can be described with the following equation

$$m\ddot{x}_r = -F_c(t) - F_f(t) + F_p^{in}(t) \tag{1}$$

The displacements in spring and dashtop elements are equal, $x_c = x_f = x_r$ where the acting forces in these elements are

$$F_c(t) = cx_r \qquad \text{and} \qquad F_f(t) = f\dot{x}_r \tag{2}$$

The expression F_p^{in} presents the inertial force according to acceleration a_p

$$F_p^{in} = m\ddot{x}_p \tag{3}$$

and it correspond to generated force given in Figure 8.

To obtain the accurate model which can be used to predict the dynamic response, it is necessary to determine the most suitable pair of parameters c and f for calculation of Voigt-Kelvin model which correspond to the experimental results for measured accelerations $\ddot{x}_r(t)$ and $\ddot{x}_p(t)$. For this purpose, the Monte Carlo simulation method is applied. According to equation (1) the appropriate model is given in Figure 10.
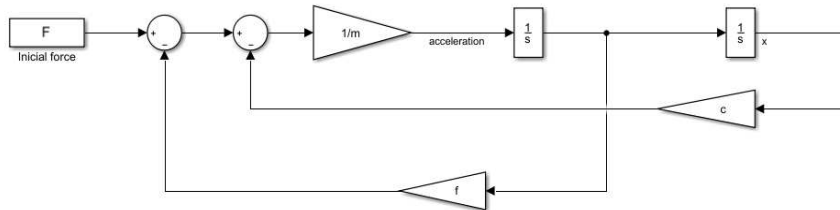
Figure 10
Simulation scheme for the system given by relation (1) and (2)

Following the Monte Carlo simulation method, the model from Figure 10 is simulated more 10000 times for various values of c and f, where the starting (initial) values of this parameters were recalculated according to obtained elastic and viscoelastic parameters in [26]. These parameters are finally estimated for the model results which gives the smallest accelerations outputs error compared to experimental acceleration values for suppressed system.
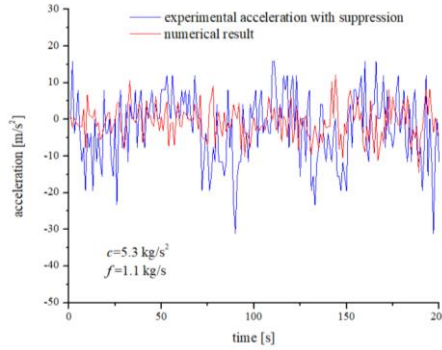
Figure 11

Voigt-Kelvin model acceleration output compared to experimental values in vertical direction

Figure 11 presents comparison of numerically determined acceleration values for a Voigt-Kelvin model and experimentally determined ODS housing response. It is evident from Figure 11 that Voigt-Kelvin model cannot accurately predict the ODS dynamic response. Although the acceleration direction is somewhat predicted, the amplitude values over time are largely missed. Because of its limitation on only two unknown parameters c and f, the Voigt-Kelvin model application is limited to analysis of smaller displacements.

Therefore, it is necessary to use a more complex constitutive model, such as, Voigt model with two Maxwell elements marked with I and II in Figure 12. Contrary to Voigt-Kelvin model, this model is more suitable in modelling of larger disturbances.
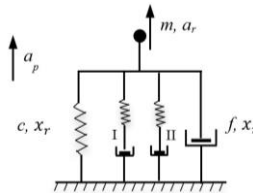
Figure 12

Voigt-Maxwell model

This applied Voigt-Maxwell constitutive model is described with following dynamic equations:

$$m\ddot{x}_r = -F_c(t) - F_f(t) + F_p^{in}(t) \tag{4}$$

where c_1, c_2 are spring stiffness and f_1, f_2 are damping coefficient in Maxwell elements I and II and:

$$F_c(t) = (c + c_1 + c_2)x_r - c_1 x_1 - c_2 x_2 \quad \text{and} \quad F_f(t) = f\dot{x}_r \tag{5}$$

The relations between Maxwell elements are given as:

$$f_1 \dot{x}_1 - c_1 x_r + c_1 x_1 = 0,$$

$$f_1 \dot{x}_2 - c_2 x_r + c_2 x_2 = 0, \qquad (6)$$

where, x_1 and x_2 are movements between elements I and II respectively.

According to relations (4) and (6), the simulation scheme of applied Voigt-Maxwell constitutive model is presented in Figure 13.
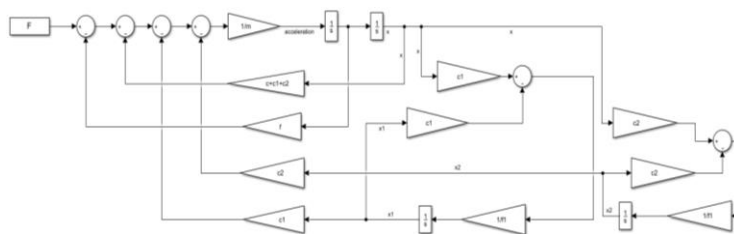
Figure 13
Simulation scheme of Voigt-Maxwell model
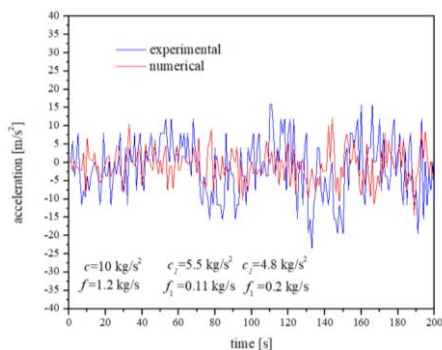
Figure 14
Voigt-Maxwell model acceleration output compared to experimental values in vertical direction

The spring stiffness (c_1, c_2) and damping coefficients (f_1, f_2) are determined by a same procedure as for Voigt-Kelvin model using the Monte Carlo simulation method.

Figure 14 presents comparison of numerically determined acceleration values for a Voigt-Maxwell constitutive model and experimentally determined ODS housing response. It is evident from Figure 14 that Voigt-Maxwell achieves better agreement between the numerically and experimentally determined acceleration values than Voigt-Kelvin model (Figure 11). There are still differences in prediction of acceleration directions and amplitude values, but the numerical and experimental determined acceleration amplitude values are somewhat comparable.

According to upper and lower limits compared through time and using into account error in experimental measurements it can be concluded this model can be successfully used for further numerical system analysis and prediction. The addition of more parallel, connected Maxwell elements would increase the accuracy of prediction of dynamic response, but at expense of increased time for determination of constitutive model parameters.

Conclusions

As vibrations can distort the images acquired by vision-based sensors, it is necessary to isolate the sensors from the source of the vibrations. This paper presents the design of a passive vibration isolation system, for a freight train, by usage of bell-shaped rubber-metal springs. The design of the vibration isolation system was generated, based on measurements of the Serbia KARGO series 444 locomotive car body on a straight portion of the track at speed of 75 km/h. The presented system can isolate vibration with frequencies larger than 10.5 Hz. The dynamic response of the ODS housing, as well as, the performance of the passive vibration isolation, was determined experimentally by measuring vibrations before and after the ODS vibration isolation system with the train in operational traffic. Based on experimental data, the designed vibration isolation system significantly reduces the amplitude of vibrations in all three directions. To predict the dynamic response of the vibration isolated ODS, viscoelastic Voigt-Kelvin and Voigt-Maxwell constitutive models were applied with real experimental data as system excitation. For both constitutive models the model parameters were determined by Monte Carlo simulation to achieve smallest error between predicted and experimental determined dynamic response. The comparison of results show that Voigt-Maxwell achieves better agreement between the numerically and experimentally determined acceleration values, over the Voigt-Kelvin model.

Acknowledgement

References

[1]   Kuchak, A. J. T., Marinkovic, D., Zehn, M., (2020) Finite element model updating-Case study of a rail damper. Structural Engineering and Mechanics, 73(1) pp. 27-35

[2]   Carrella, A., Brennan, M. J., Waters, T. P., (2007) Static analysis of a passive vibration isolator with quasi-zero-stiffness characteristic. Journal of sound and vibration, 301(3-5) pp. 678-689

[3]   Kuchak, A. J. T., Marinkovic, D., Zehn, M., (2021) Parametric Investigation of a Rail Damper Design Based on a Lab-Scaled Model. Journal of Vibration Engineering & Technologies, 9(1) pp. 51-60

[4]   Li, L., Tan, L., Kong, L., Wang, D., Yang, H., (2018) The influence of flywheel micro vibration on space camera and vibration suppression. Mechanical Systems and Signal Processing, 100, pp. 360-370

[5]   Zhao, G. W., Yuta, S. I., 1993, January. Obstacle detection by vision system for an autonomous vehicle. In 1993 Intelligent Vehicles Symposium, IV. Institute of Electrical and Electronics Engineers Inc. 1993, pp. 31-36

[6]   Abolmaali, A., Fernandez, R., Kamangar, F., Ramirez, G., Le, T., (2008) Vibration Reduction and Control for Traffic Cameras: Technical Report (No. FHWA/TX-08/0-5251-2)

[7]   SMART project, Deliverable 1.1. Obstacle Detection System Requirements and Specification

[8]   Ristić-Durrant, D., Haseeb, M. A., Banić, M., Stamenković, D., Simonović, M., Nikolić, D., (2021) SMART on-board multi-sensor obstacle detection system for improvement of rail transport safety. Proceedings of the Institution of Mechanical Engineers, Part F: Journal of Rail and Rapid Transit, p. 09544097211032738

[9]   Rysaeva, L. K., Korznikova, E. A., Murzaev, R. T., Abdullina, D. U., Kudreyko, A. A., Baimova, J. A., Lisovenko, D. S., Dmitriev, S. V., (2020) Elastic damper based on the carbon nanotube bundle. Facta Universitatis, Series: Mechanical Engineering, 18(1) pp. 001-012

[10]   Banić, M., Stamenković, D., Miltenović, A., Jovanović, D., Tica, M., (2020) Procedure for the Selection of Rubber Compound in Rubber-Metal Springs for Vibration Isolation. Polymers, 12(8) p. 1737

[11]   Sun, Y., Zhou, J., Thompson, D., Yuan, T., Gong, D., You, T., (2020) Design, analysis and experimental validation of high static and low dynamic stiffness mounts based on target force curves. International Journal of Non-Linear Mechanics, 126, p. 103559

[12]   Cao, X., Wei, C., Liang, J., Wang, L., (2019) Design and dynamic analysis of metal rubber isolators between satellite and carrier rocket system. Mechanical Sciences, 10(1) pp. 71-78

[13]   Zou, G. P., Liu, Z., Cheng, H. Z., Chang, Z. L., (2015) Effects of preloading and vibration level on the vibration characteristics of metal rubber damper. Journal of Vibration and Shock, 2015, p. 22

[14]   Carrella, A., (2012) Nonlinear identifications using transmissibility: Dynamic characterisation of Anti Vibration Mounts (AVMs) with standard approach and nonlinear analysis. International Journal of Mechanical Sciences, 63(1) pp. 74-85

[15] Ucar, H., Basdogan, I., (2018) Dynamic characterization and modeling of rubber shock absorbers: A comprehensive case study. Journal of Low Frequency Noise, Vibration and Active Control, 37(3) pp. 509-518

[16] Ramos, F. M. Vibration analysis of an engine mount. M.Sc. Thesis, Universidade Técnica de Lisboa Pais, Lisboa, Portugal, 2008: 1049-001

[17] Olsson, A. K. Finite Element Procedures in Modelling the Dynamic Properties of Rubber; Lund University: Lund, Sweden, 2007

[18] Pavlović, I. R., Pavlović, R., Janevski, G., Despenić, N., Pajković, V., (2020) Dynamic behavior of two elastically connected nanobeams under a white noise process. Facta Universitatis, Series: Mechanical Engineering, 18(2) pp. 219-227

[19] Németh, A., Fischer, S., (2021) Investigation of the Glued Insulated Rail Joints Applied to CWR Tracks. Facta Universitatis, Series: Mechanical Engineering

[20] Sysyn, M., Nabochenko, O., Kovalchuk, V., Przybyłowicz, M., Fischer, S., (2021) Investigation of interlocking effect of crushed stone ballast during dynamic loading. Reports in Mechanical Engineering, 2(1) pp. 65-76

[21] Smart Automation of Rail Transport - SMART, https://cordis.europa.eu/ project/id/730836

[22] SMART project, Deliverable 7.1. Report on evaluation of developed SMART technologies

[23] SMART project, Deliverable 2.2.- Design of the passive vibration isolation system

[24] Trelleborg IAVS Catalogue, 2017

[25] Banić, M., Stamenković, D., Miltenović, A., Simonović, M., Milošević, M., (2019) Design of Housing and Vibration Suppression for Obstacle Detection System in Railways. Proceedings of 24th International conference "Current Problems in Rail Vehicles" - PRORAIL 2019, 1, Žilina, Slovakia, 17-19 September, pp. 23-31

[26] Pavlović I., Ćirić I., Đekić P., Nikolić V., Pavlović R., Ćojbašić Ž., Radenković G. (2013) Rheological model optimization using advanced evolutionary computation for the analysis of the influence of recycled rubber on rubber blend dynamical behavior, Meccanica, 48:2467-2477

Investigation of Tramway Line No. 1, in Budapest, Based on Dynamic Measurements

Vivien Jóvér[1], László Gáspár[2], Szabolcs Fischer[1]

[1]Széchenyi István University
Egyetem tér 1, H-9026 Győr, Hungary
{jover.vivien,fischersz}@sze.hu

[2]KTI Institute for Transport Sciences Non-profit Ltd.
Than Károly u. 3-5, H-1119 Budapest, Hungary
gaspar.laszlo@kti.hu

Abstract: Determining the deterioration of superstructure systems is technical and has national economic importance. In addition to geometric deterioration, it is also very difficult to monitor the changes in the dynamic characteristics of the vehicles. The data from geometric and dynamic measurements should be properly analyzed to determine the deterioration, lifetime/life-cycle costs of superstructure systems and the casual relationships should be researched between the characteristics. In this paper, the geometric and dynamic measurement results of the two examined sections are compared. This analysis is the first step in exploring and understanding the relationship between each feature. The authors recommended methodologies for using the synchronized (static and dynamic) measurements and their evaluation possibilities related to tramway tracks. The method is a well-known solution for public railways; however, the tramways greatly differ. In Hungary, there is a great opportunity to introduce the static-dynamic parallel method, which can be applied for the determination of the life-cycle costs (LCC) of the tramway tracks that are assembled with different (super)structures.

Keywords: tramway track; superstructure systems; geometrical analysis; dynamic analysis, deterioration

1   Introduction

The deterioration of tramway tracks can be observed in several ways: the deterioration of tracks' structural elements (i.e., rails, rail fasteners sleepers, etc.) can be detected by inspection of the line; however, the changes in track geometric parameters like track gauge, alignment, longitudinal level, etc. can only be measured with instruments [1]. In addition to monitoring changes in the geometric characteristics, it is also essential to measure the dynamic characteristics of

vehicles, record and assess the measurement results [2] [3]. Considering the dynamic effect in engineering design and maintenance is quite important [4-7]. Suppose the geometric and dynamic measurements are appropriately evaluated, and the costs are known for the whole lifetime; each superstructure system's life cycle, geometric deterioration, and life cycle cost can be determined.

In Hungary, seven types of superstructure systems are currently differentiated, but they are constructed differently in each case.

The authors selected 22 standard (reference) sections in the research, at least three for each known superstructure system, but these are different ages. The goal is to determine the deterioration of these sections considering the passage of time, their lifetime, and life cycle cost by regular inspection of the line, track geometric and dynamic examination [8].

2   Survey of Tramway Track Condition in Hungary

Three methods are applied in Hungary to examine the superstructure systems of tramway tracks:

- Inspection of the tramway line

- Geometric measurements

- Dynamic measurements

In Budapest (capital of Hungary), the inspections of the lines of running tracks are executed by the persons appointed for this task. It is specified in the Guidelines of infrastructure planning of tramway tracks by BKV PLC. [9].

For many years, the measurements of tracks' geometrical characteristics have been carried out by the TrackScan 4.01 instrument developed by Metalelektro Méréstechnika Ltd. The instrument is a complex track measuring device, which is suitable for continuous measurements. This equipment is able to measure and register the following characteristics at the same time [10]:

- Track gauge [mm]

- Flange gauge [mm]

- Superelevation [mm]

- Alignment [mm]

- Longitudinal level [mm]

- Length of the railway section [in meters to the nearest mm]

- Twist [mm]

The disadvantage of this instrument (Fig. 1) is its low weight, i.e., it provides an unloaded state. For this reason, the values of some geometric parameters may show a higher value under load than the values recorded by the TrackScan 4.01 instrument.
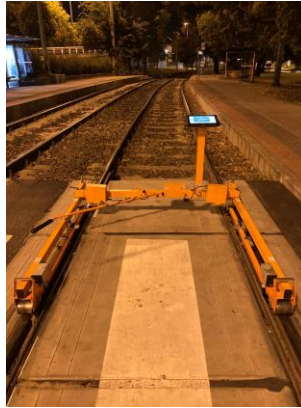
Figure 1
TrackScan 4.01 instrument (own made photo)

BKV PLC with Metalelektro Méréstechnika Ltd. commissioned the measuring tram in 2017 (Fig. 2). The vehicle dynamics measuring system has been installed on an eight-axle GANZ tram, which consists of the following fixed installation units [11]:

- Seven pieces of 3-axis accelerometer sensors

- GPS receiver and road sign receiver

- Two video cameras

Figure 2
Measuring tram (own made photo)

The sensors and cameras are connected to two systems that record the condition of the track and the catenary separately.

The data collector system of the vehicle dynamics measurement consists of the accelerometers (Fig. 3):

- Four sensors placed on wheels, which captures the tangent, radial, axial accelerations

- Two sensors placed on a longitudinal beam of boogie and one sensor placed on the car body captures accelerations perpendicular to the direction of measuring and accelerations in the direction of measuring [11].
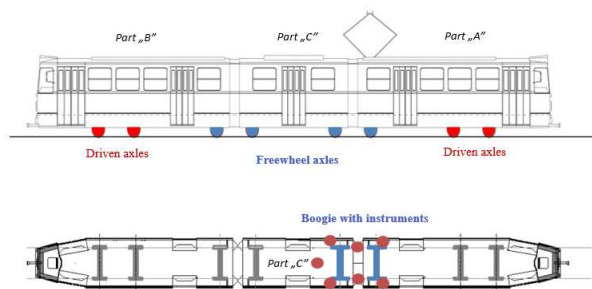
Figure 3
Placed sensors on measuring tram [11]

The accelerometers are located in the Part "C" of the tram, on the boogie closer to the Part "A".

The measuring system of tracks provides the following parameters for the rails (in parentheses are the units of each parameter, where unit 'g' means gravitational acceleration):

- Vertical impact [-]

- Transversal impact [-]

- Vertical excess load [g]

- Transversal excess load [g]

- Intensity of corrugation [-]

The parameters provided for the complete track are the following:

- Derailment safety characteristic [g^3]

- Vertical travel comfort [g]

- Transversal travel comfort [g]

- Changing of lateral acceleration [g]

- Vertical excess load of track characteristic [-]

There are cameras at the "A" and "B" ends of the tram, which takes continuous shots during the measurements. Budapest's entire tram(way) network is surveyed twice a year, usually in April and October. Measures are required at least six times at weekends because the ideal measurement speed is 25-30 km/h [11].

3 Methods

In the research, the measurements have been performed on tramway line No. 1 in Budapest. The measurements are related to three years: in autumn of 2019 and 2020; and in spring of 2021. Vehicle dynamics measurements were executed almost simultaneously with the track geometry measurements. The nearly 18 kilometers long line is the second busiest line in the capital, four of the six superstructure systems here are examined [10]:

- Concrete slab track

- ESCRB I track system (ESCRB means elastically supported continuous rail bedding system)

- ESCRB III track system

- Ballasted track system

In this article, the measurement results of two sections will be presented, which are of different ages. The sections are ESCRB III track system, which is the most modern technology today (Fig. 4). The reinforced concrete overpass was embedded by homogenous continuous elastic support along the entire length of the rails. The paved superstructure system was built with 51R1 rail (i.e., grooved rail) profiles. The special feature of this, is that, there are no steel fastenings used.
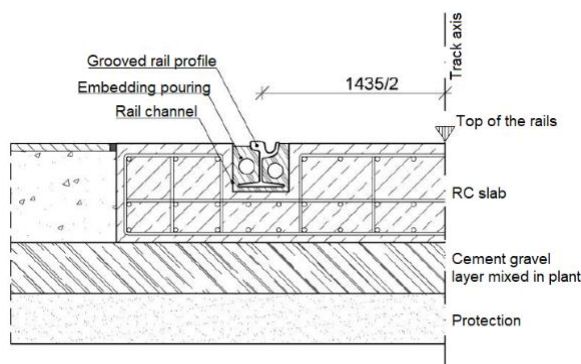
Figure 4
Cross-section of ESCRB III track system [9, 10]

Both presented sections are on bridges, the first one is the Árpád Bridge (superstructure was built in 2014), and the second one is the Kacsóh Pongrác overpass (superstructure was built in 2001). The tracks are straight, and there is no turnout or level crossing but several rail expansion devices; however, this article does not cover their examination.

In Budapest, each tramway line can be classified according to the traffic load; the classification depends on the annual through-rolled tonnages (Table 1).

Table 1
Traffic load classes [9]

Traffic load class		MGT/year/direction
I/A	Extremely heavy loaded line	> 7.5
I/B	Heavily loaded line	5.0…7.5
II	Medium loaded line	2.5…5.0
III	Low loaded line	< 2.5

The through-rolled axle tonnage is the mass of all crossing vehicles on a given line in one direction in one year. It is determined by multiplying the total number of crossing vehicles on the line and the average of the T0 loading (serviceable vehicle without crew and passenger) and T3 loading (serviceable vehicle with staff and maximum passenger capacity). In the case of the examined sections, the value of the traffic load is the same; however, it has changed in the last three years (Fig. 5).
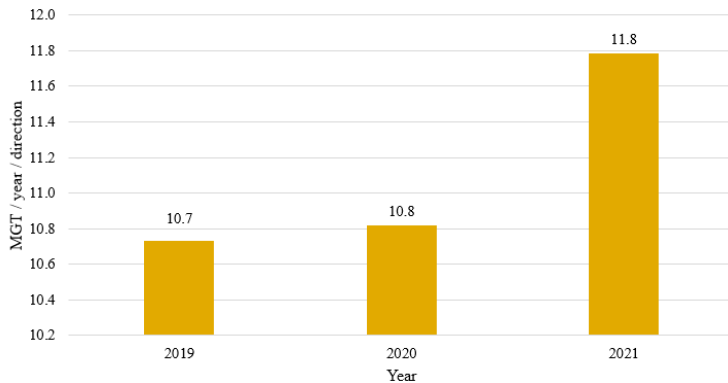
Figure 5
Traffic load of examined sections in the last three years

The figure shows that the investigated sections have extremely high loadings based on the load data. The data for 2019 and 2020 were determined on the basis of the actual completed runs, but for 2021 it is only an estimated value based on the actual completed runs in one week.

The following measured parameters of the Trackscan 4.01 instrument are considered:

- Track gauge [mm]

- Superelevation [mm]

- Alignment [mm]

- Longitudinal level [mm]

Among the dynamic characteristics measured and recorded by the measuring tram, those will be considered which can be related to track geometry parameters. These are as follows (unit 'g' means gravity acceleration):

- Vertical impact [-]

- Transversal impact [-]

- Transversal excess load [g]

- Changing of lateral acceleration [g]

- Transversal travel comfort [g]

The relationships between each track geometry and vehicle dynamics parameters are shown in Table 2 [11]. In Table 2, the "X" symbols mean there is connection; where there is not anything in the brackets there is no assumed or certified connection.

Table 2

Relationships between track geometry and vehicle dynamics characteristics

		Track geometry characteristics			
		Track gauge	Super-elevation	Alignment	Longitudinal level
Vehicle dynamics characteristics	Vertical impact				X
	Transversal impact				X
	Transversal excess load		X	X	
	Changing of lateral acceleration			X	
	Transversal travel comfort			X	

There is currently no measuring device installed on the measuring tram, to measure the values of the track geometry parameters. Therefore, the parameter is not directly or indirectly comparable to the measured dynamic characteristics. For this reason, the evaluation of the measurement results of the track geometry parameter is not reported in this article.

4   Results and Discussion

The track geometry and vehicle dynamic characteristics of the sections (see Chapter 3) are compared. Since the superelevation characteristic can only be related to one vehicle dynamic characteristic, its analysis was not fulfilled.

First of all, the possible correlations between the values of the longitudinal level track geometry parameter and the vertical and transversal impact parameters were examined for both sections. The measuring tram measures the impact values on both rails separately, the average of these was calculated during the evaluation.

Fig. 6 shows the average values of the measured and evaluated parameters. The change of average values of longitudinal level is shown as a second axis 'y' in the diagram. Based on the assumed relationship between vehicle dynamics and track geometry, the expected result is that the transversal and vertical impact values increase proportionately to the longitudinal level values. However, Fig. 6 contains the highest average of vehicle dynamic characteristics for both sections was in the third year, as the longitudinal level values decreased compared to the previous year's data.

Figure 6

Comparison of the average of transversal & vertical impact and longitudinal level

For this reason, in addition to the examined average values, it was necessary to look for points in the sections where the value of longitudinal level is high, and both vertical and transversal impact appear (Fig. 7). In general, the principal longitudinal level value appeared in the case of several cross-sections and the transversal and vertical impact values in the same or close cross-section (vertical lines in Fig. 7). But, of course, there are also cases when the examined characteristics cannot be related to each other. There may be several reasons for this, including the fact that it is difficult to reconcile the sectioning of the two instruments.
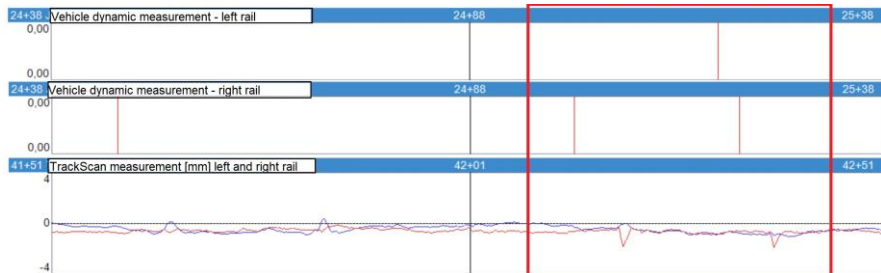
Figure 7

Comparison of transversal & vertical impact vehicle dynamic values and longitudinal level track geometry value – Section 1, 2021

Based on the hypothesized relationship between vehicle dynamics and track geometry, the alignment, and transversal excess load, changing of lateral acceleration, and transversal travel comfort's connection was also examined. Fig. 8 shows the average values of the measured and evaluated parameters and the change of average values of alignment. In this case, too, it was expected that there

would be a clear proportional relationship between the alignment and the examined vehicle dynamic values. Nevertheless, the increase of the average value of the alignment parameter characteristic of the third year is not followed by the change in the average value of the dynamic characteristics.

Figure 8

Comparison of average of transversal excess load, changing of lateral acceleration, transversal travel comfort and alignment

As in the previous case, it was necessary to find representative points from the measurement results where the values of geometric and dynamic characteristics are outstanding. Fig. 9 shows that the dynamic parameters theoretically related to the alignment parameter also appear in identical or nearly identical cross-sections. In this case, too, the values of the individual characteristics may not be compatible. The reasons for this have already been described above.
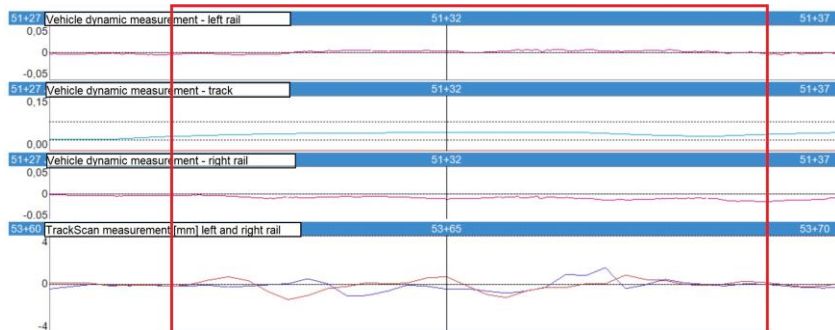
Figure 9

Comparison of transversal excess load, changing of lateral acceleration and transversal travel comfort vehicle dynamic values and alignment track geometry value – Section 2, 2021

Conclusions

The deterioration of tramway tracks can be observed in several ways: the deterioration of the tracks' structural elements or changes in track geometric parameters. In addition to monitoring changes in geometrical characteristics, it is also essential to measure the dynamic characteristics of vehicles, record and assess the measurement results.

Suppose the geometric and dynamic measurements are appropriately evaluated, and the costs are known for the whole lifetime; the life cycle, geometric deterioration, and life cycle cost of each superstructure system can be determined.

In Hungary, the TrackScan 4.01 instrument and the measuring tram are applied for examination of the superstructure systems of tramway tracks at BKV PLC. In this article, the measurement results of two sections have been presented, which are of different ages. The sections are ESCRB III track system, which is the most modern technology today.

The relationships between each track geometry and vehicle dynamics parameters were considered. Based on the assumed relationship between vehicle dynamics and track geometry, the expected result is that the transversal and vertical impact values increase proportionately to the longitudinal level values. However, the highest average of vehicle dynamic characteristics for both sections was in the third year, as the longitudinal level values decreased compa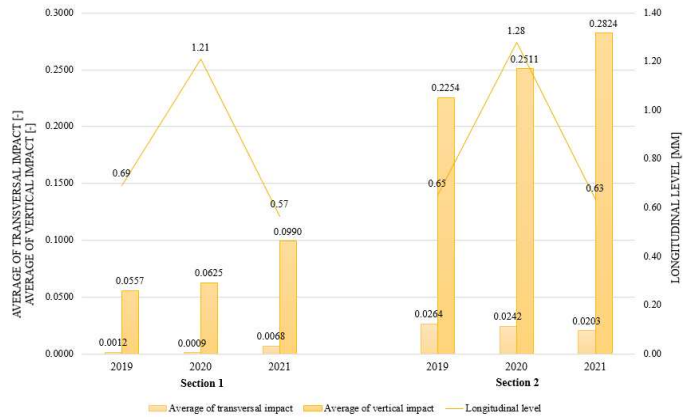red to the previous year's data. For this reason, in addition to the examined average values, it was necessary to look for points in the sections where the value of longitudinal level is high, and both vertical and transversal impact appear.

The relationship between alignment and transversal excess load, changing of lateral acceleration, and transversal travel comfort was also examined. In this case, too, it was expected that there would be a clear proportional relationship between the alignment and the examined vehicle dynamic values. Nevertheless, the increase of the average value of the alignment parameter characteristic of the third year is not followed by the change in the av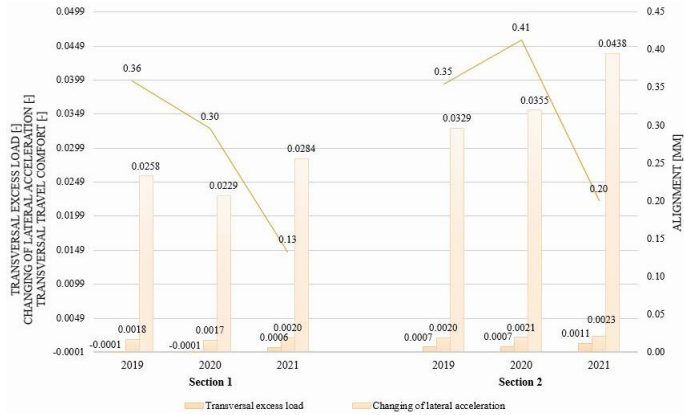erage value of the dynamic characteristics. Therefore, as in the previous case, it was necessary to find representative points from the measurement results where the values of geometric and dynamic characteristics are outstanding.

Based on the presented results, it can be stated that the relationship between track geometry and vehicle dynamics characteristics needs further investigation. As the annual change in the average values of the parameters cannot yet be related to each other, cross-sections in which both geometric and dynamic values show outliers should be examined. It is also essential to find and formulate the relationship between the parameters with further measurements and tests, thus helping to determine the lifetime, the life-cycle, geometric deterioration, and life-cycle cost of each superstructure system. The methodology for this kind of assessment is in progress, because many values (measurements), are needed for it. It will be developed and improved in future work.

References

[1]   M. Ahac, S. Lakušić, Tram track maintenance-planning by gauge degradation modelling. Transport, Vol. 30, No. 4, 2015, pp. 430-436

[2]   U. Gerber, M. Sysyn, J. Zarour, O. Nabochenko, Stiffness and strength of structural layers from cohesionless material. Archives of Transport, Vol. 49, No. 1, 2019, pp. 59-68

[3]   D. Kurhan, M. Kurhan, Modeling the Dynamic Response of Railway Track. IOP Conference Series: Materials Science and Engineering, Vol. 708, No. 1, 2019, 012013

[4]   R. M. Movahedi, S. K. Ibrahim, Optimal plastic analysis and design of pile foundations under reliable conditions. Periodica Polytechnica Civil Engineering, Vol. 65, No. 3, 2021, pp. 761-767

[5]   M. Sysyn, O. Nabochenko, V. Kovalchuk, M. Przybyłowicz, S. Fischer, Investigation of interlocking effect of crushed stone ballast during dynamic loading. Reports in Mechanical Engineering, Vol. 2, No. 1, 2021, pp. 65-76

[6]   D. Pamučar, D. Marinković, S. Kar, Dynamics under uncertainty: Modeling simulation and complexity. Mathematics, Vol. 9, No. 12, 2021, 1416

[7]   A. J. Tigh Kuchak, D. Marinkovic, M. Zehn, Finite element model updating - Case study of a rail damper. Structural Engineering and Mechanics, Vol. 73, No. 1, 2020, pp. 27-35

[8]   M. Kazemian, F. Astaraki, M. R. Movahedi, A. Taheri, Condition monitoring of vibration at weak parts of rail for ballasted railway tracks in Iran. Journal of the Korean Society for Railway, Vol. 24, No. 6, 2021, pp. 544-551

[9]   BKV Zrt. Közúti vasúti infrastruktúra tervezési irányelvek (Guidelines of infrastructure planning of tramway tracks) 2019

[10]   V. Jóvér, L. Gáspár, S. Fischer, Investigation of geometrical deterioration of tramway tracks. Nauka ta progres transportu, Vol. 86, No. 2, 2020, pp. 46-59

[11]   Metalelektro Kft., A közúti vasúti vágányok pályaállapot-felmérésére alkalmas, Ganz 8 tengelyes villamos motorkocsira felszerelt, inerciális szenzor alapú képrögzíő rendszerrel kiegészített járműdinamikai mérőrendszer (Vehicle dynamics measurement system for the track condition of tramway tracks, equipped with a Ganz 8-axle EMU with an inertial sensor-based image recording system) 2016

Study of Railway Steel Bridges' Behaviour in Order to Identify the Causes of Their Defects

Serhii Kliuchnyk, Pavlo Ovchynnykov

Dep. "Transport infrastructure", Dnipro National University of Railway Transport named after Academician V. Lazaryan, Lazaryana st. 2, Dnipro, Ukraine, 49010, e-mails: serhij_klyuchnyk@diit.edu.ua, pavlo_ovchynnykov@diit.edu.ua

Abstract: The purpose of this work is to clarify the causes and mechanism of premature origin of defects in the elements of the bridge deck with the storey connection in steel span structures of railway bridges by studying the stress-strain state of their deck beams. Research aimed at extending the service life and increasing the carrying capacity of metal girder structures with a low load class and at the introduction of a new design solution for connecting the nodes of the deck beams, which is extremely important to ensure the necessary railway capacity and train safety. Service life and reliability of stringer beams of a deck definitively defines a service life and carrying capacity of all span structure. In order to deepen the analysis of the experimental data of the tested structures, calculations of the structure with the initial data, that fully correspond to the experimental span structure, were performed. For theoretical researches the underslung span structure with through trusses, designed by "Proektstalkonstruktsiya" with the nominal span of Ln = 44,0 m with a storey carriageway was chosen, as the one having the greatest number of defects in nodes of stringers support by the floor beams. According to the results of calculations and computer simulations, it is determined that the main cause of cracks is the structural imperfection of the aforementioned nodes, that is typical of similar structures.

Keywords: railway bridge; bridge deck; storey connection; stress-strain state; truss bridge

1 Introduction

After WWII the development of bridge infrastructure occurred using girder structures designed by "Proektstalkonstruktsiya" ("Project-steel-construction", PSC). Dynamic construction of artificial structures – around 1 550 bridges constructed – occurred during the country's rebuilding period – from 1946 to 1962. These structures were designed to save materials using lightweight design load standards that do not meet modern requirements. On the railways of Ukraine at present almost 13% of metal girder structures are considered defective, and about 47% have an insufficient load class [1], so the issue of determining the real operational resource of girder structures and determining ways to increase it

becomes especially relevant. Improving the reliability of bridges is one of the main tasks of the track network maintenance, as bridges are the most responsible and complex elements of roads. In fact, it is the bridges that determine the bearing capacity of the tracks [2].

2   General Characteristics of Girder Structures according to PSC Projects

In 1944, the design bureau "Projectsteelconstruction" (PSC) in conditions when in a short time it was necessary to manufacture and install on bridges an extremely large number of destroyed metal girder structures, proposed new standard designs of truss girder structures with riding at the level of the top and bottom chords (deck-type and through-type) [3].

The design of the truss structures of the PSC (general diagrams, type of truss gratings, cross-sectional shapes of truss elements, construction of assemblies, joints, etc.) was unified for the manufacture of structures at the factory using machine riveting and maximum unification. Rated load of PSC girders is N7.

Characteristic features of the underslung girder structures of PSC are the reduction of the distance between the main trusses to 4.0 m, the use of cross ties of the main trusses and change of the deck beams design, which adopted the storey connection of stringers (S) and floor beams (F) [4, 5]. The design of the support of the stringers on the floor beams is shown in Figure 1.

For PSC span structures with a storey connection of deck beams the main defects and disorders are:

- loosening and rupture of vertical rivets or bolts attaching stringers to the floor beams;

- loose bearings of stringers by floor beams that leads to more intensive wear of metal and increase in dynamic action of a rolling stock;

- longitudinal cracks in the bottom flange angles of the stringers along the corners of the angles at their end segments;

- increasing the length of cracks and the appearance of punctures with complete separation of the horizontal edge of the stringers' flange angles;

- cracks along the corners of the top flange angles of the floor beams in the places of the stringers' bearing;

- punching horizontal edges of the top flange angles of the floor beams in the area of stringers' support.
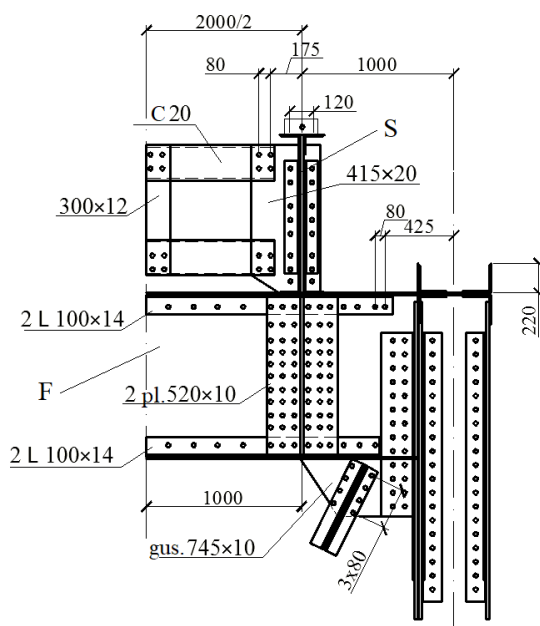
Figure 1
Design of the deck beams of the underslung PSC girder structures (S – stringer, F – floor beam)

For all girder structures, defective rivets attaching the stringers to the floor beams are replaced by high-strength bolts, which in most joints are not tightened, and in many places the bearing of the stringers by the floor beams is loosened with a gap up to 1.5-2.5 mm between the "fish-gussets" of the stringers and top flange angles of the floor beams. At passage of a rolling stock specified clearances are closed and "splashes" and wear of metal are observed. At the same time, it should be noted that at full tightening of bolts conditions occur that facilitate the emergence of local overstrains and cracks in the bottom flange angles of stringers and top ones of the floor beams in the conditions of a variable and alternating cycles of loadings.

The issue of increasing the reliability of the elements of railway and highway bridges is one of the most pressing [6, 7]. Fatigue cracks in the nodes of metal railway bridges appear in 3-20 years after the start of their operation [4, 5]. Operation of a bridge structure, with existence of fatigue damages in its nodes, can lead to restrictions in operation, decrease in loading capacity and an emergency condition of the whole structure.

3 Features of Deck Beams Work on Underslung Truss Structures

According to modern design standards for metal bridges [8, 9] as well as earlier standards, calculation of springers and floor beams of a deck is usually carried out as for simple beams on two hinged supports considering the corresponding constant and temporary loadings. In real conditions the stringers work as continuous beams on elastic supports - floor beams. Floor beams, in turn, rest on the nodes of the main trusses, which under loads yield vertical and horizontal displacements.

The influence of vertical displacements (deflections of the main truss nodes) on the stress state of the deck beams is insignificant and therefore most often is not considered. As for the continuity of the stringers, it is considered approximately. Bending moments at the support section in stringers over floor beams when calculating strength are accepted at a rate of 60% of the maximum bending moments in the middle of stringers.

Horizontal longitudinal displacements of the main truss nodes, on which the floor beams rest, occur due to the deformation of the truss chords. As a result of coupled work of stringers with chords of the main trusses, floor beams of the deck are bent horizontally. The magnitudes of the horizontal bending moments in the floor beams decrease from the ends to the middle of the span structure and depend on the distance between the main trusses (mainly on the distance between the stringer and the closest truss) [3].

To reduce deformations and horizontal bending moments in the floor beams (for medium and large spans), deformation gaps in the stringers are arranged, and in modern projects - rigid diaphragms at the end sections of the span structures. In the latter case, a reliable inclusion (according to calculation) of the stringers in the coupled work with the respective chords of the main trusses. At the same time the difference of longitudinal deformation of chords of trusses and stringers considerably decreases and operational conditions of floor beams improve. In the conditions of storey connection of the deck beams due to occurrence of large eccentricity between axes of stringers and floor beams, operation of cross beams and bearing details of stringers becomes much more complicated, and overstress and cracks occur in beams' flange angles. Connecting rivets (or bolts) of fastening of stringers to floor beams also operate in difficult conditions.

When designing metal girder structures, the transverse impacts from the rolling stock are taken into account as 6% of the design load. With beams connection in one level, the arm of the given force from cross blows is small, and with storey connection of beams this arm increases considerably that also leads to complication of work of deck beams.

In order to deepen the analysis of the work of the PSC girder structures, calculations were performed by the finite element method. For theoretical research the girder structure with through trusses of underslung type is taken, designed "Projectsteelconstruction" with the span of Ln=44,0 m with a storeyed deck. The specified truss is selected as the one with the largest number of defects in the nodes of the support of the stringer on the floor beam.

The assumption of the operation of the truss elements only on axial forces is based on the hypothesis of hinged nodes and nodal load transfer. In fact, due to inaccuracies in the centering of the elements in the nodes and the rigidity of the node connections, along with the axial forces in the truss rods, some bending moments occur. Bending moments cause additional stresses in the rods. These stresses are proportional to the linear stiffness of the elements adjacent to the nodes and, if the ratio of the heights of the elements to their length is more than 1/15, then when calculating the trusses, the stiffness of the nodes is considered [8, 9, 3].

Calculations were performed for the spatial truss span structure. This calculation scheme considers the rigidity of the nodes and most of the design features of the actual span structure.

The scheme of the metal span structure Ln=44.0 m is shown in Fig. 2.

As a computational model, a spatial scheme was constructed from rod elements, where the elements were modeled according to their geometric dimensions, which made it possible to estimate the own weight of the girder structure, as well as the corresponding distribution by elements masses for further assessment of elements masses on forces redistribution.
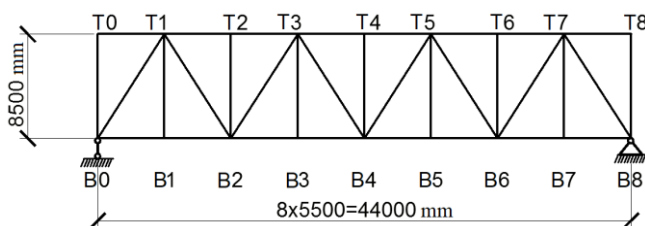
Figure 2
The scheme of the span structure Ln=44.0 m

It is very important at this stage of research by simplifying the calculation scheme not to lose the features of the entire structure of the girder and, in particular, the bridge deck – significant simplifications are unacceptable [10, 11].

The calculations were performed using the finite element method in the Selena 4.1.1 software. The solution of this problem will make it possible to objectively assess the stress-strain state in which the stringers and floor beams of metal bridges with storey connection. The main goal is to identify the interaction in the

operation of the beams with the elements of the truss and the influence of the continuity of the stringers on the stress-strain state of the floor beams.

As there is no possibility to set an addition weight of fastening elements, and also additional weight of hardware using this particular modeling, the overload factor from own weight was set as 10%.

In accordance with the design, all elements were assigned the material of the girder structure Steel 3, which allowed not only to distribute the weight in accordance with the cross-sections (depending on the cross-sectional area and density of the material), but also to consider the system in terms of material's mechanical properties.

4   Research of Deck Beams Work under Static Loading

Determination of forces in the deck beams under the static load of the span structure with a length of 44.0 m was performed in accordance with field tests of the bridge over the river Mokra Moskovka on 186 km of the line Kryvyi Rih – Volnovakha [12]. The load of the model is made according to the scheme of paired locomotives 2TE10. The scheme of static load of the locomotive 2TE10 is shown in Fig. 3, and schemes of loading for the research are shown in Fig. 4.
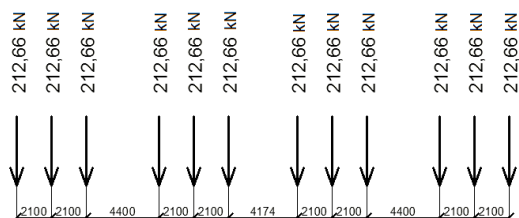
Figure 3
Scheme of static load model

The maximum values of the forces in the elements of the deck from the experimental load are shown in Tables 1 and 2.

As a result of the calculation, the fields of normal stresses along the X and Y axes, as well as the fields of tangential stresses were built.
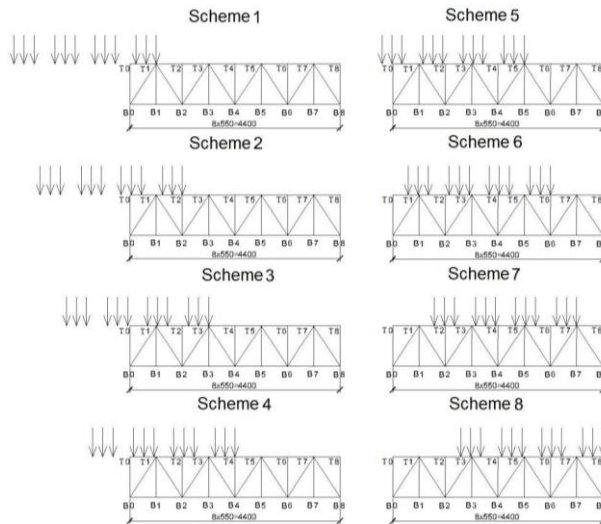
Figure 4

Schemes of loading of calculation model

Table 1

Bending moment (vertical) in the deck stringers, kN·m

Element according to the calculation scheme	Schemes of experimental loading							
	№1	№2	№3	№4	№5	№6	№7	№8
S0-1	153.6	94.3	80.3	142.5	79.7	104.9	-54.6	-14.2
S1-2	-60.5	144.8	115.1	101.2	176.0	84.1	132.9	-17.3
S2-3	2.7	16.5	155.4	138.6	93.2	178.1	109.1	148.5
S3-4	2.7	-15.6	-29.6	141.4	102.0	107.9	153.0	91.0
S4-5	1.35	8.3	7.1	-1.6	157.7	120.6	86.3	148.4
S5-6	1.3	5.3	12.3	7.6	-11.1	164.5	111.4	108.8
S6-7	1.2	5.2	11.0	17.4	20.1	-43.2	137.1	105.3
S7-8	-0.8	-3.2	-6.5	-9.3	-13.9	-19.4	-37.3	125.9

As a result of the calculation, the fields of normal stresses along the X and Y axes, as well as the fields of tangential stresses were built.

Analyzing these results yielded several conclusions:

- for the final floor beam F0, which is most intensively included in the joint work with the truss chords, the most unfavorable installation of the test load was the one according to scheme 6;

— maximum stresses occur in the floor beams of odd nodes F1, F7 (according to the loading schemes №5 and №6 for F1 and schemes №7 and №8 - for F7).

Table 2
Bending moment (vertical) in the floor beams of the deck, kN·m

Element according to the calculation scheme	Schemes of experimental loading							
	№1	№2	№3	№4	№5	№6	№7	№8
F0	105.9	129.3	20.7	122.0	46.9	34.0	-8.6	2.04
F1	148.2	216.8	253.3	241.8	229.9	249.1	66.5	-6.56
F2	-1.27	147.9	173.3	185.2	178.8	162.1	167.9	33.5
F3	-1.58	6.01	186.7	211.3	226.6	231.1	200.8	240.4
F4	-0.5	-8.04	-12.7	106.2	15.7	160.0	154.6	149.1
F5	-0.6	-1.75	-6.2	-4.7	177.8	202.1	216.1	209.2
F6	-0.7	-2.82	-5.9	-12.0	20.44	134.2	144.9	155.3
F7	-0.06	-0.08	-0.007	0.3	-1.4	9.3	191.8	216.5
F8	0.1	0.4	0.8	1.24	2.1	-1.5	-5.4	165.1

During the field test of the span structure beams F1 and F7 were not subject to stress measurement because the largest number of defects (ruptures of rivets, weakening of bolts, cracks along the edge of the stringers' flange angles at the nodes, their connection to the floor beams) was observed on these beams and measuring stress on already broken structures is virtually pointless [12].

The highest stresses σx in the flange angles of the floor beam F0 during the test reached +49.5 MPa (bottom) and -63.7 MPa (top), and the results of calculations are in the range from +87 MPa to -84 MPa, which almost coincides with the field tests results (depends on the location of strain gages).

Comparing the obtained data with the results of a field experiment [12] shows a significant match, both in qualitative and quantitative terms of almost all results (Tables 3, 4), which proves a high degree of reliability.

As it turned out, in the stringers the stress state does not exceed 100 MPa, and in the floor beams of the odd nodes F1 and F7 stresses significantly exceed the calculated strength of the material.

The reason for this is the inclusion of stringers in the joint work with the truss chords. It is believed that with spans of less than 60 m, this phenomenon may be ignored because it reduces the forces in the chords by less than 10%. At the same time, this slight force is transmitted through the floor beams to the stringers, causing not only the compression of later, but also the longitudinal bending with the torsion of the floor beams.

Table 3

Comparison of test results and calculation for floor beams

Loading schemes	Beam F0 (top)			Beam F2 (top)			Beam F4 (top)		
	Calc, MPa	Test, MPa	Δ, %	Calc, MPa	Test, MPa	Δ, %	Calc, MPa	Test, MPa	Δ, %
1	-21.50	-21.2	-1.4	3.60	3.8	5.3	-36.00	-42	14.3
2	-41.00	-47.1	13.0	8.00	8	0.0	-33.00	-36.7	10.1
3	-41.20	-41.5	0.7	-22.00	-24.5	10.2	-9.00	-9.8	8.2
4	-42.00	-40.1	-4.7	-115.00	-116.5	1.3	-51.00	-57.1	10.7
5	-60.50	-63.7	5.0	-105.00	-99.5	-5.5	-32.00	-36.8	13.0
6	-34.00	-32.5	-4.6	-105.00	-106.6	1.5	-31.00	-35.1	11.7
7	-22.00	-22.6	2.7	-93.00	-94.5	1.6	-29.00	-32.7	11.3
8	-18.50	-18.9	2.1	-124.00	-131.5	5.7	-25.00	-28	10.7

Table 4

Comparison of test results and calculation for stringers

Beam		Loading schemes							
		1	2	3	4	5	6	7	8
S1-2	Calc, Mpa	-3.6	11.0	13.5	12.75	15.0	10.8	20.0	-7.8
	Test, MPa	-3.5	10.4	13.3	12.8	15	10.9	19.7	-8.6
	Δ, %	-2.9	-5.8	-1.5	0.4	0	0.9	-1.5	9.3

The total values of stresses σx in the beams are shown in the graphs, Figures 5-8.

The appearance of unacceptable overstress, which lead to cracks and other defects, significantly reduce the durability and bearing capacity of the span structures of railway bridges in operation.
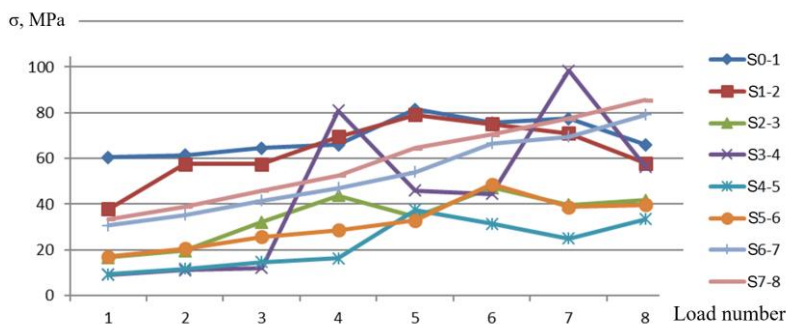
Figure 5

Total positive values of normal stresses in the deck stringers, MPa
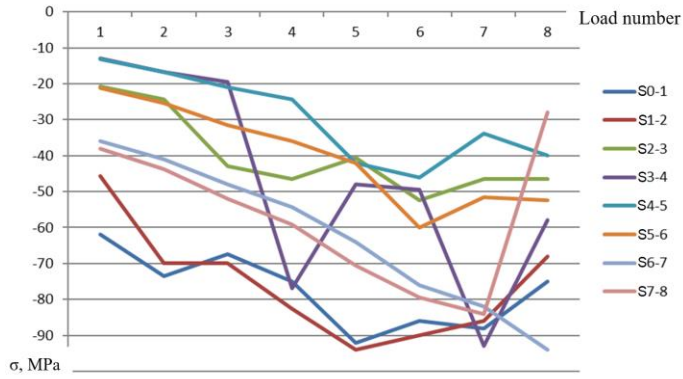
Figure 6

Total negative values of normal stresses in the deck stringers, MPa
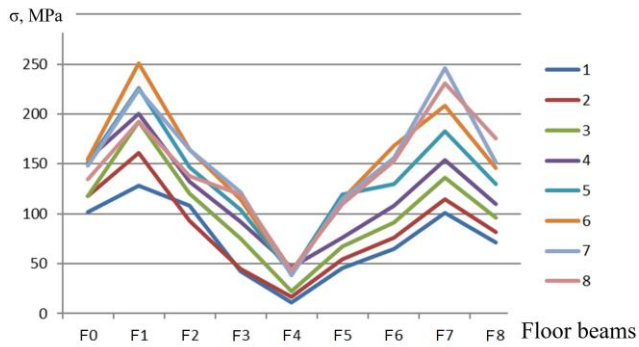
Figure 7

Total positive values of normal stresses in the deck floor beams, MPa
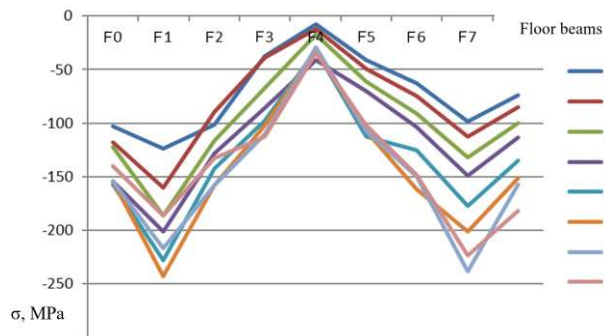
Figure 8

Total negative values of normal stresses in the deck floor beams, MPa

Conclusions

1) In almost all nodes of the support of the stringers on the floor beams of the studied span structures there is an excess of the calculated resistance of the material of the girder structures - steel St3 and in many the yield point of material is exceeded, especially in nodes where on the carried-out inspections demonstrated bearing disorders.

2) According to the results of calculations and computer simulations, it is determined that the main cause of cracks is the structural imperfection of the bearing nodes of the stringers on the floor beams of the span structure with a storey deck, that is typical for similar structures.

3) The main factor that causes the appearance of defects is the bending moment in the floor beam relative to the axis of the stringer, which due to the transfer of forces to a small area of the rivet joint leads to significant stresses in the lower edge of the bottom flange angles of the stringers. Such an occurrence is possible when the rivet joint is defect and is associated with residual deformations of the flange angles in the stringer and floor beam from the cyclic load.

4) With increasing span length and, accordingly, increasing forces in the support nodes of the stringers on the floor beams, the stress and the probability of cracks in the bottom flange angles of the stringers increases too.

5) The presence of significant main stresses in the nodes, where there are no obvious cracks may indicate the presence of hidden defects, which requires additional examination and study.

6) Analysis of the stress-strain state of the existing structure of the support node of the stringers on the floor beams indicates the complex operating conditions of the beams. Stresses in the horizontal edges of the angles reach 230-330 MPa, which significantly exceeds the calculated values of metal resistance.

References

[1] Kliuchnyk S. V.: Analysis of the current state of metal girder structures of railway bridges, Bridges and tunnels: Theory, Research, Practice. Collection of scientific works of Dnipropetrovsk National University of Railway Transport named after Academician V. Lazaryan, 12, 2017, pp. 29-40 [in Ukrainian]

[2] Soldatov K. I. and Blokhyn S. Y.: Course on strengthening and reconstruction of the operated artificial constructions of the railways of Ukraine, Bulletin of Dnipropetrovsk National University of Railway Transport, 33, 2010, pp. 262-271 [in Russian]

[3] Bychkovskij N. N and Dankovcev A. F.: Steel bridges, Saratov, 2005, 363 p. [in Russian]

[4]   Kliuchnyk S. V. and Marochka V. V.: Experience in operating a storey bridgedeck, Abstracts of the 72nd International Scientific and Practical Conference "Problems and Prospects for the Development of Railway Transport", Dnipropetrovsk, Ukraine, 2012, p. 158 [in Russian]

[5]   Kliuchnyk S. V. and Marochka V. V.: Review of options for reinforcement and repair of storey type bridgedeck beams, Bridges and tunnels: Theory, Research, Practice. Collection of scientific works of Dnipropetrovsk National University of Railway Transport named after Academician V. Lazaryan, 5, 2014, pp. 35-40 [in Ukrainian]

[6]   András Bakó and László Gáspár.: Development of a Sustainable Optimization Model for the Rehabilitation of Transport Infrastructure, Acta Polytechnica Hungarica, Vol. 15, No. 1, 2018, pp. 11-33

[7]   Németh, A. and Fischer, S.: Investigation of the glued insulated rail joints applied to cwr tracks, Facta Universitatis Series Mechanical Engineering, online first, 2021

[8]   DBN B.2.3-14:2006. Transport structures. Bridges and pipes. Design rules., Kyiv: Ministry of Construction, Architecture and Housing, 2006, 359 p. [in Ukrainian]

[9]   DBN B.2.3-26:2010 Transport structures. Bridges and pipes. Steel structures. Design rules. Part 1, 2., Kyiv: National Transport University, 2011, 108 p. [in Ukrainian]

[10]   Vaszilievits-Sömjén, B., Szalai, J., Movahedi, R. M.: Warping transfer superelement model for bolted end-plate connections subject to 3D loads, SDSS 2019 - International Colloquium on Stability and Ductility of Steel Structures, 2019

[11]   Xin Chen, Nao-Aki Noda, Magd Abdel Wahab, Yu-Ichiro Akaishi, Yoshikazu Sano, Yasushi Takase, Gusztáv Fekete: Fatigue Failure Analysis for Bolt-Nut Connections having Slight Pitch Differences using Experimental and Finite Element Methods, Acta Polytechnica Hungarica, Vol. 12, No. 8, 2015, pp. 61-79

[12]   Kluchnik S. V.: «Stress-strain state of beam staged connection point of the railway bridge track-way» Science and Transport Progress. Bulletin of Dnipropetrovsk National University of Railway Transport, 3 (69), 2017, pp. 160-170

Investigation of the Horizontal Track Geometry regarding Geogrid Reinforcement under Ballast

Szabolcs Fischer

Széchenyi István University
Egyetem tér 1, H-9026 Győr, Hungary
fischersz@sze.hu

Abstract: This paper was written concerning a test section with geogrid-reinforced railway ballast based on field tests. I aim to introduce the variation of the alignment track geometry parameter taking into consideration the geogrid reinforcement. The main advantage of the ballast reinforcement with geosynthetic inclusions is the reduction of the longitudinal level faults and the deterioration speed. I observed the alignment (i.e., the horizontal geometry) changes. The duration of the field test is approximately 11.5 years. Five different geogrid types were incorporated below the ballast bed on the Kelenföld-Hegyeshalom state board (No. 1) railway line in Hungary in 2010. The test section is only straight for 700 m in length (with reference sections with the same geometry and structural set-up), i.e., the horizontal geometry of the track does not influence the results. A statistical analysis was executed to compare the behavior of the sections, based on both the geogrid-reinforced sections and reference sections. As a result of the investigation, it can be concluded that there were some geogrid types, which seemed to be adequate to decrease the deterioration speed of the alignment parameter of the ballasted railway track. A very high variance (standard deviation) was observed in the results, this is because they cannot be determined as a general horizontal railway track stabilizing solution.

Keywords: geogrid reinforcement; railway; geometrical stabilization; ballast; alignment

1 Introduction

Railway transportation is one of the most environment-friendly solutions in the world because it chiefly uses electric hauling. The prevailing superstructure type is the ballasted track; the ballastless track set-up is mainly related to high-speed railways, bridges, tunnels, trams, and subways [1]. The railway cross-section of ballasted railways contains super- and substructure. Primarily, the superstructure is loaded by the highest forces from the railway vehicles. The most considerable inner forces arise in the rails, however, the ballast bed's top surface receives approximately 300-400 kPa normal (vertical stresses); while the subgrade is loaded by 100 kPa [2]. The high stresses can result in significant plastic vertical

deformation in the sub- and super-structures, which leads to frequent geometrical correction.

A lot of literature are concerned with the rails [3-6]. Some researchers publish about rail wear process in straight and sections with horizontal curves [3]; the rail's and wheel's corrugations, and the changed bearing capacity due to rail wear [4]. Kuchak et al. [5] analyzed rail dampers using finite element method (FEM). Kazemian et al. [6] assessed the condition monitoring of vibration of ballasted tracks in Iran based on rail problems. The fragmentation and breakage of the ballast particles connects to the environment protection because of the frequent ballast screening process, as well as the dust pollution. Benmebarek and Movahedi [7] dealt with the discrete element modeling of fragmental granular materials; hence Sysyn et al. [8] performed laboratory experiments searching the accurate relationship between interlocking effect and the testes materials, as well as the applied loading condition. Ballast interlocking is a relevant field regarding the deterioration of the ballasted track that is able to be improved by geosynthetic layers.

If someone considers the accurate geodesy and comprehensive integrated infrastructure related to railways, the papers of Kampczyk and Dybel [9], and Matejov and Sestakova [10] can be referred.

This paper is about geosynthetic reinforcement that can stabilize the track geometry of ballasted tracks. Geosynthetic reinforcement is a well-known solution for soil stabilization. The geosynthetic inclusions provide additional shear and tensile strength to the soils. It has to be mentioned that the geosynthetic reinforcement is adequate for soils, and the granular media, too [11-13].

Incorporating geogrid layer under ballast can improve the track structure's inner shear resistance and load-bearing capacity [14]. However, the interaction behavior between ballast aggregates and geosynthetic is not yet fully known.

The author started his research in this area in 2008. In 2010, a test section was built using five geosynthetic types, adequate for railway geometry stabilization; thus, 11.5 years have elapsed since then. The author assembled the measurement data recorded by railway track geometry measuring car. In this paper, he analyzed the alignment parameter in this test section, i.e., the effect of geogrid-reinforcement under the ballast bed on changing the horizontal geometry of the ballasted railway track. It is not evident whether the geogrid layer stabilizes the alignment or not. The general goal of the paper is not to declare which geosynthetic product is the best or more valuable than the others. The geogrids' original name and product type have not been used; only anonym designations (GG1 to GG5).

The author submitted a paper in Geotextiles and Geomembranes journal, in which he analyzed the vertical track geometry [15]. This current paper deals with only the horizontal geometry, i.e., the alignment railway track geometry parameter.

2 Methods

2.1 Methods for Calculation

A railway test section was configured on the No. 1 railway line in Hungary (see Fig. 1).
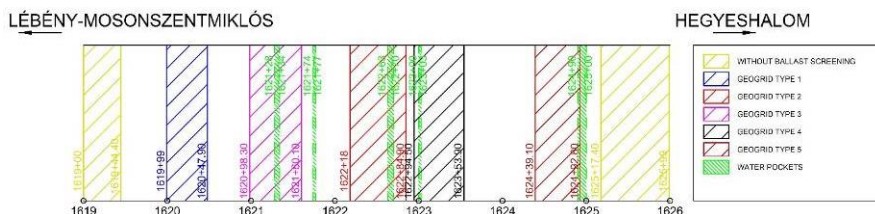
Figure 1

Locations of subsections at the test site (the internal white zones are the WG subsections; WBS: without ballast screening, WG: without geogrid))

The field tests are related to measuring, calculating, determining, and evaluating railway track geometry changes. The author details the performed measurements as below:

i) Geometric (geodetic) leveling in the time interval 2010 and 2014

ii) Railway track geometry measurements in the time interval 2010 and 2021

In i), the distance of measuring points was 1.8 m. The following parameters were determined by calculation: i) cross-level (height difference between rail heads; i.e., similar to the superelevation parameter but not only in the curve); ii) longitudinal level (i.e., the settlement; based on different chord lengths); iii) twist (i.e., the plane distortion; based on different base lengths); iv) settlement values on individual sleepers.

The author applied and dealt only with the above ii) measurements and their data processing, evaluation.

The effective field (railway track geometry) measurements were carried out using the FMK-007 type recording car of MÁV CRTI Ltd. (Central Rail and Track Inspection Ltd.) [16]. The dynamic (related to vehicle) measurements were not considered in this paper. The author summarized the measurable and countable parameters of the recording car [16]:

i) Track gauge (unit: mm)

ii) Cross-level (unit mm)

iii) Twist on five different bases (units: mm/m or mm/mm)

iv) Longitudinal level on original or on any chord, and in D1 or D2 wavelength range (unit: mm)

v)   Alignment on original or on any chord, and in D1 or D2 wavelength range (unit: mm)

vi) Gauge-changing on any base (unit: mm/m or mm/mm)

vii) Average-gauge on any base (unit: mm)

viii) Curvature (unit: 1/m or 1/mm)

ix) Twist-differences on 5 different bases (unit: mm/m or mm/mm)

x)   Longitudinal level moving standard deviation on any base (unit: mm)

Statistical methodologies were applied for the calculations and assessments of the test sections: regression analysis was executed to be able to compare the deterioration of the different subsections. Linear regression functions and approximation for the deterioration of railway track geometry were used, Nagy and Horvat [17] published and certified that this approximation is adequate for straight sections up to 10 years.

The author decided to analyze in this paper only the alignment, one of the railway track geometry parameters. In the international literature, no one has certified and published whether how the geogrid reinforcement under ballast bed influences the alignment of the railway track; in straights or in curves, as seen in Eq. (1):

$$IR\_CL = IR_{left} + IR_{right} \tag{1}$$

where IR is the measuring value related to alignment parameter calculated by area method (unit: dm^2); CL: characteristic length, based on Hungarian railway diagnostics practice [18], is 200 m; in this paper, 10 m length value was taken into consideration); IR_{left} and IR_{right}: alignment measuring values (or numbers) for the left and right rails using area method, respectively (unit: dm^2);

It has to be noted that the alignment parameter was determined with the measured data per 25 cm; ensuring the FMK-007 recording car. The IR measuring numbers was considered as chord-basis measurement, not the D1 (i.e., chord-torsion-free) assessment. The author considered only the alignment 'IR_10 m' parameter. Measurements by FMK-007 recording car: there were 34 measurement dates between 30.08.2010 and 27.07.2021.

2.2   Applied Geosynthetic Types and Their Properties

The type of installed geogrids are detailed in Tables 1, 2, 3, and Fig. 2. Fig. 2 contains the meaning of the abbreviations in Table 1, while MD means machine direction, XMD means cross-machine direction.
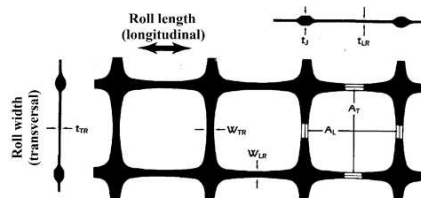
Figure 2

Meanings of geometrical characteristics of installed geogrids

Table 1

The characteristics of installed geogrids 1

Geogrid types	Base mate-rial	Prod. techn.	Uniaxial/ biaxial	A_L [mm]	A_T [mm]	W_{LR} [mm]	W_{TR} [mm]	t_J [mm]	t_{LR} [mm]	t_{TR} [mm]
GG1	PP[4]	extruded	biaxial	65.0	65.0	4.0	4.0	7.0	1.7	1.5
GG2	PP[4]	extruded	biaxial	65.0	65.0	4.0	4.0	7.0	1.7	1.5
GG3[1]	PP[4]	extruded	biaxial	65.0	65.0	4.0	4.0	7.0	2.5	1.5
GG4[2]	PP[4]	welded	biaxial	80.0	80.0	8.8	8.2	2.1	1.4	1.4
GG5[3]	PP[4]	welded	biaxial	80.0	80.0	8.8	8.2	2.1	1.4	1.4

[1]: it is the same as Geogrid type 1, but factory combined with geotextile
[2]: factory-made geocomposite; i.e., the geotextile is between the ribs
[3]: it is the same as GG4 but manually combined with geotextile under geogrid
[3]: polypropylene

Table 2

The characteristics of installed geogrids 2

Geogrid types	Ultimate tensile strength		Tensile strength at 2% elongation		Elongation at max. strength	
	MD [kN/m]	XMD [kN/m]	MD [kN/m]	XMD [kN/m]	MD [kN/m]	XMD [kN/m]
GG1	30	30	11	12	N.A.	N.A.
GG2	30	30	11	12	N.A.	N.A.
GG3[1]	26.3	28	10	9	N.A.	N.A.
GG4[2]	30	30	12	12	N.A.	N.A.
GG5[3]	30	30	12	12	N.A.	N.A.

Table 3

The characteristics of installed geogrids 3

Geotextile in the geo-composite	Puncture force [N]	Tensile strength		Elongation at max. strength		Water perme-ability [m/s]	Water perme-ability [ℓ/sm²]	Mass per unit [kg/m²]	Charac-teristic opening size [mm]
		MD [kN/m]	XMD [kN/m]	MD [kN/m]	XMD [kN/m]				
GG2	>1500	N.A.	N.A.	N.A.	N.A.	0.135	135	0.160	0.125
GG4	1670	6	11	60	40	0.110	110	0.150	0.130
GG5[3]	1670	6	11	60	40	0.110	110	0.150	0.130

3   Field Tests

In Table 4, the author gives the details of the parameters related to all the subsections.

Table 3

The characteristics of installed geogrids 3

sectioning	1619+00…1626+00 (these are hectometer section formats; i.e., 1619+00 means 161.9 km)
right or left track of the railway line; straight or curve(d) section; type of railway embankment (fill or cut)	right; straight; fill
longitudinal slope	+0.64 mm/m according to the sectioning
allowed speed and axle load; type of superstructure	V=160 km/h; Q=225 kN; ballasted CWR track
rail profiles and rail fasteners	54 E1 (i.e. UIC 54) rail profiles, rolled in Diósgyőr (Hungary) in 1980; Vossloh Skl 3 type flexible rail fasteners
sleepers and sleeper space	LM 80 type reinforced-concrete sleepers; 60 cm sleeper spaces
ballast type; effective ballast depth	31.5/50 mm A or B according to EN 13450:2002 standard [19]; effective ballast depth: 41…54 cm (based on the field measurements in 2010)
dewatering problem	there is a dirt road on the right side of the permanent way, its level is relatively high, and the precipitation was hardly able to run off/flow away from the track. This problem was partially solved in 2011 and 2014; location of water pockets: see Fig. 1
the type of installed geogrids and their location	see Tables 1, 2, and 3, as well as Fig. 1
geotechnical parameters of the site	see Fig. 1, and Tables 5 and 6

The author collected the geotechnical parameters and characteristics of the sections with water pockets in April 2010 in Tables 5 and 6, before the geogrid installation. The E_2 load bearing capacity values are according to the Hungarian standard [20], and they are measured with static load plate test.

Table 5

The characteristics of subgrade soils in/under water pockets 1

Characteristics	Sectioning			
	1620+50	1621+29	1621+70	1622+58
Soil name	silt	lean clay	silt	lean clay
Water content: w [%]	22.4 / 22.5	20.9 / 20.0	20.9 / 25.5	21.6 / 23.1
Liquid limit: w_L [%]	33.6	35.5	33.9	35.8
Plasticity index: I_P (%)	13.3	15.2	14.1	15.4

Void ratio: e [–]	0.65	0.60	0.61	0.61
Relative saturation: S_r	0.93	0.94	0.93	0.96
Compressibility (bulk) modulus: E_s (MPa)	3.7	3.7	3.1	3.2
Load bearing capacity (with static plate test): E_2 (MPa)	13.6	19.6	16.9	15.2

Table 6
The characteristics of subgrade soils in/under water pockets 2

Characteristics	Sectioning			
	1623+05	1624+00	1624+95	1625+50
Soil name	silt	silt	silt	silt
Water content: w [%]	22.4 / 20.8	19.4 / 21.1	20.8 / 18.5	20.7 / 20.8
Liquid limit: w_L [%]	34.5	31.0	32.6	37.9
Plasticity index: I_P (%)	12.8	12.4	13.3	13.9
Void ratio: e [–]	0.65	0.57	0.57	0.61
Relative saturation: S_r	0.93	0.93	0.98	0.92
Compressibility (bulk) modulus: E_s (MPa)	2.8	2.6	3.6	3.0
Load bearing capacity (with static plate test): E_2 (MPa)	15.1	19.6	18.6	21.1

The author chose this 700 m long section for his analysis due to the continuous intensive deterioration between 1999 and 2010. A ballast cleaning was planned in 2010 to repair the sections with water pockets. This work was supplemented with the geogrids' installation on nights of May 25/26 and 26/27, 2010. It has to be noted that during the ballast cleaning, there was a little rain, the contamination remained in the ballast bed due to the wet ballast particles, i.e., the work can't provide the best result.

Four different deterioration phases were considered. The author collected the elapsed days and the cumulated million gross tons, which were calculated from the last correction tamping after the geogrids' installation (June 16, 2010; 0 MGT). The Hungarian State Railway (MÁV) supplied the data below.

- Deterioration phase #9: between 25.11.2013 (Day 1257; 25.966 MGT) and 03.08.2014 (Day 1508; 37.703 MGT)

- Deterioration phase #10: between 25.11.2014 (Day 1622; 44.058 MGT) and 25.04.2016 (Day 2139; 65.707 MGT)

- Deterioration phase #11: between 15.08.2016 (Day 2251; 70.151 MGT) and 09.08.2019 (Day 3340; 115.194 MGT)

- Deterioration phase #12: between 09.12.2019 (Day 3462; 420.402 MGT) and 27.07.2021 (Day 4058; 145.132 MGT)

The dates of the tamping processes can be seen in Fig. 3.

It has to be mentioned that the geometrical deterioration of the railway track is mainly influenced by the tamping process (manually or machine). It has to be taken into consideration. Because of that, deterioration phases #1 to #8 were neglected in the calculations due to their relatively short phases.

4   Results and Discussion

The author gave his results in Figs. 3-4. The abbreviations and vertical dashed lines in the figures have the following meanings:

- GG1…GG5: sections established with GG1…GG5 type geogrids under ballast bed

- the eleven vertical dashed black lines in the figures show the date of tamping processes between June 17, 2010, and July 27, 2021 (see Chapter 3)

Figs. 3-4 contain the graphs related to variation compared to the WG subsection's behavior. Therefore, it is the only adequate basis to compare the different subsections regarding the reinforcement effect, i.e., the effect on the variation of the alignment (track geometry) parameter.

The average (A) and the standard deviation (SD) values were computed based on all the subsections (see Fig. 1), the shorter subsections (i.e., WG) were considered altogether in a common section. The relative standard deviation (RSD) values can be determined based on the ratio of SD and A; it is not calculated from the whole data series, only the estimated two numbers: standard deviation and average.

Fig. 4 has the only results related to those whose R^2 value was higher than 0.7 (mainly higher than 0.8, but some were taken into consideration with $R^2=0.7…0.8$ coefficient values).

Fig. 3 d)-f), and Fig. 4 are worth analyzing in detailed manner. Based on the results of Figs. 3 d)-f), it can be concluded that the ratio of the different subsections had varying behaviors considering the alignment (track geometry) parameter. 0.6…1.3; 0.2…2.5; 0.5…1.3 ranges can be seen, in case of VorA, VorSD, and VorRSD, respectively. The meanings of these abbreviations can be found in the title of Fig. 3.
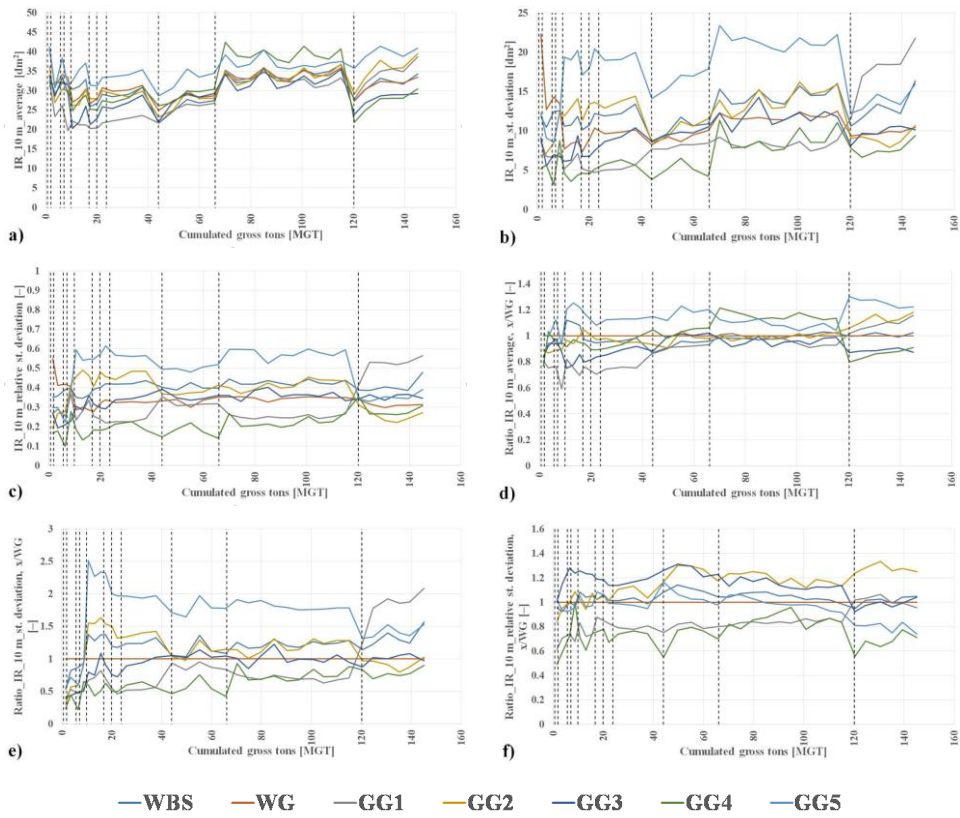
Figure 3

a) Variation of IR_10 m_average (VoA) parameter; b) Variation of IR_10 m_standard deviation (VoSD) parameter; c) Variation of IR_10 m_relative standard deviation (VoRSD) parameter; d) Variation of the ratio of IR_10 m_average (VorA) values calculated for the different subsections to the average values calculated for the WG subsection; e) Variation of the ratio of IR_10 m_standard deviation (VorSD) values calculated for the different subsections to the average values calculated for the WG subsection; f) Variation of the ratio of IR_10 m_relative standard deviation (VorRSD) values calculated for the different subsections to the average values calculated for the WG subsection
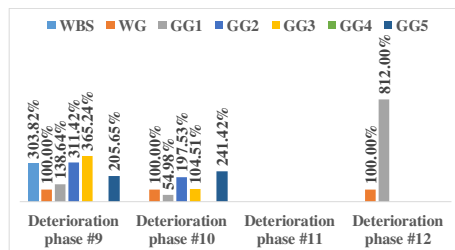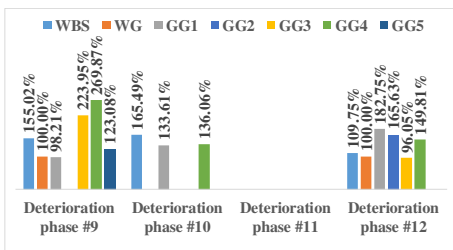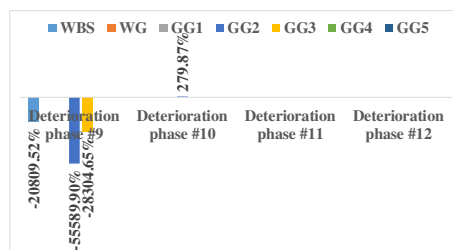
Figure 4

Above left: Deterioration speed values of IR_10 m_average related to the deterioration phases #9 to #12 compared to the deterioration speed of subsection WG; Above right: Deterioration speed values of IR_10 m_standard deviation related to the deterioration phases #9 to #12) compared to the deterioration speed of subsection WG; Bottom: Deterioration speed values of IR_10 m_relative standard deviation related to the deterioration phases #9 to #12 compared to the deterioration speed of subsection WG

First, the author can state that in Fig. 4, the above right and bottom charts show useless information, so the deterioration speed of SD and RSD functions can't be applied to assess the changing alignment track geometry parameter. The missing columns indicate that the correlations are inadequate, and they have to be neglected in the evaluation.

Based on Fig. 3, it can be concluded that the line WG show a general deterioration rate (see Fig. 3a); variation of average values of alignment). It means that the comparison can be appropriate. There are only very few types of geogrids (see Fig. 3 d)-f)) which provided better behavior than the WG subsection. If all the A, SD and RSD are considered, only the GG4 subsection can ensure reinforcement, i.e., lower ratios than the subsection WG. It is a very interesting result that GG5 shows poor achievement (even up to 1.30 ratio) in case of A and SD (Fig. 3 d) and e)), but in the case of RSD (Fig. 3 f)) its result seems to be one of the best (even lower than 0.80…0.75). GG3 can also be mentioned regarding the A (see Fig. 3, a)) as a potential adequate reinforcing solution.

If someone analyzes and assesses Fig. 4, the above-left chart in the deterioration phase #12, only the GG3 subsection is able to be noted (with 96.05%) as an appropriate one. The other sub-charts and deterioration phases don't contain consequent results, which can be adequate for correct evaluation. The highest value (182.75%) is connected to the GG1 subsection. It is extraordinary because GG1 type geogrid ensured one of the best reinforcement effects in vertical geometry [15].

The results show a very high variance (standard deviation); in this way, the author cannot state that the geogrid reinforcement unequivocally helps in stabilizing the horizontal geometry of the ballasted railway track.

Conclusions

I summarized my experiences, concerning the changing of alignment track geometry parameters, on a test site in Hungary, where five different types of geosynthetic layers were applied under the ballast bed. These geosyntetic inclusions were installed in the right track of No. 1 MÁV railway line in May 2010, since then, 11.5 years have elapsed. I presented my results in another paper related to the vertical track geometry [15], however, the work herein is about the stabilization of the horizontal geometry. FMK-007 type track geometry, recording car's measurements, can be applied for the statistical time-series analysis, to compare the sections with each other and with the reference sections (subsection WG – without geogrid reinforcement).

The International Literature is not conclusive and it is not evident that geosynthetic reinforcements under the ballast bed, in the railway superstructures, can or cannot stabilize, the horizontal track geometry. I have shown that the GG3 and GG4 geogrid types seem to be adequate. The GG3 was able to decrease the deterioration speed of the railway track geometry, regarding alignment (IR) parameter; hence, the GG4 geogrid type ensured a significantly low value, in the case of VorA, VorSD and VorRSD.

The results show a very high variance (Standard Deviation); in this way, I cannot state that the geogrid reinforcement unequivocally helps in stabilizing the horizontal geometry of the ballasted railway track.

My future plans are to continue my research related to this test site. The future measurement data can be the basis of additional and more detailed assessments.

Acknowledgement

References

[1]   V. Jover, L. Gaspar, S. Fischer, Investigation of Geometrical Deterioration of Tramway Tracks. Nauka ta Progres Transportu, Vol. 86, No. 2, 2020, pp. 46-59

[2]   A. Németh, S. Fischer, Investigation of glued insulated rail joints applied to CWR tracks. Facta Universitatis-Series Mechanical Engineering, 2021, 7642

[3]   M. Kurhan, D. Kurhan, R. Novik, S. Baydak, N. Hmelevska, Improvement of the railway track efficiency by minimizing the rail wear in curves. IOP Conference Series: Materials Science and Engineering, Vol. 985, No. 1, 2020, 012001

[4]   V. Kovalchuk, M. Sysyn, Y. Hnativ, A. Onyshchenko, M. Koval, O. Tiutkin, M. Parneta, Restoration of the Bearing Capacity of Damaged Transport Constructions Made of Corrugated Metal Structures. Baltic Journal of Road and Bridge Engineering, Vol. 16, No. 2, 2021, pp. 90-109

[5]   A. J. Tigh Kuchak, D. Marinkovic, M. Zehn, Finite element model updating - Case study of a rail damper. Structural Engineering and Mechanics, Vol. 73, No. 1, 2020, pp. 27-35

[6]   M. Kazemian, F. Astaraki, M. R. Movahedi, A. Taheri, Condition monitoring of vibration at weak parts of rail for ballasted railway tracks in Iran. Journal of the Korean Society for Railway, Vol. 24, No. 6, 2021, pp. 544-551

[7]   A. Benmebarek, M. R. Movahedi, DEM modeling of crushable grain material under different loading conditions. Periodica Polytechnica Civil Engineering, Vol. 65, No. 3, 2021, pp. 935-945

[8]   M. Sysyn, O. Nabochenko, V. Kovalchuk, M. Przybyłowicz, S. Fischer, Investigation of interlocking effect of crushed stone ballast during dynamic loading. Reports in Mechanical Engineering, Vol. 2, No. 1, 2021, pp. 65-76

[9]   A. Kampczyk, K. Dybeł, Integrating surveying railway special grid pins with terrestrial laser scanning targets for monitoring rail transport infrastructure. Measurement: Journal of the International Measurement Confederation, Vol. 170, 2021, 108729

[10]   A. Matejov, J. Šestáková, The Experiences with utilization of BIM in railway infrastructure in Slovak Republic and Czech Republic. Transportation Research Procedia, Vol. 55, 2021, pp. 1139-1146

[11]   Q. Gu, K. Shi, X. Bian, S. He, Behavior of Geogrid-Reinforced Railway Ballast under Train Traffic Loads. Lecture Notes in Civil Engineering, Vol. 165, 2022, pp. 689-701

[12]   S. F. Ibrahim Alabdullah, A. J. Kadhim, H. B. Khalaf, Life Cycle Cost Analysis for Reinforced Geogrid Railway Track. International Journal of GEOMATE, Vol. 19, No. 75, 2020, pp. 191-196

[13]   Y. Jiang, S. Nimbalkar, Finite element modeling of ballasted rail track capturing effects of geosynthetic inclusions. Frontiers in Built Environment, Vol. 5, 2019, 69

[14]   S. Fischer, Investigation of Inner Shear Resistance of Geogrids Built Under Granular Protection Layers and Railway Ballast. Nauka ta Progres Transportu, Vol. 59, No. 5, 2015, pp. 97-106

[15]   S. Fischer, Geogrid reinforcement of ballasted railway superstructure for stabilization of the railway track geometry – A case study. Geotextiles and Geomembranes, 2021, submitted manuscript

[16]   MÁV CRTI Ltd., Track diagnostics - FMK-007 track measuring wagon. http://mavkfv.hu/index.php?f=vaganydiagnosztika_fmk007 [online, last visited on: 2021.10.04]

[17]   R. Nagy, F. Horvat, Indirect determination of the measurement accuracy of the FMK-004 track geometry measuring carr used on Hungarian rail network. The 16th International Conference Computational Civil Engineering 2021, IOP Conference Series: Materials Science and Engineering, 2021, 10 p.

[18]   Hungarian State Railways, D.54, Construction and track maintenance technical data, regulations. 1988

[19]   MSZ EN 13450:2003: Aggregates for railway ballast, 33 p.

[20]   MSZ 2509-3:1989, Bearing capacity test on pavement structures. Plate bearing test., 6 p.

Risk Analysis Model with Interval Type-2 Fuzzy FMEA – Case Study of Railway Infrastructure Projects in the Republic of Serbia

Dragana Macura[1], Milica Laketić[1], Dragan Pamučar[2], Dragan Marinković[3,4]

[1]University of Belgrade, Faculty of Transport and Traffic Engineering
Vojvode Stepe 305, 11000 Belgrade, Serbia
d.macura@sf.bg.ac.rs, m.laketic@sf.bg.ac.rs

[2]University of Defence in Belgrade, Department of Logistics
Pavla Jurisica Sturma 33, 11000 Belgrade, Serbia
dragan.pamucar@va.mod.gov.rs

[3]University of Nis, Faculty of Mechanical Engineering
A. Medvedeva 14, 18000 Nis, Serbia

[4]Technische Universität Berlin, Department of Structural Mechanics and Analysis,
Strasse des 17. Juni 135, 10623 Berlin, Germany
dragan.marinkovic@tu-berlin.de

Abstract: Considering the impact of risk events to costs, time and quality of infrastructure projects, it is necessary to invest in risk management in order to prevent or mitigate negative consequences. Risk analysis should monitor the project through the whole project life cycle: from the planning through execution and controlling to finishing. In this paper, we have used Interval Type-2 Fuzzy Logic based Failure Mode and Effects Analysis (FMEA) to get a better insight into the risk events that occur in the railway infrastructure projects. The study's main contribution is developing and implementing a comprehensive and robust framework for defining and handling with the most important risk events regarding the railway infrastructure projects. The Interval Type-2 Fuzzy Logic is used to tackle the uncertainty in risk assessment. In order to illustrate the validity and capability of the model, the presented approach has been applied to the railway infrastructure projects in the Republic of Serbia. Each risk event has been analyzed through severity, occurrence and detection. The events were ranked based on the Fuzzy Risk Priority Number (RPN). This research also proposes strategies for the most important events in terms of risk.

Keywords: Risk analysis; Railway infrastructure project; FMEA; Fuzzy logic; Interval Type-2 Fuzzy Sets

1 Introduction

The economic and social development of a country depends on the enlargement of the transport infrastructure, so the investment in the infrastructure development and maintenance is mandatory for the faster economic growth of a country. Risk management should play a key role in planning, project execution and later controlling the performed infrastructure project. It should be present throughout the whole life of the project and that is what makes the difference compared to the former realization of the project. Exceeding estimated costs, delays in construction deadlines, poor cooperation between management and contractors are just some of the events that can increase costs. The construction of large transport infrastructure projects in the past has recorded large budget overruns. Dealing with the risks and uncertainties are unavoidable challenge of every infrastructure project managers.

Some risks cannot be completely eliminated, but it is necessary to identify them effectively and in a timely manner in order to make a plan to mitigate their impacts. Risk management raises the awareness of management, elevate the probability of success in achieving goals, serves to exchange views within the organization, reduces surprises, increases self-confidence when making difficult decisions, provides higher quality services and protects the organization's reputation.

An infrastructure project is most often defined as a complex technical-technological, economic, financial and legal process consisting of a set of coordinated and controlled activities with the aim of implementing the project successfully to completion. Each project has its own estimated time to be completed. Of course, shifts in infrastructure projects are usually inevitable, but even in these time shifts there must be a limit. What most often leads to exceeding the scheduled deadlines for construction or modernization is considered as risk.

Literature often defines risk as uncertainty that can positively or negatively affect the project realization. Risk management allows the investor to anticipate potential negative outcomes that may occur during the project execution. Delays of project realization are often inevitable, but a risk management plan is used to predict them.

The risk management process, based on EU projects, consists of the following steps:

- risk identification and description;
- risk assessment;
- risk management (risk response);
- monitoring and reporting on risks.

The first step in the risk management process is to identify potential risks. Some of the methods for identifying risks are: checklists, use of data from the previous period, stakeholder consultations, comparison with similar organizations, etc. The description of the risk facilitates definition of measures for its reduction.

The risk assessment, which refers to predicting the probability of the occurrence on an unwanted event and the impact of the risk, was performed by experts. The impact of risk is based on an assessment of the effect that a negative event would have on the design of the project. The remaining two steps are performed by risk management in the organization itself.

It is desirable that the risk assessment be performed objectively in order to obtain as reliable data as possible. The more the risks are talked about and the more they are studied there are less chance of surprises.

This paper discusses railway infrastructure projects, from the aspect of risks that may occur during the construction, modernization and reconstruction of the railway infrastructure. The group decision – making was included in the model presented in this paper. Based on railway experts' opinions, expressed through a survey, the values of probability of occurrence, severity and detection of risks that are most often present on railway infrastructure projects in the Republic of Serbia were obtained. The survey respondents were the railway experts who work at: University of Belgrade, Faculty of Transport and Traffic Engineering (FTTE); Ministry of Construction, Transportation and Infrastructure of the Republic of Serbia (MoCTI); and Infrastructure of Serbian Railway JSC (ISR). Six experts were from the first two institutions and two were from ISR. Their answers have different weights according to their work experience, i.e., their years of service, and description of job. A higher weight has an expert working on the railway infrastructure projects. This has been done by WGMM (Weighted Geometric Mean Method).

Given that the extension of deadlines for the completion of construction or modernization of railway infrastructure is a frequent event, this study provides a better insight into the risks involved and indicates causes of delays in the implementation of infrastructure projects. Which risks are the most relevant, the most often and with high severity in the Republic of Serbia – was researched in this study. This has been done by FMEA. Afterwards, the Interval Type-2 Fuzzy logic system (IT2-FLS) was developed in order to help managers or decision makers in assessment of the risk event. The IT2-FLS model has an ability to present the real-world projects and tackle the uncertainty.

The aim of the developed model is to define the most important risks by subjective judgments of experts on the probability and impact under IT2-FLS FMEA. The advantages of the proposed model are: reducing the individual subjective preferences with multi-group decision making process, solving the real-world issue and handling the uncertainty with the Interval Type-2 Fuzzy logic.

This paper is organized as follows. After the Introduction, there is a brief review of the relevant literature related to the Type-2 Fuzzy Logic and FMEA applications. Then, Section 3 gives a description of the methodology applied for. The results of the proposed model are presented in Section 4. The last in the series is the conclusion, as Section 5.

2   Brief Literature Review

In risk detection of infrastructure projects, FMEA is considered one of the most used tool. FMEA in cooperation with Fuzzy Logic presents the reliable way of calculating risk from aeronautical to transportation projects. In the literature review process, the papers highlighted below use the FMEA and Fuzzy Logic to assess the risk of railway projects.

Panja et al. [1] dealt with the failure analysis of Indian railway signaling systems through fuzzy Risk Priority Number (RPN) and FMEA. Twenty five rules out of one hundred have been generated and taken as serious in risk assessment. Zhu et al. [2] introduced effective strategy for analyzing and diagnose urban rail transit vehicle maintenance. Fuzzy–set based assessment for FMEA as a quantitative tool is proposed for Shanghai URT System. Ghodrati et al. [3] showed integration of fuzzy RPN and Analytical Hierarchy Process (AHP) as a method for reducing uncertainties and ambiguities. The research topic is maintenance of rolling stocks. Huang and Zhang [4] described an approach which combines FMEA and pessimistic – optimistic fuzzy information, considering Acceptable Risk Coefficient (ARC) on an example of railway dangerous goods transportation. That approach presents system problems as ranking risks based on the level of severity. Tong et al. [5] used FMEA and fuzzy multiple attribute decision making theory to evaluate risk of the full life cycle of the Maglev train system. Sarkar and Singh [6] presented two combined approaches Fuzzy Expected Value Method (FEVM) and Fuzzy Failure Mode and Effects Analysis (FFMEA) for a complex infrastructure project for the metro rail in India. The authors used interactions with experts through questionnaire survey to identify major risks. Tafazzoli [7] experimented with the crisps value of fuzzy FMEA to identified and mitigate potential causes of delay in each infrastructure project through their priority. Priority level is determined on the basis of survey and expert opinions.

Type-2 Fuzzy logic is suitable for the risk analysis in projects, when there are a lot of imprecisions and uncertainty of data. There are recently published papers dealing with the prioritization and evaluation of the decisions and initiatives with Interval Type-2 Fuzzy Logic and other methods that could be easily implemented for the risk analysis regarding the transport projects, such as: COPRAS [8], Simulated Annealing [9], Interval Agreement Approach [10], Additive Ratio Assessment [11], MABAC [12]. In the literature review process, those papers that operate with Type-2 Fuzzy logic in order to achieve the highest quality assessments within the project risk management are highlighted. Most of these papers use some additional analysis to obtain reliable data.

Seyed et al. [13] provide a better insight into the application of an interval Type-2 Fuzzy risk analysis model (IT2FRAM) in order to determine the contingency reserve in construction projects. IT2FRAM is defined as an extension of a fuzzy arithmetic-based risk analysis method which deals with uncertainties through consideration of the opinions of several subject matter experts in a way to develop

the membership functions of linguistic terms. It's explained how Type-2 Fuzzy logic can aggregate non-linear membership functions into trapezoidal. Fu et al. [14] described an approach which combines Type-2 Fuzzy logic and Multi-Criteria Optimization and Compromise Solution (VIKOR) method for operational risk assessment of railway train. This combination can be used to rank the risk of any system components considering calculated uncertainty, expert opinions and qualitative and quantitative information about the system. The authors showed the difference between static risk assessment and proposed approach through the effectiveness and feasibility. Kilic and Kaya [15] used Type-2 Fuzzy sets as helping tool for decision make in a prioritization of provinces for public grants allocation process. Crisp sets and Type-2 Fuzzy sets have been used in Multi-Criteria Decision Making (MCDM) process to illustrate better model. It also helps with creating correct strategies for socio-economic development. Yong et al. [16] deals with risk assessment of metro station with combination of Type-2 Fuzzy set and Technique for Order Preference by Similarity to Ideal Solution (TOPSIS) method. Listed methods considered: people, equipment, management and accidents factors in the same time. Obtained results reflect actual and objective risk status of metro station which can provide needed support for decision makers. Pestana et al. [17] introduced enhanced singleton Type-2 Fuzzy logic for detection of possible faults that can occur in a switch machine in railway system. The simulations are performed with real data set, and the results are compared with other models mentioned in the literature. Three main reasons for risky events are investigated and a complete model is created based on them. Kumar and Mohamed [18] presented two fuzzy models for solving transportation problems which occur due to nature of transport. Using Type-2 or Type-4 Fuzzy logic the decision maker can easier set the boundaries of acceptance for the transportation cost or profit. In order to use crisp data, Maity and Kumar [19] experimented with Type-2 Fuzzy sets and trapezoidal fuzzy numbers (TFNs). As previous paperwork, this also refers on solving transportation problem. Using this approach, the complexity of computation is reduced significantly compared to the Type-1 Fuzzy sets. Kundu et al. [20] worked on resolving multi-solid transportation problem with Type-2 triangular Fuzzy logic. Variables like transportation costs, supplies and demands are considered fuzzy variables. Deterministic problems, which occur after the calculation, are obtained by applying LINGO solver and the genetic algorithm. Soner et al. [21] suggested application of Analytic Hierarchy Process (AHP) and VIKOR methods under Type-2 Fuzzy environment in maritime transportation. AHP and VIKOR help with solving multi-attribute decision making problems, and fuzzy logic deals with uncertainties that happen during linguistics assessment of decision makers. A demonstration of proposed approach was done to show its importance in protecting cargo from external unwanted events. Another example of application interval Type-2 Fuzzy logic in transportation is showed by Deveci et al. [22] where they use Weighted Aggregated Sum Product Assessment (WASPAS), TOPSIS and Type-2 Fuzzy MCDM model to select a car sharing station. Type-2 Fuzzy sets provide a better risk insight in process of describing membership functions and non-

membership functions. Deveci et al. [23] have worked on service quality improvement of domestic airlines on Istanbul - London route. As in previous cases, Type-2 Fuzzy sets are used in order to obtain as reliable data as possible for improving the service quality.

To the best of our knowledge, the integration of Interval Type-2 Fuzzy logic and FMEA methods have not been used for the railway projects evaluation. The IT2-FLS FMEA model proposed in this study is a novel, structured, and systematic framework used to close this gap in the literature and practice. The developed model was used to evaluate priority of risks in rail infrastructure.

3   Developed IT2-FLS FMEA Model

3.1   Input Data

A survey was used in order to define the most relevant risk events for the considered case study. It was filled by experts in the field of railway transport: infrastructure, educational institutions and relevant authorities in the Republic of Serbia. The questionnaire included 26 risk events that occur during the construction or modernization of railway infrastructure projects. Potential risks (Table 1) have been utilized from previous projects dealing with similar topics [7].

Determining the most relevant risk events in our survey was done by applying the multi-group decision making process. There were 9 respondents – railway experts from FTTE, MoCTI and ISR. The importance of the decision maker is integrated into the assessment process using the WGMM method. WGMM is one of the basic methods used in group decision making. The calculation formula is [29, 30]:

$$W_i^G = \prod_{k=1}^{r} (\omega_{ik})^{\beta_k} , \ i \ \epsilon \ \{1,2,\dots,n\} \tag{1}$$

where r is the number of decision makers, k the decision maker' index ($1 \leq k \leq r$), β_k the weighting factor/importance of the k-th decision maker ($\beta_k \geq 0$) [31-34]:

$$\sum_{k=1}^{r} \beta_k = 1 \tag{2}$$

Table 1

List of potential risk events

1.	Errors in contract documents	14.	Excessive change orders by the owner during construction
2.	Delay in approving project documentation	15.	Excessive change orders by the infrastructure management during construction
3.	Delays in providing the design documents	16.	Time consuming decision making process of the owner

4.	Unrealistic schedule (bid duration is too short)	17.	Unnecessary interference by the owner
5.	Ineffective delay penalties provisions in contract	18.	Poor communication and coordination of the owner with designer and/or contractor
6.	Selecting inappropriate project delivery method	19.	Inadequate contractor's experience
7.	Complexities and ambiguities of project design	20.	Design errors
8.	Inadequate experience of the designer	21.	Misunderstanding between owner and designer about scope of the work
9.	Inadequate site assessment by the designer during design phase	22.	Delayed payments by the owner
10.	Delay to furnish and deliver the site to the contractor	23.	Financial difficulties and mismanagement by the contractor
11.	Lack of contractor staff on the project	24.	Financial difficulties with the designer
12.	Inappropriate construction methods	25.	Poor site management and Quality Control (QC) by the contractor
13.	Contractor inefficiency (in providing the labor, equipment and handling subcontractors)	26.	Legal disputes between designer and the owner

Based on years of experience and field of work, each experts is given importance as presented in Table 2:

Table 2
Values of importance factor (β_k)

Place of employment	FTTE	FTTE	FTTE	ISR	MoCTI	MoCTI	MoCTI	ISR
Years of work	-	20	10	-	2	-	5	14
β_k - importance factor	0.1	0.12	0.12	0.15	0.11	0.11	0.11	0.18

3.2   FMEA Method

Failure Mode and Effects Analysis is a method for identifying risks and effects that occur during project implementation. This method was developed in the mid 1960s in the United States for the needs of the Apollo mission as a risk control tool. After that, it found application in various industries and systems. The idea of the FMEA is to highlight the weaknesses of the system through compiling a list of priorities.

The list is compiled based on the Risk Priority Number (RPN), and it is obtained by multiplying the following elements:

- Severity (S) - refers to impact of occurred risk on project realization;

- Occurrence (O) - represent the probability of realization of risk event;

- Detection (D) - likelihood of detecting a risk event.

The respondents rated each risk event (Table 1) based on its occurrence, severity, and detection. Assessment of probability of occurrence, severity, and detection was performed on a scale of 1 to 5, where 1 represents the absence of a risky event and 5 is a higher risk event.

After the survey was finished, six critical events with the most critical grades were highlighted (Table 3). The respondents assessed these events with the highest Relative Importance Index (RII) number. According to the RII number, events can also be sorted. The calculations of RII are presented in [7].

Table 3
The most important events and their RII number

The main causes of construction delay	RII*
Poor site management and Quality Control (QC) by the contractor	0.725
Poor communication and coordination of the owner with designer and/or contractor	0.700
Lack of contractor staff on the project	0.700
Delay in approving project documentation	0.675
Ineffective delay penalties provisions in contract	0.675
Time consuming decision-making process of the owner	0.675

3.3   Interval Type-2 Fuzzy FMEA Approach

Fuzzy Logic, introduced by Zadeh in 1965 [24, 25], is used when there is a lack of information or knowledge for presenting the values of real-world parameters. In 1975 the Type-2 Fuzzy Sets was introduced by Zadeh as well, as an extension of Type-1 Fuzzy Sets. The Interval Type-2 Fuzzy Sets are used when there is uncertainty about the membership functions. The differences between Type-1 (left image) and Type-2 (right image) Fuzzy Sets are presented at the Figure 1, where it can be seen that the membership functions are fuzzy values in Type-2 Fuzzy Logic [35-37].

The introduction of fuzzy logic in FMEA is done because it allows the usage of data that are uncertain or vague. Many events have more than simple true or false values, so in that case fuzzy FMEA is the best choice for sensitive results.
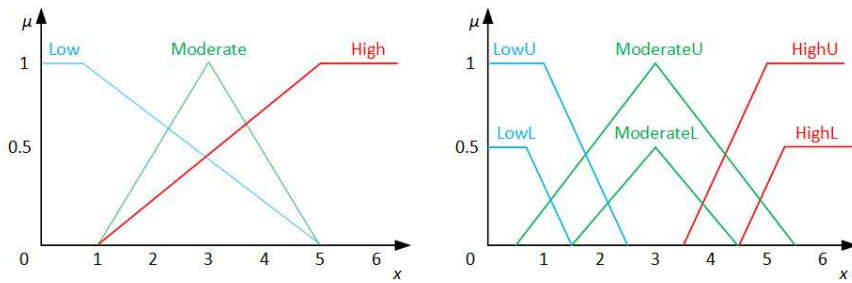
Figure 1
Type-1 and Type-2 Fuzzy Sets

Table 4 gives the quantitative description of main elements of the FMEA analysis.

Table 4
Quantitave description of severity, occurrence and detection

Level of risk (a higher number indicates a higher risk)	Severity	Occurrence	Detection
~1	Very low	Very low (Highly unlikely)	Very high
~2	Low	Low (Unlikely)	High
~3	Moderate	Moderate (It may occur)	Moderate
~4	High	High (It is expected to occur)	Low
~5	Very high	Very high (It will occur certainly)	Very low

The Interval Type-2 Fuzzy model was developed using the Matlab software (Figure 1). Fuzzy rules (If – Than rules) are defined on the basis of which the system from the combination of inputs determine the appropriate output.

The proposed Interval Type-2 Fuzzy FMEA model has three inputs: Severity, Occurrence and Detection [38,39]. Values for occurrence, severity, and detection were obtained through the survey, and these values are used as input for Interval Type-2 Fuzzy FMEA analysis.

The output value is fuzzy RPN and it was obtained by calculating the previous three inputs through Matlab-Simulink and represents the importance of the event in terms of risk. The output is in crisp form due to defuzzification.

Since all three input values are obtained using expert opinions. The domain for the severity, occurrence and detection are presented in the Table 5.
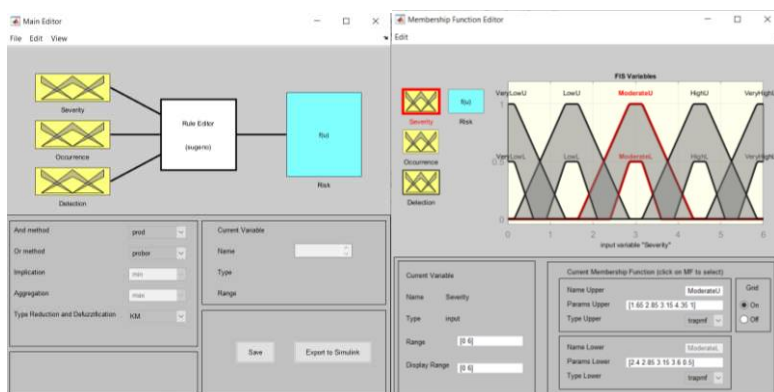
Figure 2

Developed IT2-FLS model in Matlab

Table 5

Trapezoidal Interval Type-2 Fuzzy Sets

	Upper	Lower
Very low	[-1.35 -0.15 0.15 1.35 1]	[-0.6 -0.15 0.15 0.6 0.5]
Low	[0.15 1.35 1.65 2.85 1]	[0.9 1.35 1.65 2.1 0.5]
Moderate	[1.65 2.85 3.15 4.35 1]	[2.4 2.85 3.15 3.6 0.5]
High	[3.15 4.35 4.65 5.85 1]	[3.9 4.35 4.65 5.1 0.5]
Very high	[4.65 5.85 6.15 7.35 1]	[5.4 5.85 6.15 6.6 0.5]

Here:

- Very low, Low, Moderate, High or Very high severity presents a very low, low, moderate, high or very high impact of risk event, respectively. The goal: The smaller severity is preferred.

- Very low, Low, Moderate, High or Very high occurrence presents a very low, low, moderate, high or very high chance of risk event occurrence, respectively. The goal: The smaller chance of occurrence is preferred.

- Very low, Low, Moderate, High or Very high detection presents a very low, low, moderate, high or very high chance that the risk will be detected in time, respectively. The goal: The higher chance of timely detection is preferred.

After creating the domain, the next step in conducting fuzzy FMEA analysis is to create fuzzy rules. Fuzzy rules in this case are performed based on numerical data from survey. An example of creating a rule is shown below:

Rule 1: IF the Severity is Very low and the Occurrence is Very low and the Detection is Very high, THEN the fuzzy RPN number is Very low.

Rule 2: IF the Severity is Very low and the Occurrence is Very low and the Detection is High, THEN the fuzzy RPN number is Very low.

…

Rule 125: IF the Severity is Very high and the Occurrence is Very high and the Detection is Very Low, THEN the fuzzy RPN number is High.

Once the rules are generated, it is possible to start with the calculations as a way of obtaining risk criticality. The results of calculations show the riskiness of each of the potential causes of delay. At the end, it is possible to rank the risks and notice the impact they can have on the realization of infrastructure project.

Table 6
Calculation of fuzzy RPN

Risk event	Severity	Occurrence	Detection	RPN
Poor site management and Quality Control (QC) by the contractor.	~5	~4	~4	4.1
Poor communication and coordination of the owner with designer and/or contractor.	~4	~3	~5	3.97
Lack of contractor staff on the project.	~3	~4	~3	3.3
Delay in approving project documentation.	~3	~3	~4	3
Ineffective delay penalties provisions in contract.	~2	~4	~3	3
Time consuming decision-making process of the owner.	~3	~3	~2	3

4 Results

The fuzzy RPN number, that is calculated in Matlab, provide us an assessment of riskiness of each of potential causes. The list offer essential information about risk events by which it is possible to determine corrective measures. Failure modes having a higher RPN number are considered more significant than those with a lower RPN.

As we can see, high RII number is followed by high fuzzy RPN number. The first three risk events have the highest fuzzy RPN number, the remaining three have a value of 3 which is considered a moderate risk. By calculation of severity, occurrence and detection using fuzzy logic for 'Poor site management and QC by the contractor' we have got a very high risk (RPN = 4.1) and it has to be considered a priority. Next one is 'Poor communication and coordination of the owner with designer and/or contractor' and it have RPN value of 3.97. This risk is also considered as high. The third risk event has an RPN value of 3.3 and a RII of 36. The drastic drop in RII numbers is reflected in the estimation of RPN values.

The third event has twice the value of the RII number than the first one and thus a much lower RPN value. All listed risks have observational importance but their RPN number shows what measures must be taken to prevent major consequences. The fuzzy model created to examine these events can also be used when estimating some other events related to railway infrastructure. It is also possible to reassess risk events after reduce measures have been taken.

The manner of dealing with risks is defined as actions (response) that are carried out in order to prevent the occurrence of risk, reduce the impact during the realization of risk or accept the consequences. In the world of risk management, there are four possible responses to risk:

- Risk avoidance – is used in project management if there is a situation where the cost-benefit ratio of the project is compromised and the risk can be reduced to zero by some changes.

- Risk mitigation – is based on the fact that the risk activity will continue, but the controls will be carried out regularly to minimize the possible risk.

- Risk transfer – the solution to the risk in this case is to transfer the risk to a third party or to share it with it. By transferring risk, the investor or organization reduces its exposure to that risk.

- Risk acceptance – dealing with risk's consequences directly. This solution usually develops a plan of action after a risk event has taken place.

Conclusions

Studying various infrastructure projects, it is concluded that most of them have not met the deadlines and they produce additional costs of construction and modernization. Given that such projects involve large investments, the additional costs can be unpredictably high. The solution to these problems is to improve risk management. It must be present in all phases of the project, from planning to project control after implementation.

The fact that dealing with the uncertainties is an inevitable challenge of every real-world project, makes the using the fuzzy logic appropriate for making decisions in such an unsteady environment.

The Interval Type-2 Fuzzy FMEA is suitable for project risks analysis due to the great potential to solve complex non-linear modeling task. The results of this analysis highlight the most risky events during the construction or modernization of infrastructure railway projects in the Republic of Serbia. Based on the results, a better insight into the possible consequences and measures that need to be taken in order to prevent or correct risk events is provided.

It has been observed that the events with the highest fuzzy RPN number mainly depend on the contractor and infrastructure owner, so they would be considered as responsible persons in these cases. The risk with the highest fuzzy RPN, poor site

management and QC by the contractor, can be treated by hiring external supervision. Poor communication and coordination of the owner with the designer and / or contractor should be tolerated because such a risk depends on many parties. The risk event of lack of contractor staff on the project can be improved if the right estimates of the required staff are made during the project planning.

In this paper, a model specific to the railways of the Republic of Serbia is developed. However, its application is wide and general, and does not depend on the specifics of the railway system of a country.

Since fuzzy set [24, 25, 40] was introduced, several extensions have been developed, such as: intutionistic fuzzy set, type-2 fuzzy set, type-n fuzzy set, fuzzy multiset and hesitant fuzzy set. Our future research will be dedicated to the hesitant fuzzy set theory [23, 26, 27, 28] applications for risk analysis regarding the transport infrastructure projects.

The disadvantage of FMEA analysis is reflected in the fact that it looks at individual failure modes rather than theirs combination. Research could evolve by finding ways to combine these elements. Also, it would be better if there were analytical data on risk events over the past few years in order to avoid relying on human assessment of potential risk events. Our future research will include the sensitivity analysis. Sensitivity analysis, as an in-depth study of all the variables, provides a number of benefits for decision-makers and managers in the real-world problems solving.

References

[1]   Panja, S. C., Chakraborty, R., Sarkar, D., Parida, R., Patra, S. Application of Fuzzy FMEA to Indian Railway Signaling Systems. GRD Journals, 2018, pp. 58-63

[2]   Zhu, W., Li, Ch., Xiao, X., Xu, W. Diagnosing urban rail transit vehicles with FMEA and fuzzy set. Journal of Quality in Maintenance Engineering, Vol. 21, No. 3, 2015, pp. 332-345

[3]   Ghodrati, B., Rahimdel, M. J., Vahed, A. Fuzzy Risk Prioritization of the Failure Modes in Rolling Stocks. IEEE International Conference on Industrial Engineering and Engineering Management (IEEM) 2018, pp. 108-112

[4]   Huang, W., Zhang, Y. Railway Dangerous Goods Transportation System Risk Assessment: An Approach Combining FMEA With Pessimistic – Optimistic Fuzzy Information Axiom Considering Acceptable Risk Coefficient. IEEE Transactions on Reliability, Vol. 70, No. 1, 2021, pp. 371-388

[5]   Tong, B., Duo, F., Feng, Y., Long, Zh. Research on risk analysis of suspension system in maglev train based on fuzzy multiple attribute decision-making. Proceeding of the 11th World Congress on Intelligent Control and Automation, IEEE, 2015, pp. 751-754

[6]   Sarkar, D., Singh, M. Risk analysis by integrated fuzzy expected value method and fuzzy failure mode and effect analysis for an elevated metro rail project of Ahmedabad, India. International Journal of Construction Management, 2020, DOI: 10.1080/15623599.2020.1742634

[7]   Tafazzoli, M. Dynamic Risk Analysis of Construction Delays Using Fuzzy – Failure Mode Effects Analysis. Dissertation, University of Nevada, Las Vegas, 2017

[8]   Deveci, M., Akyurt, I. Z., Yavuz, S. A GIS-based interval type-2 fuzzy set for public bread factory site selection. Journal of Enterprise Information Management, Vol. 31, No. 6, 2018, pp. 820-847

[9]   Turk, S., Deveci, M., Özcan, E., Canıtez, F., John, R. Interval type-2 fuzzy sets improved by Simulated Annealing for locating the electric charging stations. Information Sciences, Vol. 547, 2020, pp. 641-666

[10]   Deveci, M., Pekaslan, D., Canıtez, F. The assessment of smart city projects using zSlice type-2 fuzzy sets based Interval Agreement Method. Sustainable Cities and Society, Vol. 53, 101889, 2020, 101889

[11]   Karagoz, S., Deveci, M., Simic, V., Aydın, N. Interval type-2 Fuzzy ARAS method for recycling facility location problems. Applied Soft Computing, Vol. 102, No. 2, 2021, 107107

[12]   Deveci, M., Erdogan, N., Cali, U., Stekli, J., Zhong, Sh. Type-2 neutrosophic number based multi-attributive border approximation area comparison (MABAC) approach for offshore wind farm site selection in USA. Engineering Applications of Artificial Intelligence, 103, 104311, 2021

[13]   Fateminia, S. H., Sumati, V., Fayek, A. R. An Interval Type-2 Fuzzy Risk Analysis Model (IT2FRAM) for Determining Construction Project Contingency Reserve. Algorithms, Vol. 13, No. 7, 2020, 163

[14]   Fu, Y., Yong, Q., Linlin, K., Xinwang, L., Limin, J. Operational risk assessment of railway train based on type-2 intuitionistic fuzzy set and dynamic VIKOR approach. Journal of Transportation Safety & Security, 2019, DOI: 10.1080/19439962.2019.1597002

[15]   Kilic, M., Kaya, I. The prioritization of provinces for public grants allocation by a decision-making methodology based on Type-2 Fuzzy sets. Urban Studies, Vol. 53, No. 4, 2015, pp. 755-774

[16]   Qin, Y., Zhang, Z., Liu, X., Li, M., Kou, L. Dynamic risk assessment of metro station with interval Type-2 Fuzzy set and TOPSIS method. Journal of Intelligent & Fuzzy Systems, Vol. 29, No. 1, 2015, pp. 93-106

[17]   de Aguiar, P. E., Amaral, R. P. F., Vellasco M. M. B. R., Ribeiro M. V. An enhanced singleton Type-2 Fuzzy logic system for fault classification in a railroad switch machine. Electric Power System Research, Vol. 158, 2018, pp. 195-206

[18]   Kumar, S., Jamal, M. A Simple Method for Solving Type-2 and Type-4 Fuzzy Transportation Problems. International Journal of Fuzzy Logic and Intelligent Systems, Vol. 16, No. 4, 2016, pp. 225-237

[19]   Maity, S., Kumar Roy, S. A New Approach for Solving Type-2-Fuzzy Transportation Problem. International Journal of Mathematical, Engineering and Management Sciences, Vol. 4, No. 3, 2019, pp. 683-696

[20]   Kundu, P., Kar, S., Maiti, M. Multi-item solid transportation problem with Type-2 Fuzzy parameters, Applied Soft Computing, Vol. 31, 2015, pp. 61-80

[21]   Soner, O., Celik, E., Akyuz, E. Application of AHP and VIKOR methods under interval type 2 fuzzy environment in maritime transportation. Ocean Engineering, Vol. 129, 2017, pp. 107-116

[22]   Deveci, M., Canitezb, F., Gokasarc, I. WASPAS and TOPSIS based interval Type-2 Fuzzy MCDM method for a selection of a car sharing station. Sustainable Cities and Society, Vol. 41, 2018, pp. 777-791

[23]   Deveci, M., Ozcanb, E., Johnb, R., Oners Sultan, C. Interval type-2 hesitant fuzzy set method for improving the service quality of domestic airlines in Turkey. Journal of Air Transport Management, Vol. 69, 2018b, pp. 83-98

[24]   Zadeh, L. A. Fuzzy sets. Inf. Control., Vol. 8, No. 3, 1965, pp. 338-353

[25]   Zadeh, L. A. The concept of a linguistic variable and its application to approximate reasoning—II. Inf. Sci., Vol. 8, No. 4, 1975, pp. 301-357

[26]   Faizi Sh., Rashid T., Sałabun W., Zafar S., Wątróbski J. Decision Making with Uncertainty Using Hesitant Fuzzy Sets. International Journal of Fuzzy Systems, Vol. 20, 2018, pp. 93-103

[27]   Torra, V., Narukawa, Y. On hesitant fuzzy sets and decision. Proceedings of the 18th IEEE International Conference on Fuzzy Systems, Jeju Island, Korea, 2009, pp. 1378-1382

[28]   Xu Z. Hesitant Fuzzy Sets Theory. Book in Studies in Fuzziness and Soft Computing, 2014, DOI: 10.1007/978-3-319-04711-9

[29]   Blagojević, A., Vesković, S., Kasalica, S., Gojić, A., Allamani, A. The application of the fuzzy AHP and DEA for measuring the efficiency of freight transport railway undertakings. Operational Research in Engineering Sciences: Theory and Applications, Vol. 3, No. 2, 2020, pp. 1-23

[30]   Djalic, I., Ateljevic, J., Stevic, Z., Terzic, S. An integrated SWOT – fuzzy Piprecia model for analysis of competitiveness in order to improve logistics performances. Facta Universitatis-Series Mechanical Engineering, Vol. 18, No. 3, 2020, pp. 439-451

[31]   Gharib, M. R. Comparison of robust optimal QFT controller with TFC and
MFC controller in a multi-input multi-output system. Reports in Mechanical
Engineering, Vol. 1, No. 1, 2020, pp. 151-161

[32]   Gorcun, O. F., Senthil, S., Küçükönder, H. Evaluation of tanker vehicle
selection using a novel hybrid fuzzy MCDM technique. Decision Making:
Applications in Management and Engineering, Vol. 4, No. 2, 2021, pp. 140-
162

[33]   Kazimieras Zavadskas, E., Turskis, Z., Stević, Ž, Mardani, A. Modelling
procedure for the selection of steel pipes supplier by applying fuzzy AHP
method. Operational Research in Engineering Sciences: Theory and
Applications, Vol. 3, No. 2, 2020, pp. 39-53

[34]   Malbašić, S. B., Đurić, S. V. Risk assessment framework: Application of
Bayesian Belief Networks in an ammunition delaboration project. Military
Technical Courier, Vol. 67, No. 3, 2019, pp. 614-641

[35]   Milosevic, T., Pamucar, D., Chatterjee, P. Model for selecting a route for the
transport of hazardous materials using a fuzzy logic system. Military
Technical Courier, Vol. 69, No. 2, 2021, pp. 355-390

[36]   Precup, R.-E., Preitl, S., Petriu, E., Bojan-Dragos, C.-A., Szedlak-Stinean,
A.-I., Roman, R.-C., Hedrea, E.-L. Model-Based Fuzzy Control Results for
Networked Control Systems. Reports in Mechanical Engineering, Vol. 1, No.
1, 2020, pp. 10-25

[37]   Vilela, M., Oluyemi, G., Petrovski, A. A holistic approach to assessment of
value of information (VOI) with fuzzy data and decision criteria. Decision
Making: Applications in Management and Engineering, Vol. 3, No. 2, 2020,
pp. 97-118

[38]   Pamucar, D., Ecer, F. Prioritizing the weights of the evaluation criteria under
fuzziness: The fuzzy full consistency method – FUCOM-F. Facta
Universitatis-Series Mechanical Engineering. Vol. 18, No. 3, 2020, pp. 419-
437

[39]   Milosevic, T., Pamucar, D., Chatterjee, P. Model for selecting a route for the
transport of hazardous materials using a fuzzy logic system. Military
Technical Courier, Vol. 69, No. 2, 2021, pp. 355-390

[40]   Pamucar, D. S., Savin, L. M. Multiple-criteria model for optimal off-road
vehicle selection for passenger transportation: BWM-COPRAS model.
Military Technical Courier, Vol. 68, No. 1, 2020, pp. 28-64

Modification of Concrete Railway Sleeper Mix Design, Using a Hybrid Application of Steel Fibers

Jun Wang[1], Mohammad Siahkouhi[2], Farshad Astaraki[3], Sashka Uuganbayar[2], Guoqing Jing[2], Majid Movahedi Rad[3*]

[1]Shijiazhuang Tiedao University, 1 Longshan Road, Jicun Town, Yuanshi County, Shijiazhuang, 051130 Hebei, P.R.China; wangjun2011@stdu.edu.cn

[2] School of Civil Engineering, Beijing Jiaotong University, No. 3 Shangyuancun Haidian District, 100044 Beijing, China; m.siahkouhi@bjtu.edu.cn, 19119903@bjtu.edu.cn, gqjing@bjtu.edu.cn

[3] Department of Structural and Geotechnical Engineering, Széchenyi István University, Egyetem tér 1, 9026 Győr, Hungary
astaraki.farshad@hallgato.sze.hu, majidmr@sze.hu

Abstract: Concrete railway sleepers have been used for years without an update in production and design, to be compatible with demands for increasing train axle loads and speed. In the current research, concrete railway admixture is modified with consuming (0.5% straight-1.5% hooked), (1.5% straight-0.5% hooked) and (1% straight-1% hooked) steel fibers combinations. Three main mechanical experiments as compressive, flexural and splitting tensile strengths and fresh mortar "flowability" were performed. Results showed that the hybrid of 1% straight and 1% hooked steel fibers shows the optimal performance among other hybrid combinations. This hybrid admixture efficiently improves the compressive, flexural and splitting tensile strengths of the concrete railway sleeper mix design.

Keywords: Concrete railway sleeper; Steel fibers; Optimal hybrid reinforced concrete

1   Introduction

Railway sleeper are one the critical components of railway tracks, which have a role to distribute and decrease train loads from the rail foot to the underlying ballast bed and consequently to subgrade [1-3]. The traditional sleepers are manufactured using timber, concrete and steel [4]. Wooden sleepers are contained in the majority part of railway tracks, but concerning their environmental disadvantages, were gradually replaced by the other types of sleepers [5]. In order to replace wooden sleepers, steel

sleepers, as an alternative, were used [6]. Considering the performance of steel sleepers, they face problems in high speed of train and corrosion issues [7].

Concrete sleepers are extensively used in railway engineering [8]. Their performance in railway tracks leads to less maintenance cost, track stability and longer life cycles [9-, 10, 11, 12]. Pre-stressed concrete has different kinds that mono-block concrete sleeper is one of the most popular kinds implemented in railway tracks [13]. Recently, by increasing axle load, speed and traffic, finding a better quality of concrete sleepers is an approach. The common behaviors of sleepers under overloading or fatigue are tensile fracture, longitudinal and cross cracks under rail seat of railway tracks [20] [21]. Occasionally, it has been seen that the tensile strength of sleepers is not enough and leads to some physical damage. An effective solution is use of fiber reinforced concrete. Consuming short, discrete or long fibers lead to a new construction material challenges [14]. Fiber-reinforced concrete (FRC) is produced in different types mixed during fresh concrete production [15], and leads to an increase in mechanical performance of concrete [16]. Almost four popular kinds of fibers fabricated from steel, plastic, glass, and natural materials are consuming in a variety of shapes, sizes, and thicknesses. Three kinds of steel fibers in shapes of straight, hooked and crimped are commonly preferred to use [17]. It is concluded that using hybrid shape of steel fibers has the best influence on concrete performance [18].

Recently, by proving the performance of steel fibers in concrete admixtures, some researchers have tried to assess its behavior combined with concrete sleeper admixtures. Sadeghi et al. [19] followed two approaches, firstly, the effects of straight steel fibers on the mechanical behavior of pre-stressed concrete sleepers with the different percentages in contents of (0, 0.3, 0.5, 0.7 and 1% by volume) and, secondly, decreased the number of pre-stressed rebars. The results indicate that consuming steel fibers in concrete sleeper admixtures leads to an improvement in the sleeper bending strength, energy absorption capacity, and cracking resistance increase. Zhu et al. [20] investigated the effects of straight steel fibers on production cost and cracks opening in a concrete beam with polymer rebars. The results showed that all parameters of crack width, ductility and cost decreased due to presence of steel fibers. Shin et al. [21] assessed the effects of straight steel fibers mixed with different kinds of fine aggregates in pre-stressed concrete railway sleeper admixtures. The results showed that the fraction of 0.75% of steel fibers mixed with slag concrete leads to enhance its static and impact flexural capacity. Parvez and Foster [22] inspected the performance of straight steel fibers in carrying capacity and fatigue of railway sleepers. Pre-stressed concrete sleepers were researched with fiber contents of 0, 0.25% and 0.5% by volume, under cyclic and static loading. The sleepers with 0.5% fibers have higher static capacity and extended fatigue life, lower deflections and finer crack widths compared to those sleepers without fibers. Moreover, Hwang et al. [23] tried to design pre-stressed sleepers with 0.75% steel fibers by volume and features of 30 mm length and aspect ratio of 55 [24]. Results showed that toughness and durability of sleepers were improved.

None of the aforementioned papers have assessed hybrid behavior of steel fibers in railway concrete sleeper mix design. In order to decrease fiber content and increase mechanical performance of concrete, hybrid use of steel fibers with low aspect ratio is proposed that consequently, reduce the disadvantages of the presence of steel fiber in concrete admixtures. Therefore, in the current research, respect to different admixture and low aspect ratio of steel fibers, performance of single and hybrid steel fibers are investigated, to improve concrete railway sleeper mix design.

2 Experimental Program

2.1 Concrete Sleeper Test

The sleeper under test is a commercially available mono-block type used for high speed railways. The pre-stressed concrete sleeper consists of almost 320 mm × 260 mm × 2600 mm dimensions with 10 numbers of Ø7 mm strands. The lowest width and height of the sleeper structure are by 280 mm and 185 mm, respectively. European standard EN 13230-2 [25] provides guidelines for calculating reference test loads for different concrete sleeper types. As shown in Figure 1, sleeper is tested in middle negative bending moment test with flexural strength of 70 kN, (the load that the first crack is identified by operator using portable microscopes). Figure 2 shows load against deflection of sleeper under flexural load. Load is applied until 140 kN to capture bending behavior of sleeper. Until 20 kN, sleeper shows more flexibility and less stiffness, however, it has a sharp increase in sleeper stiffness after 20 kN flexural load. The first crack has been seen in almost 70 kN, when the sleeper stiffness has been reduced again due to the crack initiation.

Figure 1
The middle negative bending moment test
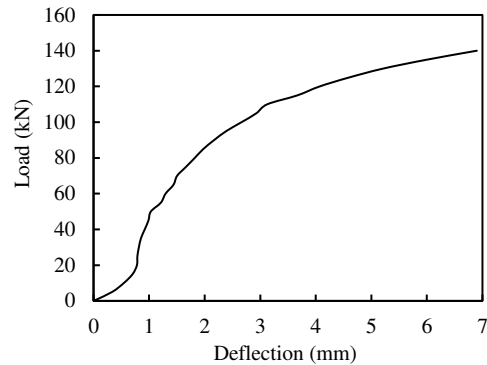
Figure 2

The flexural strength of concrete sleeper

2.2   Steel Fiber Reinforced Concrete

2.2.1   Materials and Mix Proportion

Ordinary Portland Cement (II) and silica fume was consumed in this research. A polycarboxylate superplasticizer including air entraining agent, 40% solid and 60% water with specific gravity of 1.09 and solid contents of 32% was used in all the concrete mixtures. Furthermore, steel fibers with properties according to the Table 2 have been used. 4 mixtures are presented in Table 1, Ref. mixture is without any steel fiber and is concrete sleeper mix design. The workability and mechanical properties of the concrete mixtures were considered to select the optimal admixture with hybrid use of steel fibers. To combine powder materials with concrete admixture, they are mixed before the water and superplastisizer addition, in this way particle agglomeration can be avoided. Firstly, the fine aggregates are mixed in the mixer contains quartz sand. Afterwards, the powder materials are added to mixer's contents and mixed for around 4 minutes. Then almost half of the 2% (by cement weight) high-range superplastisizer is diluted in the admixture water and is gradually added within 2 minutes. The remaining superplastisizer are gradually added during a next 4 minutes of mixing. Steel fibers are added in three parts, in first, middle and almost at the end of mixing time. The fresh concrete is placed in two kinds of molds as 100 * 100 * 400 mm prismatic and 100 mm cubical. Vibration table is used for 2 minutes. The specimens without movement are covered with plastic sheets and are kept at 240 ℃ for a day before demolding. After demolding, the samples are cured in an autoclave system with heat and vapor. By using this system, concrete sleeper cure system is simulated as Figure 3. Firstly, specimens are cured at 20 ℃ for 73 hours of cure time, then the heat is smoothly raised to 90 ℃. This much heat is stable for 50 hours, afterwards, it is slowly reduced to

20 ℃ again (Fig. 2). It should be mentioned that for validity of test results for each mix, 3 specimens are constructed and tested.

Table 1

Concrete admixtures

No.	Cement	Quartz sand	Silica fume	Water	Admixture	Volume content (%)		Notation
						Straight fiber	Hooked fiber	
1	706	1255	160	124	68	-	-	Ref.
2	706	1255	160	124	68	0.5	1.5	S05H15
3	706	1255	160	124	68	1	1	S10H10
4	706	1255	160	124	68	1.5	0.5	S15H05
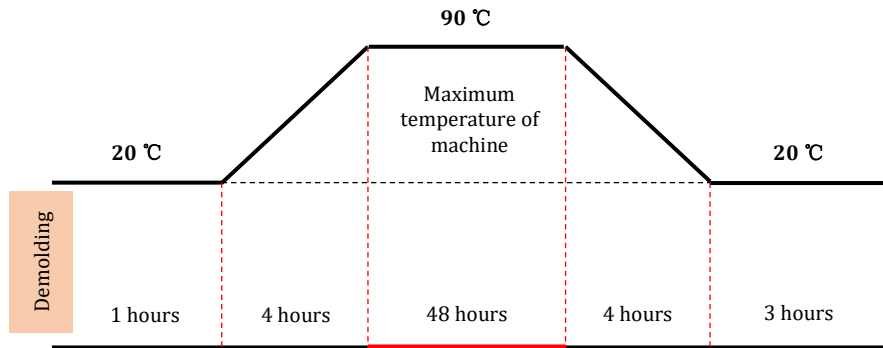
Figure 3

Steam curing process of concrete specimens in curing machine

Table 2

Steel fibers properties

Type of fiber	Diameter	Length	Aspect ratio	Density	Tensile strength	Elastic modulus	Picture
	(mm)		(l_f/d_f)	(g/cm^3)	(MPa)	(GPa)	
Straight fiber	0.2	13	65	7.8	2850	200	
Hooked fiber	0.3	22	73	7.8	2850	200	

2.2.2   Compressive Strength Test

The compressive strength results of different admixtures are shown in Figure 5. The results indicate that the presence of steel fiber increases compressive strength. Hybrid fiber content (S10H10) has more compressive strength as 171 Mpa that shows better performance. Flowability of concrete mixtures is measured using slump test. S10H10 hybrid concrete has 108 mm flowability. It should be noted that in case of concrete sleeper production, the low value of flowability cannot make a significant problem, because in production procedure of concrete sleepers a special vibration system has been used that can overcome this much of low value of flowability. The references compressive strength is about 93 Mpa, which increased by adding hybrid fibers. S05H15 has a compressive strength value by 40% greater than Ref., these percentages for S10H10 and S15H05 are almost 45% and 44% higher, respectively. Therefore, the comparison of results shows that S10H10 admixture has the maximum value of compressive strength but with minimum flowability as 108 mm.

Figure 4

An overview of compressive strength test machine
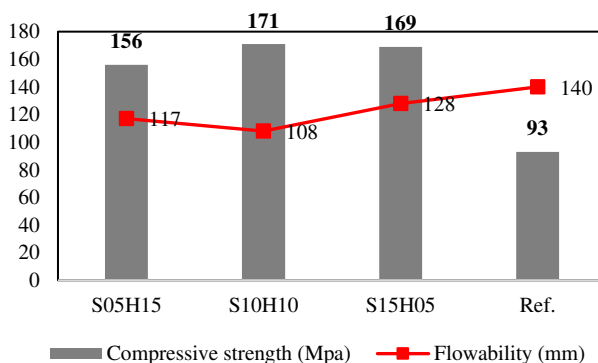
Figure 5

Compressive strength and flowability of concrete specimens

2.2.3   Flexural Strength Test

Figure 6 shows flexural test instrument machine. The diagram of flexural strength for concrete admixtures is shown in Figure 7. The results indicate that addition of steel fiber results in a significant increase in the flexural strength value. The flexural strength of S05H15, S10H10 and S15H05 increase by 52%, 55% and 50%, respectively, compared to Ref. It should be paid attention that the summation of total hybrid fiber percentage usage in every admixture is 2%. For instance, 0.5% straight plus 1.5% hooked fibers equal to 2%. Therefore, three kinds of hybrid admixtures do not show a significant difference but among those S10H10 has better performance. It should be noted that performance of 2% hybrid fiber is 55% more than Ref. Concrete sleepers according to their loading pattern with trains, may face high bending moments, therefore, flexural strength is critical in their performance.

Figure 6
An overview of flexural test layout
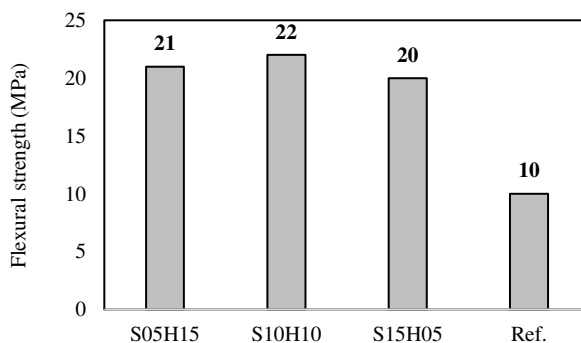
Figure 7
Flexural strength test results of concrete specimens

2.2.4   Splitting Tensile Strength

The splitting tensile strength of the different admixtures were prepared in this study that are shown in Figure 10. Concrete has weakness in tension. Thus, splitting tensile strength test is necessary to determine the load at which the concrete members may crack (Figures 8 and 9). The results indicate that the presence of fibers in admixture significantly improves the concrete splitting tensile strength. Among different admixtures considered, the highest strength value is achieved by the admixture containing S10H10. The splitting tensile strength of S05H15, S10H10 and S15H05 admixtures increase by 77%, 80% and 77% compared to Ref., respectively. In case of hybrid consumption of steel fibers, the summation of each percent of hooked or straight is 2%, therefore, a great deviation between tensile strength of admixtures cannot be seen. Maximum value of tensile strength belongs to S10H10 admixture with value of 24 Mpa. Tensile strength is part of those features that is critical in pre-stressed concrete sleepers, therefore, improving tensile strength of concrete mix design makes sleepers better in dynamic performance.
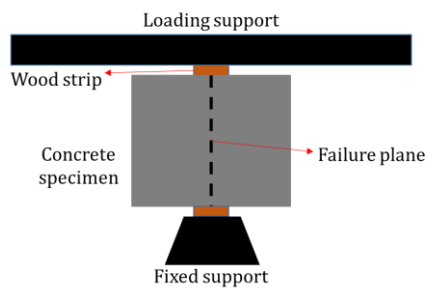
Figure 8
A schematic of Splitting tensile test

Figure 9
Splitting tensile test layout of concrete specimens
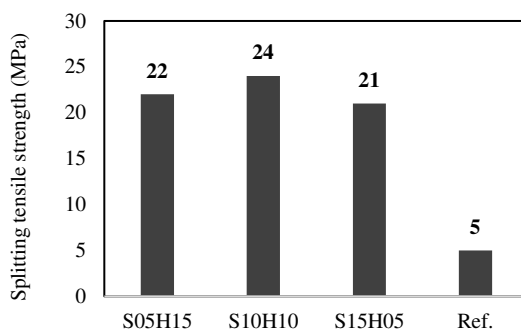
Figure 10
Splitting tensile strength of concrete specimens

3   Results and Discussion

This study shows the improvement of the physical and mechanical properties of railway concrete mixtures, by the application hybrid steel fibers. Because, content of more than 2% steel fiber in concrete mixture, generally, reduces workability and fiber dispersion, it is therefore required to apply a special mix design or special concrete casting techniques. Thus, the concrete mixture has been hybridized by adding fibers with S05H1.5, S10H10 and S15H05. The mechanical properties for all mixtures were measured and compared with compressive, tensile and flexural strengths, to determine the performance of railway concrete mix design (Table 3).

Table 3
Steel fibers properties

Notation	Compressive strength	Splitting tensile strength	Flexural strength
	MPa		
Ref.	93	5	10
S05H15	156	22	21
S10H10	171	24	22
S15H05	169	21	20

The test results show that the mechanical performance of admixture S10H10, has the best performance among all the admixtures. It can be due to the same load of single and hooked shape fibers, which provide better mechanical performance for concrete. It can be concluded that to obtain compressive strengths of more than 170 Mpa, hybrid fibers can be an effective solution. Concrete quality plays a critical role in load bearing of concrete sleepers, as well as, its pre-stressing system. Therefore, it is expected as the quality of concrete is increased and the pre-stressing systems

of conventional pre-stressed concrete sleeper and steel fiber pre-stressed concrete sleeper are identical, steel fiber pre-stressed concrete sleeper shows better performance due to the better mechanical performance of its steel fiber concrete.

Conclusions

In this study, 4 admixtures are prepared in order to investigate the performance of hybrid fibers and their influence, on concrete railway sleeper mix design. To study hybrid use of steel fibers and compare their behavior, different fiber contents as, (0.5%straght-1.5%hooked), (1%straght-1%hooked) and (1.5%straight-0.5%hooked) are considered to research. The main focus of the current study is on the mechanical behavior of concrete railway sleeper mix design, by performing compressive strength, flexural strength and splitting tensile strength experiments. The following points can be concluded from this study:

1) S05H15 has a compressive value 40% greater than Ref., these percentages for S10H10 and S15H05 are 45% and 44% higher, respectively.

2) The flexural strength of S05H15, S10H10 and S15H05 increased by 52%, 55% and 50%, respectively, compared to Ref.

3) The splitting tensile strength of S05H15, S10H10 and S15H05 admixtures increase by 77%, 80% and 77% compared to Ref., respectively.

4) **S10H10 hybrid steel fiber mix design shows the best performance in case of mechanical properties and is a good choice to fiberize concrete railway sleeper mix design.**

Acknowledgement

References

[1]   A. S. Hameed and A. P. Shashikala, "Suitability of rubber concrete for railway sleepers," *Perspectives in Science,* Vol. 8, No. Supplement C, pp. 32-35, 2016/09/01/ 2016

[2]   Fischer S. "Investigation of effect of water content on railway granular supplementary layers". Naukovyi Visnyk Natsionalnoho Hirnychoho Universytetu. (3): pp. 064-068, 2021

[3]   Gerber, Ulf, Mykola Sysyn, Jandab Zarour, and Olga Nabochenko. "Stiffness and strength of structural layers from cohesionless material." Archives of Transport" 49(1): pp. 59-68, 2019

[4]   B. Li, H. Li, M. Siahkouhi, and G. Jing, "Study on coupling of glass powder and steel fiber as silica fume replacement in ultra-high performance concrete: Concrete sleeper admixture case study," *KSCE Journal of Civil Engineering,* pp. 1-12, 2020

[5]   P. Qiao, J. F. Davalos, and M. G. Zipfel, "Modeling and optimal design of composite-reinforced wood railroad crosstie," *Composite structures,* Vol. 41, No. 1, pp. 87-96, 1998

[6]   W. Ferdous, A. Manalo, G. Van Erp, T. Aravinthan, S. Kaewunruen, and A. Remennikov, "Composite railway sleepers–Recent developments, challenges and future prospects," *Composite Structures,* Vol. 134, pp. 158-168, 2015

[7]   J.-A. Zakeri and R. Talebi, "Experimental investigation into the effect of steel sleeper vertical stiffeners on railway track lateral resistance," *Proceedings of the Institution of Mechanical Engineers, Part F: Journal of Rail and Rapid Transit,* Vol. 231, No. 1, pp. 104-110, 2017

[8]   G. Jing, D. Yunchang, R. You, and M. Siahkouhi, "Comparison study of crack propagation in rubberized and conventional prestressed concrete sleepers using digital image correlation," *Proceedings of the Institution of Mechanical Engineers, Part F: Journal of Rail and Rapid Transit,* p. 09544097211020595, 2021

[9]   G. Jing, M. Siahkouhi, J. R. Edwards, M. S. Dersch, and N. Hoult, "Smart railway sleepers-a review of recent developments, challenges, and future prospects," *Construction and Building Materials,* p. 121533, 2020

[10]   Németh A, Fischer S. investigation of the glued insulated rail joints applied to cwr tracks. Facta Universitatis, Series: Mechanical Engineering. 2021 May 14

[11]   Kurhan, M., D. Kurhan, R. Novik, S. Baydak, and N. Hmelevska. "Improvement of the railway track efficiency by minimizing the rail wear in curves." In IOP Conference Series: Materials Science and Engineering, Vol. 985, No. 1, p. 012001. IOP Publishing, 2020

[12]   Przybylowicz, Michal, Mykola Sysyn, Vitalii Kovalchuk, Olga Nabochenko, and Bogdan Parneta. "Experimental and theoretical evaluation of side tamping method for ballasted railway track maintenance." Transport Problems 15 (2020)

[13]   R. Kohoutek, "Dynamic and static performance of interspersed railway track," in *Conference on Railway Engineering 1991: Demand Management of Assets; Preprints of Papers*, 1991, p. 153: Institution of Engineers, Australia

[14]   I. Oladele, A. Akinwekomi, S. Aribo, and A. Aladenika, "Development of fibre reinforced cementitious composite for ceiling application," *Journal of Minerals and Materials Characterization and Engineering,* Vol. 8, No. 08, p. 583, 2009

[15]   W. Abbass, M. I. Khan, and S. Mourad, "Evaluation of mechanical properties of steel fiber reinforced concrete with different strengths of concrete,"

Construction and Building Materials, Vol. 168, pp. 556-569, 2018/04/20/ 2018

[16]   M. Ghahremannejad, M. Mahdavi, A. E. Saleh, S. Abhaee, and A. Abolmaali, "Experimental investigation and identification of single and multiple cracks in synthetic fiber concrete beams," *Case Studies in Construction Materials,* Vol. 9, p. e00182, 2018/12/01/ 2018

[17]   J. Katzer and J. Domski, "Quality and mechanical properties of engineered steel fibres used as reinforcement for concrete," *Construction and Building Materials,* Vol. 34, pp. 243-248, 2012/09/01/ 2012

[18]   L. Vandewalle, "Postcracking behaviour of hybrid steel fiber reinforced concrete," in *Fracture Mechanics of Concrete and Concrete Structures– FraMCoS, in: Proceedings of the 6th International Conference, Catania, Italy*, 2007, pp. 17-22

[19]   K. A. Sadeghi J, Khabbazi AS, "Improvement of mechanical properties of railway track concrete sleepers using steel fibres," *Mater Civ Eng,* p. 11, 2016

[20]   H. Zhu, S. Cheng, D. Gao, S. M. Neaz, and C. Li, "Flexural behavior of partially fiber-reinforced high-strength concrete beams reinforced with FRP bars," *Construction and Building Materials,* Vol. 161, pp. 587-597, 2018/02/10/ 2018

[21]   H.-O. Shin, J.-M. Yang, Y.-S. Yoon, and D. Mitchell, "Mix design of concrete for prestressed concrete sleepers using blast furnace slag and steel fibers," *Cement and Concrete Composites,* Vol. 74, No. Supplement C, pp. 39-53, 2016/11/01/ 2016

[22]   A. Parvez and S. J. Foster, "Fatigue of steel-fibre-reinforced concrete prestressed railway sleepers," *Engineering Structures,* Vol. 141, No. Supplement C, pp. 241-250, 2017/06/15/ 2017

[23]   C. C. Hwang CL, Lee LS, Bui LAT, Hou BS, Hsieh HY., "The material and mechanical property of heavy-duty prestressed concrete sleeper.," Mater pp. 97-98, 2011

[24]   AREMA., "Concrete ties.," in Manual for railway engineering American Railway Engineering and Maintenance-of-Way Association, 2006

[25]   E. C. f. Standardization, "Railway applications-track-concrete sleepers and bearers part 2: Prestressed monoblock sleepers," 2009

The Centrifugal Modeling of Reinforcement on Approaches to Railway Bridges

Ahmad Alkhdour[1], Oleksii Tiutkin[2], Vitalii Marochka[2], Stepan Boboshko[2]

[1]Department of Civil Engineering, Al-Balqa Applied University, Al-Salt, 19117, Jordan, a.alkhdour@bau.edu.jo

[2]Department of Transport Infrastructure, Dnipro National University of Railway Transport named after Academician V. Lazaryan, Lazaryan Str., 2, Dnipro, 49010, Ukraine, {tiutkin, vitalij_marochka, stepan_boboshko}@diit.edu.ua

Abstract: The purpose of the research is to test models of sections with transient stiffness on approaches to railway bridges in the laboratory. The feasibility of the proposed methods of reinforcing the transient stiffness areas to ensure normal operation and avoid the formation of significant deformations had been tested. Centrifugal simulation of three types of reinforcement of transition section had been performed. The deformations of the models of the section with transient stiffness on approach to the railway bridge had been obtained. A comparative analysis of the results of centrifugal experiments had been performed. The effectiveness of each of the reinforcement options had been determined and the most rational method of reinforcement had been concluded.

Keywords: centrifugal modeling; reinforcement; railway bridge

1 Introduction

The problem of the normal operation of sections with transient stiffness on approaches to railway bridges is that the dynamic impact of rolling stock adversely affects the embankment. Changing the significant rigidity of the bridge elements, that is, the abutment and superstructure, to a lesser rigidity of the embankment causes its considerable, and sometimes excessive, deformation. This requires measures that impair the operation: reducing the speed of movement, repairing, redeveloping or reconstructing the embankment.

This problem was engaged in very fruitful in 1990-2020, but the proposed solutions (geogrid reinforcement [1-2], ballast material [3-5], bitumen emulsion [6], soil cement piles [7], variable stiffness [8, 9], boring and mixing technology [10]) were not always rational. This is due to the fact that the sections with

transient stiffness on approaches to the railway bridges were not thoroughly investigated. There are several research methods, the main ones being mathematical modeling, experimental research, and field tests [10, 11]. Because full-scale bridge testing requires a large amount of time and financial cost to implement, experimental modeling becoming increasingly popular [10-12]. One of the methods of experimental modeling based on physical device – centrifuge [12]. It is this method of research that gives knowledge of the general nature of deformation, which is of great importance for the correct formulation of theoretical studies and for the explanation of certain phenomena occurring in nature.

The essence of the centrifugal simulation method is that the field of centrifugal forces created by the rotation of the centrifugal machine is used as a force field similar to gravity [12]. A model of a soil structure made of natural material is placed in a centrifuge, creating a rotating field of centrifugal forces similar to gravity, which has a much higher intensity. Thus, centrifugal modeling ensures the complete preservation of the nature of processes occurring in the structure.

It is worth noting that the similarity conditions that apply to models with the location of individual simulation regions at different distances from the center of rotation are practically unworkable, since it is impossible to ensure the rotation of these simulation regions at different angular velocities. For correct centrifugal simulation experiments, the same starting conditions for each iteration must be carefully observed. As a result, minimal changes to starting conditions can lead to incorrect results.

2   Methods and Resources

The experimental model was based on a real railway bridge on the Loshkarovka – Pavlopillya section of the Merefa – Kherson line in Ukraine. An experimental model with a total length of 32.5 m covers the abutment construction and the approach area 20 m behind it.

The tests had been performed at a unique centrifuge of the Soil Mechanics Research Laboratory of Dnipro National University of Railway Transport (DNURT) named after Academician V. Lazaryan. The DNURT machine is one of the most powerful centrifugal devices used in the world. Thus, with a large mass of test models (2×120 kg) and an effective rotation radius of 2.28 m, the device is able to develop any speed within the range from 0 to 250 rpm. The total acceleration is from 1g to 160g.

The kinematic scheme of the centrifugal machine is constructed in such a way that the torque from the traction motor through the gear reducer is transmitted to the vertical shaft of the machine, with which the two-shoulder yoke rotates, at the

ends of which are pivotally suspended carriages. As the machine is overclocked, the carriages are rotated and mounted horizontally (Figure 1).
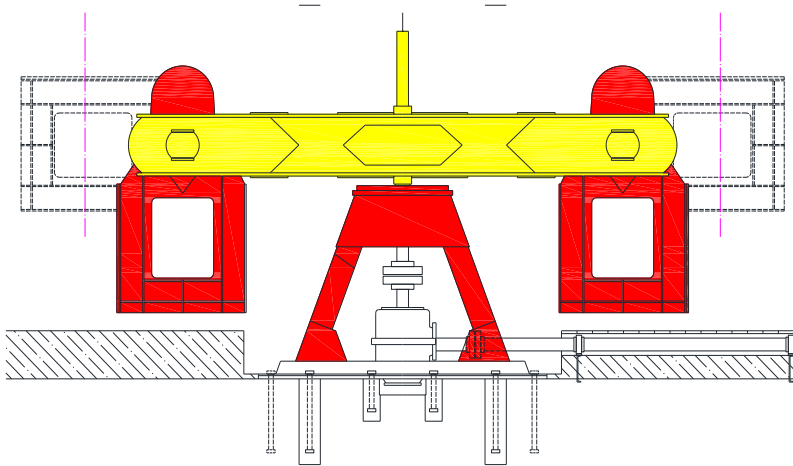
Figure 1
The design of the centrifuge

The model of the investigated structure, which is in the carriage, is the total attachment root of the centrifugal force and gravity that is, the process of modeling. The tray, which is made for modeling, made of metal, one of the walls can be removed. The internal dimensions of the tray are 650×235×360 mm. The abutment model (Figure 2) is mounted in a test tray on a soil cushion 2 … 3 cm thick.

Figure 2
The model of the abutment of the bridge made of cement

The soil is compacted by manual ramming to the specified density. The model is covered with layers of soil 4 … 5 cm, which are further compacted in accordance with the first layer to model the embankment as a solid array. The lateral topsoil of the soil array had been divided by a pencil grid (Figure 3) into 2×2 cm squares for better inspection and processing of test results.

Figure 3
Model appearance in the centrifuge cassette

The resulting soil mass is given an embankment shape by cutting slopes according to the real bridge.

The physical and mechanical characteristics of the soil of the base are as follows: clay of dark brown color of plastic consistency with index of fluidity I_L=0.7, plasticity index I_P=0.23, the density of the soil when making the model ρ=1.884 … 1.911 g/cm^3, dry soil density ρ_c=1.299 … 1.317 g/cm^3, humidity W=0.40 … 0.41, porosity coefficient e=1.106 … 1.135, the degree of humidity S_r=0.94.

The tray had been mounted in a centrifuge. To counterbalance on the other side of the centrifuge lever had been set counter. Centrifugal acceleration equal to the inverse of the scale of the model, i.e. 50 g had been given to simulate the loading on the soil of the bulkhead of the centrifuge. Acceleration of the centrifugal machine in all experiments had been carried out uniformly with the increase of scale of simulation for 5 min and corresponded to time in kind 24 months.

After stopping the centrifuge, a visual description of the condition of the model, removal of deformation of the mesh and photographing had been performed. After completing the program and checking the model, it had been found that the model was built without significant deviations. The marked grid made it possible to outline the intensity of the load distribution on the soil of the embankment.

3   Output Data of the Experiment

Weight of the container with model No. 1: 194.5 kg; weight of the container of counterweight No. 1: 194.5 kg.

Weight of the container with model No. 2: 205.0 kg; weight of the container with counterweight No. 2: 205.0 kg.

Weight of container with model No. 3: 200.0 kg; weight of the container counterweight No. 3: 200.0 kg.

Weight of container with model No. 4: 201.5 kg; weight of the container of counterweight No. 4: 201.5 kg.

Modeling Scale: 1: 10000 (1 hour equals 10.000 hours); rotation time: 60 minutes (equal to 416 days); central gearbox conversion factor: 1.576; (1 turn of the centrifuge = 1.576 engine turns). This is an equation example:

$$a_c = \omega^2 R \,, \tag{1}$$

$$\omega = 2\pi f \,, \tag{2}$$

where "f" is the speed of centrifuge (desired value):

$$a_c = (2\pi)^2 f^2 R \,, \tag{3}$$

$$f^2 = \frac{a_c}{4\pi^2 R} \,, \tag{4}$$

$$f = \sqrt{\frac{a_c}{4\pi^2 R}} \,, \tag{5}$$

where "R" is the effective radius of the centrifuge $R = 2.28$ m; a_c – centrifugal acceleration ($a_c = 50$g);

$$f = \sqrt{\frac{50 \cdot 9.81}{4\pi^2 \cdot 2.28}} = 2.334 \quad \text{Hz}. \tag{6}$$

Engine speed:

$$n_o = f \cdot 1.576 = 2.334 \cdot 1.576 = 220.74 \quad \text{rpm, or} \tag{7}$$

$$n_o = \frac{60 f_c}{4} \,. \tag{8}$$

Frequency of current:

$$f_c = \frac{4 n_o}{60} = \frac{4 \cdot 220.74}{60} = 14.72 \quad \text{Hz}. \tag{9}$$

4   Results

Three types of reinforcement of the embankment consignment had been selected for verification and comparison: 1) reinforcement by gabion boxes; 2) reinforcement by vertical soil cement piles; 3) the use of reinforced and sorted soils.

The reinforcement of the gabion boxes was as follows. As in the non-reinforced ones, the abutment model is mounted on a dense, cushioned pillow, after which layers of 4 … 5 cm had been rammed to form the main soil mass. During backfilling and ramming of the upper layers, part of the backfill soil is replaced by models of gabion boxes of three sizes: 3000×2500×1500 mm, 3000×2500×1200 mm and 3000×2500×900 mm (Figure 4).

a)

b)
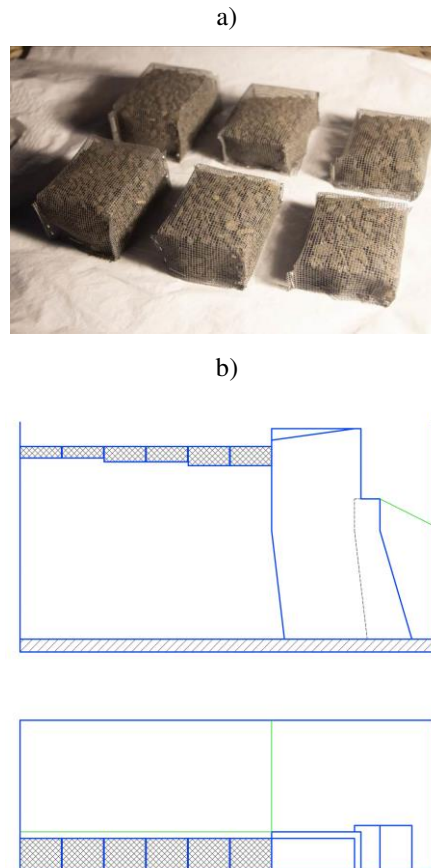
Figure 4
a) The appearance of models of gabion boxes;
b) their arrangement scheme in the centrifuge cassette

Polymer mesh and crushed stone of fraction 3 … 5 mm had been used for modeling of gabions. The resulting soil mass is provided with an embankment shape by cutting slopes according to a real bridge (Figure 5).

a)

b)

Figure 5
View of model with gain gabion boxes: a) in plan; b) in top

After stopping the centrifuge, a visual description of the model's condition, mesh deformation, and photographing had been performed.

Reinforcement with soil cement piles has several advantages over the earlier method. First of all, it is an opportunity to strengthen the existing railway bridge embankments without dismantling the upper structure of the track, which not only

reduces the labor costs for the reinforcement works, but also reduces the rail losses from closing the line for the period of repair. The reinforcement is performed by paired soil cement piles with a diameter of 30 cm of various lengths with a step of 1 m between them along and across the bridge. Reinforcement begins at a distance of 2 m from the abutment structure to ensure the safety.

The reinforcement model is as follows: as in the non-reinforcement test, the abutment model is mounted on a tightly packed pillow, after which layers of 4 … 5 cm are formed and the main soil mass is formed by the ram. After giving the array an embankment shape, vertical holes of the design length are drilled in the upper part of the embankment, which are tightly filled with soil cement solution (Figure 6).

a)

b)
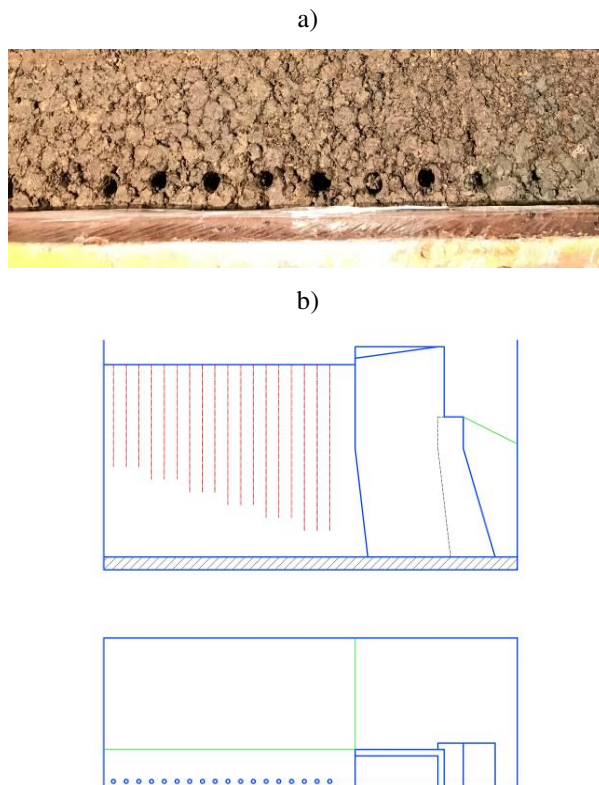
Figure 6
a) The appearance of model with soil cement piles;
b) Their arrangement scheme in the centrifuge cassette

Reinforcement with the help of sorted soils is performed by stabilizing part of the embankment 2.5 … 3 % of cement, using sorted soil and performing a horizontal pillow of tightly compressed soil (Figure 7) [13].
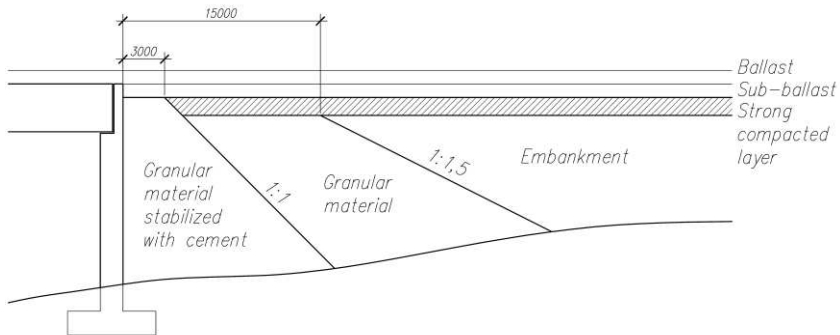
Figure 7
Reinforcement of the transitional area by sorted soils (drawing taken from work [13])

In contrast to the non-reinforcement test, one part of the layer of rammed soil is cement-stabilized soil, the second is sorted soil, and the other is ordinary soil (Figure 8).

a)

b)
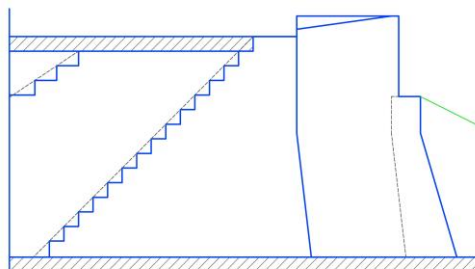
Figure 8
a) The appearance of model with sorted soil;
b) their arrangement scheme in the centrifuge cassette

After stopping the centrifuge, a visual description of the condition of the model, deformation of the grid and photographing had been carried out. In Figures 9-11 models of three variants of reinforcement after deformation in a centrifuge are presented.

Figure 9
Deformed bridge and embankment models with reinforced gabion boxes
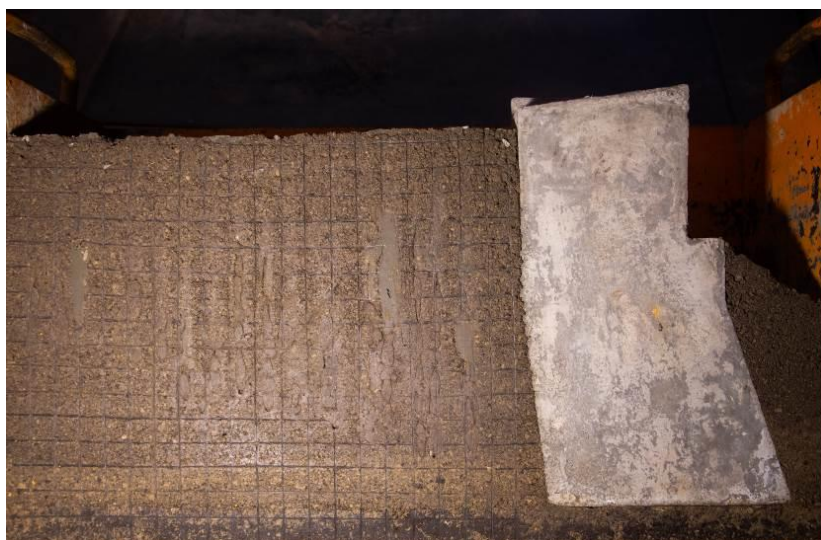
Figure 10
Deformed bridge and embankment models with reinforced soil cement piles

Figure 11
Deformed bridge and embankment models with reinforced sorted soil

After processing the results, the original photos and the results of each test had been converted to a digital vector view and overlaid for comparison. The comparison showed the following results of maximum vertical deformation: for the test without reinforcement – 20.56 mm; for the test with reinforcement gabion boxes – 5.46 mm; 9.77 mm for soil reinforcement piles; 5.33 mm for graded soil reinforcement test.

Conclusions

Thus, studies conducted using centrifugal modeling of reinforced sections with transient stiffness on approaches to railway bridges allow comparative analysis. It testifies that the use of all three variants of reinforcement (gabion boxes, soil cement piles and sorted soil) has a positive effect on the reduction of vertical deformations (2.10 … 3.86 times). It is also possible to conclude that two of the three variants of reinforcement are almost equal from the point of view of reduction of vertical deformations: reinforcement by gabion boxes – 3.77 times, reinforcement by sorted soil – 3.86 times. The option of reinforcing soil cement piles, which is effective in other cases, in a particular reinforcement of sections with transient stiffness on approaches to railway bridges is less effective. Further research, which will compare the technologies of gabion-box reinforcement and sorted soil, will prove the most rational technology in terms of financial and labor costs.

References

[1]   Sz. Fischer, F. Horvát. Investigation of the reinforcement and stabilisation effect of geogrid layers under railway ballast. Slovak Journal of Civil Engineering, Vol. XIX, 3, 2011, pp. 22-30

[2]   E. Juhasz, S. Fischer. Investigation of railroad ballast particle breakage. Pollack Periodica, Vol. 14(2), 2019, pp. 3-14

[3]   D. Bannikov, A. Radkevich. Analytical method for compiling and applying a ballast map for the traction unit Pe2U. Eastern-European Journal of Enterprise Technologies, Vol. 2(1-98), 2019, pp. 6-14

[4]   M. Sysyn, V. Kovalchuk, U. Gerber, O. Nabochenko, A. Pentsak. Experimental study of railway ballast consolidation inhomogeneity under vibration loading. Pollack Periodica, Vol. 15(1), 2020, pp. 27-36

[5]   M. Amine Benmebarek, M. M. Rad. Dem modeling of crushable grain material under different loading conditions. Periodica Polytechnica Civil Engineering, Vol. 65(3), 2021, pp. 935-945

[6]   M. Iwański, A. Chomicz-Kowalska. Application of the foamed bitumen and bitumen emulsion to the road base mixes in the deep cold recycling technology. Baltic Journal of Road and Bridge Engineering, Vol. 11(4), 2016, pp. 291-301

[7]   O. Dubinchyk, V. Petrenko, D. Ihnatenko, V. Kildieiev. Comprehensive analysis of the retaining pile structure with the determining the stability factor by numerical methods, International Conference Essays of mining science and practice, E3S Web of Conferences 109, 00020, 2019

[8]   D. Kurhan, M. Kurhan, M. Husak. Impact of the variable stiffness section on the conditions of track and rolling stock interaction. IOP Conference Series: Materials Science and Engineering, Vol. 985, 2020, 012005

[9]   D. Kurhan, M. Kurhan. Modeling the Dynamic Response of Railway Track. IOP Conf. Ser.: Materials Science and Engineering. Vol. 708, 2019, 012013

[10]   O. L. Tiutkin, L. Neduzha, J. Kalivoda. Finite-element Analysis of Strengthening the Subgrade on the Basis of Boring and Mixing Technology. Transport Problems, 16(2), 2021, pp. 1-10

[11]   J. E. Nicks. The bump at the end of the railway bridge. Doctoral dissertation, 2009, Texas A&M University

[12]   D. Ignatenko, O. L. Tiutkin, V. D. Petrenko, A. M. Alkhdour. Application of centrifugal modeling for the study of landscape structure stability. International Journal of Civil Engineering and Technology, Vol. 10(01), 2019, pp. 2179-2187

[13]   V. V. Marochka, S. H. Boboshko. Analysis of the problems of sections with the transitional rigidity indicator in world bridging. Bridges and tunnels: Theory, Research, Practice, 16, 2019, pp. 82-92

Train Driving Parameters Optimization to Maximize Efficiency and Fuel Consumption

Miloš Milovančević[1], Dragan Milčić[2], Boban Andjelkovic[3], Ljubomir Vračar[4]

[1] University of Niš, Faculty of Mechanical Engineering,
  Aleksandra Medvedeva 14, 18000 Niš, Serbia
  milos.milovancevic@masfak.ni.ac.rs

[2] University of Niš, Faculty of Mechanical Engineering,
  Aleksandra Medvedeva 14, 18000 Niš, Serbia; dragan.milcic@masfak.ni.ac.rs

[3] University of Niš, Faculty of Mechanical Engineering,
  Aleksandra Medvedeva 14, 18000 Niš, Serbia
  boban.andjelkovic@masfak.ni.ac.rs

[4] University of Niš, Faculty of Electronic Engineering,
  18000 Niš, Serbia; ljubomir.vracar @elfak.ni.ac.rs

Abstract: Progress in air and fuel management has greatly increased the efficiency of modern automotive train diesel engines, also achieving significant reductions of pollutant emissions. The increased flexibility of the air and fuel management systems also means a higher number of control parameters and complex interactions between different parameters. The task of tuning the engine control parameters to find the right combination to maximize the efficiency and reduce pollutant emissions is referred to as engine calibration. The task of engine calibration for modern automotive diesel engine has become extremely challenging, requiring large amount of time and money to be spent on engine test bench. The main aim of the study was to test and evaluate driving quality of train diesel engine. The subject of this test is a diesel engine train. The diesel engine train series was made with respect to running safety and dynamic behavior, under the test conditions fulfilled. It meets the prescribed requirements of the standard EN 14363: 2005.

Keywords: train; diesel engine; engine calibration

1   Introduction

Energy consumption is one of the focus points of modern train operation. In the last decade, almost every train company has taken measures to diminish its carbon footprint, and to save energy. Railways are considered energy efficient compared

to other transport modes such as air travelling. These energy reduction goals also affect high-speed railways (HSR), which are expanding throughout the world. The progress in air and fuel management has greatly increased the efficiency of modern automotive train diesel engines, also achieving significant reductions of pollutant emissions. Many studies have been carried out with regard to this issue, in order to reduce the HSR energy consumption. As the operational speed of HSR is much faster than metro train, the efficiency of the HSR can't be ensured only by traditional automatic driving methods, which increase the energy consumption and impair the intelligence of train operation. Increased flexibility of the air and fuel management systems also means a higher number of control parameters and complex interactions between different parameters. The task of tuning the engine control parameters to find the right combination to maximize the efficiency and reduce pollutant emissions is referred to as engine calibration. The task of engine calibration for modern automotive diesel engine has become extremely challenging, requiring large amount of time and money to be spent on engine test bench.

The study [1] defines a set of key performance indicators (safety, timeliness, energy consumption, workload of the driver, environment, cost of maintenance and brand image) relevant to train operation that are specific, measurable, assignable, realistic and time-related, and that are influenced by the driving strategy of the driver. The results show that a maximal coasting strategy causes the least environmental pollution, and in most scenarios its energy consumption coincided with the optimal energy-efficient train control strategy or it had an energy efficiency close to the optimal one. Eco-driving is an energy efficient traffic operation measure that may lead to important energy savings in high-speed railway lines [2, 3, 4]. Rail operations are housed inside a complex and extremely dynamic system where work is distributed in time and space [5]. Finding the way to reduce environmental impact and to produce cleaner energy is the main task of engine manufacturers. Hence, the paper [6] presents different methods and systems of diesel emission control, especially exhaust gas recirculation (EGR) techniques that regulate emissions during their formation, as well as exhaust after treatment techniques which reduce already generated harmful emissions based on the catalytic effect of precious metals, various catalytic converters and particle filtering (DPF). The article 7 has developed and evaluated two models to predict instantaneous exhaust emissions of CO_2, NOx, particle number concentration and geometric mean diameter in accumulation mode (30-560 nm) and in nucleation mode (5.6-30 nm) of a 2.0 euro 4 diesel engine fueled with pure diesel and animal fat in different proportions. Today, diesel engines are no longer mentioned for generating huge amount of soot and high-level of noise. These achievements have been made owing to the employment of numerous mechatronic systems implemented in the engine [8]. Potential of an artificial neural network platform to emulate the performance, emissions and stability indices of an existing single cylinder diesel engine operating in dual-fuel mode with methanol port injection under varying fuel injection pressure has been explored in articles [9, 10, 11, 12, 13, 14]. The main aim of the study was to test and evaluate driving quality of train diesel engine. The subject of this test is

a diesel engine train - DMV manufactured in "Metrovagonmaš" for Serbian Railways. Testing was conducted in respect to a vibration dumping based on research [15, 16] in order to determent driving stability as well as vibration.

2   Methodology

2.1   Experimental Testing Procedure of Diesel Engine Train Series 711

The subject of this test is a diesel engine train - DMV conducted by simplified method and partial procedure according to standard: EN14363. This test was conducted in accordance with the methodology and criteria of the standard: EN14363 -testing for the acceptance of running characteristics of railway vehicles.

The test was conducted on the first train set in the series. Set of diesel engine train is composed of two motor wagons for passengers. Each of the two motor wagons have two axle bogies and the control room in front. Bogies in frontside of the driver's cabs have driving axels, while the axels at the side of the clutch are not driving. Train has four bogies in total. Acceleration in the lateral direction was measured on the two bogies frame.

2.2   Test Conditions

The test was carried out by a simplified method, i.e. measuring vertical and lateral acceleration of the bogie frame.

The procedure was applied according to the standard EN 14363. The test speed of train in both directions, while large radius track (R > 2500 m) was:

$$V_{isp} = 1{,}1 \times V_{max} = 1{,}1 \times 100\,\text{km/h} = 110\,\text{km/h} \tag{1}$$

If it was not possible to achieve testing speed since the maximum speed allowed, in some sections, was considerably smaller. Maximum lateral acceleration at the level of the upper edge of rail needs to be in the limits of $0.81 \div 1.19$ m/s^2, for this type of train and the range of speeds according to EN 14363, annexes G.

Running safety and ride quality testing was performed according to EN 14363. Information about the test:

- Train number: 711 - 001/101
- Type of vehicle: Two diesel engine train
- Manufacturer: "Metrovagonmaš"
- Net weight train: m_0 = 87.663 t

- Maximum train speed: V_{max} = 100 km/h

- Centre bolt distance: 2a = 15,000 mm

- Number of driving units: 2

- Number of bogies by driving units: 2

- Type of bogies: Twin axle with two-stage suspension

- Primary suspension: Double coil springs

- Secondary Suspension: Air

- Primary oscillation damping: Vertical hydraulic dampers

- Secondary oscillation damping: Vertical and horizontal hydraulic dampers

- Leading axle: Pivot

2.3   Geometric Quality of Track

According to EN14363 quality rail track for testing is evaluated through a standard deviation prominence of the left and right rails by profile (vertical deviation - z) and deviation per direction (lateral deviation - y). Levels of quality tracks are marked with QN1, QN2 and QN3. The recommendation of EN14363 of the test track includes:

- 50% of quality sections better than or equal to QN1,

- 40% of the quality sections between QN1 and QN2,

- 10% of cut quality between QN2 and QN3.

The segments in which the deviation has exceeded maximum allowed by quality QN3, was not considered in the assessment of the results. The value of 1.3xQN2 was taken as the limit of QN3. Limit values for evaluating the quality of tracks depends on the maximum constructive speed of the tested vehicle Vmax. In the straight tracks and tracks with large curve radius maximum testing speed was V max + 10 km/h. In the small curves radius (R≤600 m), a testing speed of 80 km/h < V ≤ 120 km/h was applicable. An overview of the relevant track parameters is shown in Table 1.

Railways Serbia used for measuring the geometric parameters gauge measuring the round: Plasser & Theurer type EM - 80 L. Assessment of the geometric quality of the tracks on Serbia Railways is performed according to: "Instruction 339 on unique criteria for the control of the condition of the railways, while recording the following parameters: stability of the left and right rails, which corresponds to the parameter of uneven rail profiles in the vertical direction.

Table 1
An overview of the relevant track parameters

parameters track	Limits for quality of tracks in curves of small radius			Limits for quality of track in the corners of a large radius and the direction		
	QN1 [mm]	QN2 [mm]	QN3 [mm]	QN1 [mm]	QN2 [mm]	QN3 [mm]
Standard deviation by profile (z-deviation, irregularities): - σz	1.8	2.1	2.73	1.4	1.7	2.2
Standard deviation in direction (y-deviation): - σy	1,2	1.5	1.95	1.0	1.3	1.7
Maximum single deviation per profile, irregularities: Zmax	8.0	12,0	15.6	6.0	10	13,0
Maximum single deviation per direction - Ymax	8.0	10,0	13,0	6.0	8.0	0.4

The geometric quality of the track from the standpoint of maintenance criteria is defined in three levels:

- QN 1 value, which results from the track control or from the rate of maintenance in the context of the normal planning tasks of maintenance rails.

- QN 2 value, which results from short-term measures to maintain track.

- QN 3 value, in which exceedances are observed, track segment is excluded from the tests because the geometrical quality of track is not typical of tracks quality. This value still doesn't correspond to the most unfavorable condition, but it is an allowed form the aspect of maintenance.

2.4   Test Train Composition and Condition

Set of diesel engine train is composed of two motor wagons for passengers, which are attached by clutch. Figure 1.

Figure 1
Diesel engine train series 711, equipped with measuring devices

The train was tested in the ready for service mode. The mass of a motor vehicle with toilet is 44.019 kg. Mass of train without toilets is 43,644 kg. Total train mass is 87,663 kg.

For testing purposes, 18 people boarded the train. If the average mass of passengers with luggage is 80 kg, total mass of passengers was 1440 kg, thus, the total mass of the train during testing was 89 103 kg. The rolling surfaces of wheels on a train have a UIC - ORE profile. Before the test, the train has passed about 1500 km so that the profiles of rolling surface of the wheels were a little worn. On Figure 3 is shown measuring points from acceleration.
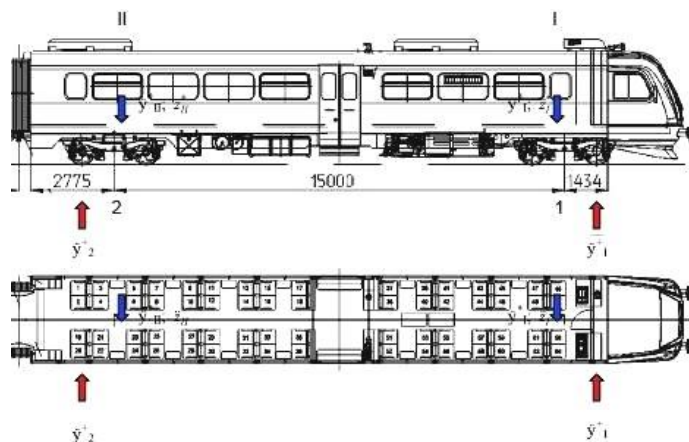
Figure 3

Sensors for acceleration setup

Red arrow are marked measuring points on the bogie frame abovethe axle and, a blue arrow are marks measuring at floor level above the central bogie pivot.

Lateral acceleration of bogie frame was measured (Figure 2), as well as lateral and vertical acceleration on train floor Figure 3. The measuring signals from the channels are shown in Table 2:

Table 2

Measuring signals from the channels

Sizes	Units	Measuring locations	Filter when recording to computer
Transverse acceleration of the frame rotating stand above the front axle assembly lead (drive) rotating stand	m/s^2	1	50 Hz
Transverse acceleration of the frame rotating stand above the rear axle assembly medium (free) working pedestals	m/s^2	2	50 Hz

Sizes	Units	Measuring locations	Filter when recording to computer
Transverse acceleration in the axis of the crate above the lead (drive) bolt rotating stand	m/s2	I	50 Hz
Transverse acceleration in the axis of the crate above the rear pivot of the middle (free) pivot pedestals	m/s2	II	50 Hz
Vertical acceleration in the axis of the crate above the lead (drive) bolt rotating stand	m/s2	I	50 Hz
Vertical acceleration in the axis of the crate above the bolt of medium (free) rotating stand	m/s2	II	50 Hz
Driving speed	km/h	-	50 Hz
Road trip	m	-	50 Hz

During the recording, measurement signals were sampled at a frequency of 300 Hz. Measurement signals of acceleration and speed are provided in Table 3.

Table 3

Measuring equipment

Name	Type	Number	Manufacturer
Encoder acceleration 1	V 12/200	074510716	HBM
Encoder acceleration 2	V 12/200	7321	HBM
Encoder acceleration 3	V 12/200	3047	HBM
Encoder acceleration 4	V 12/200	3052	HBM
Encoder acceleration 5	V 12/200	3290	HBM
Encoder acceleration 6	V 12/200	074510708	HBM
Impulse encoder	Faively	5030	ESPAS
Measuring acquisition system	Quantum X MX 840	0009E5001B2D	HBM
Computer	Notebook	-	DELL

Figure 2

The encoder of acceleration on the frame rotating by - century and above the outer shaft signal

Figure 3
Sensors of acceleration above the main pivot

The characteristics of the measuring equipment used are given in Table 4.

Table 4
Characteristics of measuring equipment

Size	Extended measurement uncertainty
Speed up	± 0,43%
Speed	≤ 0.1%

3   Test Results

The test results are, in the following order:

1)   Track sections with directions and curves of very large radius R ≥ 2500 m

-   motor car 1 forward

-   motor car 1 back

2)   Track sections with curves of large radius 600 m ≤ R <2500 m

-   motor car 1 forward

-   motor car 1 back

3)   Track sections with curves of small radius 400 m ≤ R <600 m

-   motor car 1 forward

-   motor car 1 back

4)   Track sections with curves of very small radius 250 m ≤ R <400 m

-   motor car 1 forward

-   motor car 1 back

The maximum recorded speed driving on a track section was 112.8 km/h. Since minimum speed of 105 km/h was not achieved at this section, the criterion for running speed in test area 1 was reduced to 103 km/h. Criterion of the overshoot Cd ≤ 40 mm was fulfilled during driving in the right curvature radius of 5000 m.

All mathematical expectations of running safety parameters are well below the limit values. The smallest reached factor of safety - λ min is 2.24 for the transverse acceleration above the central pivot of the bogie.

Measuring sections for statistical processing in the test area are presented in Table 5.

Table 5

Test results, measuring sequences for statistical data analyses

Nr. The sections	Stationary		l [m]	R [m]	h [mm]	In P [km/h]	Cd [mm]
	From the [km.m]	To [km.m]					
Section: A							
1	2	3	4	5	6	7	8
1	61.774	62.524	250	∞	-	111.9	-
2	61.524	61.274	250	∞	-	110.6	-
3	61.274	61.024	250	∞	-	109.2	-
4	61.024	60.774	250	∞	-	107.9	-
5	60.774	60.524	250	∞	-	107.4	-
6	60.524	60.274	250	∞	-	107.5	-
7	60.274	60.024	250	∞	-	107.4	-
8	60.024	59.774	250	∞	-	107.8	-
9	59.774	59.524	250	∞	-	108.8	-
10	59.524	59.274	250	∞	-	110.8	-
11	59.274	59.024	250	∞	-	112.1	-
12	59.024	58.774	250	∞	-	112.4	-
13	58.774	58.524	250	∞	-	112.6	-
14	58.524	58.274	250	∞	-	112.8	-
15	58.274	58.024	250	∞	-	112.3	-
16	58.024	57.774	250	∞	-	112.4	-
17	57.774	57.524	250	∞	-	112.9	-
18	57.524	57.274	250	∞	-	112.8	-
19	57.118	56.868	250	5000 / D	0	111.1	29
20	56.868	56.618	250	5000 / D	0	110.5	29
21	56.618	56.368	250	5000 / D	0	109.7	28
22	56.368	56.118	250	5000 / D	0	109.0	28
23	56.118	55.868	250	5000 / D	0	109.2	28
24	55.868	55.618	250	5000 / D	0	110.0	29
25	55.618	55.368	250	5000 / D	0	110.2	29
26	55.368	55.118	250	5000 / D	0	110.3	29
27	55.118	54.868	250	5000 / D	0	109.2	28
28	219.600	219.850	250	∞	-	104.2	-

Nr. The sections	Stationary		l [m]	R [m]	h [mm]	In P [km/h]	Cd [mm]
	From the [km.m]	To [km.m]					
29	217.100	217.350	250	∞	-	105.3	-
30	216.850	217.100	250	∞	-	104	-
31	215.850	216.100	250	∞	-	103.6	-

All mathematical expectations of dynamic behavior parameters are below the limit values. The smallest reached factor of safety - λ min is 1.39 for the effective value of the transverse acceleration of the bogie.

4   Discussion

Testing of diesel engine train Series 711 working abilities verification was performed by program test security running and the quality of driving. Testing was carried out by a simplified method, by measuring the acceleration on the bogie frames.

Tests have included all test areas, i.e. categories of curves, which are provided by standards EN 14363 considering number and total length of the rail track sequence that meets the requirements of the standard.

Maximum speeds are reaching a value of 112.8 km/h, weather conditions during testing, and the state of rail have been appropriate. All mathematical expectation of parameters for secure train running are below the limit value in all test areas.

On the basis of the results of testing, it was concluded that the diesel engine train series 711, product of "Metrovagonmaš" with respect to operational safety and dynamic behavior, during determined test conditions, meets the prescribed requirements of the standard EN 14363: 2005.

References

[1]   Scheepmaker, G. M., Willeboordse, H. Y., Hoogenraad, J. H., Luijt, R. S., & Goverde, R. M. (2019) Comparing train driving strategies on multiple key performance indicators. *Journal of Rail Transport Planning & Management*, 100163

[2]   Fernández-Rodríguez, A., Fernández-Cardador, A., & Cucala, A. P. (2018) Balancing energy consumption and risk of delay in high speed trains: A three-objective real-time eco-driving algorithm with fuzzy parameters. *Transportation Research Part C: Emerging Technologies*, *95*, 652-678

[3]   Cheng, R., Chen, D., Cheng, B., & Zheng, S. (2017) Intelligent driving methods based on expert knowledge and online optimization for high-speed trains. *Expert Systems with Applications*, *87*, 228-239

[4]   Fernandez-Rodriguez, A., Fernández-Cardador, A., & Cucala, A. P. (2018) Real time eco-driving of high speed trains by simulation-based dynamic multi-objective optimization. *Simulation Modelling Practice and Theory*, *84*, 50-68

[5]   Naweed, A. (2014) Investigations into the skills of modern and traditional train driving. *Applied ergonomics*, *45*(3), 462-470

[6]   Kozina, A., Radica, G., & Nižetić, S. (2020) Analysis of methods towards reduction of harmful pollutants from Diesel engines. *Journal of Cleaner Production*, 121105

[7]   Domínguez-Sáez, A., Rattá, G. A., & Barrios, C. C. (2018) Prediction of exhaust emission in transient conditions of a diesel engine fueled with animal fat using Artificial Neural Network and Symbolic Regression. *Energy*, *149*, 675-683

[8]   Nikzadfar, K., & Shamekhi, A. H. (2019) Investigating a new model-based calibration procedure for optimizing the emissions and performance of a turbocharged diesel engine. *Fuel*, *242*, 455-469

[9]   Németh, A., & Fischer, S. (2021) Investigation of the glued insulated rail joints applied to cwr tracks. Facta Universitatis, Series: Mechanical Engineering, doi: 10.22190/FUME210331040N

[10]   Shatrov, Mikhail G. et al. Influence of pressure oscillations in common rail injector on fuel injection rate. *Facta Universitatis, Series: Mechanical Engineering,* [S.l.], v. 18, n. 4, pp. 579-593, Dec. 2020

[11]   Shatrov, Mikhail G. et al. Method of conversion of high- and middle-speed diesel engines into gas diesel engines. *Facta Universitatis, Series: Mechanical Engineering*, [S.l.], v. 15, n. 3, pp. 383-395, Dec. 2017

[12]   Sinyavski, V., Shatrov, M., Kremnev, V., & Pronchenko, G. (2020) Forecasting of a boosted locomotive gas diesel engine parameters with one- and two-stage charging systems. *Reports in Mechanical Engineering*, 1(1), 192-19

[13]   S. Fischer, Investigation of effect of water content on railway granular supplementary layers, Naukovyi Visnyk Natsionalnoho Hirnychoho Universytetu, ISSN 2071-2227, E-ISSN 2223-2362, 2021, № 3, doi.org/10.33271/nvngu/2021-3/064

[14]   Sysyn, M., Nabochenko, O., Kovalchuk, V., Przybyłowicz, M., & Fischer, S. (2021) Investigation of interlocking effect of crushed stone ballast during dynamic loading. Reports in Mechanical Engineering, 2(1), 65-76, https://doi.org/10.31181/rme200102065s

[15]   Kuchak, A. J. T., Marinkovic, D., Zehn, M. Parametric Investigation of a Rail Damper Design Based on a Lab-Scaled Model (2021) Journal of Vibration Engineering and Technologies, 9 (1), pp. 51-60

[16]   Tigh Kuchak, A. J., Marinkovic, D., Zehn, M. Finite element model updating - Case study of a rail damper (2020) Structural Engineering and Mechanics, 73 (1), pp. 27-35

Investigation of the Track Gauge in Straight Sections, Considering Hungarian Railway Lines

Dalma Németh, Henriett Horváth, Majid Rad Movahedi, Attila Németh, Szabolcs Fischer

Széchenyi István University
Egyetem tér 1, H-9026, Győr, Hungary
nemeth.dalma@hallgato.sze.hu,
{horvath.henriett,majidmr,nemeth.attila,fischersz}@sze.hu

Abstract: In this work, considering the MÁV's (i.e., the Hungarian Railways) five small and five high-traffic railway lines, the statistical distribution and change of the track gauge parameter were analyzed, under a ten year, on time-series analysis, related to straight track sections. The analysed data, were bottom track gauge measurements, of the FMK-004 and FMK-007 type railway track geometry, measuring and recording car & wagon. Taking into account the railway tracks, the track gauge parameter cannot be controlled and improved upon by large machine methods, but its permitted value depends on the allowed speed (and vice versa). The main independent variables were the elapsed time and the through-rolled axle tons (as a function of time, i.e., the MGT). To generate the statistical analyses, Vaszary-like shape numbers were computed, considering the distribution functions of the measured data series of the track gauge parameter every 25 cm. The authors examined the change of the shape numbers, the average and standard deviation values of the track gauge, and the shape of the distribution functions (skewness and kurtosis properties). In the end, a spectrum analysis of the measured data series was produced. In conclusion, the Authors provide relevant statements regarding the track gauge parameter.

Keywords: railway track; track gauge; statistical analysis; time-series analysis; distribution

1   Introduction

Railway transportation is one of the most significant modes of continental transportation. The most relevant advantages of it – compared to road transportation – are the following [1]:

- The high travel/transportation performance (it can be more comfortable);

- The environment protection property (it causes less pollutant emission);

- The speed can reach 350 km/h (or higher) in passenger transport and up to 200 km/h (or higher) in freight transport.

In fixed-rail transportation, it is essential to have a system of geometrical size limits for the fixed-rail track, i.e., to keep specific track geometry and rail geometry parameters within the prescribed and requested values. These parameters are essential due to the lack of maneuverability, high vehicle weights, high speeds, and severe consequences of accidents. The parameters primarily depend on the allowed speed on the track in each case. In addition, track monitoring [2] [3] and the geometrical deterioration [4] [5] of the tracks are significantly essential.

In the case of tramways and (ordinary public) railway tracks, the following are usually distinguished in terms of track geometry parameters:

1) Track gauge, it is generally characterized by deviation from the nominal track gauge in mm unit;

2) Alignment, it is usually distortion-free and filtered for wavelengths D1 (3-25 m) or arc-height (chord height) data defined in the middle of a symmetrical 10.0 m long chord from baseline to peak or from peak to peak (value on a straight line 0, in the case of a curve, the alignment parameter is a function of the change in curvature);

3) Longitudinal level, it is usually distortion-free and filtered for D1 (3-25 m) wavelengths or arc height (chord height) data determined at the intermediate point of a chord of 11.8 m (5.0 + 6.8 m) in mm unit, 'from baseline to peak' or 'from peak to peak' in mm unit (its value is 0 in the section between vertical curves on a faultless railway track section; in the case of a vertical curve the value of longitudinal level is a function of the radius of vertical curvature);

4) Superelevation (cross-level): height difference between outer and inner rail in mm unit;

5) Plane distortion (twist), it is the difference in cross-level (cross-level deviation) for a given base length (1.5–2.5–6.0–8.0 m), its unit is mm/m; the value of twist depends on the superelevation transition;

6) Curvature, it is the reciprocal of the radius of curvature belonging to the instantaneous topographical (i.e., horizontal) tangent, its unit is 1/m or 1/km;

7) Other, e.g., calculated parameters (change of track gauge, etc.).

The definition of the track gauge is the distance of two rails (interpreted between lines perpendicular to the rails' running surface) in a given track section. The value of Z_p is generally 14 mm for flat-bottom rails (this is true for Vignol rail profiles; however, it is 9 mm for grooved (Phoenix) rails); the measurement principle is shown in Fig. 1. This 14 mm depth allows the measurement to be less affected by the rail head's lateral wear and the enclosure radius [6].
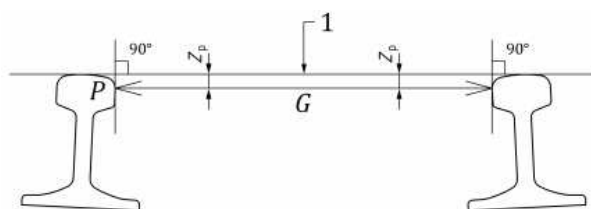
Figure 1
The measurement principle of track gauge [6]

Table 1 contains the various types of track gauge on world railways currently operated without claiming completeness.

Table 1
Various track gauges on world railways [7] (Remark: the 1520 mm track gauge is also a well-known and widely used value as the 1524 mm track gauge)

Type of track gauges	Size of track gauge [mm]	Size of track gauge [feet]	% of total length	Countries
Standard gauge	1435	4'8.5"	62	England, USA, Canada, Turkey, Persia and China
Broad gauge	1676	5'6"	6	India, Pakistan, Ceylon, Brazil, Argentina
Broad gauge	1524	5'0"	9	Russia, Finland
Cape gauge	1067	3'6"	8	Africa, Japan, Java, Australia, New Zealand
Metre gauge	1000	3'3.5"	9	India, France, Switzerland, Argentina
23 various other gauges	different gauges	different gauges	6	various countries

In the case of track gauges occurring in Hungary, it is worth mentioning the value of 760 mm; railway line No. 7 (Children's Railway) and No. 39 (Balatonfenyves narrow gauge railway) in Hungary also have this track gauge value.

The following options are available for measuring the track gauge on railway tracks (taking into account the cases in Hungary):

- Hand-operated track gauge and superelevation measuring equipment
- Track measuring system for surveying railroad geometry
- Track geometry measuring cars and wagons: FMK-004 track geometry measuring car, and FMK-007 track measuring wagon

One of the basic requirements for ensuring accident-free traffic is to keep the factors describing the condition of the railway within the size limits (geometrical tolerances) prescribed for compliance with the standards and regulations.

The neglected track also has an economic issue; i.e., the worse the track state is, the higher the cost of traction energy, the higher the amount of operation, maintenance and rehabilitation, and renewal costs [8].

It is not evident whether the track gauge (as a track geometry) parameter is influenced by the traffic (i.e., the million gross-tons; MGT) and the allowed speed (categories). The aim of the authors is to examine this dependence and variation. They have chosen ten railway lines in Hungary (with the help of the MÁV PLC.) and analyzed the track gauge parameter considering the last ten years.

2   Methods

While selecting the railway lines for the analysis (investigation), the authors covered the possible widest range, even in terms of quality, their role, the permitted speed of the vehicles running on them, and the gross tonnage loaded (i.e., the MGT). The railway lines have different geometric and line designs; they have other constructions (structures) and rail types in the diverse terrain of Hungary.

The following lines (line numbers) were chosen (see Figs. 2-7):

- 11, 13, 145, 146, 147
- 1, 30, 70, 100, 120 (these are double-track lines, only the data of the right track were processed and analyzed)

(The numbering is based on the line numbering system applied in track maintenance according to the Network Business Rules of the Hungarian Railways.)

The inspection time interval was the between 2011-2020. In some analyses, the authors slighty modified this time range.

The track geometry measurements were performed with FMK-004 and FMK-007 track geometry recording cars/wagons, owned, and operated by MÁV Central Rail and Track Inspection Ltd. (MÁV KFV). Thus, the authors were able to work with the raw data sets recorded every 25 cm.
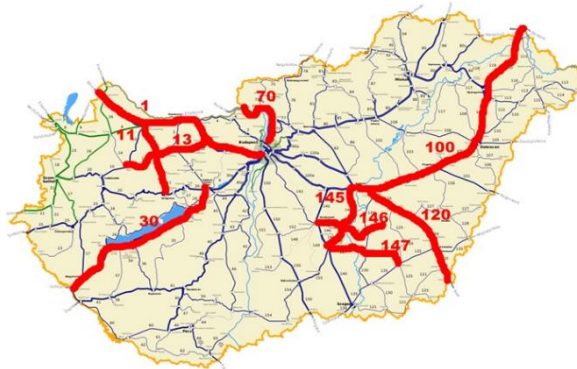
Figure 2
The investigated railway lines in Hungary

	1 – rigth track	11	13	30 – right track	70 – right track	100 – right track	120 – right track	145	146	147
■ Average MGT	37.755	0.574	0.324	11.872	23.221	23.177	19.664	0.458	0.244	0.205
■ Maximal MGT	55.438	0.856	1.904	28.198	28.114	44.086	22.835	0.687	0.335	0.334
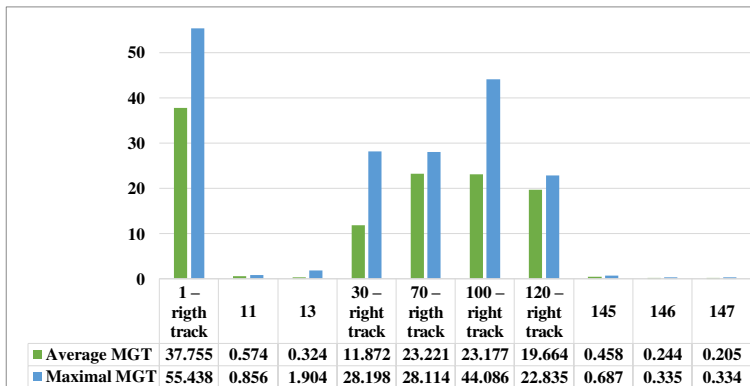
Figure 3

The average and maximal MGT values on the examined railway lines (between 2013 and 2019)
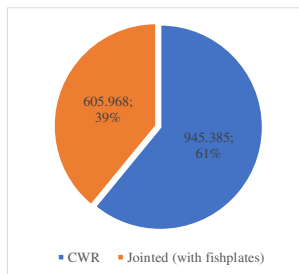
Figure 4

The ratio of the CWR tracks and the jointed tracks on the investigated railway lines (the numbers in the circle mean length values in kilometers)
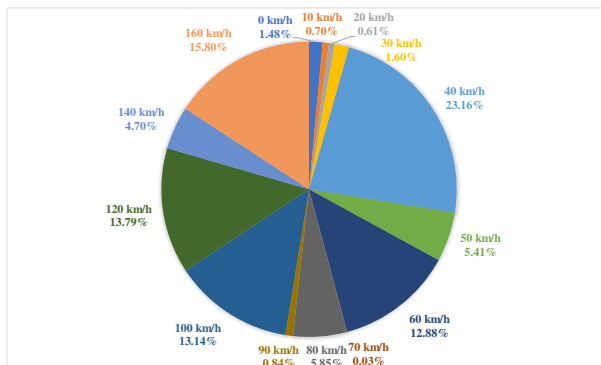
Figure 5

The ratio of the allowed speed values on the investigated railway lines
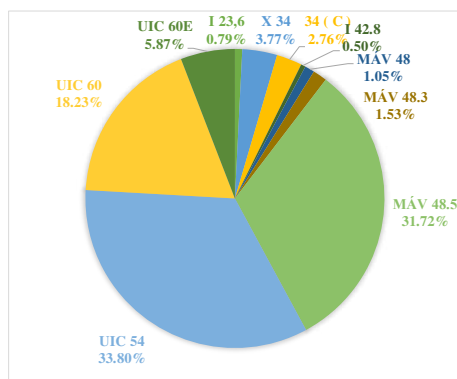
Figure 6

The ratio of the applied rail profiles on the investigated railway lines
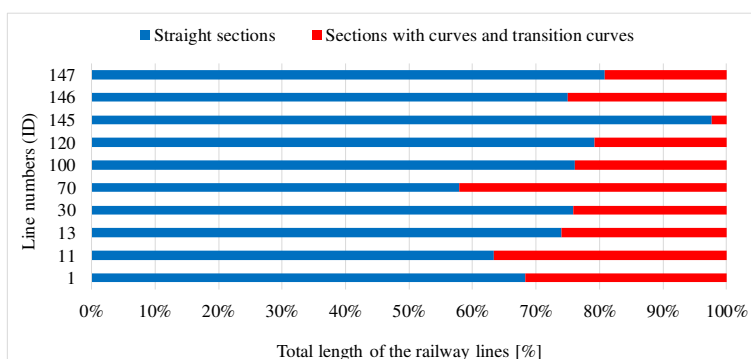
Figure 7

The ratio of the straights and curves sections on the investigated railway lines

In our research, we performed a large-sample statistical analysis.

The authors examined the rate of change of track gauge parameter as a function of time, its dependence on load and speed, the distribution of faults, and the descriptive statistical characteristics only on the straight sections of the railway lines.

To be able to easily plot and manage the 'change of the state or condition' described by the data, the Vaszary-type shape numbers were calculated for the distribution functions (curves) [9]. This shape number allows describing the condition of a track (or a whole railway line) characterized by big data set with a single number. The values for the quantiles of the distribution functions (i.e., 15%, 50%, and 85%) had to be determined. Based the measurements, the characteristics of the condition was calculated in Eq. (1).

$$I_{track\ gauge} = \frac{(i_{15\%}^2 + i_{50\%}^2 + i_{85\%}^2)}{10} \tag{1}$$

The authors randomly selected 1-1 random data sets for each railway line for which they performed a statistical test. The authors examined whether the measurement data sets show a normal or lognormal distribution. To the lognormal distribution, 10 mm (in some cases 20 mm) was added to the measured values so that their e-based logarithm (e=2.718) could be interpreted. It was only a transformation that did not modify the fundamental property of the statistical distribution. The calculations were executed with Kolmogorov-Smirnov statistical test in MS Excel software (chi-square, Shapiro-Wilk, Jarque-Barre, D'Agostino-Pearson tests would also have been possible). The authors also defined the skewness and peak characteristics for the distributions, which show how much and how the given distribution deviates from the normal distribution.

In the case of track geometry measurements, according to the TSI regulation [10], for the longitudinal level (i.e., settlement) and alignment parameters, it is compulsory to filter the measurement results so that only the part representing them in a specific wavelength range appears in the result. For example, filtering is often used for the wavelength range D1 (wavelength between 3 and 25 m).

There is no such filtering requirement for track gauge measurements. Still, the question arises as to what typical wavelengths are included in the national track gauge measurements' data sets, as it is possible to deduce from them the causes and nature of track gauge differences. Therefore, Fourier transformation was performed on the arbitrarily selected signal sequences so that the share of each wavelength component in the examined sample becomes visible.

3   Results and Discussion

During the time series analysis, the authors applied one measurement per year for the railway lines, which preferably covers the most extensive length of the railway line and contains various data from summer and winter. However, it has happened that specific measurement zones have been left out of the data series, so there is a difference in the number of pieces per year, which can have a minimal effect on the output results. However, the number of measurement data is still the case that they represent hundreds of thousands, millions of items each year.

The figures calculated for the data series are first the time followed by the traffic load (MGT). The main question is whether any dependency can be detected from the data. Fig. 8 illustrates the change of the calculated $I_{track\ gauge}$ as a function of a time related to each railway line.
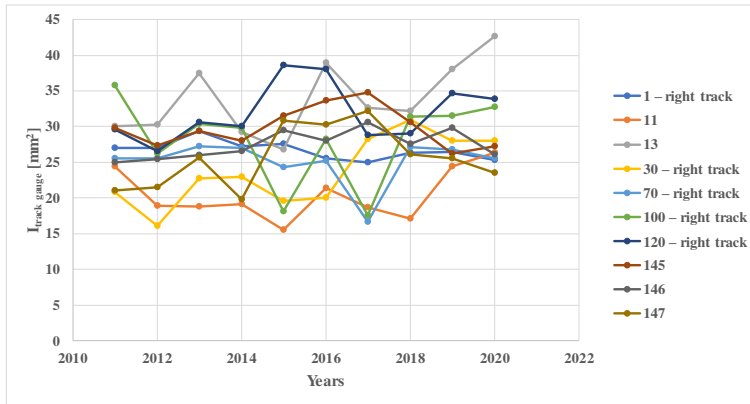
Figure 8

Change of the $I_{track\ gauge}$ shape number as a function of the time

It can be seen in Fig. 8 that the charts (lines) approximately remain in the range of 15… 40 mm^2. No significant trend can be observed for any of the railway lines. It is typically more alternating each data set in a given band. The larger the number of shapes, the flatter the defects distribution curve, i.e., the track gauge parameter moves over a broader range. Traffic load was also an aspect to be examined. However, the authors did not consider the above 'point graph' but a bar graph display expedient.

Fig. 9 illustrates the results, where the base railway line is railway line No. 1 (and its right track), while the authors chose 2019 as the base year. It can be stated that the result values depicted in Fig. 9 don't depend on traffic load (MGT), i.e., the track gauge parameter (and its change) does not rely on it either.
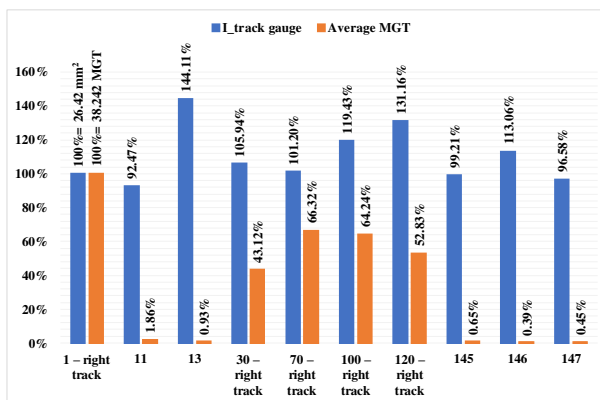
Figure 9

Change of the $I_{track\ gauge}$ shape number as a function of the through-rolled axle tons (MGT); basis year is 2019

Fig. 10 shows the change of the $I_{track\ gauge}$ shape number as a function of the time considering the allowed speeds.
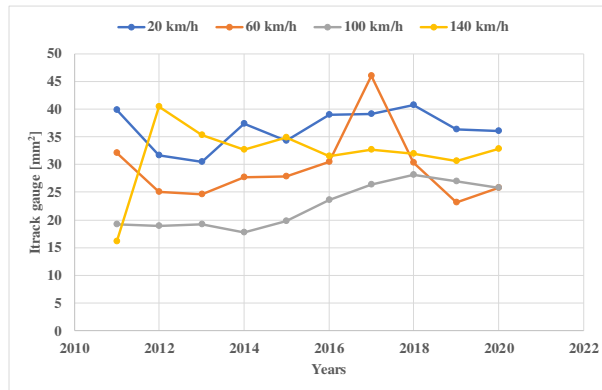
Figure 10

Change of the $I_{track\ gauge}$ shape number as a function of the time considering the allowed speeds

Based on Fig. 10, in 2011, the expected order developed between the speeds, but it is characterized by volatility in the other years. The authors think the alternation can be the different speeds are a set of data from different types and qualities of tracks. In this way, the speed data set containing more data from subsidiary railway lines resulted in worse (higher) values than those related to only main railway lines.

Fig. 11 shows the mean and the standard deviation values in the whole inspected time range.

	2011	2012	2013	2014	2015	2016	2017	2018	2019	2020
Mean	-0.543	-1.050	-0.571	-0.545	-0.808	-0.410	-0.126	-0.233	-0.067	-0.415
St. Deviaton	2.885	2.509	2.933	2.703	3.016	2.816	3.333	2.666	2.704	2.587
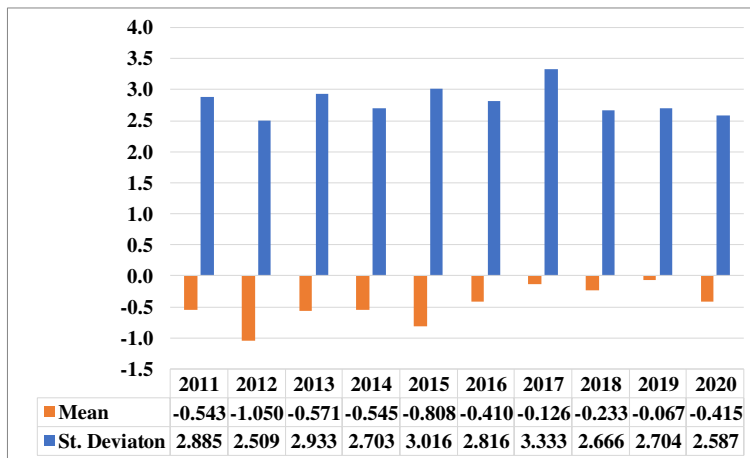
Figure 11

Change of the $I_{track\ gauge}$ shape number as a function of the time considering the allowed speeds

From the annual average values, it can be seen that Hungary is characterized by mainly track gauge narrowing (in the range of 0…–1.05 mm in the case of the examined railway lines).

The standard deviation of the examined straight track sections can be said to be uniform in the elapsed time; the difference between the maximum and minimum values is 0.824 mm. The most significant rise occurred between 2016 and 2017, which means 0.517 mm in the current case, the most significant decrease between 2017 and 2018 is –0.667 mm.

Fig. 11 presents the results of the spectrum analysis related to the examined ten railway lines.

It can be seen that the extensions are located higher with several errors compared to the main lines (as expected). They contain a larger weight, a larger amplitude from a given wavelength.

The authors executed distribution analyses related to the data sets. Because of the limited space, there is no possibility to show the details; however, the results indicated that the received measurement data neither have Gaussian nor lognormal distribution. The analyses were related to Kolmogorov-Smirnov tests (i.e., the lognormal distributions were checked by the log(e)=ln values of the original data sets).

The authors plan to continue their research in the future with considering only the curves and transition curves, analyzing the Fuzzy or Fuzzy-random behaviors of the measurements, etc.
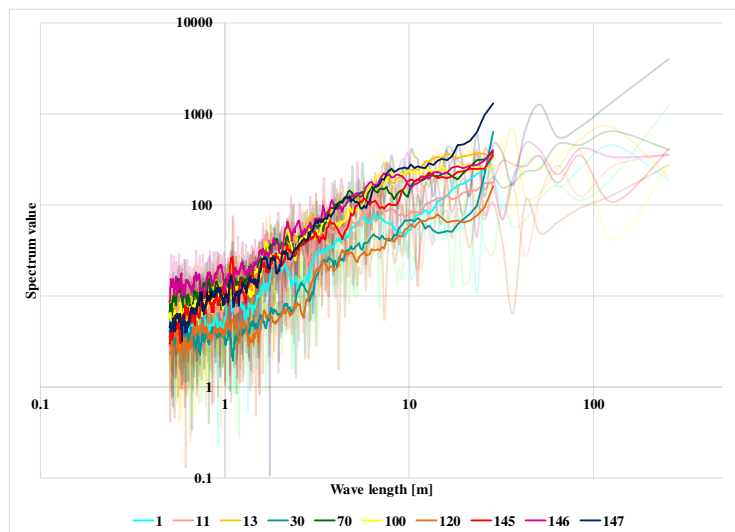
Figure 12
Result of the spectrum analysis

Conclusions

The following conclusions can be drawn, based on the authors' research and results:

1) Considering the examined ten (10) railway lines, there is no significant correlation between the change of the track gauge, average and standard deviation values, elapsed time and traffic loading (i.e., MGT).

2) Typically, in Hungary, there is a narrowing of the track for the straight sections. As a result, the standard deviation of the errors is balanced.

3) The measured data sets of the 10 examined track gauge parameters have neither a Gaussian, nor a lognormal distribution.

4) The examined parameter is characterized by a peak and right-sloping shape distribution every year. Larger values in the sideline indicate that they deviate better from the normal distribution.

5) Lower velocities have a flatter distribution curve, steeper for higher speeds. Thus, it can be stated that the parameters deviated more from the nominal value at lower speeds.

6) In the case of the track gauge parameter, the distribution curves of the sidings were flatter, so the condition of the track is worse than expected.

7) The subsidiary contains a more considerable weight and amplitude from the given wavelength; they have more errors than expected.

Acknowledgement

References

[1]   M Sysyn, V Kovalchuk, U Gerber, O Nabochenko, B Parneta, Laboratory evaluation of railway ballast consolidation by the non-destructive testing. Communications-Scientific letters of the University of Zilina, Vol. 21, No. 2, 2019, pp. 81-88

[2]   A. Kampczyk, K. Dybeł, The fundamental approach of the digital twin application in railway turnouts with innovative monitoring of weather conditions. Sensors, Vol. 21, No. 17, 2021, 5757

[3]   A. Matejov, J. Šestáková, The Experiences with utilization of BIM in railway infrastructure in Slovak Republic and Czech Republic. Transportation Research Procedia, Vol. 55, 2021, pp. 1139-1146

[4]   M. Sysyn, O. Nabochenko, V. Kovalchuk, M. Przybyłowicz, S. Fischer, Investigation of interlocking effect of crushed stone ballast during dynamic loading. Reports in Mechanical Engineering, Vol. 2, No. 1, 2021, pp. 65-76

[5]   A. Németh, S. Fischer, Investigation of glued insulated rail joints applied to CWR tracks. Facta Universitatis-Series Mechanical Engineering, 2021, 7642

[6]   MSZ EN 13848-1:2004, Railway applications/Track. Track geometry quality. Part1: Characterisation of track geometry, 24 p.

[7]   S. Chandra, M. M. Agarval, Railway Engineering, Oxford University Press, India, 2013, 676 p.

[8]   D. Kurhan, M. Kurhan, M. Husak, Impact of the variable stiffness section on the conditions of track and rolling stock interaction. IOP Conference Series: Materials Science and Engineering, Vol. 985, No. 1, 2020, 012005

[9]   D. Németh, H. Horváth, Statistical distribution and time variation of the track gauge parameter on the lines of the Hungarian railways, taking into account several low- and high-traffic railway lines, SIU, 2020, 55 p.

[10]   TSI.   https://eur-lex.europa.eu/legal-content/EN/TXT/PDF/?uri=CELEX: 32014R1299&from=HU [online, last visited on: 2021.10.15]

A Review of Research on Detection and Evaluation of the Rail Surface Defects

Lei Kou

Institute of Railway Systems and Public Transport, TU-Dresden, Reitbahnstr. 35, 01069 Dresden, Germany; lei.kou@tu-dresden.de

Abstract: Defects on the rail surface will hasten the wear of the wheels. At the same time, when the wheel is periodically hitting and rolling surface defected, the defects will gradually develop into the interior, which significantly increases the possibility of a train derailment and serious safety accidents. A timely checking of the railway tracks to find defects as early as possible is a basic condition for ensuring the safety of railway operations. It also prolongs the service life of railways because most of the rolling contact fatigue (RCF) can be eliminated during rail grinding. Such defects appear as spalling and cracks in the first stage of the rail surface. Manual detection has been challenging to meet the large-scale railway running mileage. Therefore, a more efficient automatic detection method is indispensable. This article reviews the latest research and exploration on the defect inspection of rail surfaces in recent years. In the article, not only the application of traditional ultrasonic and acceleration detection methods but also contributing computer vision and deep learning to detect defects on the rail surface. The new detection technology can even classify and evaluate the damage, further improving the efficiency of the detection system. Besides, the emerging research on defect state prediction to reduce inspection costs is interesting.

Keywords: rail surface defects; machine learning; detect; CNN

1   Introduction

In the 21st Century, railway transport will be an increasingly important task related to the developed world and society. It started in the 19th and 20th Centuries with enormous railway construction procedures worldwide [1-3]. Railway construction investment has been continually increasing. It can be said that traffic safety is an important consideration for traffic users when choosing a particular means of transport. It is critical to the scale of traffic implementation, revenue, and overall business performance [4]. The total railway mileage in the world is about 1.5 million kilometers, and the European Union accounts for about 25% [5]. The rail is an important part of the railway. The defects on the surface of the rails have caused great damage to the wheelsets and bearings of the rail vehicles. When the

wheels are moving on the track with defective surfaces, periodic impacts will cause the coupled vibration of the entire vehicle and the track system. It will reduce the service life of the train components and a significant cause of vehicle derailment overturning and combustion axles. Therefore, defect detection of railway tracks is an essential means to ensure the safety of railway transportation. The annual railway inspection cost in the EU (European Union) alone is about 70 million euros [6]. Finding rolling contact fatigue (RCF) as early as possible cannot only avoid traffic accidents but also take timely measures to extend the service life of rails [7], both of which can reduce railway running costs [8]. The detection of track surface defects has long relied on manual inspections. This detection method needs experts to visually inspect components and use specific tools to identify any defects in the rail surface [9]. However, this method is cumbersome, hardworking, and prone to human error. In addition, the personal safety of the inspectors is also an issue that needs to heed. With the increase in demand for high-speed railway transport and advanced technology, it is necessary to develop an automatic intelligent detection system to replace manual detection in detecting track surface defects.

Although the continual improvement of technology has reduced the probability of internal defects in the rail, the probability of fatigue cracks on the surface of the rail is still high [10]; harsh environments can also cause surface defects, which may irritate worsening the rail [11, 12]. Surface defects of rail can be divided into the wave-shaped abrasion and discrete disease of the rail. Wave-shaped abrasion refers to the irregularity of the wavy shape of the periodic disease that appears on the surface of the rail in the longitudinal direction [13]. Discrete damage occurs randomly on the surface of the rail [14]. With developing technology, people have fully researched and applied the detection methods of rail surface defects by using the above technologies. Non-contact detection methods based on machine vision have gradually developed and been widely used in electrical, electronic, mechanical, automotive, and industrial inspections. Machine learning can even predict some regular damage.

This article reviewed the rail surface defect detection, recognition, classification, and evaluation methods proposed and improved in the past ten years. Technical analysis, the characteristics of technology, cost performance, accuracy, and the object to which the method is applicable. However, the results of each method and the matching limits are recorded. Through comparing and analysis methods that can evaluate the size or severity of rail surface defects or classify them to select the best rail surface damage detection method. The organization of this article is as follows: Chapter 2 expounds on the research results of detection and recognition, discusses and emphasizes the advantages and limits of each method in the paper. Chapter 3 introduces the research results of classification, evaluation, highlights the accuracy and background conditions of every method in the article. Chapter 4 discusses the results, analyzes the characteristics of the method, and shows the overall progress in the field. Finally, Chapter 5 summarizes the purpose and results of this article, and prospects for detecting technologies.

2   Detection Methods

In the paper, the detection methods shown in 70 research papers regained by Scopus can be divided into six categories: geometry measuring, detecting wheel track motion (vibration or acceleration), using electric or magnetic field changes, using acoustic or light waves (thermal sensors), Image processing and machine learning. The research field is mainly concentrated in the emerging image processing and machine learning fields. Because other detection methods have been around for a long-time and have been thoroughly studied, the new research mainly explores improving detection technology and optimizes a particular step. In this section, a comprehensive review of these papers will be conducted. Analyze the performance, results, and limits of each technology.

2.1   Geometric Measurement

Although measuring geometric information can get the situation of the railway track through many indicators [15], good results have been achieved. A single geometric measurement method is used to obtain the geometric data of the track surface, mainly through a mechanical stylus or laser reflection. These methods can only detect a cross-section and cannot provide macroscopic inspection data. Later manual inspections are still required to confirm the location and size of surface defects, but most inspections in the railway industry do not use 3D reconstruction technology. To complete 3D technology combines cross-sectional data with a longitudinal plane positioning based on geometric detection, making 3D model reconstruction possible in defect detection on the rail surface. Ye et al. present a novel 3D perceptual system based on a low-cost 2D laser sensor [16]. This method uses the 2D laser sensor detection system and a drawing sensor to decide the longitudinal position movement. The data are formed into a three-dimensional point set. 3D modeling by Matlab. Use the 3D model to identify rail surface defects. Rikhotso et al. also applied this method to measure rail profile and detect defects on the track surface [17]. Casey Jessop and Naeimi each proposed a 3D modeling method combining the stylus Profile-metric and X-Ray scan data. The results showed a geometry similar to the squat network, also possible to infer the crack tip of the surface to a deeper depth that needs improvement. Still, the description of the mid-depth squat crack network is sufficiently accurate [18, 19].

The above methods can theoretically detect surface defects, but they also have obvious shortcomings. Radiography is mainly used to detect internal defects. Surface defects are just derived properties and cannot be quickly moved to detect. The geometric detection of mechanical contacts also has this disadvantage. Laser sensors are sensitive to the environment, too strong light will affect the measurement results, and strenuous exercise will cause high deviations. Niu et al. proposed a method based on a binocular line scanning system, which can obtain contour information in the high-precision image while avoiding the decoding

distortion of the structured light reconstruction method [20]. Sysyn et al. applied the modeling method to detect surface wear of turnouts, using the measurement data on the surface scanning device to establish the 3D model of the turnouts and analyze the change of the wheel/rail trajectory to detect the defect of turnouts [21]. This method has high 3D modeling accuracy while high detection speed, which is a research direction worth looking forward to.

2.2   Electromagnetic Detection

Electromagnetic detection is a broad region of technologies used in railways. Due to surface inspection of blind subjects in conventional ultrasonic technology, an eddy inspection method based on electromagnetic principles has been proposed to detect the rail surface and near-surface defects [22]. Eddy testing uses alternating magnetic fields to create vortex-like induced alternating currents in the measured conductive Rail. The conductivity, magnetic permeability, defects, defect size, and shape of the measured part affect the distribution and size of the eddy. Through the coil-detection to measure the magnetic field change caused by the eddy. The distribution, size, and phase of the eddy in the test piece were measured without contact. It can perform high-speed inspections but has a skin effect and can only detect the surface and near-surface structure status of conducive materials [23]. The eddy testing technology has matured application examples in Eurailscout in Germany and Sperry in the United States [24]. However, lift-off has a more significant impact on the accuracy of rapid inspection. Huang and others, the Chinese Academy of Railway Sciences, and others have studied the card-type eddy sensor used to detect surface defects of curved turnout rails [25]. The research team of Nanjing University of Aeronautics and Astronautics has been continuously researching magnetic flux leakage detection technology in recent years. The team studied the development of array-type magnetic flux leakage inspection equipment and quantitative analysis of rail cracks to get defect location and distribution characteristics. Under the simulated conditions of the laboratory, the inspection speed of cracks with a width of 0.2 mm can reach up to 200 km per hour, which is in the leading position in the field [26]. This team added a ferrite in a sensor to reduce the reluctance to increase the magnetic intensity above the defects to increase the MFL signals [27]. It also gives an improved adaptive filtering method is proposed to solve the problem caused by filtering the MFL signal on the rail top surface [28].

The alternating magnetic field measurement method detects material defects by measuring the changes in the induced magnetic field on the surface of the Rail, which can realize the accurate positioning and measurement of defects. The data Rows Handel collects from ACFM sensors are processed offline by combining threshold and feature matching methods rather than simple threshold methods. Even in the presence of peeling changes and noise, the automatic detection of surface damage defects has high reliability [29]. Chacón Muñoz et al. presents the

B-Spline approach used for the accurate filtering of the noise of the raw ACFM signal gained during high-speed tests to improve the reliability of the measurements [30]. Papaeias et al. studied the applicability of ACFM technology in detecting and assessing the severity of surface cracked RCF defects [31]. ACFM technology has an extensive development prospect in detecting and quantifying RCF cracks. However, it is necessary to overcome the influence of the probe on the detection sensitivity caused by being too far from the object's surface. It is needed to continue improving the sensitivity of corrugated and polished track detection.

2.3   Track-side and On-board Vibration and Acceleration Detection

The dynamic interaction between the wheels and the track produces vibrations and varying accelerations transferred through the track system, air, and rolling stock. This vibration is generally used to measure rail defects in squats. Axlebox acceleration (ABA) measurement is often used to identify railway and track irregularities. The squat is a kind of rolling contact fatigue defect, and early detection is conducive to the safe operation of railways [32]. Mykola Sysyn et al. deal with measurement interpretation problems by analyzing vibration to estimate the health of the turnout [21]. Some scholars try to use this technology to detect spalling defects on the rail surface. Andrew Keong Ng aims to model and simulate three common defects with three degrees of damage, process and analyze the simulated RSD-driven ABA signal, and create explicit dynamic finite element models of wheel-rail interaction for tracks with and without RSDs [33]. Sysyn et al. introduced a method to detect the defect of the turnout by using the ESAH-F system to perform the machine learning on the inertial measurement data of the axle box on the running train [34]. The research team then discussed the Hilbert-Huang transform method used to overcome the relationship between the measured acceleration component and impact lateral distribution and the life cycle of ordinary turnout contact surface [35]. However, this detection method is challenging to use to detect cracks and small peeling. Besides, it is not practical outside the laboratory, because the vertical acceleration of the train in operation is affected by too many reasons.

2.4   Sound and Light Wave Detection

Acoustic wave detection uses the characteristics of sound wave reflection, diffraction, and transmission to determine whether there are defects inside the measured rail by watching the waveform, echo, sound velocity, attenuation, and resonance of the ultrasonic wave in the measured rail. Conventional ultrasonic technology has been widely applied in the detection of internal defects in steel rails. Defects extending in the horizontal direction and longitudinally close to the

gauge angle will reflect the ultrasonic wave, and obstruct the incidence of the sound beam so that the dangerous cracks buried under it cannot be detected. There is a prominent detection blind zone, defects with a depth of less than 4 mm from the surface of the tested part. There will be missed inspections. Therefore, ultrasound is generally not used for surface defect detection. However, Yi Jiang et al. and Hui Zhang et al. still tried to detect near-surface damage [36, 37]. The outstanding research is that Yuehong Zhang et al. studied the technology of rapid laser ultrasonic detection of rail surface defects and designed an interlaced laser ultrasonic defect detection imaging method: laser ultrasonic signals are excited on both sides of the rail to detect, and the images are fused and registered by algorithms. Filtering and image registration, obtaining a complete rail surface inspection image, displaying defect characteristics, and solving laser ultrasonic insensitive to defects [38]. Also, Bilawal Ramzan et al. proposed a research method to use Active Thermography to detect railroads surface crack [39]. The reflection of microwaves can be used to measure distance. Andrey Zhuravlev et al. proposed using the microwave or short waves to detect the rail surface, but it has become a method [40].

2.5   Image Processing Detection

Accurate judgment and cognition through computer vision research have been applied in many fields with the development of science and technology. The basic principle of rail computer visual damage detection is to use an image acquisition device to obtain information on the surface of the rail and convert it into an electronic image signal. By filtering the image, the contrast and equal processing are enhanced. According to the data characteristics of the pixel, the interference will interfere with various code operations. The background information is eliminated, and the characteristics of the rail surface damage, such as size, length, number, etc., are extracted. It even uses deep learning to mine the potential features of the data to classify and judge damage. The basic computer vision inspection system, the important part of the composition, includes the image acquisition module, the image-the preprocessing module, and the result judgment module. The research in computer vision also focuses on the optimization and exploration of these three modules. Usually, an inspection system is constructed by combining the improved methods of all stages. Liu and Wei presented a detection system based on image processing and edge detection to find the defect on the rail surface [41-44].

About improving the image acquisition module, it is mainly to adopt better equipment and optimize the method of acquiring images. The more creative research is that Francisco Javier de la Calle Herrero, etc. proposed a system that uses visual algorithm processing to find changes in pixel values between images [45]. Besides, Jia Ge et al. present an improved traditional system by combining a speed adaptive (SAA) system to adjust the appropriate exposure frequency and

uniform image quality at any time according to the speed of the vehicle [46]. Guangyu Dai et al. studied an image processing system that is useful for online real-time detect the defects of the railway track surfaces. When the images are obtained by linear CMOS camera, the train detection speed can be 50 km/h while the image is a planar array CMOS camera; the train speed can be 100 km/h [47].

More researches focus on the image-processing module and the defect recognition module. The irregularity of rail surface defects makes automatic visual inspection very difficult. Because irregular defects appear randomly on the surface of the rail, the defects can only be located according to the image pixels. Moreover, in the natural environment, the uneven illumination and different reflectivity received by the curved surface of the rail will greatly impact the grayscale distribution of the image. The electronic interference in the image acquisition process will inevitably add some noise to the image [48]. At the same time, effective image enhancement and automatic threshold segmentation of defective images can improve detection efficiency. The image processing process mainly goes through the following steps. First: Track positioning, using the principle that the track surface and the background are quite different, such as edge detection, gray value positioning [49], etc. Second: Image noise reduction, the commonly used noise reduction methods are: mean filtering, median filtering, non-local means, Gaussian filtering, etc. Third: Image enhancement, traditional methods are global histogram equalization, adaptive histogram equalization, contrast-limited adaptive histogram equalization [50], local contrast enhancement [51], low-rank matrix decomposition, etc. At Last: Threshold segmentation, commonly used methods are: Ostu, Maximum between-class variance method, maximum entropy method, Iterative threshold method, etc.

The research on image processing has mainly improved and innovated on the original methods. Li et al. propose the Michelson-like contrast (MLC) measure image enhancement method with a new threshold algorithm, named proportion emphasized maximum entropy (PEME) [46]. Wu and Li optimized the background difference method by reducing the template preprocessing to reduce the influence of shadows and a loop threshold algorithm using histogram judgment [52]. Jinrui Gan et al. proposed a background-oriented defect detector (BODI), which uses modeling to determine specific image features of the track to distinguish background and defects to improve detection efficiency. The perfect detection rate of 100% for large defects, but only 41.78% for relatively small defects [53]. The defect-recognition rate reached 92.2%. Yu et al. proposed a coarse-to-fine model (CTFM) to identify defects of different scales. Using different image processing methods to identify various defects has achieved better results than the previous method. The accuracy rate reached 100% in the actual evaluation [54] Hu et al. proposed an optical rail surface spalling detection algorithm based on visual saliency. Use a two-dimensional differential Gaussian (2D DoG) filter to reduce noise [55]. Wu Yunpeng et al. proposed the LWLC-GSME model in a drone-based visual inspection system, using a new image

enhancement algorithm based on local Weber-like contrast (LWLC) to enhance railway images and gray-scale stretched maximum entropy (GSME) segmentation images [56].

The image processing method of visual inspection shows better performance than other detection methods in detecting the rail surface peeling damage. However, in practical applications, it may be affected by more factors to reduce the accuracy. Therefore, some new image processing technologies have also been used. For example, Ashwani Kumar Dubey proposed using the maximally stable extremal region marking on the original system [57]. In the turnout surface wear detection field, Sysyn et al. introduced the application of computer vision in the diagnosis of common cross frogs [58]. However, technology has insufficient detection accuracy in detecting the rail surface cracks or more minor defects. With the continuous research of computer machine learning, the efficiency and accuracy of machine learning methods in image classification have surpassed the traditional classification methods. Since 2010, many scientific research institutions have conducted a lot of research on the categorization of rail surface defects in this field and make specific predictions about the development of cracks or defects. Machine learning methods are necessarily accompanied by defect assessment and prediction, so they are introduced in the next section.

3   Classification Evaluation and Prediction

Advances in technology have made it possible to automatically classify or evaluate the damage to the track surface, whether it is based on ultrasonic inspections or, of course, more visual images. Now the final evaluation and classification step almost have to rely on machine learning. Current methods for predicting features of track defects and even more minor cracks must also use machine learning. This section mainly introduces some research results in this field in the past ten years. Machine learning is divided into deep learning and shallow learning methods. The shallow machine learning calculation logic is relatively simple, and the classification analysis of available features is more accurate. Deep machine learning is more complex and has advantages in the classification and analysis of uncertain features.

3.1   Shallow Machine Learning

The traditional data classification method is a shallow machine-learning model. The basic process of using image information classification is as follows: First, image features are extracted. Commonly used image features include HOG (Histogram of Oriented Gradient) features [59], LBP (Local Binary Pattern) features [60], HAAR features, and SIFT (Scale Invariant Feature Transform)

features [61]. After extracting the feature words, use the word bag model or clustering method (Marker controlled watershed segmentation (MCWS), K-means (KM) clustering, Expectation-Maximization (EM), and canny edge detection (CED), etc.) to reshape extracted features. Then, send the reshaped features to the classifier to get the classification result. Commonly used classifiers include support vector machines (SVM), decision trees, random forests, and Bayesian classification. Mercy et al. introduced three machine-learning methods for the prediction of track surface defects. Decision trees have the highest accuracy in predicting distortions and inhomogeneity. The random forest has the highest accuracy in predicting specific defects [62]. Regardless of accuracy, the recognition rate and complexity of the detection task. Machine learning has reached or even surpassed traditional methods.

Table 1 summarizes some research on the detection and judgment of track surface defects using image processing methods and the recently studied shallow machine learning methods. Shallow machine learning can already perform evaluation tasks other than the detection of rail surface defects, such as classification. Nearly 90% of the classification tasks of multi-class classification have been well applied in practice. With the research and development of deep learning, the effect of deep learning in target detection tasks surpasses all the above methods. And people gradually turn to the study of deep learning rail surface defect detection.

3.2   Deep Machine Learning

The deep learning model can learn deep abstract features layer by layer from the data set through supervised and unsupervised modes to achieve an abstract description of learning goals. The concept of deep learning has been produced since 1986. Deep learning models can learn deep abstract features layer by layer from the data set through supervised or unsupervised learning methods to achieve abstract descriptions of learning goals. In 2016, Hinton et al. elaborated on the deep learning system and proposed related technologies such as deep neural networks. In recent years, the wave of deep learning research has come and has produced many significant results.

The deep learning models currently used in the field of image and visual recognition mainly include Stacked auto-encoders, SAE, Deep belief network, DBN, and Convolutional Neural Networks, CNN), among which CNN has achieved satisfactory research and application results. A multi-layer convolutional neural network (convolutional neural network, CNN) can adaptively input data for feature learning and classify or recognize the learned features. CNN-based target detection is mainly divided into three categories: regression-based network models, such as YOLO, network models generated based on candidate regions, such as R-CNN, Fast R-CNN, Faster R-CNN; search-based network models, such as AlexNet; and VGGNet. Since deep learning simulates the human visual

perception system, avoids the weaknesses of manual design features, and has the advantages of non-linearity and high parallelism, it has a wide range of applications.

Table 1
Image Processing and machine learning methods for rail defect detection

Method	Features	Dataset	Results	Ref.
Decision Tree	Rail surface defect	Data from East Coast Railway division	Precision= 93.02%	[62]
Random Forest			Precision= 95.23%	
Region growing	The area of defect	Rail Images Acquisition	Sensitivity=100%	[63]
MCWS			Sensitivity=90.9%	
K-means			Sensitivity=72.7%	
Canny edge			Sensitivity=81.8%	
SVM	Crack	17000 Rail images from CRH and CM	Accuracy=99.87%	[64]
Random Forest			Accuracy=100%	
logistic regression			Accuracy=99.74%	
boosted tree			Accuracy=99.92%	
AdaBoost multiclassifier +CART decision tree	Rail surface defect classifier recognition	1200 rail images	Recognition rate(%): Scale peeling crack=81.45; Stripping block =79.64;Tread cracks=82.27	[65]
Deep Forest	Peeling and Crack classification	Video from X5 PTZ camera	Classification accuracy =100%	[66]
LWLC+GSME	$25<$T-I Defect $<$ 255 mm^2; T-II > 255mm^2	HD video from DJI Matrice 600	T-I Precision=88.63.22%; T-II Precision=90.32%	[56]
GMM+MRF	Rail surface defect	Image detection system	Precision =88.8%, recall =92.0%	[67]
Bayesian classification + EM	Onboard detection RUL prediction	Data from 3D acceleration sensors	RUL predicted accuracy= 75%	[68]
MODWPT+ Lasso regression	Trackside detection RUL prediction	Data from 3D acceleration sensors	RUL predicted accuracy= 50%	[69]

There have also been a lot of researches in the detection of rail surface defects. The surrounding set is the RSDD data released by Beijing Jiaotong University. By combining Wavelet Scattering and Neural Networks, Yang Jin improved classification accuracy up to 97.20% and 94.74% for the two datasets [70].

Combining the advantages of the bilateral full convolutional network and CRF proposed by Zhang Ziwen and others will also significantly improve detection accuracy [71]. This article introduces the use of deep learning, mainly neural convolution, to detect rail surface defects in the past ten years. Part of the research on classification and evaluation is shown in Table 2. Various methods can be intuitively compared.

3.3   Prediction

The losses caused by the catastrophic railway failures caused by RCF are difficult to estimate. Although the rails are very expensive, the defects are found in time, and the prediction and evaluation are carried out. The forecast reduces the number of inspections and avoids disasters, which is an economical and safe method. In the field of state prediction, many methods of finite element analysis are used. For example, H. M. El-Sayed establishes a wheel-rail stress model, simulates the rail head's damage state through finite element analysis, and predicts the service life of the rail through long-term data [72]. The ability of machine learning in the field of prediction has also been proven to have more potential. In recent years, there have been more studies for the prediction of rail damage. Ahmed Lasisi et al. proposed an integrated learning framework. It takes advantage of the advantages of a single machine learning tools and overcomes assuming basic distribution (such as Weibull) to predict the deviation of the defect, and also consider the railway characteristics except for the traffic volume (Mt) to achieve the purpose of optimizing the prediction results [73]. Sysyn's research team conducted two studies on the remaining useful life (RUL) prognosis of common crossings as shown in Table 2 on the inspection data obtained by the on-side and the onboard intrinsic measurement system of the turnout.

The two machine learning methods proposed in the research systematically carry out the processes of feature extraction, selection, fusion, and degradation modeling and are then used to deal with the problem. It corresponds to about 50% and 75% of the condition indicator reached. Therefore, the available period would be sufficient for maintenance planning, thus avoiding operational hindrance costs [66].

Table 2
Deep learning detection methods

Method	Features	Dataset	Results	Ref.
DCNN	Classification: Weld, large, middle and small Squat; Joint	22408 images; size 100 × 50	Accuracy=92%	[74]
CNN	Defect on Surface	25.000 profiles per second	Accuracy=98%	[75]
CNN	Defect on Surface	7897 images size 4096x3000	Precision=61.14%; Recall=75.52%	[76]

Cropped i-CNN	Rail Surface location	5793 images; size 960 × 1280	Recall=92.54%;Precision=92.8%	[77]
MOLO	Classification: corrugation, fatigue block, stripping off block	96944 images; size 224×224×3	Corrugation AP=95.28%;Fatigue block AP=84.60%; Stripping off block AP=82.33%	[78]
SegNet	Rail surface defects	120 rail training images; size 1250 × 55	Detection Rate=100%	[79]
YOLOv3	Rail surface defect	184images; size 416 × 416	Recognition rate more than 97%	[80]
MRF-GMM and CNN	Rail surface defects	6 categories, 2700 samples; size 250 × 160	Precision=96.74%, Recall =94.13% Overlap =95.18%	[81]
DCNN	Detection and classification of abrasion scar crack corrugation	38000 training images; size 512×512	The accuracy of defect classification achieves 96.55%	[82]
Faster R-CNN	Rail surface defect	1000 images in environments	Average Precision =97.8%	[83]
OC-IAN & OC-TD	Rail surface defect	RSDDs	T-I: pre.=84.21%; T-II: pre.=91.76%	[84]
RBGNet & LWLC-ME	Rail surface defect	video images resized to 1280 × 720	Precision over 90%	[85]
Mcnet	Rail surface defect	3936 NRSD images,; size 400 × 400	Manmade Pre.=85.28% Natural Pre.=72.74%;	[86]

4   Results and Discussion

In this article, various methods for detecting railway surface defects are discussed. The detection of defects on the rail surface is challenging because the cracks have an irregular form and have no specific shape or size. Each detection method may have some advantages and some disadvantages. However, visual inspection and electromagnetic technologies such as ACFM and MFL have significant benefits in comprehensively comparing inspection efficiency and accuracy. In terms of detecting speed, both methods can be used to obtain data on a running train. However, the sensitivity of electromagnetic technology at high speeds is not high. ACFM is generally less sensitive to short or shallower discontinuities than traditional eddy currents. MFL cannot detect relatively small defects. From the distribution of the number of papers, it can also be shown that more scholars are engaged in the research of visual inspection, especially the visual inspection direction in machine learning, on rail surface defects.

The visual inspection method of image processing has been well certified in the laboratory, but in the actual environment, there is a lot of external interference, different texture characteristics, changing lighting conditions, and stains on the rails, etc., will cause the image processing process significant interference reduces the accuracy of detection. The shallow machine learning methods shown in Table 1 have achieved 90% or more accuracy in defect detection. Even for some major defect categories, the accuracy can reach 80%. The deep machine learning shown in Table 2 further strengthens this effect. The detection accuracy is further improved by 5-7%. Many neural convolution processes are combined with other image processing or SVM, random forest, and other machine learning methods to achieve better detection results. Many methods have proved the feasibility and relative accuracy in real track surface damage detection. Enlarging the data set can avoid overfitting of the model and enhance the accuracy of detection. But larger data sets require more data collection time and investment, and deep machine learning requires a lot of computing time in working hours and also has high requirements for computing equipment. The method of deep machine learning in the classification of rail surface damage has shown considerable prospects. There are still very few studies used to predict the surface defect of railroad tracks, and the prediction results are also relatively unstable. The primary research method does not use deep machine learning because shallow machine learning methods are easier to control the number and focus of features.

Conclusions

This article focuses on reviewing the most advanced rail surface damage detection methods in the past decade. These results have been published in top journals and conferences. We reviewed the criteria of the 70 research articles screened after the application and checked their content in detail. These articles are evaluated based on the detection methods they use, performance results, and limitations. Through analysis, we can infer that machine learning visual inspection methods can be widely used to detect railway surface defects. Combining multiple methods with sub-gradient detection of different types of defects has a better detection effect. More research needs to focus on the detection of rail surface cracks. At present, satisfactory results have been achieved for spalling and squats, while relatively small surface crack research has hardly made significant progress. For the reasonably complicated in 3 classifications task, orbital surface defect classification accuracy can reach 75% or even 85%. After more data sets and more research results to overcome false defects or even minor defects are proposed in the future, the accuracy of classification will be further improved. In the future, research on crack damage detection on the surface of the steel rail will mainly focus on the optimization and improvement of deep machine learning, especially in the field of CNN. The research on detection can be extended in the direction of evaluating the defects and then predicting the service life of the rail. More image processing methods suitable for real environments are also necessary.

References

[1]   A. Németh, S. Fischer, Investigation of glued insulated rail joints with special fiber-glass reinforced synthetic fishplates using in continuously welded tracks. Pollack Periodica, Vol. 13, No. 2, 2018, pp. 77-86

[2]   A. Németh, S. Fischer, Investigation of glued insulated rail joints applied to CWR tracks. Facta Universitatis Mechanical Engineering, 2021, 7642

[3]   S. Fischer, Investigation of effect of water content on railway granular supplementary layers. Naukovyi Visnyk Natsionalnoho Hirnychoho Universytetu, No. 3, 2021, pp. 64-68

[4]   Blagojević, Aleksandar, Željko Stević , Dragan Marinković , Sandra Kasalica, and Snježana Rajilić. "A Novel Entropy-Fuzzy PIPRECIA-DEA Model for Safety Evaluation of Railway Traffic." MDPI Symmetry, 2020

[5]   Wikipedia. List of countries by rail transport network size. 2017. https://en.wikipedia.org/wiki/List_of_countries_by_rail_transport_network _size

[6]   Popvic, Zdenka, V. Radovic, Luka Lazarevic, and G. Tepic. "Rail inspection of RCF defects." Metalurgia-Sisak, Oct 2013, pp. 537-540

[7]   Ovchinnikov, Dmitry, Alexey Bondarenko, Lei Kou, and Mykola Sysyn. "Extending service life of rails in the case of rail head defect." Gradevinar, 2 2021, pp. 119-125

[8]   Falamarzi, Amir, Sara Moridpour, and Majidreza Nazem. "Areview on Existing Sensors and Devices for Inspecting Ralway Infrastructure." Jurnal Kejuruteraan, 2019, pp. 1-10

[9]   Oliveira, H. and Correia, P. L. "Automatic road crack detection and characterization." IEEE Transactions on Intelligent, 2012, pp. 155-168

[10] Marais, J J, and K C. Mistry. "Rail integrity management by means of ultrasonic testing." FFEMS, 2010, pp. 931-938

[11] Shang, Lidan, Qiushi Yang, Jianing Wang, Shubin Li, and Weimin Lei. "Detection of rail surface defects based on CNN image recognition and classification." International Conference on Advanced Communication Technology. IEEE, 2018

[12] Cannon, D. F., K. O. Edel, S. L. Grassie, and K. Sawley. "Rail defects: an overview." Fatigue Fract ENgng Mater Struct, 2003, pp. 865-887

[13] Li, Q Y, and S W Ren. "A visual detection system for rail surface defects." IEEE Transactions on Systm, 2012, pp. 1531-1542

[14] Lu, Z W. "Overall comments on track technology of high speed railway." Journal of Railway Engineering Society, 2007, pp. 41-54

[15]   Kurhan Dmytro and Maksym Havrylov. "The Mathematical Support of Machine Surfacing for the Railway Track." Acta Technica Jaurinensis, 2020, pp. 246-267

[16]   Ye, Jiaqi, Edward Stewart, and Clive Roberts. "Use of a 3D model to improve the performance of laser-based railway track inspection." Proc IMechE Part F: J Rail and Rapid Transit, Aug 2018

[17]   Rikhotso, Vonani, Nico Steyn, and Yskandar Hamam. "3D Rail Modelling and Measurement for Rail Profile Condition Assessment." IEEE Africon 2017 Proceedings, 2017, pp. 1522-1527

[18]   Jessop, Casey, Johan Ahlstrom, Lars Hammar, Soren Faester, and Hilmar K. Danielsen. "3D characterization of rolling contact fatigue crack networks." Wear, 2016, pp. 293-400

[19]   Naeimi, meysam, et al. "Reconstruction of the rolling contact fatigue cracks in rails using X-ray computed tomography." NDT and E International Elsevier Ltd, 2017, pp. 199-212

[20]   Niu, Menghui, et al. "Unsupervised saliency detection of rail surface defects using stereoscopic images." Transactions on Informatics, 2021, pp. 2271-2281

[21]   Sysyn, Mykola, Kluge Franziska, Gruen Dimitri, Vitalii Kovalchuk, and Olga Nabochenko. "Experimental analysis of rail contact fatigue damage on frog rail of fixed common crossing 1:12." Journal of Failure Analysis and Prevention, 2019, pp. 1077-1092

[22]   Bentoumi, M, and Pbloch G. Aknin. "online rail defect diagnosis with differential eddy current probes and specific detection processing." The European Phzsical Journal Applied Physics, 2003, pp. 227-233

[23]   Pohl, R, and R Krull. "A new eddy current instrument in a grinding train." In Proceeding of the ECNDT, 2006, pp. 178-184

[24]   Thomas, H, and Thanspach G。 Heckel. "Advantage od a combined ultrasonic and eddy current examination for railway inspection trains." Insight-Non-destructive Testibf abd Condition Monitoring, 2007, pp. 341-344

[25]   Huang, F Z, D H Gao, and X H Ding. " The Design and Application of the Card-type Eddy Current Sensor for the Detection of the Surface Defects of the Switch Rail." Nondestructive Testing, 2014, pp. 63-68

[26]   Wang, Ping, Yunlai Gao, Guiyun Tian, and et al. "Velocity effect analysus of dynamic magnetuyation in high speed magnetic flux leakage inspection." NDT & E International, 2014, pp. 7-12

[27]   Jia, Yinliang, Kangwu Liang, Ping Wang, Kailun Ji, and Peng Xu. "Enhancement method of magnetic flux leakage signals for rail track

surface defect detection." IET Science, Measurement & Technology, 2020, pp. 711-718

[28]   Ji, Kailu, Ping Wang, Yinliang Jia, Yunfei Ye, and ShunziI Ding. "Adaptive Filtering Method of MFL Signal on Rail Top Surface Defect Detection." IEEE Access, 2021, pp. 87351-87360

[29]   Hamed, Rowshandel and L Nicholson Gemma, et al. "An integrated robotic system." journal of rail and rapid transit, 2013, pp. 310-322

[30]   Chacón Muñoz, J. M., F. P. García Márquez, and M. Papaelias. "Railroad inspection based on ACFM employing a non-uniform B-spline approach." 2013, pp. 605-617

[31]   Lugg, Martin, and Mayorkinos P Papaelias. "Detection and evaluation of rail surface defects using alternating current field measurement techniques." journal of rail and rapid transit, 2012, pp. 530-542

[32]   Li, Zili, Maria Molodova, Alfredo Núñez, Senior Member, and Rolf Dollevoet. "Improvements in Axle Box Acceleration Measurements for the Detection of Light Squats in Railway Infrastructure." Transactions on Industrial electronics, 2015, pp. 4385-4399

[33]   Keong Ng, Andrew, Landong Martua, and George Sun. "Dynamic Modelling and Acceleration Signal Analysis of Rail Surface Defects for Enhanced Rail Condition Monitoring and Diagnosis." The 4th International Conference on Intelligent Transportation Engineering. Sep. 2019

[34]   Sysyn, Mykola, Dimitri Gruen, Ulf Gerber, Olga Nabochenko, and Vitalii Kovalchuk. "Turnout Monitoring with Vehicle Based Inertial Measurements of Operational Trains: A Machine Learning Approach." Communications, 2019, pp. 42-49

[35]   Sysyn, Mykola, Olga Nabochenko, Franziska Kluge, Vitalii Kovalchuk, and Andriy Pentsak. "Common Crossing Structural Health Analysis with Track-Side Monitoring." COMMUNICATION, 2019, pp. 77-84

[36]   Jiang, Yi, et al. "Non-contact ultrasonic detection of rail surface defects in different depths." Proceedings of Front 2018. 2018

[37]   Zhang, Hui, et al. "Wavenumber Imaging of Near-Surface Defects in Rails using Green's Function Reconstruction of Ultrasonic Diffuse Fields." Sensors, April 2019

[38]   Zhang, Yuehong, Lin Luo, Yu Zhang, Xiaorong Gao, and Jiang Long. "Interlaced scanning by laser ultrasonic for defects imaging of train rail surface." Eleventh International Conference on Information Optics and. Xi an, 2019

[39]   Ramzan, Bilawal, Sohail Malik, S. M. Ahmad, and Milena Martarelli. "Railroads Surface Crack detection using Active Thermography." 2021, pp. 183-198

[40]   Zhuravlev, Andrey, Vladimir Razevig, Sergey Ivashov, Aleksey Skrebkov, and Viktor Alekseev. "On the Use of Microwave Holography to Detect Surface Defects of Rails and Measure the Rail Profile." sensors, 2019

[41]   Liu, Yuxin, and Xiukun Wei. "Track Surface Defect Detection Based on Image Processing." Proceedings of the 3rd International Conference on Electrical. Singapore, 2018, pp. 255-232

[42]   Fu, Shengwen, and Zhanjun Jiang. "Research on Image-based Detection and Recognition Technologies for Cracks on Rail Surface." 2019 International Conference on Robots & Intelligent System (ICRIS) Lan Zhou, 2019, pp. 98-102

[43]   Wu , Yunpeng, Yong Qin, and Limin Jia. "Research on Rail Surface Defect Detection Method Based on UAV Images." 2018 Prognostics and System Health Management Conference. 2018, pp. 553-559

[44]   Min, Yongzhi, Benyu Xiao, Jianwu Dang, Biao Yue, and Tiandong Cheng. "Real time detection system for rail surface defects based on machine vision." l. EURASIP Journal on Image and Video Processing, 2018

[45]   Herrero, Francisco Javier de la Calle, Daniel F. García, and Rubén Usamentiaga. "Inspection System for Rail Surfaces Using Differential Images." IEEE Transactions on Industry Applications, 2018, pp. 4948-4958

[46]   Li, Qingyong, Shengwei Ren, Member, and IEEE. "A Visual Detection System for Rail Surface Defects." IEEE Transactions on Systems, 2012, pp. 1531-1543

[47]   Dai , Guangyu, et al. "Online real-time detection method for defects of railroad track surface." Applied Mechanics and Materials, 2013, pp. 1017-1020

[48]   Tang, Bo, Jianyi Kong, and Shiqian Wu. "Overview of surface defect detection based on machine." Chinese Journal of image and graphics, 2017

[49]   Zhao, Kang, Laizhen Luo, Zhengmin Ren, and Qingchen Fu. "A surface defect detection system for railway track based on machine vision." MCTE. 2020

[50]   Mohan, S., and M. Ravishankar. "Optimized histogramm based contrast limited enhancement for mammogram." American Council for an Energz-efficiept Economy Intternational Journal on Information Technology, 2013, pp. 66-71

[51]   Gordon, R., and Rangayan. "Feature enhancement of film mammogram using fixed and adaptive neighborhoods." Applied Optic, 1984, pp. 560-564

[52]   Wu, Yidi, and Lin Li. "Inspection of Rail Surface Defects Image Based on Histogram Processing by the Judgment Threshold." Proceedings of 2018 Chinese Intelligent Systems Conference. Singapore, 2019, pp. 199-209

[53] Gan, Jinrui and Jianzhu Wang, Haomin Yu, Qingyong Li, and Zhiping Shi. "Online Rail Surface Inspection Utilizing Spatial Consistency and Continuity." IEEE Transactions on Systems, Man, and Cybernetics: Systems, 2018, pp. 2741-2751

[54] Yu, Haomin, et al. " A coarse-to-fine model for rail surface defect detection." IEEE Transactions on Instrumentation and Measurement, 2018, pp. 656-666

[55] Hu, Zhixin, Hongtao Zhu, Ming Hu, and Yong Ma. "Rail Surface Spalling Detection Based on Visual Saliency." IEEJ Transactions on Electrical and Electronic Engineering, 2018, pp. 505-509

[56] Wu, Yunpeng, Yong Qin, Zhipeng Wang, and Limin Jia. "A UAV-Based Visual Inspection Method for Rail Surface Defects." applied sciences, 2018

[57] Dubey, Ashwani Kumar, and Zainul Abdin Jaffery. "Maximally Stable Extremal Region Marking) based Railway Track Surface Defect Sensing." IEEE Sensors, 2016, pp. 9047-9052

[58] Sysyn, Mykola, Ulf Gerber, Olga Nabochenko, Dmitri Gruen, and Franziska Kluge. "Prediction of Rail Contact Fatigue on Crossings Using ImageProcessing and Machine Learning Methods." Urban Rail Transit, 2019, pp. 123-132

[59] Dalal, N, and B Triggs. "Histograms of oriented gradients for human detection." IEEE Computer Society, 2005

[60] Rodriguez, Y, and S Marcel. "Face authentication using adapted local binary pattern histograms." Springer Verlag, 2006, pp. 321-332

[61] Mercy, K. Grace, and Sri. K. Srinivasa Rao. "A Framework for Rail Surface Defect Prediction Using Machine Learning Algorithms." Proceedings of the International Conference on Inventive Research in Computing Applications (ICIRCA 2018) IEEE Xplore, 2018, pp. 972-978

[62] Jaffery, Zainul Abdin, Nadeem Ahmad , and Deependra Sharma. "Performance comparison of segmentation techniques for detection of defect in rail head surface images." 2017, pp. 132-137

[63] Wang, Long, Li Zhuang, and Zijun Zhang. "Automatic Detection of Rail Surface Cracks with a Superpixel-Based Data-Driven Framework." J. Comput. Civ. Eng, 2019

[64] Yue, Biao, Yangping Wang, Yongzhi Min, Zhenhai Zhang, Wenrun Wang, and Jiu Yong. "Rail Surface Defect Recognition Method Based on AdaBoost Multi-classifier Combination." Proceedings of APSIPA Annual Summit and Conference 2019, LanZhou, 2019

[65] Long Wang; Li Zhuang; and Zijun Zhang. "Rail Surface Defect Recognition and Classification Method Based on Deep Forest." EITRT 2019, 2019, pp. 493-503

[66]   Zhang, Hui, Xiating Jin, Q. M. Jonathan Wu, Yaonan Wang, Zhendong He, and Yimin Yang. "Automatic Visual Detection System of Railway Surface Defects With Curvature Filter and Improved Gaussian Mixture Model IEEE Transactions on Instrumentation and Measurement, 2018, pp. 1593-1608

[67]   Sysyn, M., U. Gerber, F. Klug, O. Nabochenko, and V. Kovalchuk. "Turnout remaining useful life prognosis by means of on-board inertial measurements on operational trains." International Journal of Rail Transportation, 2019, pp. 1-23

[68]   Sysyn, Mykola. "Improvement of inspection system for common crossings by track side monitoring and prognostics." Structural Monitoring and Maintenance, 2019, pp. 219-235

[69]   Lowe, D G. "Distinctive Image Features from Scale Invariant Keypoints." International Journal of Computer Vision, 2004, pp. 91-110

[70]   Jin, Yang. "Wavelet Scattering and Neural Networks for Railhead Defect Identification." Materials, 2021

[71]   Zhang, Ziwen, Mangui Liang, and Zhe Wang. "A Deep Extractor for Visual Rail Surface Inspection." IEEE Access, 2021, pp. 21798-21801

[72]   El-sayed, H. M., M. Lotfy, H. N. El-din Zohny, and H.S. Riad. "Prediction of fatigue crack initiation life in railheads using finite elementanalysis." Ain Shams Engineering Journal, 2018, pp. 2329-2342

[73]   Lasisi, Ahmed, and Nii Attoh-Okine. "Machine Learning Ensembles and Rail Defects Prediction: Multilayer Stacking Methodology." Journal of Risk and Uncertainty, 2019

[74]   Faghih-Roohi, Shahrzad, Siamak Hajizadeh, Alfredo Nu´nez , Robert Babuska, and Bart De Schutter. "Deep Convolutional Neural Networks for Detection of Rail Surface Defects." 2016 International Joint Conference on Neural Networks (IJCNN) IEEE, 2016, pp. 2585-2591

[75]   Santur, Yunus, Mehmet Karaköse, and Erhan Akın. "A New Rail Inspection Method Based on Deep Learning Using Laser Cameras." IEEE, 2017

[76]   García, Daniel F., Iván García, Francisco J. delaCalle, and Rubén Usamentiaga. "A Configuration Approach for Convolutional Neural Networks used for Defect Detection on Surfaces." 2018 5th International Conference on Mathematics and Computers in Sciences and Industry (MCSI) 2018, pp. 44-52

[77]   Shang, Lidan, Qiushi Yang, Jianing Wang, Shubin Li, and Weimin Lei. "Detection of Rail Surface Defects Based on CNN Image Recognition and Classification." International Conference on Advanced Communications Technology(ICACT) 2018

[78] Yuan, Hao, Hao Chen, ShiWang Liu, Jun Lin, and Xiao Luo. "A deep convolutional neural network for detection of rail surface defect." IEEE Xplore, 2020

[79] Liang, Zhicong, Hui Zhang, Li Liu, Zhendong He, and Kai Zheng. "Defect Detection of Rail Surface with Deep Convolutional Neural Networks." Proceeding of the 2018 13th World Congress on Intelligent Control and Automation. Chang Sha: IEEE, 2018

[80] Song, Yanan, Hui Zhang, Li Liu, and Hang Zhong. "Rail Surface Defect Detection Method Based on YOLOv3 Deep Learning Networks." IEEE, 2018, pp. 1564-1572

[81] Jin, Xiating, et al. "DM-RIS: Deep Multimodel Rail Inspection System With Improved MRF-GMM and CNN." IEEE Transactions on Instrumentation and Measurement, 2020, pp. 1051-1066

[82] Li, Xiaoqing, Ying Zhou, and Hu Chen. "Rail Surface Defect Detection Based on Deep Learning." Eleventh International Conference on Graphics and Image Processing. Hang Zhou, 2019

[83] Chen, Xiaobo, and Huimin Zhang. "Rail Surface Defects Detection Based on Faster RCNN." 2020 International Conference on Artificial Intelligence and Electromechanical Automation (AIEA) IEEE Xplore, 2020

[84] Zhang, Defu, Kechen Song, Qi Wang, Yu He, Xin Wen, and Yunhui Yan. "Two Deep Learning Networks for Rail Surface Defect Inspection of Limited Samples With Line-Level Label." IEEE Transactions on Industrial Informatics, 2021, pp. 6731-6742

[85] Wu, Yunpeng, and Yong Qin, et al."Hybrid deep learning architecture for rail surface segmentation and surface defect detection." Computer-Aided Civil and Infrastructure Engineering, 2021, pp. 1-18

[86] Zhang, Defu, Kechen Song, Jing Xu, Yu He, Menghui Niu, and Yunhui Yan. "MCnet: Multiple Context Information Segmentation Network of No-Service Rail Surface Defects." IEEE Transactions on Instrumentation and Measurement, 2021

Analysis of the Safety Level of Obstacle Detection in Autonomous Railway Vehicles

Slobodan Rosić[1], Dušan Stamenković[1], Milan Banić[1], Miloš Simonović[1], Danijela Ristić-Durrant[2], Cristian Ulianov[3]

[1] University of Niš, Faculty of Mechanical Engineering
Aleksandra Medvedeva 14, 18106, Niš, Serbia
slobodan.rosic@masfak.ni.ac.rs, dusan.stamenkovic@masfak.ni.ac.rs,
milan.banic@masfak.ni.ac.rs, milos.simonovic@masfak.ni.ac.rs

[2] Institute of Automation, University of Bremen
Otto-Hahn-Allee NW1, 28359 Bremen, Germany
ristic@iat.uni-bremen.de

[3] School of Engineering, Newcastle University
NE1 7RU, Newcastle upon Tyne, the UK;
cristian.ulianov@newcastle.ac.uk

Abstract: Traffic safety of fully automated train operations is one of the most complex challenges in the field of railway traffic automation. One of the biggest problems with the introduction of driverless trains to the public railway infrastructure are the risks associated with the obstacles on the line, which represent one of the most common and most significant safety risks in railway traffic. The Obstacle Detection System (ODS), should meet the safety requirements, but also should not lead to a deterioration of the railway traffic. In addition to the purely technical issues of ODS development, the issue of determining the necessary requirements in terms of safety, reliability and efficiency must be considered. The paper analyses the current European regulations in the field of railway safety, safety requirements for certification of ODS, as well as risk control measures by the types of obstacles on the line. A survey of train drivers in the Republic of Serbia was conducted to understand the significance of particular obstacles and the manner of reaction of train drivers in case of their occurrence. The results of the survey and the available statistical indicators were used to assess the impact of certain categories of obstacles on railway safety. The criteria for defining the safety requirements necessary for the certification of ODS in autonomous vehicles have been proposed.

Keywords: safety; autonomous railway vehicles; certification; obstacle detection

1 Introduction

One of the main goals of modern railway transport is to increase its quality, as well its effectiveness and capacity while maintaining a very high level of safety [1] through automation. Automation is currently one of the most important trends in the railway development in order to oppose the strong competence of other transport means [2] and reduce Greenhouse Gas emissions [3], thus reaching the goals of the Green Deal. It is considered that, after electrification and the introduction of high-speed trains, it represents the third revolution in the development of railway traffic. This is one of the most complex areas in the field of automation. While other components in the process of automatic train operation (ATO) have already been successfully developed (automatic train control, optimal energy consumption, automatic door control and departure from station, etc.) train operation without a driver, the so-called Grade of Automation (GoA) level 4 has so far been successfully developed only for systems in specific environments (metro systems and mining lines in uninhabited areas). One of the biggest problems for the introduction of driverless trains on the public railway infrastructure are the risks associated with the obstacles on the line. Obstacles on the line represent the most common and most significant safety risk in railway traffic. Accidents caused by obstacles on the line account for over 83% of all significant accidents on European railways, and the casualties in such accidents make up over 99% of the total number of casualties in railway traffic. Almost 1,000 people die in such accidents on the EU railways every year. Obstacles on the railway also cause significant material damage [4]. Even insignificant obstacles such as fallen leaves on the track can have a significant negative impact - according to some estimates, the negative financial impact of this phenomenon on the railway system in the UK reaches up to 350 million pounds [5] and 100 million SEK in Sweden [6]. Obstacles on the line, including the implementation of the procedures associated with such events are significant cause of traffic delays and increased costs in the railway system. For this reason, it is necessary that the obstacle detection system (ODS) in the driverless train operation (DTO) regime successfully meets the requirements in terms of safety, but also not to lead to a deterioration in the efficiency and economy of railway traffic. Therefore, in addition to purely technical issues of development of these systems, it is also crucial to determine the necessary requirements for them in terms of safety, reliability and efficiency. The issue of defining the requirements for the ODS within the DTO is related to the regulatory conditions for their certification or authorization. It is very specific because according to the current regulatory framework in the EU, the area of detection and response to obstacles belongs to both structural and functional subsystems, and their introduction undoubtedly represents a significant change of both technical and operational character. Existing specifications and national regulations currently do not cover on board obstacle detection devices, so the conditions for their certification need to be defined in accordance with the EU regulatory framework. Alternative to ODS

would be complete fencing of the railway lines which is not considered feasible by most EU infrastructure managers as the installation cost would be quite high. Furthermore, the current practical experience shows that fences cannot fully prevent occurrence of obstacles on the track [7].

Previous research in this area is mainly related to the technical aspect of the development of obstacle detection devices and the possibility of their application on railways. The authors [1, 8, 9] provide an overview of the different types of sensors that can be used to detect obstacles and the possibility of using them for DTO. Hyde et al. [10] discusses the concept of an ODS and an overview of possible Use cases. Several researchers [11-13] are considering the use of neural networks in the field of detection of obstacles in railway traffic. The area of defining safety requirements for ODS has not been the subject of special research so far. This issue is being addressed as part of the SMART 2 [14] project which considers on board and track side ODS. At the end of 2020, the German Centre for Rail Traffic Research (DZSF) launched a study to define the requirements for authorizing the automated train operation [15]. The main goal of this study is to identify the requirements that must be met to ensure that automated trains provide at least the same level of safety as manually operated trains. There are still no academic papers on this topic, however, there are several papers [16, 17] that consider the problem of certification of signalling devices in which neural networks and artificial intelligence would be applied or discuss the safety evaluation by noted technologies [18].

This paper analyses the current European regulations in the field of railway safety, safety requirements for certification of obstacle detection devices, risk control measures by types of obstacles and proposes criteria for defining safety requirements that would be needed for certification of ODS in autonomous railway vehicles.

2 Regulatory Requirements that the ODS should Meet and the Manner of Their Certification in Accordance with EU Legislation

The European regulatory framework for railways is very complex due to the required interoperability and open market for railway services. According to this framework, the railway system is divided into structural and functional subsystems and implies the participation of a large number of actors like railway companies, independent bodies, national state bodies and European institutions.

The area of certification is largely defined by Directive 2016/797 on the interoperability of the railway system in the EU [19]. This directive prescribes requirements for all the parts of the railway system as well as a way of proving

their fulfillment. The basic elements of the certification process according to this document are sublimated in a form diagram presented as Figure 1.

The Interoperability Directive defines a number of general and specific safety requirements. Relevant to the development of a system for the detection of obstacles are the following:

- General requirements

a) The ODS must be designed and constructed to guarantee safety at the level corresponding to the aims (goals) laid down for the network.

b) The components of the ODS must withstand all specified normal or exceptional stresses during their use. Impact of accidental failures on the safety must be limited.

c) The design of ODS must be aimed at limiting the negative consequences of a fire.

d) The supervision and maintenance of the ODS must be organized, carried out and quantified in such a manner that their operation is carried out under the intended conditions.

Requirements Defining

- High level - essential requirements that EU rail system, subsystems and constituents and interfaces shall meet. This requirements are defined in Annex III Directive 2016/797
- Technical specification for interoperability' (TSI) which define the technical and operational standards which must be met to satisfy the 'essential requirements' and to ensure the interoperability. TSIs are defined for each subsystem
- National rules which defining the requirements for so-called open issues and special cases in TSIs

Demonstration of compliance with the requirements

- Conformity assesment with TSIs and national rules acording Article 13 Directive 2016/797
- Verification of conformiti assesment

Authorisation for the placing in service

- Proving verification declaration
- Proving technical compatibility
- Proving safe integration
- Proving procedure is carried out acording Article 18 Directive 2016/797

Figure 1
Basic elements of the certification process in accordance with EU regulations

- Specific requirements

The ODS and interface with control-command and signalling (CCS) installations and procedures used must enable trains to travel with a level of safety which corresponds to the objectives set for the network. This system must continue to ensure the safe passage of trains which are allowed to run in degraded conditions (failures in CCS system).

The first-mentioned general requirement and the specific requirement for CCS systems are virtually identical. This practically means that the introduction of an ODS must ensure a level of safety that corresponds to the objectives envisioned for the railway network. The Safety Directive EU 2016/798 [20] states that the basic objective for the railway network in the EU is to preserve the existing level of safety. Article 7 of the same Directive also defines the Common Safety Targets (CST) as the minimum levels of safety that the system as a whole and its various parts need to achieve. CSTs can be expressed in risk acceptance criteria or target safety levels. CSTs relevant to the ODS are aims related to train collisions with trains and obstacles on the line (within the clearance profile), for accidents at level crossings, for accidents involving people involving a moving railway vehicle and for passing a signal prohibiting further driving (SPAD). Although there are many doubts about the use of CST in the certification process, the study [21] states that for the development of new elements of the subsystem on the railway it is necessary to define individual, specific objectives based on the value of CST. When considering the method of their calculation [22], CSTs based on the level of safety achieved in the previous period. Therefore, these conditions practically assure reaching at least the existing level of safety in their areas.

Finally, safety objectives may exist at the level of a network and individual actors in the railway system (Infrastructure managers and Railway undertakings). Since these goals must be harmonized with the CST also, they are almost without exception based on the existing level of safety. Deviations from the achieved level of safety are possible only if this level is not satisfactory for an area. However, there is a constant improvement in safety in the EU railway system [4] and there are currently no strong arguments to justify raising safety levels as a condition for certification of obstacle detection devices. For the development and implementation of DTOs, these safety objectives imply that the level of safety required of the ODS must be at least equal to the level of safety achieved by the train driver in relation to line obstacles on the line. This can also be considered a basic high-level requirement in terms of the functional aspect of system safety. Other specified general and specific conditions relevant for the development and certification for ODS related to reliability, applicability, maintenance, and technical aspects of safety (RAMS). The requirements in this regard are mostly based on the EN 50126 Railway applications standard - The specification and demonstration of Reliability, Availability, Maintainability and Safety (RAMS) [23].

The second level of safety requirements is defined in the TSI. However, as such a system has not existed so far on the railways in the TSI CCS, to which by the nature of things ODS should belong, there are currently no requirements related to this system. This area is currently covered by TSI OPE. It defines safety requirements regarding the occurrence of hazards on the railway, which includes the occurrence of obstacles on the line. But these requirements are defined at a general level and mainly refer to national and internal regulations. A safety

requirement to record and store all relevant vehicle control and operation data before and after an accident could be considered an explicit requirement for this system. Therefore, the existing TSIs need to be supplemented with provisions relating to the ODS. Interoperability Directive requires that all proposals for amendments to existing or new specifications within the TSI must be proven to meet the existing essential requirements. Similar to TSIs, national regulations currently do not have defined requirements for such a system. However, some requirements for it can be deduced from the operational rules for train drivers. They are mostly identical for all European countries, but there are also certain differences. For example, in Great Britain, it is prescribed that the train driver is obliged to take appropriate measures in case of noticing leaves on the tracks and to report it to the traffic control, which is not the case in many other countries [24]. There are also significant differences between European countries in terms of procedures in the case of the appearance of animals on the line.

In addition to the above safety requirements, European regulations stipulate that during the certification of subsystems and their elements, the safe integration into the existing railway system must be ensured [19]. Since the introduction of an ODS instead of a train driver is undoubtedly a change of great importance for the traffic safety, the fulfilment of this requirement implies the application of the Common safety methods for assessing the risk of changes in the railway system (CSM RA). Regarding the basic requirement of the functional aspects of safety, in CSM RA procedure, the principle of risk acceptance GAME (Globalement au moins équivalent) should be applied. From the recapitulation of the stated regulatory requirements for the certification of the ODS, it can be concluded that it must meet the following conditions:

1) The level of safety of this system in functional terms must correspond to the set objectives for the network, which practically means that the ODS must provide the least achieved general level of safety, and the achieved level of safety defined by individual CST. This requirement is an essential requirement for the development of this system. Based on this safety objectives, the necessary technical specifications should be further developed.

2) The Reliability, Availability, Maintainability and Safety (RAMS) requirements for the ODS should comply with the EN 50126 standard. For the technical aspect of safety, the requirements should be at least at the same Safety Integrity Level (SIL) level as for other onboard CCS devices [23].

3) The achievement of the existing level of safety as well as the acceptability of the risks associated with the introduction of an ODS in the existing railway system should be determined by applying the ZBM RA using the GAME principle of acceptability of risk. Deviations from this principle are possible only if an increase in the level of safety is explicitly required.

4) The system must meet the requirements of national regulations regarding the occurrence of obstacles on the line at the same safety level as train drivers, and if that is not possible, other ways and measures of risk control must be defined and introduced.

3   Analysis of the Existing Level of Safety in the Railway System Related to Obstacles on the Line

The term existing or achieved level of safety is very important in the EU regulatory framework for the railway system and is stated in a number of legal documents. Its achievement in the case of change (including innovation) is a crucial safety requirement. It also has an important legal aspect because it represents the limit of what is legally allowed and what is not, in the railway system. But, despite the great importance of this term in the regulations, there is no defined way in which it is determined in the railway system. This problem is not considered in more detail in academic papers either. In practice, the existing level of safety is usually determined based on so-called "historical records" about accidents. However, common statistics do not provide enough information to adequately establish the achieved level of safety associated with railway barriers. The main reasons for this are:

- accident statistics cover only events that had harmful consequences. Most obstacle-related events end without such consequences, so the number of accidents alone does not give a true picture of the frequency of hazards.

- a number of accidents does not represent unsuccessful events from the aspect of reacting to the appearance of obstacles. These are events in which the train crash could not be avoided due to the circumstances, but the timely response resulted in the maximum possible reduction of the consequences of the crash.

- the classification of accidents is not detailed enough in terms of different types of obstacles, so it does not give a true picture of the degree of risk of individual categories of obstacles.

An analysis of the available safety data on European railways was performed, to adequately describe the existing level of safety. The main source of data are the safety reports issued at the EU level by the European Union Agency for Railway and for individual members by their National safety authority. This data is contained in the ERADIS database [25], which combines all the data relevant to the safety and interoperability on the European railways.

Analysis of the data from these reports for 2019 (the last year for which all the data are available) showed that collisions, which are in terms of possible consequences the most dangerous type of event, are very rare events. They make

up only about 0.6% of the total number of accidents and the number of casualties in them is about 1% of the total number in all railway accidents in Europe. The vast majority of accidents related to obstacles, and casualties in them, are accidents at level crossings and unauthorized people crossing the track. On European railways, between 250 and 300 people are killed at level crossings every year, and over 600 people are killed by moving railway vehicles (without suicides). This relationship between the number of collisions, level crossings accidents and accidents with people and the consequences of these events is very similar in almost all European countries [25].

An analysis of the reports of all national safety authorities showed that the Danish National Safety Authority TBB has the best detailed information on the dangerous events related to obstacles. Their report includes data on serious accidents, minor accidents as well as other dangerous events (precursors) that include avoided collisions (near misses) with some types of obstacles.

As part of the research conducted during the SMART2 [14] project in 2020, a survey of train drivers in Serbia was conducted, to determine the existing level of safety. The survey included a total of 68 train drivers from three operators in Serbia (one incumbent and two private freight operators). The average work experience of the surveyed train drivers is 21.7 years. The survey included 3 categories of questions:

1) Questions about work experience: company name, the type of traffic it performs (international / domestic, cargo passenger, shunting, hazardous materials), years of service;

2) Questions about dangerous situations: types of dangerous situations the driver has experienced (collision with a railway vehicle, collision with an object with a description of the type of object, collision at a level crossing, collision with a person, collision with an animal, near-miss by the same categories, other dangerous situations with obstacles according to one's own description, the number of these events or the frequency (in each shift, monthly, annually, in several years) and the assessment of the hazard to the safety of the train or people and the environment that a certain type of event represents;

3) Questions about the risk control measures they take in individual cases and about the effects of those measures (most often consequences of individual types of events).

Table 1

Most important results of the survey of 68 train drivers in Serbia

1 Experience of train drivers	Number of drivers	Percentage
all kinds of traffic	51	75%
passenger	3	4,5%
freight	13	19%
shunting	1	1,5%

2 The types of dangerous events he has experienced	The number of train drivers who had that event	The total number of these events[*]
2.1 Collision		
with train	7	7
with an object that endangers the safety of the train	22	27
on level crossing	49	69
with person	51	53[**]
with big animal	14	18
2.2 Near miss		
with train	5	6
with an object that endangers the safety of the train	41	54
on level crossing	67	217
with person	66	255[*]
with big animal	21	37

*the total number of events for all 68 surveyed train drivers (multiple events occurred)
**this number also includes suicides that are not covered by safety reports

Drivers were asked to state the exact number of different types of dangerous events in which they participated, and if they could not, to state the approximate frequency of these events at the stated intervals. The vast majority of surveyed train drivers (92.65%) stated the exact numbers of events only for collisions with a railway vehicle, collisions with a landslide and collisions with people. For other categories, approximate frequencies are generally given. For this reason, it was decided to use the data from the safety report of the Danish national safety authority as the main source for the frequency of events, and to use the data from the train driver survey as their supplement. Although there are some differences in the number of individual categories of dangerous events between Denmark and Serbia, the relationship between the total number of significant and minor accidents and precursors of dangerous events (including near-miss) is similar. The most important results of the train driver survey are shown in Table 1.

The data from the driver's survey was the basis for determining the classification of obstacles and determining the risk control measures that are applied in the event of the occurrence of a certain type of obstacles.

3.1 Classification of Obstacles in the Railway System

Any object (object or a living being) that is or can be found on the train's running path in clearance (free) profile and that can affect its normal movement can be considered an obstacle for the train. This means that in addition to the object in the clearance (free) profile of the railway, any object in the area next to the railway

that is in the zone of the train stopping distance and can realistically be found on the train's running path is also considered an obstacle. The classification of the obstacles depending on the type and possible harmful effects as well as risk control measures applied in case of their occurrence is given in Table 2.

Table 2

Classification of the obstacles and risk control measures taken in case of their occurrence

Type of the obstacle	Risk control measures taken	Severity
1 Immovable objects in the free profile of the railway line stones / earth, railway vehicles, parts of railway equipment, vegetation, liquids, construction material, packaging, etc. accidentally or intentionally left on the tracks. A signal that prohibits further driving can also be considered in this class of obstacles.		
1.1 Immovable objects which, due to their dimensions and physical characteristics, do not endanger the safe movement of the train and cannot cause harmful consequences *packaging, small items, thin branches*	It is not necessary to take risk control measures, i.e., the usual way of driving the train does not change.	No consequences
1.2 Immovable objects that do not endanger the safe movement of the train but may cause minor damage to vehicles or traffic disturbances *thick branches, leaves, deeper liquid, parts of railway equipment*	reduction of train speed, if necessary, until stopping but without emergency braking, activation of anti-slip devices, notifying the control centre of an obstacle on the track	Material damage, traffic disruption Only indirect safety consequences are possible (in case another irregularity in the system occurs at the same time)
1.3 Immovable objects that endanger the safe movement of trains *railway vehicles, larger deposits of earth/stones, construction materials*	imperative stopping of a train in front of an obstacle, if the distance to the obstacle requires it with the introduction of emergency braking, informing the control centre about the obstacle on the line	Catastrophic consequences in the railway system
2 Movable objects in the free profile of the railway *animals, people, vehicles*		
2.1 Movable objects that do not endanger the safe movement of the train but the consequences for them can be fatal *small and medium-sized animals, people, light vehicles*	activation of warning signals (sound and light) and possible reduction of train speed; in case the person cannot safely leave the free profile stopping of train	Minor material damage; Victims outside the railway system (third parties, human environment)

Type of the obstacle	Risk control measures taken	Severity
2.2 Movable objects that endanger the safe movement of trains *large animals, heavy vehicles*	activation of warning signals (sound and light) and reduction of train speed; in case the object cannot safely leave the free profile stopping the train, in case of heavy vehicles possible emergency braking	Significant consequences in the railway system; Victims outside the railway system (third parties, human environment)
3 Immovable objects in the immediate vicinity of the railway that may endanger the free profile and endanger the safety of the train *damaged catenary equipment, damaged buildings and vegetation, running water, unstable soil and rock masses*	notifying the control centre and possibly acting on its order	Only indirect consequences for safety are possible. These consequences can be significant
4 Movable objects in the immediate vicinity of the line that can enter in the free profile *animals, people, road vehicles*		
4.1 Movable objects in the immediate vicinity that cannot endanger the safe movement of the train, but the consequences for them can be fatal *small and medium-sized animals, people, light vehicles*	activation of warning signals (sound and light); in case the object continues to move towards the free profile, reducing of the speed and, if necessary, stopping the train	Minor material damage; Victims outside the railway system (third parties, human environment)
4.2 Movable objects in the immediate vicinity that endanger the safe movement of trains *large animals, road vehicles*	activation of warning signals (sound and light); in case the object continues to move towards the free profile, reducing the speed and, if necessary, stopping the train, in the case of heavy vehicles possible emergency braking	Significant consequences in the railway system; Victims outside the railway system (third parties, human environment)

3.2   Determining the Frequency of Occurrence of Different Categories of Obstacles

As in other European countries, dangerous events on the Danish railways are divided into serious accidents, minor accidents, and incident precursors [26].

According to the 2019 Railway Safety Report, there were a total of 13 serious accidents related to railway obstacles in Denmark, 5 less than in the previous year. The number of accidents related to obstacles that are categorized as minor in 2019 was 186 in Denmark, 28 more than in the previous year. Their distribution is shown in Figure 2.

Although the division of events in these reports does not fully correspond to the categories of obstacles listed in Table 2, we can consider that the data on serious collisions with railway vehicles and facilities is relevant for the category of obstacles "1.3. Immovable objects that endanger the safe movement of trains". Data on accidents at level crossings is relevant for the category "2.2 Movable objects that endanger the safe movement of trains", and data on collisions with people is relevant for category "2.1 Movable objects that do not endanger the safe movement of the train, but the consequences for them can be fatal".
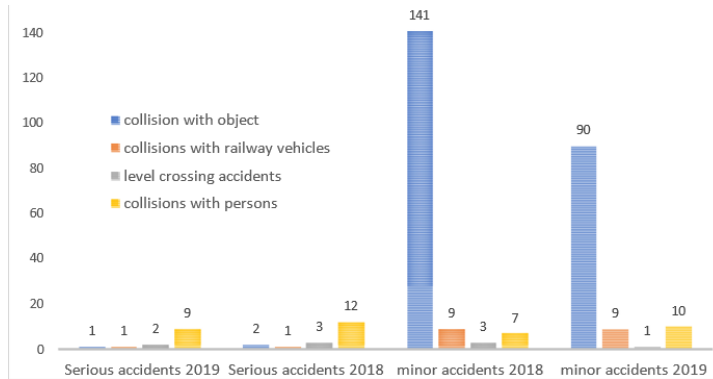

Figure 2

The number of serious and minor accidents related to obstacles on the Danish Railways

Data on collisions with people, accidents at level crossings and collisions with railway vehicles is relevant for the same categories of obstacles as in the case of serious accidents. Collisions with objects that are categorized as minor accidents according to the mentioned safety report are mainly collisions with larger animals (horses, cows, deer), felled trees, smaller objects and pieces of equipment. There is no more detailed division of these events, but it is estimated that about half of these events are smaller objects and that this is a relevant parameter for the category of obstacles "1.2 Stationary objects that do not endanger safe train movement but can cause minor damage to vehicles or traffic disturbances". The other half of these events are considered to be collisions with larger animals and this number is relevant for category "2.2 Movable objects that endanger the safe movement of trains ".

The largest number of dangerous events is in the precursors. Precursors relevant to the hazard of obstacles are Risky events with people and Risky events at level crossings. In Denmark, over 1,200 such events related to obstacles were recorded in 2019, about 200 such events more than in 2018.

Risky events with people and at level crossings are mostly events in which the train could have hit a person or a vehicle, but it was avoided, the so-called near-miss. Risky events with people are relevant for category "4.1 Movable objects in

the immediate vicinity that cannot endanger the safe movement of the train, but the consequences can be fatal", and risky events for category "4.2 Movable objects in the immediate environment that endanger the safe movement of trains".

3.3   Assessment of the Impact of Certain Categories of Obstacles on Railway Safety

From the available data in the report of the Danish National Safety Authority, data for category "1.1 Immovable objects that cannot endanger train" safety cannot be extracted. To understand the significance of certain obstacles and the manner of reaction of train drivers in case of their occurrence, data from the survey of train drivers was used. From it can be concluded that this is an everyday occurrence. The most common objects from that category are smaller pieces of vegetation, empty boxes, and smaller stones, but some unusual objects such as, e.g., snowman on the track were also recorded. Since this category of obstacles has no impact on safety, it is not necessary to quantify it for the process of defining safety requirements.

This is also the case for the obstacles from category "3 Immovable objects in the immediate vicinity of the railway line that may endanger the free profile and endanger the safety of the train". The relevant Safety Reports do not provide appropriate data for their quantification, but this category of obstacles does not have a direct impact on the safety of the train that detects these obstacles, so its quantification is not necessary within the procedure for defining safety requirements. However, in the risk assessment process related to the safe integration of the ODS into the existing railway system, it is necessary to determine the capabilities of this system for the detection of this type of obstacle and informing the control centre about them. In case that this cannot be at the level that the train drivers have (which is to be expected), it is necessary to consider other ways of controlling these risks. For example, if the ODS is not able to successfully detect the appearance of wet leaves on the track, information from the adhesion control sensor or anti-slip protection can serve as a risk control measure.

The data from the Danish report is incomplete for category "4.2 Movable objects in the immediate vicinity of the line that endanger the safe movement of trains" because they do not include risky events with large animals, i.e. near-miss. This type of incident is not covered by safety reports in any European country, so that number was estimated on the basis of a survey conducted in Serbia. According to the survey, the number of near misses with large animals is twice the number of collisions with them, so according to that key, the number of these events can be determined.

Based on the analysis of the frequency and possible consequences of certain categories of obstacles to railway safety, the following can be concluded:

- Collisions with immovable obstacles from category 1.3, which represents the greatest hazard in terms of possible consequences, are very rare events. Risk control measures within other parts of the railway system obviously control these risks at a very high-level. However, the ODS must be able to detect such objects in a timely manner to avoid them or at least reduce the harmful consequences. The system must be able to correctly classify objects from this category of events because incorrect classification can cause unnecessary safety risks (unnecessary emergency braking) or reduce the efficiency of the railway system (stopping in front of an obstacle when it was not necessary).

- The largest number of events refers to moving obstacles and over 93% of these events refer to avoided collisions with them. From the aspect of individual and social risk, these obstacles represent by far the greatest risk in the railway system. Primary safety requirement is the condition that the ODS must not exceed the level of risk that exists with train drivers in the case of moving obstacles. In the category of moving obstacles, the largest number of these events is from category 4.1 and they individually represent the highest risk. The system must be able to detect these obstacles, initiate the activation of the warning signal and then monitor the movement of the obstacle, i.e. whether it passes into category 2.1 or ceases to be an obstacle. The system must be able to correctly classify objects from this category of events because incorrect classification can cause additional safety hazards (occurrence of a much larger number of obstacles in category 2) or reduction of railway system efficiency (stopping in front of an obstacle when it was not necessary).

- In the case of the obstacles that do not have a direct impact on the railway safety and do not cause harmful consequences outside the railway system (category 3 and partially 1.2), the ODS does not need to fully detect them. But in the process of risk assessment, it is necessary to establish other risk control measures that will replace the measures implemented by the driver in such cases.

4   Requirements for the ODS based on the Assessment of the Impact of Obstacles on Railway Safety

The need for proper classification of obstacles and monitoring the movement of moving obstacles places high demands on the ODS. The application of the traditional safe-side principle on the railway (to treat everything as the worst case) for the ODS in DTO mode has certain limitations. The worst case involves emergency braking that can cause the train to derail [27]. In addition, the absolute application of the safe-side principle would mean that the train should be stopped in case of any detected obstacle, which would, given the large number of events

that do not pose a danger or pose only a potential safety hazard (obstacle categories 1.1, 3, 4.1 and 4.2) significantly jeopardize the efficiency and economy of railway traffic. Especially having in mind that there are no staff on the train in the DTO mode. Carrying out the procedures after stopping the train would require far more time than in the case when the driver is on board.

For these reasons, it is necessary that the ODS can monitor and classify obstacles, at least at the level that the train drivers can achieve. This is not an easy task, especially in the case of moving obstacles. For successful classification of obstacles, it is necessary to determine several parameters, some of which are not easy to determine. Unlike road traffic, trains have very long stopping distances and this drastically increases the number of possible risk situations. Practically every living being or vehicle that is located at a distance of a kilometre or two (depending on the type of train) near the railway represents a potential danger that must be detected and assessed. Based on a survey with train drivers conducted in Serbia, it can be concluded that they assess the risk of moving obstacles based on distance, position of the obstacle in relation to the free profile, its movement, but also some characteristics of the obstacle itself. In case of humans this assessment can be based even on the so-called body language. At the same time, none of the parameters has an unambiguous influence on the risk assessment. In some cases, a more distant obstacle may be more risky than a closer one.

a   b

Figure 3

The vehicle in a free profile at the level crossing (a) and moving towards the level crossing at high speed (b)

For example train drivers will not assess a railway worker in a free profile, even at a very short distance, as a great hazard because they know that they are professionals, trained for such situations and medically fit to timely move from a free profile. Hence, in case of detecting a railway worker in a free profile, train drivers will not take any measures other than the warning sign. On the other hand, some categories of people (e. g., small children, people with special needs) will be considered a great risk, and drivers will start to brake even at a great distance. Also, in some cases, a moving obstacle outside the free profile at a greater distance will be considered as a higher risk than one that is in the free profile at a

shorter distance. A vehicle that is in a free profile leaving the level crossing (Figure 3 a) will not be considered a big risk (except at a very short distance), while, on the other hand, a vehicle moving towards the level crossing at high-speed will be considered a big risk even at a greater distance (Figure 3 b).

In addition to the movable obstacles, immovable ones also require classification based on the risks they pose to safety. For example, whether a cardboard box in the free profile of the track poses a significant risk depends on its size, position in the free profile and content. This issue is also greatly influenced by the type of the railway vehicle, because the risk of immovable obstacles is drastically different for, e.g. a heavy locomotive on freight trains and a light diesel motor train.

The need to classify and monitor obstacles obviously requires the application of advanced object detection and classification methods. In recent years, the advancement in neural network technology has enabled great improvement in object (obstacle) detection based on Artificial Inteligence (AI) in rail road traffic applications [8]. However, introduction of AI-based obstacle detection and classification can be a problem when meeting technical safety requirements. The usual approach to certifying CCS devices involves reaching the required SIL. However, certification of systems that contain AI for SIL 4 level can be problematic, some standards do not recommend the use of AI for systems where a level higher than SIL 1 is required [17]. Given the large number of possible obstacles in the railway system and the complexity of this issue, machine learning will be a long - term process that will require extensive experimental application of this system before starting the process of its certification. A rational approach to solving this problem would therefore be to introduce an AI-based ODS in ATO level 3 (attended train operation). Mass application of this system in that regime could enable adequate training of the AI system for the classification of obstacles and raising its level of safety to the level required to reach SIL 4. In addition, the acceleration of mass application would be supported by using of eXplainable Artificial Intelligence (XAI)-based object detection and classification as opposed to current primarily "black box" use of AI-based methods [28]. Namely, "black box" approaches usually cause uncertainty regarding the way they operate and, ultimately, the way that they come to decisions. This ambiguity is problematic for machine learning systems to be adopted in sensitive yet critical domains, such as obstacle detection in railway. XAI can explain how AI obtained a particular solution (e.g., classification or object detection) and can also answer other "wh" questions, such as "which object features dominated when making AI-based decision on object classification?". Using of XAI could increase trust in and transparency of an AI-based object detection and classification.

Conclusions

ODS are one of the basic conditions for the introduction of DTO. In the European regulatory framework, the condition that they must at least provide a level of safety in relation to the obstacles on the line that is achieved by train drivers, can

be considered the basic safety requirement. This aspect is particularly important in the case of DTOs where the responsibility for accidents is shifted from the human control factor to the design and approval of the automatic control device.

Autonomously operated trains can increase the existing level of safety as they can lead to the elimination of human errors or improve the recognition of obstacles in difficult conditions. On the other hand, they can reduce that level in unexpected and more complex situations. They can also negatively affect the efficiency and economy of railway traffic.

To determine the achieved level of safety, the most important is the analysis of risks related to obstacles and the ways of their control by train drivers. It is therefore essential that the system must be able to classify all obstacles and monitor moving obstacles. This requires the application of an artificial intelligence system that is not easy to certify according to existing standards in the European railway system. One solution to this problem is the mass introduction of a detection system in ATO level 3 mode that should serve as a training phase for the system.

Acknowledgement

References

[1]   Banić, M., Miltenović, A., Pavlović, M. and Ćirić, I., (2019) Intelligent machine vision based railway infrastructure inspection and monitoring using UAV. Facta Universitatis, Series: Mechanical Engineering, 17(3), pp. 357-364

[2]   Sysyn, M., Nabochenko, O., Kovalchuk, V., Przybyłowicz, M. and Fischer, S., (2021) Investigation of interlocking effect of crushed stone ballast during dynamic loading. Reports in Mechanical Engineering, 2(1), pp. 65-76

[3]   Petrović, N., Bojović, N., Petrović, M. and Jovanović, V., (2020) A Study of The Environmental Kuznets Curve For Transport Greenhouse Gas Emissions In The European Union. Facta Universitatis, Series: Mechanical Engineering, 18(3), pp. 513-524

[4]   ERA, "Report on Railway Safety and Interoperability in the EU 2020", 2021

[5]   RSSB, "Trial of Sander Configurations and Sand Laying Rates", T1107 Project Report, Issue 1, 2018

[6]   Olofsson, U. and Sundvall, K., (2004) Influence of leaf, humidity and applied lubrication on friction in the wheel-rail contact: pin-on-disc

experiments. Proceedings of the Institution of Mechanical Engineers, Part F: Journal of Rail and Rapid Transit, 218(3), pp. 235-242

[7]   Rail Accident Report - Derailment at Godmersham, Kent on 26 July 2015. Report 05/2016. Rail Accident Investigation Branch, Department for Transport. April 2016

[8]   Ristić-Durrant, D., Franke, M. and Michels, K., (2021) A review of vision-based on-board obstacle detection and distance estimation in railways. Sensors, 21(10), p. 3452

[9]   Pavlović, M., Nikolić, V., Simonović, M., Mitrović, V. and Ćirić, I., (2019) Edge detection parameter optimization based on the genetic algorithm for rail track detection. Facta Universitatis, Series: Mechanical Engineering, 17(3), pp. 333-344

[10]   Hyde, P., Ulianov, C., Liu, J., Banic, M., Simonovic, M. and Ristic-Durrant, D., (2021) Use cases for obstacle detection and track intrusion detection systems in the context of new generation of railway traffic management systems. Proceedings of the Institution of Mechanical Engineers, Part F: Journal of Rail and Rapid Transit, p. 09544097211041020

[11]   Yu, M., Yang, P. and Wei, S., 2018, May. Railway obstacle detection algorithm using neural network. In AIP Conference Proceedings (Vol. 1967, No. 1, p. 040017) AIP Publishing LLC

[12]   Zhang, S., Tang, T. and Liu, J., (2021) A Hazard Analysis Approach for the SOTIF in Intelligent Railway Driving Assistance Systems Using STPA and Complex Network. Applied Sciences, 11(16), p. 7714

[13]   Amartuvshin D., Bilguunmaa M., Tadachika N., "Railroad Near-Miss Occurrence Detection and Risk Estimation System with Data from Camera Using Deep Learning", 5th ICISPC IEEE conference, 2021

[14]   https://smart2rail-project.net/, accessed on 24.10.2021

[15]   https://www.railtech.com/innovation/2020/11/26/two-new-ato-research-projects-launched-in-germany/?gdpr=accept

[16]   Braband, J. and Schäbe, H., (2020) On Safety Assessment of Artificial Intelligence. arXiv preprint arXiv:2003.00260

[17]   K Kurd, Z. and Kelly, T., (2003) September. Safety lifecycle for developing safety critical artificial neural networks. In International Conference on Computer Safety, Reliability, and Security (pp. 77-91) Springer, Berlin, Heidelberg

[18]   Németh, A., Fischer, S. (2021) Investigation of the Glued Insulated Rail Joints Applied to CWR Tracks. Facta Universitatis, Series: Mechanical Engineering, doi: 10.22190/FUME210331040N

[19] Directive (EU) 2016/797 of the European Parliament and of the Council of 11 May 2016 on the interoperability of the rail system within the European Union, http://data.europa.eu/eli/dir/2016/797/oj

[20] Directive (EU) 2016/798 of the European Parliament and of the Council of 11 May 2016 on railway safety, http://data.europa.eu/eli/dir/2016/798/oj

[21] El Koursi, E. M., Fletcher, S., Tordai, L. and Rodriguez, J., (2006) SAMNET Synthesis Report-Safety Management and Interoperability

[22] 2009/460/EC: Commission Decision of 5 June 2009 on the adoption of a common safety method for assessment of achievement of safety targets, as referred to in Article 6 of Directive 2004/49/EC of the European Parliament and of the Council (notified under document number C(2009) 4246)

[23] EN 50126 Railway applications standard - The specification and demonstration of Reliability, Availability, Maintainability and Safety (RAMS)

[24] Rail Delivery Group, "AWG Manual", Sixth Edition, January 2018

[25] ERADIS - European Railway Agency Database of Interoperability and Safety, https://eradis.era.europa.eu/

[26] Sikkerhedsrapport for jernbanen 2019, Trafik-, Bygge- og Boligstyrelsen, København, September 2020

[27] Assessment of freight train derailment risk reduction measures Part A final report for ERA, Det Norske Veritas, July 2011

[28] Linardatos, P., Papastefanopoulos, V. and Kotsiantis, S., (2021) Explainable ai: A review of machine learning interpretability methods. Entropy, 23(1), p. 18

Development of the High-Speed Running of Trains in Ukraine for Integration with the International Railway Network

Dmytro Kurhan, Mykola Kurhan, Nelya Hmelevska

Department of Transport Infrastructure, Dnipro National University of Railway Transport named after Academician V. Lazaryan
Lazaryan st. 2, 49010 Dnipro, Ukraine
{kurhan.d, mykolakurhan, hmelevnela}@diit.edu.ua

Abstract: Most European countries successfully solve the problem of national passenger transportation due to a significant increase in speed. Such measures are carried out both on existing railways through their modernization, and on specially built lines. Mass passenger transportation along the HSN has confirmed their extremely high reliability, safety, economic efficiency, ecological cleanness, and attractiveness for passengers. The creation of international networks based on the potentials of individual countries leads to the need for establishing the following operational and technical parameters of domestic high-speed railway lines, which would have operational compatibility with the Trans-European HSN. The interconnection between the volume of passenger traffic with the specified factors allows to predict promising passenger flow and evaluate the effectiveness in the organization of high-speed running in a particular direction. The economic integration of countries in the European Union allows increasing passenger flows on international travel. This circumstance leads to the problem solution in connecting national high-speed highways into a single European network.

Keywords: railway; train traffic; high-speed network; Net Present Value

1 Introduction

One of the priority directions in the development of railway transport is increasing the speed of passenger trains and further implementing a rapid and over the medium term a high-speed running both in Ukraine and in traffic between Ukraine and Western Europe.

The first-priority problem that needs to be carried out in accordance with the National Transport Strategy of Ukraine [1] includes providing a comprehensive innovative development of transport, in particular by creating conditions for the implementation of the high-speed passenger running on railways (up to

400 km/h), the expedited delivery of high-value goods (up to 350 km/h), faster delivery of containers (not less than 200 km/h).

At all times, the travel speed was the only integral indicator that characterized the development of passenger transport and in general the level of engineering-technical and economic development of the society. The way has gone from establishing the record levels of speed and painstaking work on the adaptation of the railway to the movement with high speeds to the organization of constant rotation of high-speed trains.

2   Review of the Literature

Most European countries successfully solve the problem of national transportation due to a significant increase in speed. Such measures are carried out both on existing railways through their modernization, and on specially built lines [2-7].

According to the National Transport Strategy of Ukraine for the period up to 2030, it is planned to provide conditions for the rapid traffic of passenger trains between regional centers from 160 to 200 km/h, and by 2030 – from 250 to 350 km/h. Also, it is expected the expedited delivery of high-value goods at a speed of up to 350 km/h and creating conditions for faster delivery of containerized freight – up to 200 km/h [8].

In solving the tasks of the first stage – the rapid traffic on existing lines of the railway is considered as an entire system consisting of devices and structures which because of the imperfection of the technical condition can limit the speed of trains on each particular section. Therefore, it is necessary to know the allowable speed of trains on each section of the railway, as well as the parameters of devices, according to which the railway should be rebuilt for the implementation of these speeds. Papers [9-11] describe suggestions concerning parameters definition for the reconstruction of the railway while implementing the rapid traffic of trains on the existing line.

The main criteria for choosing the direction of the way were grounded on a balanced accounting of such fundamentally important requirements as the maximum reduction in the length of HSN, providing optimal technical, operational and structural characteristics of the line (reduction in the number of turns, large artificial structures, volumes of earthworks, demolition of buildings, etc.), reduction in areas of operational lands, providing normative ecological and sanitary requirements in the zone of HSN impact [12-14].

On the example of Chinese railways, there is a full assessment of speeds implemented during operation [15-17]. The articles offers indicators and an integrated structure for a comprehensive assessment of the working speed on the high-speed railway.

The question about the accessibility of the railway corridor is interesting. In papers [18-20] it is noted that accessibility to the railway corridor is provided both by a conventional railway (CR) and high-speed railway (HSR). Studies illustrate the importance of CR and HSR coordination, evaluating and comparing the railway accessibility of the Shanghai-Hangzhou corridor (SH) in China and the Osaka-Nagoya corridor (ON) in Japan, the corridor of high-speed trains Madrid-Barcelona-French border.

Article [21] is devoted to the analysis of accessibility of high-speed railways in Korea. As tools for evaluation, a dispersion analysis test (ANOVA) and cartographic audit based on geographic information systems (GIS) are used.

Based on the analysis of perspective tasks, issues in the implementation of rapid traffic (161-200 km/h) of trains in Ukraine is subject to substantiation; application of rolling stock with forced bodies tilt of cars; construction of the new railway track of the European standard, which in its parameters can provide the implementation of high-speed (250-350 km/h) traffic of trains.

3 Methods and Results of the Research

3.1 Implementation Activities upon Passenger Trains Traffic with Speeds of 160-200 km/h in Kyiv-Lviv and Kyiv-Odesa Directions

To conduct research at various stages in the functioning of the railway, it (system) is divided into the subsystem of the 1st level (station-to-station blocks, interstations), which, in turn, are divided into the subsystem of the 2nd level (objects, barrier sites). Horizontal curves, defective artificial structures, areas of the weak roadbed, etc. act as barrier sites.

The authors in [22] reviewed the local optimization. It envisages the possibility of setting the maximum allowable speed not only within each station-to-station block, but also for each object (barrier site). The solution of such a problem is much more complicated because it is necessary to consider interdependent sections (objects). For such sections it is characteristic that reducing the train traffic time received on each section after removal of constraints in traveling speed is not equal to the advantage in time if authors remove all speed limits. That is, it is possible to obtain proved initial data only after carrying out tractive calculations at various combinations of removal of speed limits (eliminating barrier sites).

Table 1 shows the summarized results of executed tractive calculations for three technical states: option 1 – the initial condition of the railway, option 2 – reconstruction of the plan of the line, Option 3 – reconstruction of the plan and replacement of railroad switches on interstations for train handling with higher speeds.

Table 1

Results of tractive calculations for trains of various categories

Section	Length, km	Train type	Option 1		Option 2		Option 3	
			Travel time, min.	Average speed, km/h	Travel time, min.	Average speed, km/h	Travel time, min.	Average speed, km/h
Kyiv-Fastiv	63.83	Passenger	79.1	96.8	77.1	99.4	77.1	99.4
		Intercity+	60.7	126.3	56.3	136.1	51.3	149.3
		Pendolino	59.5	128.8	55.9	137.0	50.8	150.8
Fastiv-Kozyatyn	95.16	Passenger	114.2	100.0	113.7	100.5	113.7	100.5
		Intercity+	80.2	142.4	77.9	146.6	72.0	158.6
		Pendolino	79.8	143.2	77.5	147.3	71.4	159.9
Kozyatyn-Zhmerynka	109.48	Passenger	135.1	97.3	134.9	97.4	134.9	97.4
		Intercity+	104.4	125.8	100.2	131.1	88.3	148.8
		Pendolino	103.9	126.4	98.3	133.6	85.9	152.9
Zhmerynka-Pidvolochysk	165.87	Passenger	205.2	97.0	201.4	98.8	201.4	98.8
		Intercity+	155.0	128.4	143.4	138.8	138.1	144.1
		Pendolino	150.6	132.2	137.0	145.3	130.2	152.9
Pidvolochysk-Ternopil	52.94	Passenger	69.4	91.5	65.4	97.1	65.4	97.1
		Intercity+	57.0	111.5	51.7	122.9	50.6	125.6
		Pendolino	53.5	118.7	47.6	133.5	45.8	138.7
Ternopil-Krasne	90.10	Passenger	117.2	92.3	111.6	96.9	111.6	96.9
		Intercity+	104.4	103.6	87.3	123.8	85.3	126.8
		Pendolino	100.4	107.7	81.4	132.8	78.4	137.9
Krasne-Lviv	50.98	Passenger	67.2	91.0	63.3	96.6	63.3	96.6
		Intercity+	55.2	110.8	47.2	129.6	44.6	137.2
		Pendolino	51.5	118.8	44.7	136.9	41.9	146.0
Kyiv - Lviv	628.36	Passenger	787.4	95.8	767.3	98.3	767.3	98.3
		Intercity+	616.9	122.2	564.0	133.7	530.2	142.2
		Pendolino	599.2	125.8	542.4	139.0	504.4	149.5

The required capital investments to perform work on the modernization of infrastructure and reconstruction of the plan of the line are presented (Fig. 1) in the form of such components: track works, contact network and traction substations, reconstruction and modernization of signalling control devices, construction and reconstruction of passenger facilities at running lines and stations: railway stations, foot bridges, platforms, etc.
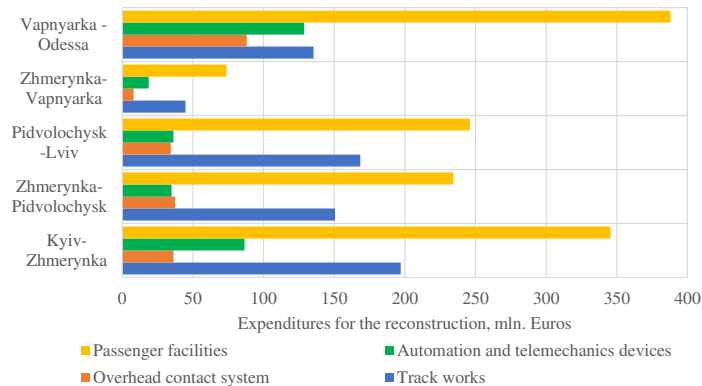
Figure 1

Expenses for the reconstruction of Odesa-Kyiv-Lviv direction

The total costs amounted to 2.5 million Euros/km (74.8 million UAH/km), which was adopted for the next assessment of the design decision.

3.2 Application of Rolling Stock with the Forced Bodies Tilt of Cars

One of the common ways to increase the speed of trains in the curved track is the use of rolling stock with a forced bodies tilt of cars. Trains such as "Pendolino" run in Italy, France, Great Britain, Spain, Portugal, Austria, Czech Republic, Slovenia, etc. Optimistic predictions that the purchase of rolling stock with the forced bodies tilt of cars will solve the issue of increasing the traffic speed in curves by 25-40% compared to the trains of locomotive traction without investing in the development of the railway infrastructure in real conditions may be incorrect. This is attested by the results of the above studies [3, 5, 9].

The conclusion that rolling stock with a forced bodies tilt of cars passes with a larger by 25-45 % speed compared to a conventional passenger train was obtained by the non-exceedance criterion of the allowable level of unbalanced acceleration within one circular curve acting at the passenger, without taking into account other factors. The presence of fitted curves, short transition curves and steep grade due to elevation of the outer rail does not allow to provide a high speed on the sections of the track and the reduction of motion time in average is 10-15%.

Thus, after the reconstruction on the Kyiv-Lviv section (see Table 1), the average passenger train speed will be 98 km/h, Intercity+ train – 142 km/h, Pendolino train – is about 150 km/h, which is 1.5 times higher compared to passenger and 5 % higher compared to Intercity+. Accordingly, the travel time will be 12.8 hours, 8.8 hours and 8.4 hours.

Based on the above, it can be concluded that a technique of adjusting a slope angle of a car body can not be an alternative to existing railways with the complex plan of the line. Using Pendolino Trains can lead to a tangible advantage in time at the train traffic, if authors consider the option of the new route with the corresponding parameters of the curves.

3.3 The Engineering of the New Route to Ensure Transportation by High-Speed Transport

In order to develop the network of railways in Ukraine, a systematic approach that envisaged the design and construction of new high-speed railways and modernization and reconstruction of existing ones was introduced.

In 2016, the predictive update program for rolling stock for the period up to 2021 was prepared including the section: "Organization of high-speed running". The Kyiv-Lviv-state border direction with the countries of Western Europe with further integration of the line with the European Network of the HSN is proposed to be the primary direction in the implementation of high-speed running in Ukraine (up to 350 km/h). The next stages in the implementation of projects for construction of HSN can be directions: Kyiv-Odesa; Kyiv-Poltava-Kharkiv-Donetsk; Kyiv-Poltava-Dnipro.

If the railroads can be included in HSN where a speed of 250 km/h and higher is realized, then the length of such railways in the world is about 110 thousand km, of which 53% and 47% are in operation at the stage of new and modernization of existing railways.

At the low percent of HSN in the total length of main railways (China – 29.0 %, Spain – 25.0 %, Taiwan – 22.0 %, Japan – 11.7 %, France – 11. 7%), the volume of passenger work performed by them many times exceeds the total volume of passenger transportation. It indicates high competitiveness and demand in this type of transport [23]. Figure 2 shows countries in alphabetical order.

Today there are many scientific research devoted to the study of ways for the further development of the Trans-European high-speed railway network. One of these projects is NGT (Next Generation Train) developed by eight Institutes in the German Aerospace Center (DLR). The main idea of NGT is to determine the HSN ground in Europe, calculated at the movement of new generation trains (NGT) at a speed of 400 km/h.

According to research [16], there are four types of operating models. They can be identified in various high-speed rail systems, which are currently working around the world, and their connection with ordinary rail systems.

The first type of model is characterized by a complete separating from traditional services, it is used in Japan.
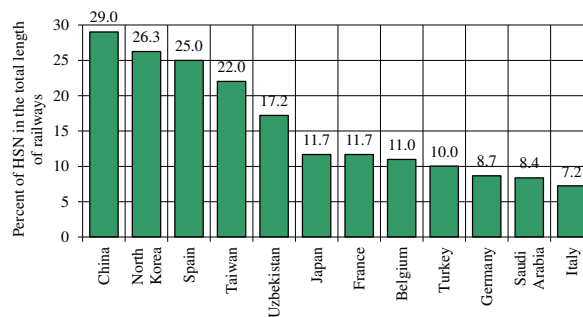
Figure 2

HSN in the total length of railways

The second model of exploitation is a mixed high-speed model in which a rapid train can move both on a specially built new line, and on upgraded sections of ordinary lines, which ultimately leads to a reduction in construction costs. This model is in agreement with the French system TGV (Train à Grande Vitesse).

The third model of operation is a mixed conventional model adopted in the Spanish rail system, it allows handling of some ordinary trains along the high-speed railways.

The fourth model is a fully mixed model. It involves using both high-speed, and ordinary trains on one infrastructure. This model is used for the German ICE system, where high-speed trains use upgraded ordinary lines, and freight trains – a reserve crossing capacity on the high-speed lines at night.

Thus, it can be considered advisable to build the new electrified double-track railroad in a length of 900 km, specialized for the movement of high-speed passenger transport and faster delivery of container and high-value goods. At the same time, high-speed trains can go to the existing Odesa-Kyiv-Lviv line to service them at the existing passenger stations, but trains of the existing railway are forbidden to go on the high-speed line. Travel time is 1.5-2.0 hours, route speed is about 270 km/h.

4   Performance Evaluation of Design Decisions

The essential factors determining the success of the HSN projects are the economic indicators of the country's development, as well as the financial position of citizens living in the HSR load region. The interconnection between the volume of passenger traffic with these factors allows to predict a promising passenger flow and evaluate the effectiveness in the organization of high-speed running on a particular direction. As world practice and calculations show, the construction of

the HSR can be effective in Ukraine in directions when the population of the load region is 20-25 million people, the length of the line does not exceed 800-900 km, and passenger flow is not less than 5-6 million people per year.

The authors analysed the dynamics, the main trends of passenger transportation and calculated flow factors [24]. Designed in long-distance traffic, the flow factor is significantly different in the regions and ranges from 0.9 to 2.28; On average, it is about 1.5 trips per year.

Methods are taken as the basis of the preliminary assessment of the project's efficiency [25-27] in accordance with which this assessment can be performed by six indicators. Authors turn our attention to the most common NPV (Net Present Value of Discounted Cash Flow) which is a difference of aggregate income and all types of expenses taking into account the factor of time.

For comparison of options: the reconstruction of the existing railway, the implementation of rolling stock with the construction of the European track and the implementation of high-speed running in Ukraine. The authors developed a model for predicting and evaluating the efficiency of rail transportation, taking into account all expenses by the *NPV* indicator [23, 28].

The analysis of the results showed that with the cost of reconstruction for Odesa-Kyiv-Lviv infrastructure (1010 km) of 2.5 million euro/km, the organization of rapid traffic will be economically justified at annual volumes of freight traffic 10-15 million tons and volumes of passenger traffic 15-20 pairs of trains per day.

To determine the most optimum compromise of high-speed passenger and specialized freight transportation on the new route, various combinations were considered. The issue of choosing the track gauge when designing a new railway remains relevant. The choice of 1,520 mm or 1,435 mm track gauge for use on the Ukrainian network is one of the most important issues. Each option has both negative and positive factors [29].

In the construction of the European standard railway (900 km) with the implementation of rolling stock with titling trains, the net present value depends on the volume of freight and passenger transportation and the cost of 1 km of the new railway. As it is seen from the graph (Fig. 3), the largest economic effect and in the shortest term can be achieved with the volumes of specialized freight transportation of 20-25 million tons per year (*G*) and passenger transportation of 15-20 pairs of trains per day (*n*). According to the results of tractive calculations in the Kyiv-Odesa and Kyiv-Lviv directions, the delivery time will be about 2 hours without taking into consideration the time to stop at a route speed of about 220 km/h.

In the construction of a railway of the Ukrainian standard with the implementation of high-speed rolling stock, type TGV POS, the net present value also depends on the volume of freight and passenger transportation and cost of 1 km of the new railway (Fig. 4). As it follows from the graph, the largest economic effect and in

the shortest term can be achieved with the volumes of special freight traffic 25-30 million tons per year (*G*) and passenger transportation 15-20 pairs of trains per day (*n*). According to the results of tractive calculations, the delivery time of passengers on the Kyiv-Odesa and Kyiv-Lviv sections will be about 1.5 hours without taking into account time to stop at a route speed of 280 km/h.
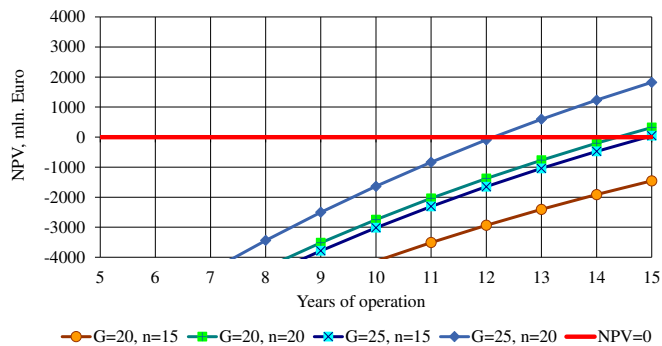

Figure 3

The term when the net present value arises depending on the volume of freight and passenger transportation in the construction of a new railroad with a track gauge of 1,435 mm
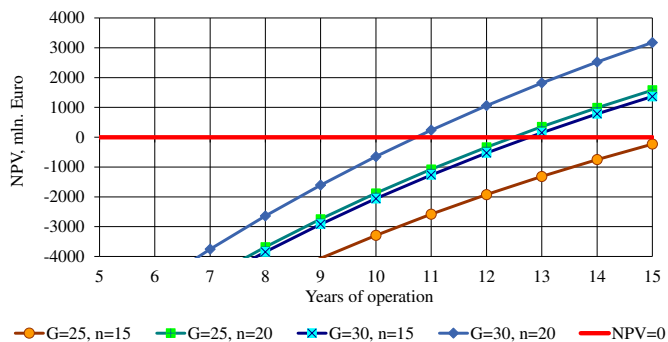

Figure 4

The term when the net present value arises depending on the volume of freight and passenger transportation in the construction of a new railway track with a track gauge of 1,520 mm

Conclusions

The creation of international networks based on the potentials of individual countries leads to the need for establishing the following operational and technical parameters of domestic high-speed railway lines, which would have operational compatibility with the Trans-European HSN.

The essential factors determining the HSN projects' success are the economic indexes of the national development, as well as the financial position of citizens living in the HSN load area. The interconnection between the volume of passenger traffic with the specified factors allows to predict promising passenger flow and evaluate the effectiveness in the organization of high-speed running in a particular direction. As evidenced by world practice and the performed calculations, the construction of the HSN can be effective in Ukraine in directions when the population of the load area is 20-25 million people, the length of the line does not exceed 800-900 km, and passenger traffic is not less than 5-6 million people per year. When designing the HSN, a new independent route must be laid in the shortest distance, without entering the main same cities, which allows relying on electricity savings, a decrease in ecological damage, to reduce the time of passengers staying by 2-3 times. To serve the population of cities and transfer of passengers to other types of transport one should be provided with technological connections of it with the existing general network of railways with the entry of the part of expresses to reconstructed stations in the central part of cities.

The construction of the proposed network of high-speed railways in Ukraine should be carried out in several stages. Implementation of the first stage (it is performed) will ensure the introduction of high-speed running between Kyiv and the main regional cities: Kharkiv, Dnipro, Lviv, Odesa, etc. The task of the second stage is to create a network of high-speed highways with technical and operational parameters that provide the motion of high-speed express trains at a speed of up to 350 km/h. The implementation of the HSM in Ukraine requires significant investments for the construction of transport infrastructure and the purchase of rolling stock. Many issues arise with the land allotment for construction, the cost of land plots, the possibility of private capital participation, construction organization.

The implementation of rapid traffic on the territory of Ukraine together with rapid lines Kyiv-Lviv, Kyiv-Odesa, Kyiv-Kharkiv, Kyiv-Dnipro will allow creating a single network of rapid traffic that will be attractive to users, which in turn will increase the number of transit passengers in the directions of the West - Ukraine - North East. The economic integration of countries in the European Union allows increasing passenger flows on international travel. This circumstance leads to the problem solution in connecting national high-speed highways into a single European network.

References

[1]   National transport strategy of Ukraine for the period up to 2030. https://mtu.gov.ua/news/28581.html [online, last visited on: 2021.09.30]

[2]   R. Pittman, M. Jandová, M. Król, L. Nekrasenko, T. Paleta. The effectiveness of EC policies to move freight from road to rail: Evidence from CEE grain markets. Research in Transportation Business & Management, Vol. 37, 2020, 100482

[3]   G. Bureika, L. Bielousova, V. Nozhenko. Estimation of Ecological Effectiveness of Rail Vehicle Operation in Eurasian Railway Corridors. Transport Means, 2019, pp. 460-465

[4]   A. Németh, S. Fischer. Investigation of glued insulated rail joints applied to CWR tracks. Facta Universitatis Series Mechanical Engineering, 2021, 7642

[5]   A. Massel. Train Commercial Speed Versus Maximum Line Speed – Central-European Experience. Transport Means, 2019, pp. 358-366

[6]   A. Massel, A. Soczówka. Evolution of High-Quality Express Passenger Train Services in Poland in 1989-2019. Transport Means 2020, pp. 49-56

[7]   R. Pittman. Reforming and restructuring Ukrzaliznytsia: a crucial task for Ukrainian reformers. Science and Transport Progress, Vol. 1(67), 2017, pp. 34-50

[8]   A. Shevchenko, O. Matviienko, V. Lyuty, V. Manuylenko. M. Pavliuchenkov. Ways of introduction of the high-speed movement of passenger trains in Ukraine. MATEC Web Conf. 230, 2018, 01014

[9]   S. Fischer. Comparison of railway track transition curves. Pollack Periodica, Vol. 4(3), 2009, pp. 99-110

[10]   I. Lebid, I. Kravchenya, T. Dubrovskaya, N. Luzhanska, M. Berezovyi, Y. Demchenko. Identification of the railway reconstruction parameters at imposition of high speed traffic on the existing lines. MATEC Web of Conferences 294, 2019, 05003

[11]   O. Hubar, R. Markul, O. Tiutkin, V. Andrieiev, M. Arbuzov, O. Kovalchuk. Study of the interaction of the railway track and the rolling stock under conditions of accelerated movement. IOP Conf. Ser.: Materials Science and Engineering, Vol. 985, 2020, 012007

[12]   O. M. Pshinko, L. V. Ursulyak, K. I. Zhelieznov, A. O. Shvets. To the problem of train running safety. IOP Conf. Ser.: Materials Science and Engineering, 985, 2020, 012014

[13]   M. Kurhan, D. Kurhan. Problems of providing international railway transport. MATEC Web of Conf., 230, 2018, 01007

[14]   K. Grębowski, M. Zielińska. Dynamic Analysis of Historic Railway Bridges in Poland in the Context of Adjusting Them to Pendolino Trains. International Journal of Applied Mechanics and Engineering, Vol. 20(2), 2015, pp. 283-297

[15]   J. Zhang, J. Zhang. Comprehensive Evaluation of Operating Speeds for High-Speed Railway: A Case Study of China High-Speed Railway. Mathematical Problems in Engineering, Vol. 1, 2021, pp. 1-16

[16]   D. Sun, S. Zeng, H. Ma, J. J. Shi. How Do High-Speed Railways Spur Innovation? IEEE Transactions on Engineering Management, 2021

[17]   China's High-Speed Rail Technology. Zhejiang University Press, Hangzhou and Springer Nature Singapore Pte Ltd., 2018, 587 p.

[18]   A. Li, J. Liua, H. Katoc, Q. Peng. Accessibility for a railway corridor integrating high-speed railway and conventional railway. Transportation Research Board Annual Meeting, 2021

[19]   J. Jiao, J. Wang, F. Jin. Impacts of High-Speed Rail Lines on the City Network in China. Journal of Transport Geography, Vol. 60, 2017, pp. 257-266

[20]   S. L. Shaw, Z. Fang, S. Lu, R. Tao. Impact of high speed rail on the rail network Accessibility in China. Journal of Transport Geography, Vol. 40, 2014, pp. 112-122

[21]   J. S. Chang, J.-H. Lee. Accessibility Analysis of Korean High-speed Rail: A Case Study of the Seoul Metropolitan Area. Transport Reviews, Vol. 28(1), 2008, pp. 87-103

[22]   M. B. Kurhan, D. M. Kurhan. Scientific-technical support of the railway Ukraine - European Union. Dnipro, Ukraine, 2018, 268 p.

[23]   M. B. Kurhan, D. M. Kurhan. Theoretical bases for introduction of high-speed train operation in Ukraine. Dnipro, Ukraine, 2016, 283 p.

[24]   M. Kurhan, D. Kurhan. Forecasting of Passenger Traffic upon Implementation of High-Speed Running. Science and Transport Progress. Vol. 67(1), 2017, pp. 117-130

[25]   Dac Criteria for Evaluating Development Assistance https://www.oecd.org/dac/evaluation/49756382.pdf [online, last visited on: 2021.09.30]

[26]   Results-Based Management approach as applied at UNESCO https://unesdoc.unesco.org/ark:/48223/pf0000177568 [online, last visited on: 2021.09.30]

[27]   Guide to Cost-Benefit Analysis of Investment Projects. https://ec.europa.eu/regional_policy/sources/docgener/studies/pdf/cba_guid e.pdf [online, last visited on: 2021.09.30]

[28]   M. Kurhan, D. Kurhan. Providing the railway transit traffic Ukraine–European Union. Pollack Periodica, Vol. 14(2), 2019, pp. 27-38

[29]   M. Kurhan, D. Kurhan, M. Husak, N. Hmelevska. Perspectives of High-speed Train Traffic in Ukraine at the Stage of Integration with the European Network. Transport Means, 2021

Relaxation of the Elastic Clamp in Rail Fastenings

Maxim Arbuzov, Serhii Tokariev, Oleksii Hubar, Volodymyr Andrieiev, Volodymyr Suslov

Department of Transport Infrastructure, Dnipro National University of Railway Transport named after Academician V. Lazaryan, Lazaryan st. 2, 49010, Dnipro, Ukraine; {maximarbuzov, serhiitokariev, oleksiihubar, volodymyrandrieiev}@diit.edu.ua
Company LLC Research and Production Enterprise "KRT CORPORATION", Komarnivska st. 66, 81500, Gorodok city, Gorodotskiy district, Lviv region, Ukraine; spc@krt.co.ua

Abstract: The main purpose of a rail fastening system is to provide the strength and reliability of joining rails to sleepers and, thus, prevents the longitudinal rail displacement and track disturbance. In a railway fastening, the joining function is performed by an elastic clamp. Over time, the clamping force of the elastic clamp is decreased due to various factors. The elastic clamp relaxation phenomenon is studied in present work. The observation of the clamp residual deformation was carried out on predetermined sleepers in different operating conditions. According to the research results of the elastic clamp relaxation of the rail fastenings, the following conclusions can be made: there is a relaxation process in the elastic clamps of the rail fastening, which has a curvilinear dependence on time; the intensity of the elastic clamps relaxation attenuates after one year of operation; in addition to the time factor, the relaxation of elastic clamps is influenced by the level of operating stresses; greater value of operating stresses corresponds to greater relaxation.

Keywords: elastic clamp; residual deformation; relaxation

1 The Research Program

Today in the countries of the European space [1] the design of elastic intermediate rail fastening is used, which combines all advanced achievements. Elastic fastenings are manufactured in many countries around the world. In order for this work not to be an advertisement, this paper does not indicate the type of rail fastening. Elastic fastening has different design options. But all elastic fastenings have a common element. This is an elastic clamp. The elastic clamp is the main element in rail fastening system. The elastic clamp must work for a long time.

The present work, studies the behavior of elastic fastening over time. Elastic fastening in its design includes elastic clamps that press a rail to a sleeper. In a free state, the elastic clamp has initial sizes. During mounting of the clamp, elastic deformations and mounting mechanical stresses occur. This creates a force that presses the rail to the sleeper. The mechanical properties of elastic clamps change over time. The reducing phenomenon of elastic deformations and mounting mechanical stresses is called relaxation. During relaxation of the elastic clamps, part of the elastic deformation transforms into plastic. As a result, the clamping force of the rail to the sleeper is decreased. At low values of the clamping force, the rail track malfunctions and the level of train safety decreases.

The research object is the elastic clamps of the intermediate rail fastening. The aim of present work is to research the effect of time on the geometric sizes of elastic clamps installed in a railway track.

An elastic rail fastening that is in operation is subject to research. When studying the relaxation of elastic clamps, it is necessary to establish how different factors affect. Experimental elastic fastening is affected not only by time but also the force effect from the wheels of the rolling stock. It is also necessary to determine how the track horizontal curvature affects the rail track, how the dismantling of the elastic clamp itself affects. It is necessary to determine whether the temperature affects the deformation of the elastic clamp.

The answer to the question "affects or does not affect" can be got by a special experiment or by factor analysis. Factor analysis of variance is performed under the Regulations on the procedure for conducting acceptance tests of railway track superstructure element prototypes [2, 3].

Analysis of variance task is to compare the estimation of the variance caused by the influence of a factor with the estimation of the variance caused by the influence of a random component. Comparing this relationship with Fisher's criterion $[F]$, a conclusion is made about the influence of the factor on the study parameter [4]. If the calculated value of the criterion F more than $[F]$, the factor affects. If the calculated value of the criterion F less than $[F]$, the factor is not affected.

Object No. 1. To study the relaxation process of the elastic clamp, a test section of the track in operation was selected. A new elastic fastening was placed on this section of the track, which was monitored. Measurements were periodically performed at the test section to accumulate passed tonnage of over 100 million tons, which is 1 year and 4 months. These elastic clamps were affected by all the factors listed in paragraph 1.2.1.

Object No. 2. A rail-and-sleeper grid with a new fastening was also assembled and placed outside of the track. The movement of trains on it was not carried out. The rail-and-sleeper grid is straight. The elastic fastening of the rail-and-sleeper grid was not affected by the rolling stock. The study of this fastening was carried out simultaneously with the fastening that was in operation (object No. 1).

Table 1
Frequency of measurements of elastic clamps

Measurement number	Date	Operation time, months	Passed tonnage at the time of measurement, million tons gross
0	August 2018	0	0
1	November 2018	3	21.96
2	March 2019	7	49.10
3	June 2019	10	72.30
4	December 2019	16	107.01

Objects No. 3 and No. 4. To study the relaxation process over a longer period of time, additional control track sections were selected, which worked for a long time. The control sections are sections of the same track construction as the test section (object No. 1), the operating conditions of which (a radius, passed tonnage, an axial load) do not differ by more than 10% from the operating conditions of the test facility (object No. 1), and a load intensity differ by at least 50% and 75%. In this case, the operating conditions of the elastic fastening of objects No. 1, No. 3, No. 4 differ only in the operating time. One-time measurements were performed at the control sections.

An information search in literary sources was also conducted about the elastic fastenings which worked over a long period of time. Periodically at the test section and once at the control sections evaluations were conducted monitoring the failure of the fastening units and observation of residual deformation of the elastic clamps.

The observation of the clamp residual deformation was carried out on predetermined sleepers - control cross sections. The control cross sections were located in the middle of the circular curves and on the straight section of the track. The distance between the control cross sections is approximately 10 m from each other. The clamps did not replace during the research period.

During the observation, the actual geometric sizes of the elastic clamps were determined and compared with their initial values. Thus, the plastic deformation of the elastic clamp was determined, which reflects the relaxation process. The initial values of the geometric sizes of the elastic clamps were obtained during measurements taken before laying into the track.

Dismantling of the fastening unit was carried out by by the track facility workers, measurements were performed by scientists of the Dnipro National University of Railway Transport named after Academician V. Lazaryan.

The elastic clamp of the rail fastening has a symmetrical curvilinear shape. One part of the clamp is rigidly attached to the sleeper, and the other elastically presses on the rail. The elastic clamp is dismantled and the sizes "S" and "Z" are measured in the free state (Fig. 1). Measurements are performed with a caliper with an accuracy of 0.1 mm. An auxiliary equipment is also used for measurement.
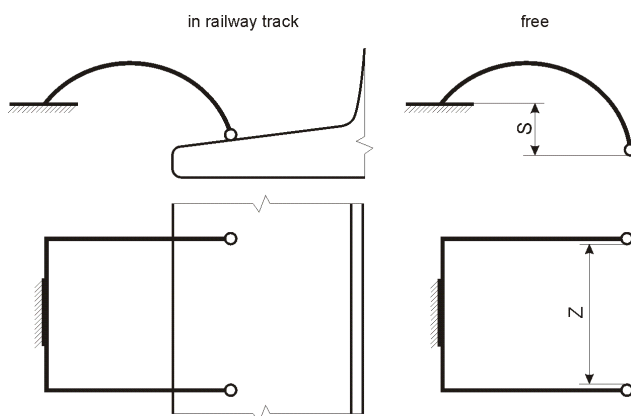
Figure 1

The measurement schema of the size "S" and the size "Z" of the elastic clamp

The residual deformation of the elastic clamp was estimated by changing the sizes "S" and "Z" according to formula (1) and (2), respectively.

$$\Delta S = S_n - S_0 \tag{1}$$

where ΔS is the vertical residual deformation of the elastic clamp;

S_n is the size "S" during the *n*-th dismantling of the elastic clamp for measurements;

S_0 is the size "S" before the initial laying of the elastic clamp into the track.

$$\Delta Z = Z_n - Z_0 \tag{2}$$

where ΔZ is the horizontal residual deformation of the elastic clamp;

Z_n is the size "Z" during the *n*-th dismantling of the elastic clamp for measurements;

Z_0 is the size "Z" before the initial laying of the elastic clamp into the track.

2   Analysis of Research Data

The track facility workers observed the elastic fastening operation every day. Scientists periodically conducted a control inspection when measuring the elastic clamps. The frequency of follow-up surveys was once every three months. During the entire period of operational tests, the elastic clamp failures due to passed tonnage or high load intensity of the section were absent. Failures of other fasteners during operational tests were also not observed.

Measurements of elastic clamps were carried out after their dismantling. The elastic clamps were in a free state. After measurements, the elastic clamp was mounted into the track in its place. It worked for some time and was dismantled again during subsequent measurements. In such studies, it is important to know whether the dismantling process itself affects the elastic clamp. To answer this question, the following experiment was conducted. Dismantled the elastic clamp. Size "S" and size "Z" were measured. Mounted the elastic clamp in its place. Dismantled the elastic clamp again. Size "S" and size "Z" were measured again. This was repeated five times. Size "S" and size "Z" have not changed. Therefore, the dismantling of the elastic clamp does not affect its residual deformation.

Measurements of elastic clamps were carried out at different ambient temperatures. Measurements were performed in August, November, March, June, and December. There were positive and negative temperatures. It is known that when heated, the metal expands. The elastic clamp has internal stresses from its production. It is important to know how temperature affects the deformation of the elastic clamp. The following experiment was performed to answer this question. Dismantled the elastic clamp. Size "S" and size "Z" were measured. The temperature of the elastic clamp was measured. The elastic clamp was heated to 15°C. Size "S" and size "Z" were measured again. The elastic clamp was heated to another 15°C. This was repeated five times. Size "S" and size "Z" have not changed. Therefore, the change in temperature of the elastic clamp does not cause its deformation. The effect of seasonal temperature fluctuations was also not detected.

The influence of the track radius on the residual deformation of the elastic clamp is estimated from the measurements of the object No. 1 via one-factor analysis. The elastic clamps at object No. 1 were located in the straight section of the track, in a curve with a radius of 874 m and in a curve with a radius of 1062 m. Therefore, three levels of factor were adopted for one-factor analysis.

Table 2 shows the results of one-factor analysis for the significance level $\alpha = 0.05$. Calculations were made for the different passed tonnage. The results for passed tonnage equal to zero are not shown, as the elastic clamps have not yet been mounted into the rail track. The results show that at the beginning of operation the track radius has a negligible effect on the geometric sizes of the elastic clamp. Then this effect disappears. This phenomenon is called "adaptation".

Passed tonnage influence on the elastic clamp residual deformation is estimated from the measurements of the object No. 1 via one-factor analysis. The elastic clamps at object No. 1 were measured five times. Therefore, five factor levels were adopted for one-factor analysis. Table 3 shows the results of one-factor analysis for the significance level $\alpha = 0.05$. The results show that passed tonnage is a very influential factor.

Table 2

One-factor analysis results of the track radius influence on the residual deformation of the elastic clamp

Passed tonnage, million tons gross	for size "Z"			for size "S"		
	F	[*F*]	conclusion	*F*	[*F*]	conclusion
21.96	4.284	3.074	affects	0.816	3.074	does not affect
49.10	0.198	3.074	does not affect	3.514	3.074	affects
72.30	2.361	3.074	does not affect	0.850	3.074	does not affect
107.01	0.886	3.074	does not affect	1.925	3.074	does not affect

Table 3

The results of one-factor analysis of the passed tonnage influence on the residual deformation of the elastic clamp

for size "Z"			for size "S"		
F	[*F*]	conclusion	*F*	[*F*]	conclusion
62.467	2.387	affects	46.190	2.387	affects

It is known that the dynamics of the track and rolling stock interaction in the straight section and in curve differ. In the curved section of the track there is a centrifugal horizontal force, which is transmitted through the rail to the fastenings. Simultaneous influence of two factors – radius and passed tonnage – is investigated by two-factor analysis, the results of which for the significance level $\alpha = 0.05$ are shown in Table 4. The results show that the simultaneous influence of the radius and passed tonnage has a minor effect on geometric sizes of the elastic clamps.

Table 4

The results of a two-factor analysis of the simultaneous effect of the curve radius and passed tonnage on the residual deformation of the elastic clamp

for size "Z"			for size "S"		
F	[*F*]	conclusion	*F*	[*F*]	conclusion
2.645	1.954	affects	2.518	1.954	affects

The observation results of the horizontal residual deformation ΔZ of the elastic clamps of the object No. 1 are shown in Figure 2. The data for the straight section of the track is shown here so it can be compared with the data for the section No. 2. The points on the graph show the average values of measurements at different passed tonnage. The obtained data are approximated by the function $\Delta Z = A \cdot \operatorname{atan}(B \cdot T)$, where *A* and *B* are constant approximations: $A=0.9$; $B=0.05$. Along the ordinate axis is the residual deformation ΔZ. Passed tonnage *T* is on the abscissa.

The results show that at the beginning of operation passed tonnage has a significant effect on the size "Z" of the elastic clamp. Then this effect fades. The results of the relaxation intensity, which fades over time, is confirmed by the classical mechanics [5].

The observation results of the vertical residual deformation ΔS of the elastic clamps of the object No. 1 are shown in Figure 3. The data for the straight section of the track is shown here so it can be compared with the data for the section No. 2. The obtained data are approximated by the function $\Delta S = C \cdot \text{atan}(D \cdot T)$, where C and D are constant approximations: $C = 0.6$; $D = 0.05$. On the y-axis - the residual deformation ΔS. The abscissa axis is the paseed tonnage T. The results show that at the beginning of operation the paseed tonnage has a significant effect on the size "S" of the elastic clamp. Then this effect fades.
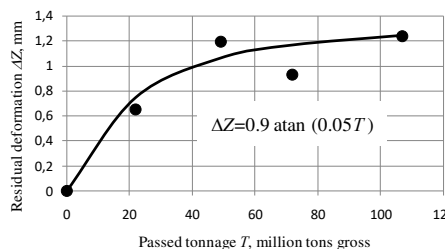

Figure 2

Influence of passed tonnage on horizontal residual deformation of the elastic clamp in straight section of track
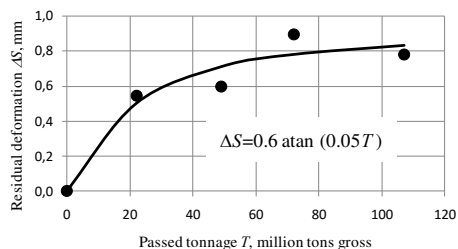
Figure 3

Influence of passed tonnage on vertical residual deformation of the elastic clamp

As the factor analysis showed, passed tonnage is a very influential factor. Here, it should be understood that passed tonnage is the sum of the loadings of the rolling stock axles. And the rolling stock moves through the track section for a certain period of time. While the pressure of the axles sums up, time goes by. Therefore, the passed tonnage influence on the elastic clamps is the effect of time under the rolling stock impact and the mounting forces of the clamps. Hence, it is necessary to observe the track of the object No. 2, which technical characteristics are similar to the technical characteristics of the track of the object No. 1, but the rolling stock impact is absent. Under this condition, it is possible to determine the time influence when only the mounting forces of the fastenings are acting. In this work, elastic fastenings that meet the requirements of regulatory and technical documentation were used. Thus, it is supposed that, at the beginning of the tests, the mounting forces of the clamps are the same.

The observation results of the horizontal residual deformation ΔZ of the elastic clamps of the object No. 2 are shown in Figure 4. The points on the graph show the average values of measurements at different times. The obtained data are approximated by the function $\Delta Z = E \cdot \text{atan}(F \cdot t)$, where E and F are constant

approximations: E=0.9; F=0.33. Along the ordinate axis is the residual deformation ΔZ. Time t is on the abscissa.

The results show that the approximating functions in Figure 2 and Figure 4 are the same. It is interesting that $F=B\cdot107/16$. The ratio 107/16 is the track load intensity of the object No. 1 expressed in months (Table 1).

The observation results of the vertical residual deformation ΔS of the elastic clamps of the object No. 2 are shown in Figure 5. The obtained data are approximated by the function $\Delta S=G\cdot\mathrm{atan}(H\cdot t)$, where G and H are constant approximations: G=0.8; H=0.33. On the y-axis - the residual deformation ΔS. On the abscissa is time t.
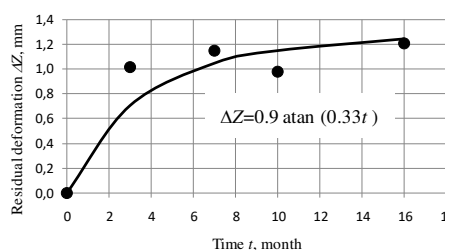

Figure 4

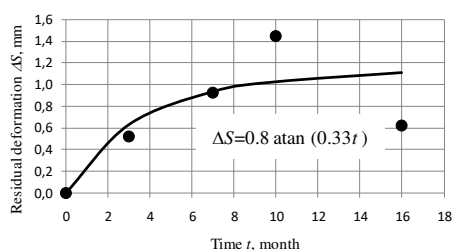Influence of time on horizontal residual deformation of the elastic clamp

Figure 5

Influence of time on vertical residual deformation of the elastic clamp

The results show that the approximating functions in Figures 3 and 5 do not match. Approximation constant $H=D\cdot107/16$. The ratio 107/16 is the track load intensity of the object No. 1 expressed in months. It is interesting that the vertical residual deformation of the elastic clamps, where there was a movement of trains, is less. This is due to the fact that under the wheel, the under-rail pad is compressed, and the operating stresses in the clamp are periodically reduced. The relaxation is the higher, the higher the level of operating stress. [6]. Thus, the dynamic vertical forces of the track and rolling stock interaction reduce the vertical residual deformation.

Then it is obvious that in Figures 2 and 4, the approximating functions of the horizontal residual deformations coincide due to the lack of dynamic lateral forces in the straight lines. If this statement is true, then the graph of horizontal residual deformations ΔZ for the curve should have a larger amplitude compared to the graph in Figure 2 due to the influence of lateral horizontal forces [7, 8].

Figure 6 shows a graph of horizontal residual deformations ΔZ for a curve section with a radius of 874 m. The obtained data are approximated by the function $\Delta Z=J\cdot\mathrm{atan}(K\cdot T)$, where J and K are constant approximations: J=1.2; K=0.05. Since $J>A$ then, indeed, the higher the relaxation, the greater the level of operating stresses.
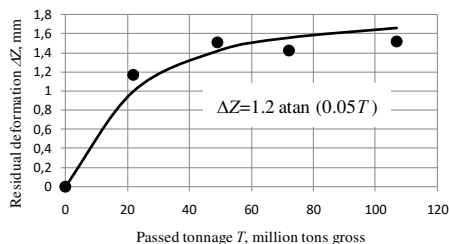
Figure 6

Influence of passed tonnage on horizontal residual deformation of clamp in curved section of track

As the factor analysis showed, the radius of the track has an effect, although insignificant, on the residual deformation of the elastic clamp. The combination of track radius and passed tonnage factors has a greater impact. Therefore, these track specifications of the object No. 3 and object No. 4 should be similar to those track specifications of the object No. 1. Under this condition, they can be compared with each other.

Further studies were performed by comparing sections of track with the same passed tonnage, the same curvature. The difference was in the operation time, there was an another load intensity.

On the track section of the object No. 3, the fastening measurements in the curved section with a radius of 745 m were performed. Passed tonnage was 49.7 million tons gross. Load intensity is 7.1 million tons gross/year/direction. Operation time is 7 years.

On the section of the track of the object No. 4, the fastening measurements in the curved section of the track with a radius of 885 m were performed. Passed tonnage was 46.9 million tons gross. Load intensity is 49.7 million tons gross/year/direction. Operation time is 0.9 years.

On the section of the track of the object No. 1, the fastening measurements in the curved section of the track with a radius of 874 m were performed. Passed tonnage was 46.1 million tons gross. Load intensity is 87.1 million tons gross/year/direction. Operation time is 0.5 years.

Table 5

The results of measuring the residual deformation of the elastic clamp at different sections of the track

Track section	Load intensity, million tons gross/year/direction	ΔZ, mm	ΔS, mm	Operation time, years
object No. 3	7.1	1.9	1.7	7.0
object No. 4	49.7	1.7	1.3	0.9
object No. 1	87.1	1.6	0.8	0.5

Table 5 shows the results of measuring the residual deformation of the elastic clamp of the track sections with the same passed tonnage of 48 ± 5% million tons gross, the same radius of 815 ± 9% m and different load intensity.

3   Results and Discussion

The influence level of time on the residual deformation of the elastic clamp is estimated using one-factor analysis based on the measurements of the object No. 2. The elastic clamps at object No. 2 were measured five times. Therefore, five factor levels were adopted for one-factor analysis. Table 6 shows the results of one-factor analysis for the significance level $\alpha = 0.05$. The results show that time is a very influential factor.

Table 6

One-factor analysis results of the time influence on the residual deformation of the elastic clamp

for size "Z"			for size "S"		
F	$[F]$	conclusion	F	$[F]$	conclusion
7.516	2.467	affects	16.803	2.467	affects

Table 7 shows the results of determining the vertical residual deformation of the elastic clamp with a passed tonnage of 50 million tons gross and a different load intensity, obtained from the literature [9-11], describing the similar studies. The data in Table 7 are reduced to the passed tonnage of 50 million tons gross using the established functions of the influence of passed tonnage on the residual deformation of the elastic clamp.

Table 7

The results of determining the residual deformation of the elastic clamp according to literary sources

Literary sources	Load intensity, million tons gross/year/direction	ΔS, mm	Operating time, years
[9]	15	1.6	3.3
[9]	57	1.3	0.9
[10], [11]	211	0.5	0.2

The data in Table 7 clearly confirm the conclusion of the one-factor analysis that the operating time affects the residual deformation of the elastic clamp. In addition, the data in Table 7 can be used as a supplement to the data in Table 5.

Figure 7 shows the effect of time with train load on the horizontal residual deformation of the elastic clamp for curved track sections with a radius of 815 ± 9% m. The vertical wear influence of under-rail pads and insulators on the horizontal residual deformation ΔZ is not established. Therefore, the data can be combined for different passed tonnages. The points on the graph show the data of

Figure 6 and Table 5. The obtained data are approximated by the function $\Delta Z = P \cdot \text{atan}(Q \cdot \tau)$, where P and Q are constant approximations: $P = J = 1.2$; $Q = K \cdot 12 \cdot 107/16 = 4$. The ratio $12 \cdot 107/16$ is the track load of the object No. 1 expressed in years. On the y-axis is shown the residual deformation ΔZ. On the abscissa axis - time with train load τ. Time with train load is the ratio of passed tonnage to load intensity, that is $\tau = T/(12 \cdot 107/16)$.

Figure 8 shows the effect of time with train load on the vertical residual deformation ΔS of the elastic clamp for curved sections of track with a radius of $815 \pm 9\%$ m and passed tonnage up to 50 million tons gross. The points on the graph show the data of Figure 8 (partially), Table 5 and Table 7. The obtained data are approximated by the function $\Delta Z = U \cdot \text{atan}(V \cdot \tau)$, where U and V are constant approximations: $U = L = 1.0$; $V = M \cdot 12 \cdot 107/16 = 4$. On the y-axis is shown the residual deformation ΔS. On the abscissa axis - time with train load τ.
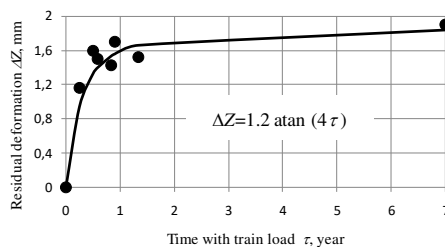

Figure 7

Time influence with train load on horizontal residual deformation of the elastic clamp
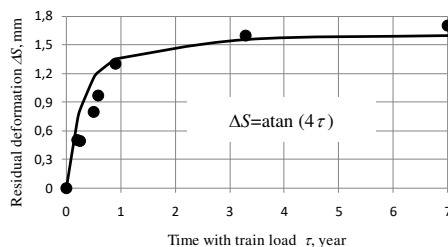
Figure 8

Time influence with train load on vertical residual deformation elastic clamp

Conclusions

According to the research results of the elastic clamp relaxation of the rail fastenings, the following conclusions can be made:

- there is a relaxation process in the elastic clamps of the rail fastening, which has a curvilinear dependence on time;

- the intensity of the elastic clamps relaxation attenuates after one year of operation;

- in addition to the time factor, the relaxation of elastic clamps is influenced by the level of operating stresses;

- greater value of operating stresses corresponds to greater relaxation;

- the influence of operating stresses is manifested as a factor of passed tonnage, a factor of the curve radius;

- the factor of passed tonnage is expressed by the impact of vertical and horizontal forces: vertical force reduces relaxation by the pad compression and reduction of level of the elastic clamp working stresses;

- the factor of the curve radius is expressed by the action of horizontal forces that increase the relaxation of the elastic clamps by their additional deformation and increase the level of operating stresses;

- no effect on the relaxation of the mounting-dismantling operation of the elastic clamp was detected;

- the effect of temperature on the relaxation of the elastic clamp is not detected.

References

[1]   M. Kurhan, D. Kurhan. The effectiveness evaluation of international railway transportation in the direction of "Ukraine – European Union", Transport Means, 2018, pp. 145-150

[2]   Regulations on the procedure for conducting acceptance tests of prototypes of the elements of the upper structure of the track. CP-0139. - Kyiv, 2006. – 39 p.

[3]   A. K. Mitropolskiy. Technique of statistical computations. Ed. 2., "Science", M.: 1971. – 576 p.

[4]   A. G. Bondar, Planning an experiment in chemical engineering. "Graduate school", K.:1976. – 184 p.

[5]   S. V. Grachev, L. A. Maltseva. Stress relaxation of the spring tape during bending. GOU VPO "Ural State Technical University – UPI". 2005. – 18 p.

[6]   V. P. Belogur, V. V. Voroshilin, G. A. Danilin. Investigation of the relaxation resistance of helical cylindrical springs during prolonged exposure under load. Metal working, No. 3, 2014, pp. 30-35

[7]   S. Fischer. Comparison of railway track transition curves. Pollack Periodica, Vol. 4(3), 2009, pp. 99-110

[8]   M. Kurhan, D. Kurhan, R. Novik, S. Baydak, N. Hmelevska. Improvement of the railway track efficiency by minimizing the rail wear in curves. IOP Conf. Ser.: Materials Science and Engineering, Vol. 985, 2020, 012001

[9]   K. V. Moiseenko, V. M. Suslov, A. A. Taturevich. Justification of the need to abolish the restrictions on the use of fasteners type PPC-5 by the criterion of load. Railway transport of Ukraine. 2/2017, – 55 p.

[10]   Conclusion on the results of field tests of intermediate rail fastenings KPP-5 and KPP-7. OJSC "Railway Transport Research Institute", 2010

[11]   Test protocol No. 2 gasket subrail type PRP-3.2 made of polyurethane based on polyesters Elastolan 90A. Institute of Ferrous Metallurgy of the National Academy of Sciences of Ukraine. Dnipro, 2016

Increasing the Efficiency of the Railway Operation in the Specialization of Directions for Freight and Passenger Transportation

Mykola Kurhan, Dmytro Kurhan, Marina Husak, Nelya Hmelevska

Department of Transport Infrastructure, Dnipro National University of Railway Transport named after Academician V. Lazaryan
Lazaryan st. 2, 49010 Dnipro, Ukraine
{mykolakurhan, kurhan.d, marinahusak, hmelevnela}@diit.edu.ua

Abstract: It is shown that in the mixed traffic of trains compared to the directions specialized for transportation of freight and passengers, the traffic capacity is sharply reduced, and costs on repairs and maintenance of track infrastructure increase by 1.5-2 times. The paper outlines ways to solve the problem in the distribution of directions with mainly freight and passenger traffic to increase the traffic capacity of transportation on the rail network. Among the activities, there is the transmission of transit freight flow on parallel runs. Furthermore, changing the operation conditions of railways in the case of implementing the high-speed trains traffic requires strengthening the existing railway lines in the event of insufficient reserves.

Keywords: railway; high-speed trains; trains traffic; traffic capacity

1   Introduction

The topicality of the paper is defined by the need to address a rather complex problem in the distribution of directions with mainly freight and mainly passenger traffic and increase of the traffic capacity on the rail network. Domestic and foreign studies demonstrate that in the mixed traffic of trains compared to the directions specialized for transportation of freight and passengers, the traffic capacity and reliability in fulfillment of a schedule is sharply reduced and costs on repairs and maintenance of a railway track increase by 1.5-2 times. As a result, the transmission of transit freight flow on parallel runs is often used in practice. Consequently, it is necessary to reconstruct such directions for developing the freight flow that is being transmitted. The relevance of the research is also defined by changing the operating conditions of Ukrainian railways in the case of the

high-speed trains traffic implementation, which requires strengthening the existing railway lines in the event of insufficient reserves.

In this regard, there is a need to substantiate, develop and implement the specialization of railway directions on the following principles:

- high-speed directions of passenger trains traffic;
- directions of intensive carrying capacity;
- directions of mixed traffic of passenger and freight trains.

The distribution of freight and passenger traffic is the main principle in organizing high-speed traffic in Europe. The analysis of contemporary publications shows that research on the choice of priority areas of international transportations include a wide range of issues, the main ones are:

- substantiation of logistics schemes of transportations, acceleration of the freight delivery time;
- increase in speed and traffic capacity;
- reduction of operating costs for current maintenance of infrastructure;
- research of the rolling stock/track interaction when changing the operating conditions.

2 Review of the Literature

Studies conducted on the Netherlands railways [1] consider the decision making issues faced by managers of the railway transport infrastructure in rail networks with dedicated tracks and corridors of public usage. The strategy upon consolidation of corridors, where the track serves passenger and freight trains is analysed. Various characteristics of passenger and freight trains are specified and the optimal distribution of tracks and consolidation time is analytically determined using two different patterns of models. The realistic parameters based on the Dutch railway system will be used in the experiments.

The optimization method for selecting a route for the everyday planning of freight trains is proposed in [2].

The mixed traffic of trains on the same tracks directly or indirectly affects the design, construction, operation, and maintenance of the railway system. In this context, the article [3] qualitatively and quantitatively evaluates the impact of some of the listed characteristics on the components of the rail system and presents the elements of the costs for the construction of the railway infrastructure, taking into account various exploitation scenarios.

The choice of optimal transport decision includes the rationale of the most profitable routes, the choice of rolling stock in accordance with the type of freight, the freight transportation mode [4], the state of railway traffic safety [5], the influence of train velocity [6], the work technique of border stations [7, 8], etc.

In [9], models of decision making to evaluate the effectiveness of the transport system in Europe-Asia are presented and in [10], the model for the distribution of transit freight on the railway network is proposed.

Article [11] highlights theoretical foundations and empirical results of analyzing and modeling Poland's transport networks. Properties of complex networks (Scale Free and Small World) and network-specific parameters are described.

Work [12] considers applying the simulation model of the transport system in Poland as a tool for sustainable transport development and reasonably substantiate the scientific and technical use of rail transport in the international carriage.

Methods of research and solving current transport issues were considered at the International Scientific Conference Transportation of the 21st Century, June 9-12, 2019, Rin, Poland [13].

Most European countries successfully solve the problem of national passenger traffic based on a significant increase in the speed of trains on specially built lines [14].

The article [15] highlights the impact of existing speed limits of trains on the amount of additional energy on the haulage of trains. On the example of the Budapest–Kelenfold–Hegyeshalom line, the efficiency in removal of constraints of speed limits on the tracks is shown.

The evolution of high-quality express-passenger trains in Poland is described in [16], and in work [17], the driving mode of mixed multispeed freight trains with the distribution of passenger and freight transport is investigated.

When solving tasks with increasing the traffic and carrying capacity, the railway is considered as a holistic system consisting of devices and structures that due to the imperfect technical condition can restrict the speed of trains on one or another section. Therefore, for each barrier site on the railway, it is necessary to know the allowable speed of trains and parameters of devices according to which one needs to reconstruct the railway to realize these speeds [18].

It has been a considerable growth of freight and passenger transportation on the British railway network over the past 20 years [19], which raises concerns about its ability to absorb continued growth. A number of infrastructure initiatives aimed at increasing the traffic capacity and reducing conflicts were implemented. The impact of new railway infrastructure for the distribution of passenger and freight traffic on the operational characteristics of freight trains was studied.

On the railways of North America [20, 21], there is a rapid growth in demand for transportation, and a rise in traffic capacity is increasingly required to meet them. Non-uniformity in a combination of characteristics of various types of trains leads to more considerable delays than with uniform traffic. The analysis given in the work included the impact on the delay of various vehicles and the characteristics of trains. The simulation program of dispatching developed by the authors was used to analyze the model of a single-track line with characteristics typical for the railways of North America. The purpose was to determine the impact of various operating and infrastructure changes to reduce train delays. The reduction of delays was considered the advantage of the project for each scenario. In contrast, any increase in delays leads to the necessity of using additional locomotives and extra fuel consumption, increased costs for infrastructure maintenance.

North American railways experience a growth in demand for transportations, and increasingly require a rise in the traffic capacity of their lines, which requires changing a cycle process of operational work and modernization of infrastructure. In [22], it is shown that the expansion of infrastructure involves a long time and capital-intensive operations, and as an alternative, it is proposed to reach additional power by changing the operational work regime, which is often cheaper and faster in realization.

Article [23] presents a model of reliable freight routing in the intermedial network of automobile and rail transport. The model is aimed at providing an optimal route. The main contribution of this work is that a program of actions is provided, which allows you to determine the amount of reducing traffic capacity, which should be taken into account when planning routes to obtain a level of reliability specified by the user.

The implementation of large-scale investment projects (new construction, reconstruction of railways) that foresee high investment expenses and the need to include many factors entails the use of appropriate efficiency assessment methods. The following principles are the basis for evaluating the effectiveness of the project: consideration of an option (project) during the entire estimated period, positive and maximum effect, the consideration of time factor, the impact of inflation, uncertainty, risks, etc. The preliminary assessment is based on methods [24-26].

Years of research have proved that the most minor operating costs upon the maintenance of the railway track would be provided with the corresponding ratio of the load intensity of a track, the level of dynamic load on a track from the rolling stock, and the power of a railway track.

This principle is used in regulatory documents of Ukrzaliznytsia. For example, a category of a railway track is determined depending on the traffic density and from the governed speed of passenger and freight trains. In papers [27, 28], the load intensity of a track is also determined by traffic loading and the level of dynamic load on a track from rolling stock by the governed speed of trains.

In [29], the railway track/rolling stock interaction results are presented under conditions of rapid and high-speed trains traffic.

In the existing rules of engineering of Hungarian railways, there are no design parameters for speeds exceeding 160 km/h. However, in the relevant international standard (ENV 13803), a similar speed limit is 300 km/h. The article [30] presents the results of comparing these rules.

A behavior pattern of the strain-stress state for the railway track based on the joint usage of propagation equations of an elastic wave to describe the topography of a part in the system involved in the interaction at a given moment of time, and equations of the dynamic equilibrium of its deformation are proposed in [31]. It enables to take into consideration the dynamics during the traffics of trains at high-speed.

3   Methods and Results of the Research

3.1   Purpose of the Research

Due to its geographical position and advanced transport infrastructure, Ukraine has significant potential in the development of international transportation, in particular as a transistor country in the logistics chain of trade between Asia and Europe [32]. However, in Ukraine, a classical form in the organization of traffic, which is to use infrastructure in the transportation of both passengers and freight (mixed traffic) has become an obstacle in the transition toward innovation-based development. The disadvantages of organizing such traffic are the insufficient comfort of passengers and the impossibility of using a new progressive rolling stock. A possible option for solving this problem is the separation of the freight traffic from the passenger one.

Problems of operational and technical nature arising during mixed traffic are primarily related to the disorders of the permanent way. When there is a changeover of the train flows to parallel runs, the traffic density of freight and passenger trains and other operational indicators change. These indicators affect the stress-strain state of a track and, consequently, on expenses associated with repair and maintenance of a track.

While dividing the freight and passenger transportation (even partly), the number of trains overtaking significantly reduces passenger and freight directions, leading to a decrease in operating expenses associated with braking, stops, and acceleration of trains.

The first steps in this direction were made in Ukraine: a program has been developed, according to which freight flows should be evenly distributed in all directions, and not concentrated on the most heavy-traffic rail lines, for example, such as Kyiv-Dnipro. To that end, the secondary, so far little involved runs on which one can changeover the freight flows are put in a proper condition. Simultaneously, there are several operational and technical challenges associated with the ratio of speeds of freight and passenger trains, a decrease in traffic-carrying capacity of railways, where high-speed traffic is being introduced [14].

The purpose of the study is to develop mathematical models for the rational distribution of freight and passenger flows based on vector optimization to ensure a minimum of the indicator: car-mileage (train-km), time of traffic (train-hour), energy intensity (mechanical work of locomotives, tonne-kilometer, or electricity costs, kWh), other technical and economic indicators.

3.2 The Mathematical Model for the Rational Distribution of Train Flows

To solve the problem of optimal distribution of train flows between the origin and destination, the network of railways was presented in the form of $G(V, E)$ graph, where stations are the graph vertex (set V), and sections between them – edges of graph (set E). Furthermore, the trains flow is given in a form of P_{ij} matrix, $i, j = \overline{1, n}$, where n is a number of stations, and P_{ij} is a number of trains from point i to point j [33].

Considering that one can reach from one station to another in various ways, following the graph between points i and j there are W_{ij} simple ways. Each edge $e \in E$ will be characterized by three parameters: edge length, train's traffic time on edge and mechanical work when driving a train on edge.

Let us denote a number of trains by X_{ijw}, moving from point i to point j along w-th simple route from list W_{ij}.

Then

$$\exists w = \{e, v\} : \sum_{i=1}^{n-1} \sum_{j=i+1}^{n} \sum_{w \in W_{ij}} f(w) X_{ijw} \to \min , \tag{1}$$

where $f(w)$ is the total value of an indicator of the simple way w from list W_{ij}.

The minimum value is determined with consideration to train flows, namely

$$\sum_{w \in W_{ij}} X_{ijw} = P_{ij};$$
$$i = \overline{1, n-1}; i+1 \le j \le n. \tag{2}$$

The limits upon the traffic capacity of each edge is added to these limits:

$$\sum_{i=1}^{n-1}\sum_{j=i+1}^{n}\sum_{w\in W_{ij}}I_w(e)X_{ijw}\leq N(e),\tag{3}$$

where $N(e)$ is traffic capacity of edge e;

$I_w(e)$ is the edge indicator e for the way w:

$$I_w(e)=\begin{cases}1,\,e\in w;\\0,\,e\notin w.\end{cases}\tag{4}$$

For example, Fig. 1 shows the optimization results by various indicators. One can consider multiple optimization indicators: train-kilometers (f_1), train-hours (f_2), mechanical work of a locomotive (f_3). Thus, train-kilometers and ton-kilometers (gross) reflect railways' technical and freight work, train-hours is the average speed of the trains' traffic, and the mechanical work of the locomotive is the costs of electricity or diesel fuel.
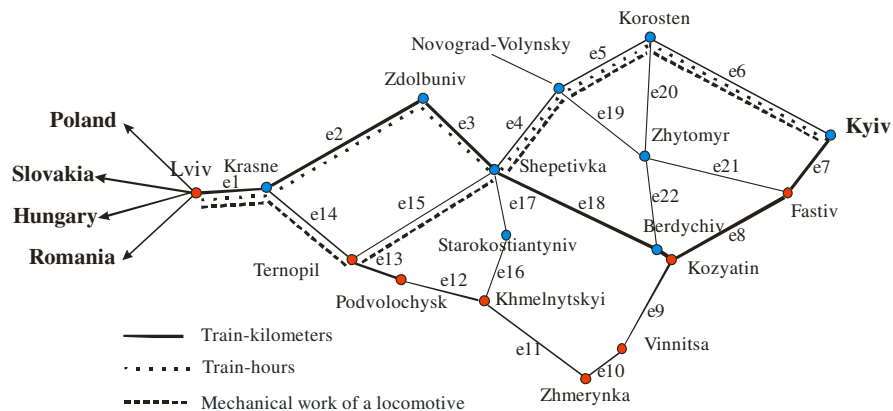

Figure 1

Distribution of trains between Kyiv-Lviv stations by different indicators of optimization

The final decision should be taken concerning the operating costs for the passage of freight and passenger trains, capital investments to enhance parallel runs, and the available opportunity in investing projects.

Therefore, further improvement of the transport process will be effective in the simultaneous specialization of railway directions.

3.3   Modeling the Trains Flow Traffic

The approach offered by the authors is based on the alleged modeling of the trains flow traffic. The trains flow is presented in the form of a three-dimensional surface, which is an approximation for the real distribution of masses and speeds of trains.

The statistical data analysis showed that the distribution of motion speeds in one cross-section of the track for all trains of this type is approaching the normal law. While evaluating the deviations of empirical distribution from normal upon fitting criterion, it has been established that in most samples, these deviations are insignificant. In subsequent calculations, we can use theoretical distribution curves of actually implemented speeds.

When modeling the flow of trains, the standard deviation can be taken approximately such as before the reconstruction of the railway according to the results of the statistical processing of the speed recorder tapes. Calculations show that in most cases, the value of the standard deviation is 5-20 km/h.

When dividing the freight and passenger traffic, the directions will be set depending on the structure of the train flows: categories and masses of rotating trains, and motion speeds (Table 1).

On the sections of passenger and freight traffic, the working conditions of the track are improved due to the uniform load of both rail lines as an elevation of an outer rail in curves is set in accordance with the speed of passenger and freight trains, which leads to a decrease in the deterioration of track and rolling stock. The article [34] highlights the analysis results of the measurement parameters for the railroad track and the ratio of vertical and side wear of rails in curves of various radii under the different operating conditions. It is shown that the set elevations of the outer rail do not meet the current requirements of increasing the operability of the track when minimizing the wear of rails, and therefore dividing the freight and passenger traffic is a vital problem.
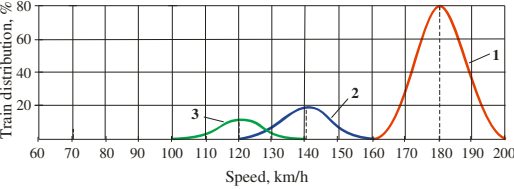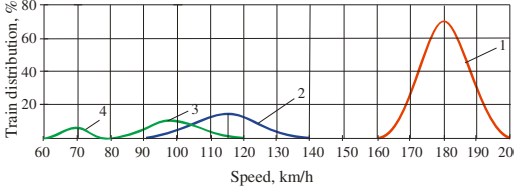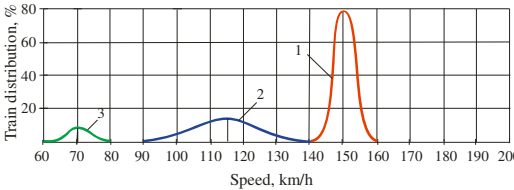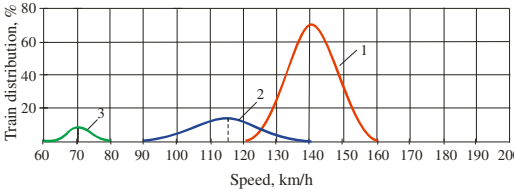
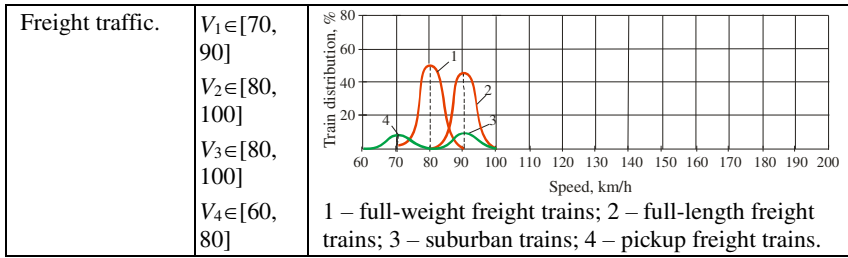## 3.4   Transmission of Freight Trains on Parallel Runs

In the study of parallel runs, it is necessary to consider the technical condition of both railway directions. For example, a passenger run may be a single-track section or single-track with double-track inserts or double-track railways. In this case, the freight (parallel) run can also be in one of these technical states. Therefore, at least nine possible combinations occur.

There is a need to investigate the conditions under which the transfer of parts of freight traffic to the parallel run can be effective. The analysis showed that in the presence of parallel directions with two main tracks, there are almost no problems with the transfer of the train flow. The question is considerably more complex

when one of the directions is single-track or with double-track inserts. The results of calculations for parallel directions represented by sections with double-track inserts are presented in the work. The basis of such an analysis can be the Program adopted by Ukrzaliznytsia concerning the increase of traffic capacity for sections with double-track inserts of Poltava-Kremenchuk-Burty-Korystivka-Dolynska-Mykolaiv due to the construction of the second main track.

Table 1
Classification of directions by categories of trains

Characteristics of the direction	Speed (V), km/h	Distribution graphs of trains speeds
High-speed passenger traffic:	$V_1 \in [160, 200]$ $V_2 \in [120, 160]$ $V_3 \in [100, 140]$	1 – day expresses; 2 – passenger rapid; 3 – suburban rapid.
Mixed traffic of high-speed passenger with pickup freight and suburban trains:	$V_1 \in [160, 200]$ $V_2 \in [90, 140]$ $V_3 \in [80, 120]$ $V_4 \in [60, 80]$	1 – day expresses; 2 – passenger rapid trains; 3 – suburban rapid trains; 4 – pickup trains.
Rapid passenger traffic of trains mixed with rapid traffic of suburban trains:	$V_1 \in [140, 160]$ $V_2 \in [90, 140]$ $V_3 \in [60, 80]$	1 – passenger rapid; 2 – suburban rapid; 3 – pickup freight.
A mixed traffic of rapid passenger trains with pickup freight and suburban ones.	$V_1 \in [120, 160]$ $V_2 \in [90, 140]$ $V_3 \in [60, 80]$	1 – passenger rapid; 2 – suburban rapid; 3 – pickup freight.

Freight traffic.	$V_1 \in [70, 90]$ $V_2 \in [80, 100]$ $V_3 \in [80, 100]$ $V_4 \in [60, 80]$	
		1 – full-weight freight trains; 2 – full-length freight trains; 3 – suburban trains; 4 – pickup freight trains.

It was adopted that a parallel freight run has the same technical condition as a passenger one, and the necessary traffic density is changed by a linear law $G_t = G_0 + \Delta G_t$. At the same time, three options were considered when the growth of traffic density occurs with different paces on a parallel run, namely $\Delta G_t = 2t, 3t, 3.5t$, at $G_0 = 5.0$ million nons / years.

From the graphs of traffic support (Figs. 3, 4) it is established, that with the available technical equipment and $G_t = 5.0 + 4.5t$ the railway will provide transportation till the 6th year of operation with the subsequent transition to a more powerful technical condition – the construction of the second track.

In the case of changeover, a part of freight ΔG_t on the parallel run the postponement of capital expenditures is achieved. The term in the postponement of the second track depends primarily on the value ΔG_t. For example, when transferring 10 million tons/year on a parallel run, the construction of the second track is postponed till the 9th year of operation; during the transfer of 20 million tons/year, postponing construction is possible till the 11th year (Fig. 3).
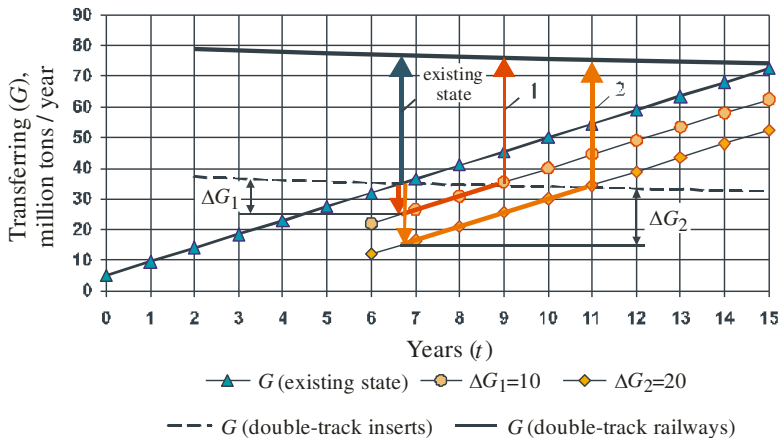

Figure 3

The graph of traffic support on a passenger direction when transferring 10 and 20 million tons/year on the parallel run

With the growth of traffic density by law $G_t = 5.0 + 2.0t$ (the 1st option) the parallel run can provide the necessary volumes of transportation until the 13th year. When transferring freight flow in the 6th year in a volume of 10 million tons/year, the reinforcement of the line will need to be performed in the 9th year, during the transfer of 20 million tons/year – a line in the year of transferring the freight flow should be double-track (Fig. 4).
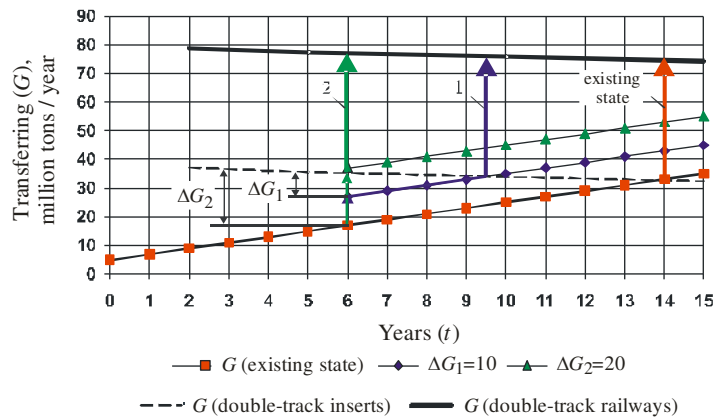

Figure 4

The graph of traffic support (freight traffic) on parallel run $G_t = 5.0 + 2.0t$

At other growth rates of traffic density (the 2nd and the 3rd options), the capacity of the parallel run is not enough, and therefore already in the 6th year, the line needs to be reinforced by building a second main track.

Conclusions

1) The analysis of the technical equipment and parameters of the route for the main directions of international transport corridors passing through the territory of Ukraine, showed that it is impossible to meet European requirements, especially for the maximum speed of motion without dividing the freight and passenger traffic and restructuring the plan of a line. The results of the analysis confirm the timeliness of the work.

2) The classification of directions of railways by categories of trains and the structure of the train flow is specified and detailed. Five types of directions are proposed: purely passenger, mainly passenger, rapid, mixed, and freight traffic, which corresponds to the safety criteria, smoothness, and comfort of traveling.

3) Problems of operational and technical nature arising during mixed traffic, are primarily related to the disorders of the permanent way. When there is a changeover of the train flows to parallel runs, the traffic density of freight and passenger trains and other operational parameters change. These parameters affect the stress-strain state of a track and, consequently, on expenses associated with repair and maintenance of a track.

4) In the dividing freight and passenger traffic, the total effect in each direction should be determined separately. On the sections of passenger and freight traffic, the working conditions of the track are improved due to the uniform load of both rail lines as an elevation of an outer rail in curves is set in accordance with the speed of passenger and freight trains, which leads to a decrease in the deterioration of track and rolling stock.

5) The number of trains overtaking significantly reduces passenger and freight directions, leading to a decrease in operating expenses associated with braking, stops, and acceleration of trains. In addition, it allows receiving additional profits by reducing the track disorder.

6) The proposed approach makes it possible to consider the opportunity to transfer the part of trains on parallel runs and evaluate the profit by dividing the freight and passenger traffic. The mathematical model of mixed formation for the scheme of traffic support for parallel railway lines makes it possible to take into consideration the specifics of each from the parallel directions (passenger, freight, mixed traffic) and obtain problem solving with minimal operating costs and rational investments, including reorganization of the railway to increase. The speed of passenger trains.

References

[1]   E. Ursavas, Stuart X. Zhu. Integrated Passenger and Freight Train Planning on Shared-Use Corridors. Transportation Science, Vol. 52(6), 2018, pp. 1297-1588

[2]   S. Li, H. Lv, C. Xu, T. Chen, C. Zou. Optimized Train Path Selection Method for Daily Freight Train Scheduling. IEEE Access, Vol. 8, 2020, pp. 40777-40790

[3]   C. Pyrgidis, E. Christogiannis. The Problems of the Presence of Passenger and Freight Trains on the Same Track. Procedia - Social and Behavioral Sciences, Vol. 48, 2012, pp. 1143-1154

[4]   A. Shvets. Dynamic Indicators Influencing Design Solution for Modernization of the Freight Rolling Stock. FME Transactions, Vol. 49(3), 2021, pp. 673-683

[5]   A. Blagojevic, Ž. Stevic, D. Marinkovic, S. Kasalica1, S. Rajilic. A Novel Entropy-Fuzzy PIPRECIA-DEA Model forSafety Evaluation of Railway Traffic. Symmetry, Vol. 12(9), 2020, 1479

[6]   V. Kovalchuk, M. Sysyn, U. Gerber, O. Nabochenko, J. Zarour, S. Dehne. Experimental investigation of the influence of train velocity and travel direction on the dynamic behavior of stiff common crossings. Facta universitatis - series Architecture and Civil Engineering, Vol. 17(3), 2019, pp. 345-356

[7]   N. Chornopyska, K. Stasiuk. Logistics Potential of the Railway as a Key for Sustainable and Secure Transport Development. Transport Means, 2020, pp. 421-425

[8]   M. Kurhan, D. Kurhan, L. Černiauskaite. Rationale of priority areas of rail operation in north-eastern Europe. Transport Means, 2019. pp. 1439-1444

[9]   M. Szkoda, A. Tulecki. Decision Models in Effectiveness Evaluation of Europe-Asia Transportation Systems. 8th World Congress on Railway Research, Seoul, Korea, 2008

[10]   D. Kozachenko, V. Skalozub, B. Gera, Y. Hermaniuk, R. Korobiova, A. Gorbova. A model of transit freight distribution on a railway network. Transport Problems, Vol. 14(3), 2019, pp. 17-26

[11]   Z. Tarapata. Modelling and analysis of transportation networks using complex networks: Poland case study. The Archives of Transport, Vol. 36(4), 2015, pp. 55-65

[12]   M. Jacyna¸ M. Wasiak, K. Lewczuk, M. Kłodawski. Simulation model of transport system of poland as a tool for developing sustainable transport. Archives of Transport, Vol. 31(3), 2015, pp. 23-35

[13]   M. Siergiejczyk, K. Krzykowska. Research Methods and Solutions to Current Transport Problems. Proceedings of the International Scientific Conference Transport of the 21st Century, Ryn, Poland, 2019

[14]   A. Németh, S. Fischer. Investigation of glued insulated rail joints applied to CWR tracks. Facta Universitatis Series Mechanical Engineering, 2021, 7642

[15]   S. Fischer. Traction Energy Consumption of Electric Locomotives and Electric Multiple Units at Speed Restrictions. Acta Technica Jaurinensis, Vol. 8(3), 2015, pp. 240-256

[16]   A. Massel. Train Commercial Speed Versus Maximum Line Speed – Central-European Experience. Transport Means, 2019, pp. 358-366

[17]   H. Zhipeng, N. Huimin. The Mode of Combined Multi-speed Freight Trains under Separation of Passenger and Freight Transport. Procedia - Social and Behavioral Sciences, Vol. 43, 2012, pp. 709-717

[18]   R. Pittman. Reforming and restructuring Ukrzaliznytsia: a crucial task for Ukrainian reformers. Science and Transport Progress, Vol. 1(67), 2017, pp. 34-50

[19]   A. Woodburn. The impacts on freight train operational performance of new rail infrastructure to segregate passenger and freight traffic. Journal of Transport Geography, Vol. 58, 2017, pp. 176-185

[20]   M. H. Dingler, Y-C. (Rex) Lai, C.P.L. Barkan. Impact of Train Type Heterogeneity on Single-Track Railway Capacity. Transportation Research Record, Vol. 2117(1), 2009, pp. 41-49

[21]   M. H. Dingler, Y-C. (Rex) Lai, C. P. L. Barkan. Mitigating train-type heterogeneity on a single-track line. Proceedings of the Institution of

M. Kurhan *et al.*

Increasing the Efficiency of the Railway Operation
in the Specialization of Directions for Freight and Passenger Transportation

Mechanical Engineers, Part F: Journal of Rail and Rapid Transit, Vol. 227(2), 2013, pp. 140-147

[22] Y-C. (Rex) Lai, Y-J. Lin, Y-F. Cheng. Assessment of Capacity Charges for Shared-Use Rail Lines. Transportation Research Record, Vol. 2448(1), 2014, pp. 62-70

[23] M. Uddin, N. Huynh. Reliable Routing of Road-Rail Intermodal Freight under Uncertainty. Netw Spat Econ, Vol. 19, 2019, pp. 929-952

[24] Guide to Cost-Benefit Analysis of Investment Projects. https://ec.europa.eu/regional_policy/sources/docgener/studies/pdf/cba_guide.pdf [online, last visited on: 2019.09.11]

[25] Dac Criteria for Evaluating Development Assistance https://www.oecd.org/dac/evaluation/49756382.pdf [online, last visited on: 2019.09.11]

[26] Results-Based Management approach as applied at UNESCO https://unesdoc.unesco.org/ark:/48223/pf0000177568 [online, last visited on: 2019.09.11]

[27] B. Leitner, D. Rehak, R. Kersys. The new procedure for identification of infrastructure elements significance in sub-sector railway transport. Communications - Scientific Letters of the University of Zilina, Vol. 20(2), 2018, pp. 41-48

[28] G. Bureika, L. Bielousova, V. Nozhenko. Estimation of Ecological Effectiveness of Rail Vehicle Operation in Eurasian Railway Corridors. Transport Means, 2019, pp. 460-465

[29] O. Hubar, R. Markul, O. Tiutkin, V. Andrieiev, M. Arbuzov, O. Kovalchuk. Study of the interaction of the railway track and the rolling stock under conditions of accelerated movement. IOP Conf. Ser.: Materials Science and Engineering, Vol. 985, 2020, 012007

[30] S. Fischer. Comparison of railway track transition curves. Pollack Periodica, Vol. 4(3), 2009, pp. 99-110

[31] D. Kurhan, M. Kurhan Modeling the Dynamic Response of Railway Track. IOP Conf. Ser.: Materials Science and Engineering. Vol. 708, 2019, 012013

[32] M. Kurhan, D. Kurhan. The effectiveness evaluation of international railway transportation in the direction of "Ukraine – European Union", Transport Means, 2018, pp. 145-150

[33] D. M. Kurgan, M. A. Zayats. The definition of rational allocation of train-flows on the rail network. Science and Transport Progress, Vol. 34, 2010, pp. 88-93

[34] M. Kurhan, D. Kurhan, R. Novik, S. Baydak, N. Hmelevska. Improvement of the railway track efficiency by minimizing the rail wear in curves. IOP Conf. Ser.: Materials Science and Engineering, Vol. 985, 2020, 165475